Ss. Cyril and Methodius University
Institute of Earthquake Engineering and Engineering Seismology
Skopje, Macedonia

Innovative method for improvement of the seismic resistance of the masonry infill walls in RC frame structures

DOCTORAL DISSERTATION

Jordan Bojadjiev, M.Sc.

Supervisor:

Prof. Roberta Apostolska, Ph.D

August, 2019

Универзитет Св. Кирил и Методиј
Институт за земјотресно инженерство и
инженерска сеизмологија
Скопје, Македонија

Иновативен метод за зголемување на сеизмичката отпорност на зидовите од исполната во армирано-бетонски рамовски конструкции

ДОКТОРСКА ДИСЕРТАЦИЈА

М-р Јордан Бојаџиев

Ментор

Проф. Д-р Роберта Апостолска

Август, 2019

Резиме

Неармираната исполна од ѕидарија широко се користи како внатрешни или надворешни преградни ѕидови кај армиранобетонските конструкции во светот. Во повеќето кодови за проектирање, панелите со исполна се сметаат како неконструктивни елементи и вообичаено се занемаруваат во процесот на проектирање на конструкции. Конвенционалната ѕидана исполна има поволно влијание од аспект на зголемување на крутоста на рамката во рамнина и е корисна во спротивставувањето на мали земјотреси. Сепак, во случај на силни сеизмички побуди, силната интеракција меѓу ѕидовите на исполна и околната рамка може да доведе до крт лом на АБ столбовите од смолкнување и оттука катастрофални рушења и целосен колапс. Во изминатите неколку декади, за време на секој катастрофален земјотрес, направени се многу извештаи за забележани големи оштетувања и неповолно сеизмичко однесување на АБ рамки со ѕидана исполна, вклучувајќи и многу ново пректирани, особено за време на земјотресот во Измит (Турција) во 1999, земјотресот во Венчуан (Кина) во 2008 и земјотресот во Покхара (Непал) во 2015. Неспорно е дека многу проблеми во врска со анализата и методите на проектирање на рамовски конструкции со соодветна исполна се се уште нерешени и дека инструкциите за проектирање и оцена на АБ рамки со исполна во различни земји се се уште далеку од задоволителни од аспект на комплетност и доверливост.

Примарната цел на оваа докторска дисертација е да се предложи и тестира иновативна врска која ефективно ќе ги ублажи несаканите штети врз АБ рамовски конструкции со исполна од ѕидарија како резултат на нивната интеракција и ќе го минимизира хазардот во однос на безбедност на животи во случај на можна земјотресна побуда. Ова предложено техничко решение се состои од поврзување на панелот на исполна со столбовите кои го опкружуваат со помош на врски со арматурни прачки сместени во слоевите од малтер и анкерувани во самите столбови. Предложената едноставна врска е практична, евтина и лесна за имплементација без некоја специфична технологија, што е многу важно за земјите во развој во сеизмичките региони. За оцена на ефективноста и адаптибилноста на предложената иновативна врска во однос на ублажувањето на штетите од земјотрес, беа извршени обемни квази-статички, тестови на вибро-платформа и нумерички истражувања врз основа на кои можат да се развијат и предложат понатамошни критериуми за однесување како и да се дадат генерални препораки за употреба на предложениот метод.

Земајќи ги предвид барањата за сличност, модел на трикатна, трибродна АБ зграда со предложената врска беше внимателно проектиран согласно Еврокодовите и беше применет на ѕидовите со исполна. Истиот беше тестиран на вибро-платформата во ИЗИИС, Скопје, Македонија. Беа направени серија од сеопфатни истражувања кои ги вклучија динамичките карактеристики, хистерезисното однесување како и механизамот на лом во услови на реални земјотресни побуди скалирани во размер кој одговара на моделот и прототипот. Глобалното однесување на конструкцијата во однос на предложената врска беше симулирано во компјутерскиот програм SAP2000, почнувајќи од моделирање на предложената врска, преку „push-over“ анализа и нелинеарна динамичка анализа на временски истории на интегралниот модел. Беа извршени динамички и монотони симулации и беше направена споредба со опсервациите од експериментите. Нумеричките и експерименталните резултати укажуваат на тоа дека предложениот концепт за ублажување на штети од земјотрес може значително да ја

намали непосакуваната интеракција меѓу панелите со исполна и околната рамка, да ги заштити столбовите од директен лом од смолкнување во рана фаза и да обезбеди способност на конструкцијата да се спротивстави на високи нивоа на земјотресни побуди. Конструктивната стабилност и интегритет, дуктилноста на поместување како и капацитетот за дисипација на енергија на АБ рамката со исполна се глобално подобрени. Од аспект на големиот број на рамовски конструкции со исполна од ѕидарија во Македонија, презентираното истражување се очекува да даде вредни насоки за сеизмичка оцена и проектирање на побезбедни рамовски конструкции. Резултатите од тестирањето и генералните насоки/препораки за проектирање од предложеното истражување исто така се очекува дека ќе придонесат за развој на градежништвото во други земји изложени на земјотреси, особено на Балканот и Медитеранот.

Клучни зборови: исполна од ѕидарија, АБ згради, иновативна врска, сеизмичка оцена, тестови на вибро-платформа

Summary

Unreinforced masonry panels are widely used as interior or exterior partitions in reinforced concrete frame structures around the world. In most design codes, infill panels are considered as non-structural elements and are commonly neglected in the structural design process. The conventional masonry infill walls have some favourable effects regarding an increase of the frame's in-plane stiffness and are beneficial for resistance to minor earthquakes. However, under strong earthquake excitation, the severe interaction between the infill walls and the bounding frame can introduce brittle shear failure in the RC columns and hence lead to catastrophic failures and collapse. For the past few decades, during each disastrous earthquake, severe damage and poor seismic performance of masonry infilled RC frames, including many newly designed ones, have been reported extensively, particularly during the 1999 Izmit earthquake in Turkey, the 2008 Wenchuan earthquake in China, and the 2015 Pokhara earthquake in Nepal. It is indisputable that inherent problems related to analysis and design methods for tight-fit infilled frame structures have not yet been solved, and some design guidelines for evaluation of infilled RC frames provided in different countries are recognized as being far from satisfactory in terms of completeness and reliability.

The primary objective of this doctoral dissertation is to propose and test an innovative connection detailing method, which can effectively mitigate undesirable interaction damage to masonry infilled RC frame structures and minimize the life-safety hazard under potential earthquake excitation. This proposed technical solution consists of connection of the infill panel to the bounding columns with steel wire connections deployed in mortar layers and anchored to the columns. The proposed simple connection is practical, cheap and easy to implement without any specific technology, which is very important for developing countries in seismic regions. To evaluate the effectiveness and adaptability of the proposed innovative connection for seismic damage mitigation, extensive quasi-static, shake-table tests and numerical investigations were conducted, based on which, further performance criteria and comprehensive design recommendations could be developed and proposed.

Taking into account the similitude requirements, a three story, three bay RC building model with the proposed connection implemented on the infill walls, was carefully designed according to the Eurocodes and tested on the shake-table in IZIIS-Skopje, Macedonia. A series of thorough investigations including dynamic characteristics, hysteretic behaviour, failure mechanism under real earthquake excitation properly scaled to fit the model and the prototype were rigorously carried out. The global performance of the structure in respect to the proposed connection was simulated in the computer program SAP2000, starting with modelling of the proposed connection, through push over analysis and nonlinear time history analysis of the integral model. Dynamic and monotonic push simulations were carried out and compared with the experimental observations. The numerical and experimental results indicate that the proposed seismic damage mitigation concept can considerably reduce the undesirable interaction between the infill panels and the bounding frame, protect the columns from direct shear failure at an early stage, and provide structural redundancy at high levels of excitation. Globally, the structural stability and integrity, displacement ductility, and energy dissipation capacity of the infilled RC frame are improved. In view of the large number of masonry-infilled frame buildings in Macedonia, the presented research is expected to provide valuable guidance for seismic assessment and design of safer frame structures. The test results and design guidelines/recommendations from the proposed research are also expected to benefit the

infrastructural development in other countries threatened by earthquakes, preferably in the Balkan and the Mediterranean region.

Keywords: masonry infill, RC buildings, innovative connection, seismic assessment, shake-table tests.

Acknowledgments

Contents

List of figures

List of tables

1. INTRODUCTION

1.1. Problem statement

Reinforced concrete frame structures infilled with unreinforced masonry infills, are recognized as one of the most widely adopted structural forms throughout the world. The cost-effective, easy construction and flexible layout characteristics of masonry infill panels make them a popular choice for architects to arrange interior and exterior partitions. Most of the seismic codes of practice nowadays tend to designate masonry infill panels as non-structural elements and neglect their structural participation during earthquake excitation. However, as demonstrated by many researchers (Liauw and Kwan, 1985; Mehrabi and Shing, 1997; Mosalam, et al., 1997a, 1997b; Fardis et al., 1999; Kakaletsis and Karayannis, 2009; Griffith 2008), infill panels may completely alter the structural behaviour by their nonnegligible bracing actions during strong earthquake excitation. The severe interaction between infill walls and bounding frame, especially in the case of non-seismic frames, can be detrimental to the seismic performance of buildings, resulting in irreparable damage or even collapse of the whole structure, tremendously endangering peoples' lives and property (Zhang, 2015).

Figure 1.1 Collapse of a two-storey infilled RC building during the 2008 Wenchuan earthquake (Photo creator: Zhe Wang) (Zhang, 2015)

Kuang and Zhang, 2014, pointed out that it has extensively been reported that in almost every moderate to high excitation earthquake during the past decades poor seismic performance and severe damage of masonry-infilled frames have been observed, including many newly designed ones, particularly in the 1999 Izmit earthquake in Turkey, the 2008 Sichuan earthquake (Figure 1.1) and 2013 Lushan-Ya'an earthquake in China, the 2010 Maule earthquake in Chile, the 2009 L'Aquilla, Italy, the

2016, Italy. The most recent one in our country, the Skopje earthquake from 11.09.2016 with magnitude 5 was characterized with masonry infill damage in RC structures.

Even with dozens of lessons from past earthquake events, the structural reliability and adequacy of infilled frame buildings are utterly not guaranteed by the current design and analysis methods. The intractable conflict between the expectations from engineers' computational analysis and the realistic observations of the seismic performance of infilled RC frame buildings remains unresolved.

Seismic design, in general, has two main objectives, namely to: i) prevent local or global collapse of the structure in the event of the design seismic action, retaining structural integrity and residual load bearing capacity after the event - Ultimate Limit State requirement; ii) withstand a more frequent seismic action without significant damage – Serviceability Limit State requirement.

In other words, human lives have to be protected and damage has to be limited in order to keep the rehabilitation of the structure economically feasible. These are the objectives clearly stated in Eurocode 8 (EC8) (Eurocode-8, 2004). Furthermore, this new standard imposes new rules for non-structural members, as in the case of masonry infills. It is stated in article 4.3.6.4 of part 1 of EC8 (Eurocode-8, 2004) that the brittle collapse of the infills has to be avoided and that light wire meshes or bed joint reinforcement have to be used. Besides this general information, no more details are given, so there is insufficient information for the structural engineer to correctly design the infills.

In the new buildings design according to Eurocode 8, (EN 1998: Eurocode 8.2004) the masonry infill are threat as a source of structural additional strength and so called "second line defense". So the reduction of input seismic action as a result of favorable infill effects is not allowed. Considering this, design of RC buildings with masonry infill according to EC8 is on safety side but it is not rational because leads to significant increase of reinforcement in the structural element in comparison with the bare frame. Having in mind that the design EC8 method for RC frames with infill are conservative it is necessary to quantify the effects of the infill on seismic performance of the structure properly, which means:

- The infill should be explicitly incorporate in the structural model for analysis and design
- Performance of the infill should be verified against seismic demands as a results of the nonlinear analysis and design of structures

The problem is even more complex in the case of seismic performance assessment of the existing RC buildings with masonry infill. It is already know that the influence of the infill wall is most significant when the structural system itself does not possess adequate seismic resistance, which is often case in large number of substandard RC buildings in south Europe and Mediterranean (Necevska-Cvetanovska et al., 2015).

1.2. Thesis originality

The previously mentioned contradiction has led to the formulation of two earthquake-resistant design philosophies. One requires the infills to be tightly placed in the frame and behave as beneficial structural elements. The symmetrically arranged and tight-fit infill panels may serve as the first line of earthquake defense and provide structural redundancy and an alternative vertical load transfer path. The rationale behind this design philosophy is “Avoid unnecessary masses” and “If a mass is necessary, use it structurally to resist seismic effects” (Bertero and Brokken, 1983). With this concept the unreinforced masonry infill (URM) behaviour could be simplified and considered as an equivalent diagonal strut. Some modelling techniques have been proposed (Stafford-Smith, 1966; Saneinejad and Hobbs, 1995; Mehrabi and Shing, 1997; Flanagan and Bennett, 2001; El-Dakhakhni et al., 2003; Cavaleri et al., 2014) and practically presented in design pre-standards (FEMA 306, 1998; FEMA 356, 2000; ATC 40, 1996). However, the tightly placed strategy failed to achieve satisfying seismic performance as introduced before and the strut model for URM infill walls cannot clearly define the complex interaction itself and reveal the inherent brittle properties of materials. As a result, under moderate and high seismic excitation, tight fit URM infilled frames exhibit poor performance due to premature shear failure in the frames, or rapid degradation of stiffness and strength in infill walls. These global and local vulnerabilities could trigger a catastrophic soft-storey failure mechanism and progressive collapse of a whole RC frame structure, which is far beyond the anticipated seismic behaviours during the design process.

The conventional tight-fit layout of infill panels may also conflict with the performance based seismic design criteria, since the enormous debris of infill panel from in-plane and out of-plane failure not only cause severe life and property loss during earthquakes, but also cause a burden for the economy and society. When the expense of repairing and retrofitting of an infilled RC frame structure after earthquake events could exceed the cost of building a new structure, alternative solutions should be proposed, which form the main concern of this thesis.

Another design philosophy requires that the infills be effectively isolated from the structural system so that their structural effect and undesirable interaction can correctly be neglected; nevertheless, difficulties lie in the lack of convenient and satisfying solutions for fire and acoustic protection of the gaps. Furthermore, plenty of lessons learnt from past earthquake events show that isolating infill panels without proper connection detailing leads to catastrophic out of plane throw-off failure, which blocks crucial escape/rescue routes and endangers people’s lives inside and outside the structure.

In a nutshell, no reliable analytical method and design guidelines together with convenient and engineering applicable technological solutions have been developed to reflect poor seismic

performance and to model the major possible failure modes of infills and frames. Therefore, there is an urgent need to propose an innovative seismic damage mitigation solution to fill the gap between previous studies and present problems and to provide more rational and accurate guidelines for the future seismic design of infilled RC frame structures. The proposed method in this thesis is consisted of connection of the infill panel to the bounding columns with steel reinforcement which are deployed in mortar layers and anchored to columns. The proposed simple connection is practical, cheap and easy to implement without any specific technology, which is very important for developing countries in seismic regions.

1.3. Thesis organization

The research programme includes the development of concept, designing and construction of the models, shake-table testing, computational simulations and finally proposing a design approach and recommendations for the seismic damage mitigation as an alternative to the construction of infill walls.

Chapter 1 provides the background information about the seismic performance of infilled RC frame structures under earthquake excitation. The research significance is also presented. Chapter 2 present the research objectives and used methodology in this study.

Chapter 3 is literature review in the masonry infill in RC buildings. At the beginning the global and local vulnerabilities of infilled frame structures based on lessons learnt from past earthquakes are given. A comprehensive literature review for analytical models developed during the past few decades is compared and discussed. Some of the most popular design codes of practice relating to the seismic assessment of infilled RC frames are also systemized. Previous studies with masonry infill performed in IZIIS are also presented.

Chapter 4 in the first part gives detailed information about the experimental programme, including introduction of the shake-table system, derivation of similitude requirements, design and construction of models, test setup and instrumentations, and the mechanical properties of the test material used. At the second part, shake table tests results are presented as well comparison with a reference model previously tests with standard infill construction.

Chapter 5 presents the results of 3-D finite element modelling of the three-storey three-bay RC frame structure with the standard infill connection and the new proposed connection detailing method. Dynamic excitations and in-plane pushover analysis are simulated and compared with the shake-table experimental data. Chapter 6 summarizes the major findings in this research. A conclusion and general

design recommendations are made. Possible further research work is also discussed. Finally the used bibliography in the research is given.

2. OBJECTIVES AND METHODOLOGY

The main objective of this research is to propose and test an innovative method for the connection of column-infill which minimizes unexpected seismic damage and to provide optimal solutions and design recommendations for masonry infilled RC frame structures in seismic prone areas. With this optimal solution, the RC frame column members are protected from premature shear failure and tend to deform as initially designated in the design, while providing favourable integrity and out-of plane stability of infill panels. The proposed detailing method will achieve optimal and favourable force-displacement behaviour between a fully infilled RC frame and bare frame. The complicated failure modes of tight-fit infill panels dominated by a large number of interacting parameters, and the dangerous soft/weak storey phenomenon are also anticipated to be solved.

More specifically, the goals of the dissertation are as follows:

- Understand the seismic performance and failure modes of conventional infilled RC frame structures through an elaborate literature review.
- Evaluate the problems and the missing gaps in the current seismic codes dealing with the masonry infill walls in reinforced concrete structures.
- Design and construct scaled RC frame models based on the seismic code of practice and rigorous similitude requirements. Design and validate experimental instrumentations and test protocols.
- Investigate the effectiveness of the proposed seismic damage mitigation detailing method by conducting shake table tests on scaled three-storey two-bay specimens.
- Contribution towards development of seismic performance criteria for infilled RC frame structure with connections based on systematic analysis and assessment of experimental results.
- Conduct computational simulations with the developed numerical models and compare and validate the results with experimental data.
- Propose design guidelines identifying the advantage of the proposed connection system and make intro towards design recommendations for infilled reinforced concrete frames.

In order to meet the goals envisaged in this dissertation, an integral experimental and analytical methodology based on several main components is proposed, described in more details in the following paragraphs.

This research project focuses on developing and upgrading a method for increasing the seismic capacity of reinforced concrete building structures with masonry infills. In this manner the planned dissertation's main activities are:

A. Experimental investigation program

1. Laboratory testing of concrete, steel, masonry unit (bricks) specimens for definition of their strength characteristics.

2. Quasi-static testing of different types of masonry wall samples, for definition of mechanical characteristics and failure mechanism.

3. Construction of the model of three story RC building with different types of masonry infill, to a scale 1:2.5 and preparation for shake- table testing.

4. Shake- table testing of the scaled models applying programme of experimental tests by gradual increase of the intensity of input earthquake excitation, aimed at monitoring the progressive development of cracks (damages?) and the phases of dynamic behaviour of the models.

In this dissertations several experimental investigations performed in IZIIS are used as well as the experimental investigations which are performed in the frames of the research project "Frame – masonry composites for modeling and standardizations (**FRA**med-**MA**sonry)" realized by the Faculty of Civil Engineering and Architecture Osijek, Josip Juraj Strossmayer University of Osijek, Croatia**,** and The Institute of Earthquake Engineering and Engineering Seismology, IZIIS from Skopje in the period between September 2014 and August 2017 (Necevska Cvetanovska et al., 2015). The principal investigator was Prof. Vladimir Sigmund and the funding was provided by Croatian Science Foundation.

B. Numerical investigation program

Several approaches of modelling the global behaviour of the model, using sophisticated finite element computer programs, are considered in order to adequate simulate response of the RC structures with infill recorder during experimental investigations:

- Selecting the right modeling approach for modeling the infill walls
- Defining nonlinear models for defined frame elements
- Modelling of the infill walls
- Defining Hysteresis Model for analysis
- Nonlinear static (pushover) analysis
- Nonlinear direct integration dynamic "time–history" analysis

3. LITERATURE REVIEW

3.1. Seismic performance of RC structures with masonry infill – lessons learnt from past earthquakes

Design and construction of RC buildings with masonry infill are common in European engineering practice especially in its seismic active southern part. The effects of infill on seismic performance of integral structure are very important. The infill walls have demonstrated poor performance even in moderate earthquakes: due to their brittle behaviour and little or no ductility, they suffer damage ranging from cracking to crushing and eventually disintegration (Fig.3.1). However, it is recognized that they could have a beneficial effect on the seismic performance of buildings in that they reduce the lateral storey drift at which the maximum shear force is attained, by more than 2 times compared with the bare frame, except for partial-height walls that may cause shear failure of the adjacent RC columns.

Figure 3. 1 Damages on infill walls (Photos: L.D. Decanini & L. Liberatore, L'Áquila EQ, 2009; R. Milanesi, P. Morandi, G. Magenes & B. Binici, Emilia EQ, 2012)

A review of the literature shows that consensus on the effects of the interaction between frames and in-plane masonry walls is still lacking. Some researchers have suggested that infill walls have led to collapse of many buildings (Aschheim, 2000; Sezen et al., 2003, Kyriakides, 2008) and that infill walls may affect the response of frames detrimentally (Murty et al., 2006). Some others have suggested

that masonry infill panels may be beneficial (Akin, 2006; Hassan, 1996; Fardis and Panagiotakos, 1997; Henderson, 2002; Mehrabi et al., 1997).

Fardis (2006) reported that the effects of masonry infill could be positive-in case that the bare structural system has little seismic resistance and negative-if the contribution of masonry infill to lateral strength and/or stiffness is large relative to that of the frame itself. In such a case the infill may override the seismic design and render ineffective the efforts of the designer to control the inelastic response by spreading inelastic deformation demands throughout the structure.

The unfavorable effects can be representing throughout: (1) loss of the integrity of the infill in the ground storey that may produce “soft storey” and trigger global collapse, (Fig. 3.2); (2) brittle failure of frame member, notably columns, (Fig. 3.3); (3) concentration of inelastic demands in the part of the building which have more sparse infill etc.

Figure 3. 2 Negative effect of infill on seismic performance of structure – “soft storey” mechanism (Photos: L.D. Decanini & L. Liberatore, L’Áquila EQ, 2009)

Figure 3. 3 Negative effect of infill on seismic performance of structure (Photos: L.D. Decanini & L. Liberatore, L’Áquila EQ, 2009)

Hermans et al. (2011) reported that the differences in stiffness and ductility between the structural model (without infill) and the built structure can be very large. As masonry infill walls may significantly affect the way in which the building responds to the seismic event it should not be surprising that some buildings collapse although the magnitude of the earthquake is not very high. In this case the seismic loads that are used to analyze the seismic response of the structure may vary significantly from what the building will be subjected to.

Dolsek and Fajfar (2008) captured the essence of the problem stating: “The infill walls can have a beneficial effect on the structural response, provided that they are placed regularly throughout the structure, and that they do not cause shear failures of columns.”

The similar conclusion was given by Varum et al. (2017) after Ghorka 2015 Nepal earthquake. From the reconnaissance trip they observed that material properties of the infills and their construction process technique contributed to increase significantly the lateral stiffness of the buildings. For the cases of regular distributions such in terms of height or plant, their contribute was positive and no significant damages were observed, however the common practice of use the ground-floor of the buildings for commercial purposes originated vertical stiffness irregularities that was particularly catastrophic by causing several soft-storey mechanisms which lead to the collapse of a significant number of buildings around Kathmandu.

The recent investigations point to the engineering design of masonry infills for post-earthquake structural damage control where horizontal sliding joints were designed as a weak points where the deformations are concentrated (Preti at el., 2015).

Another study, which analyzes the response assessment of nonstructural building elements (S. Taghavi and E. Miranda, 2003), reported that the largest percentage of cost breakdown during an earthquake actions belongs to the nonstructural components of the analyzed buildings (Figure 3.4).

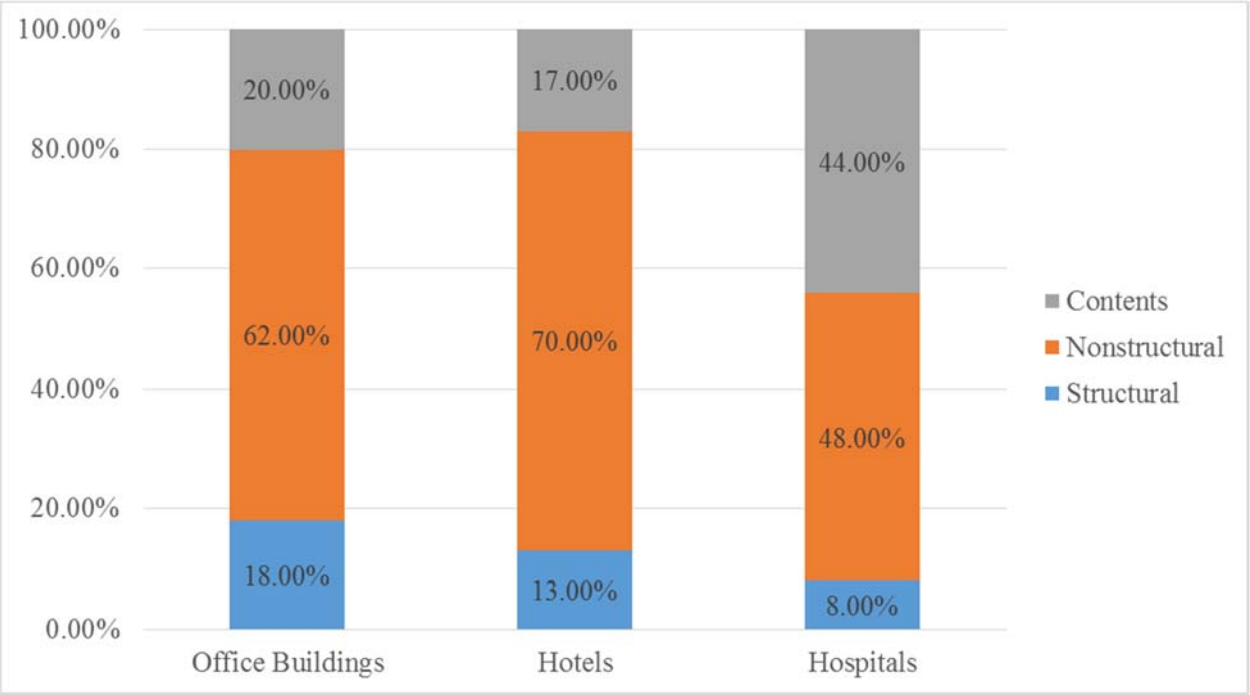

Figure 3. 4 Cost Breakdown of office buildings, hotels and hospitals
(S. Taghavi and E. Miranda, 2003)

The existence of such contradictions in the views of the research community have led to the deconstruction of the frame-masonry system by many regional building codes that contain warnings about the interaction of frames and infill walls but are mostly silent on providing recommendations and bounds on their proper detailing.

In the new buildings design according to Eurocode 8, (EN 1998: Eurocode 8.2004) the masonry infill are threat as a source of structural additional strength and so called “second line defense”. So the reduction of input seismic action as a result of favorable infill effects is not allowed. Considering this, design of RC buildings with masonry infill according to EC8 is on safety side but it is not rational because leads to significant increase of reinforcement in the structural element in comparison with the bare frame. The problem is even more complex in the case of seismic performance assessment of the existing RC buildings with masonry infill. It is already know that the influence of the infill wall is most significant when the structural system itself does not possess adequate seismic resistance, which is often case in large number of substandard RC buildings in south Europe and Mediterranean constructed before implementation of seismic codes, as well as in the case of newly designed buildings without respecting capacity design approach. In such buildings the explicitly consideration of infill wall in analytical model and their verification are necessary.

In RC frames infilled with masonry (framed-masonry) the infill walls stiffen the frame and reduce the first-mode period leading to a reduction in drift response to strong ground motion. At the same time, the addition of the masonry wall to the frame tends to increase the base-shear response and reduce the drift capacity of the structure. The increase of lateral force and reduction of drift capacity leads to serious vulnerabilities unless proper proportioning is exercised. Solution of the problem requires understanding the behavior of masonry and concrete subjected to dynamic and random loading reversals, a challenge that demands testing under reasonably realistic conditions for confident analysis of the problem and its generalization.

3.2. Current codes of practise

According to the inherent complexity and difficulties in modelling infilled frame structures, there is still no uniform design approach or guideline in current codes of practice world-wide. Some guidelines for the evaluation of tight-fit infilled frames have been provided in different countries, but they are well recognized to be far from satisfactory in terms of completeness and reliability. Kaushik (2006) offered a comprehensive summary of the development of codes.

Table 3. 1 Summary of contents of national codes on masonry infilled RC frames

			Min. design force (%)		Irregularity				Infill			
Country/Code	D[1]	T_a[2]	Frame	Infill	Plan	Elev.	K[3]	Drift	σ_i[4]	K_i[4]	O[4]	Out-of-Plane
Albania (1989)	Y	Y	×	×	×	×	1.2–1.5	×	×	×	×	×
Algeria (1988)	Y	Y	25	×	×	×	1.42	×	×	×	×	×
Bulgaria (1987)	Y	×	×	×	×	Y	1.5–3.0[5]	×	×	×	×	×
China (GBJ-11-89 1989)	Y	×	×	×	×	×	×	Y	×	×	×	×
Columbia (NSR-98 1998)	Y	Y	25	100	×	×	×	Y	×	×	×	×
Costa Rica (1986)	Y	Y	×	×	Y	Y	×	Y	×	×	×	×
Egypt (1988)	Y	Y	25	100	×	×	2.0	×	×	×	×	×
Ethiopia (ESCP-1 1983)	Y	Y	25	100	×	×	1.25	×	×	×	×	×
Eurocode 8 (2003)	Y	Y	50–65	×	Y	Y	1.2	Y	×	×	Y	Y
France (AFPS-90 1990)	Y	Y	×	×	×	×	×	×	×	×	×	×
USA (IBC 2003)	×	×	×	×	×	×	×	×	×	×	×	×
India (IS-1893 2002)	Y	Y	×	×	×	Y	×	×	×	×	×	×
Israel (SI-413 1995)	Y	Y	25	×	Y	Y	1.15	×	Y	×	×	×
Nepal (NBC-105, 201 1995)	Y	Y	25	×	Y	Y	2.0	Y	Y	×	Y	Y
Philippines (NSCP 1992)	Y	Y	×	×	×	×	1.5	×	×	×	×	×
Venezuela (1988)	Y	Y	25	×	×	×	×	×	×	×	×	×
FEMA-306[6]	Y	×	×	×	×	×	×	Y	Y	Y	Y	Y

[1] Dynamic analysis is required for *irregular* buildings, tall buildings, important buildings, and buildings located in high seismic regions. The specific requirements vary among different codes.
[2] T_a is the fundamental natural period of vibration for MI-RC frames.
[3] K is the ratio of seismic design forces for MI-RC frames to that for the RC frames without MI due to the difference in response reduction factor.

The key points of different codes of practice considering masonry infill wall are summarized in the following parts.

3.2.1. Eurocode 8

- Empirical formulae for natural period

The natural vibration period of a building system depends on mass and lateral stiffness. Non-isolated masonry infill walls increase both the mass and stiffness and consequently decrease the natural period of the frame system compared with base frames. Although all national codes explicitly specify empirical formulae for the fundamental natural period calculations of bare frame, only a few specify the formulae for masonry infilled RC frames. Eurocode 8 (2003) recommends the following equations for buildings up to a height of 40 m:

$$\boldsymbol{T_a = C_t h^{0.75}}$$

where:

$$\boldsymbol{C_t = \frac{0.075}{\sqrt{A_c}}\ and\ A_c = \sum A_i \left(0.2 + \frac{l_{wi}}{h}\right)^2 ; \frac{l_{wi}}{h} \leq 0.9}$$

It should be noted C_t is the correction factor for masonry infill, A_c is the combined effective area of masonry in the first storey, A_i is the effective cross-sectional area of wall i in the first storey, and l_{wi} is the length of wall i in the first storey in the considered direction.

- Lateral load sharing between infill and frame

For tight-fit infilled frames, the infill panel attracts most of the lateral force under earthquake excitations. However, infill panels usually fail prematurely due to their brittle nature. In such cases, RC frames must have sufficient strength to avoid collapse of the structure. Eurocode 8 (2004) requires RC frames to resist full vertical loads and at least 50-65% of horizontal loads on buildings.

- Vertical and in-plane irregularities

The consequences of irregularities in plane and elevation produced by the masonry infills are highlighted in Eurocode 8 (EN 1998-1 2004) (Clause 4.3.6.2). In plane irregularity conditions, strongly irregular, unsymmetrical or non-uniform arrangements of infills should be avoided. In the very special case with severe irregularities, the spatial models should be used in the analysis, and infills should be included in the model (Clause 4.3.6.3.1). In the irregularities in elevation condition (e.g. drastic reduction of infills in one or more storeys compared to the others), the calculated seismic action effects of the vertical element in the respective storeys should be amplified by a magnification factor η, and is defined as follows (Clause 4.3.6.3.2):

$$\boldsymbol{\eta_a = 1 + \frac{\Delta V_{RW}}{\sum V_{Ed}} \leq q}$$

where:

ΣV_{RW} is the total reduction of the resistance of masonry walls in the storey concerned, compared to the more infilled storey above; and

ΣV_{Ed} is the sum of the seismic shear forces acting on all vertical primary seismic members of the storey concerned.

- Stiffness of masonry infill

Eurocode 8 recommends modelling the masonry infill as equivalent diagonal struts.

- Measures to avoid infill failure

Appropriate measures should be taken to avoid brittle failure and premature disintegration of the infill walls (in particular of masonry panels with openings or of friable materials), as well as the partial or total out-of-plane collapse of slender masonry panels.

1. Particular attention should be paid to masonry panels with a slenderness ratio (ratio of the smaller of length or height to thickness) of greater than 15.

2. In accordance with 1, to improve both in-plane and out-of-plane integrity and behaviour, include light wire meshes well anchored on one face of the wall, wall ties fixed to the columns and cast into the bedding planes of the masonry, and concrete posts and belts across the panels and through the full thickness of the wall.

3. If there are large openings or perforations in any of the infill panels, their edges should be trimmed with belts and posts.

3.2.2. FEMA-273, FEMA-306, 307

The National Earthquake Hazards Reduction Program (NEHRP) Guidelines for the seismic rehabilitation of buildings (FEMA-273, 1997) is a comprehensive document for use in designing and analysis of seismic rehabilitation projects. FEMA-273 includes design criteria, analysis methods and material specific evaluation procedures. Section 7.5 addresses masonry infill systems and specifies that masonry infill panels shall be represented as equivalent diagonal struts. The struts may be placed concentrically across the diagonals, or eccentrically to directly evaluate the infill effects on the columns, as shown in Figure 3.5.

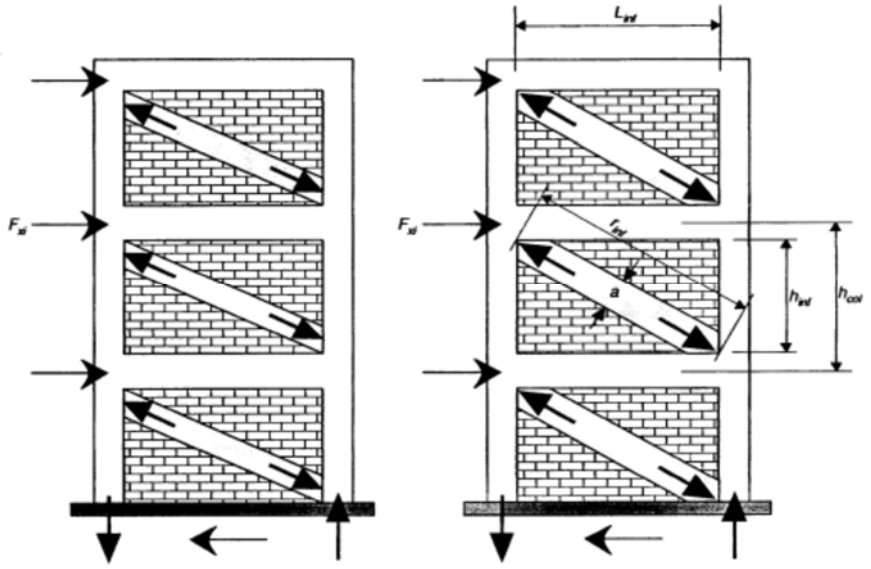

Figure 3. 5 Compression Strut Analogy-Eccentric and Concentric Struts (FEMA-273)

The equivalent diagonal compression strut of width is recommended with the following equation:

$$\boldsymbol{a = 0.175(\lambda_1 h_{col})^{-0.4} r_{inf}}$$

$$\boldsymbol{\lambda_1 = \left[\frac{E_{me} t_{inf} sin2\theta}{4 E_{fe} I_{col} h_{inf}}\right]^{\frac{1}{4}}}$$

where E_{me} and E_{fe} are the expected modulus of elasticity of masonry (secant modulus of elasticity between 5% and 33% of masonry prism strength) and frame material, respectively. In the absence of tests, the recommended value of E_{me} is specified as 550 times the prism strength of masonry (f_{me}'). t_{inf} is the actual thickness of masonry infill in contact with the frame and, θ is the inclination of diagonal struts with the horizontal. In 1999, FEMA publications on the "Evaluation of Earthquake damaged concrete and masonry wall buildings" (FEMA-306 1999; FEMA-307 1999) were developed to provide practical criteria and guidance. The modelling infill panel has equivalent struts in accordance with FEMA-273. Deformation capacity guidelines are given in the form of inter-storey drift ratios. These vary from 1.5% for brick masonry to 2.5% for ungrouted concrete block masonry. As diagonal cracking is initiated at drifts of 0.25% and essentially complete by about 0.5%, this represents a high level of ductility in the panel system.

3.2.3. American Standard ACI 530.1-11 Building Code Requirements and Specifications for Masonry Structures and Related Commentaries.

The Masonry Standards Joint Committee (MSJC) has updated the code into the 2011 version by adding a new chapter 'Appendix B- Design of masonry infill'. In Appendix B, the masonry infills are simply divided into two categories, nominated as 'Non-participating infills' and 'Participating infills' according to the width of the in-plane isolation joints. The value of the in-plane isolation joints is specified as 9.5mm. In addition, it should be emphasized that the in-plane isolation joints shall be designed not only at the sides, but also the top of bounding frame. The connectors shall be provided with a maximum spacing of 1.22 m along the supported perimeter of the infills.

3.2.4. Canadian Standard (CSA S304.1-2004)

CSA S304.1 design provisions for masonry infill walls, introduced for the first time in the 2004 edition of the code, are summarized below:

General design requirements:

- Masonry infill walls are treated as shear walls and should be designed to resist all in-plane and out-of-plane loads (Cl.7.13.1).
- Masonry infill walls should be designed to resist any vertical loads transferred to them by the frame (Cl.7.13.2.4).
- The increased stiffness of lateral load-resisting elements that consist of masonry infill shear walls working with the surrounding frame, should be taken into account when distributing the applied loads to these elements (Cl.7.13.2.5).
- When a diagonal strut is used to model the infill shear wall according to Cl.7.13.3, an infill frame can be designed using a truss model (see the note to Cl.7.13.2.5).

According to Cl.7.13.3, when there are no openings or gaps between the masonry infill and the surrounding frame, and the infill is not tied or bonded to the frame, the infill should be modelled as a diagonal strut:

$$\boldsymbol{w = \sqrt{\alpha_h^2 + \alpha_L^2}}$$

$$\boldsymbol{\alpha_h = \frac{\pi}{2}\sqrt[4]{\frac{4E_f I_c h}{E_m t_e sin2\theta}}}$$

$$\boldsymbol{\alpha_L = \pi\sqrt[4]{\frac{4E_f I_b h}{E_m t_e sin2\theta}}}$$

α_h vertical contact length between the frame and the diagonal strut

α_L horizontal contact length between the frame and the diagonal strut

3.2.5. Chinese Code for Seismic Design (GB50011-2010)

In the National Code for Seismic Design of Buildings (GB50011-2010), the masonry infill walls are treated as non-structural elements; however, the natural period of the frame system is recommended to be reduced by a factor ranging from 0.6-0.7 taking the stiffening effect of masonry panels into account.

3.2.6. New Zealand NZS 3101 1995

A very few codes specifically recommend isolating the MI from the RC frames such that the stiffness of MI does not play any role in the overall stiffness of the frame such as NZS-3101 1995 in New Zealand and SNIP-II-7-81 1996 in Russia (Kaushik et al., 2006). As a result, MI walls are not considered in the analysis and design procedure. The isolation helps to prevent the problems associated with the brittle behavior and asymmetric placement of MI.

3.2.7. Rulebook on Technical Norms for Construction of High-rises in Seismically Prone Areas – PIOVS'81 (Official Gazette of RM 31/81)

In the official code in Macedonia, the masonry infill influence is also not taken into account in the analysis and is not mention in any article. The seismic performance of the structure is only controlled through the displacements which is the following:

- - the maximum relative floor displacement from linear analysis of the structure should be $\Delta y \leq hi/350$,
- - the maximum relative floor displacement for design earthquake in nonlinear dynamic analysis should be $\Delta u \leq hi/150$,

Where h_i is the height of the i- floor in cm.

3.3. Experimental investigations

In providing the earthquake protection of the structures, the experts are permanently challenged by the fast development and the improved performance of new materials and techniques. However, their implementation depends on the extent it has been investigated and verified. The delicate problem of proving the effectiveness of the selected structural system/material/technique/device can be successfully overcome by using the methodology of design assisted by testing, which as methodology, has been recently codified in all Eurocodes.

Understanding the behavior of masonry and concrete structures, specially RC buildings with masonry infill subjected to dynamic and random loading reversals, is a challenge that demands testing under reasonably realistic conditions for confident analysis of the problem and its generalization. Many of these types of buildings are built in regions that have been strongly affected by medium and high magnitude earthquakes in the past. For each significant event, specialists have gathered relevant information with respect to their protection, which calls for verifications based on experimental testing. To obtain the experimental values of the main parameters (physical-mechanical and chemical characteristics of the built-in material, strength and deformability characteristics, ductility capacity and energy dissipation capacity of the structural elements and structures as whole), different testing techniques are applied in practice.

The experimental investigation of models on a seismic shake table is the most corresponding way of investigation from the aspect of dynamic structural performance during real earthquakes. Applying an appropriate modeling technique and according to the similarity laws, the models can be designed to different scales and tested under various seismic inputs. Founded on experimental data obtained from site testing of buildings, as well as the results of the seismic hazard analysis, the laboratory testing of models gives very reliable data on the seismic performance and stability, pointing out the weak points of the structures. These data are of a great importance for further analysis and verification of seismic performance of building structures.

Most of the aforementioned experimental works, both in-plane and out-of-plane investigations, were carried out under monotonic or cyclic lateral loading. These studies provide evaluations of: (1) the stiffness and strength of the infilled frames, (2) the failure modes for both the infill panel and frame members, and (3) the strength and stiffness degradation upon loading reversal. It is necessary to notice that these investigations were performed using static, quasistatic or pseudo-dynamic loading methods which may not reveal the dynamic performance of an infilled frame structure under real earthquake excitation. Limited data exist relating to the dynamic characteristics of masonry infill structures since relatively few shake table tests are performed in the literature.

Fardis et al. (1999) report shake-table tests performed on a single-bay two-storey RC frames with eccentric masonry infill walls subjected to bidirectional ground accelerations. The study focused on the effects of displacement demand on corner columns because of eccentricity. They also reported that infill panels survived out-of-plane peak accelerations up to 0.6 g at the base.

Zarnic (2001) presents shake-table test results performed on 1/4 scale one- and two storey RC frames with strong-block weak mortar masonry infill walls subjected to unidirectional sinusoidal motions, as shown in Figure 3.6. He found the model response compares well with the global performance of real structures.

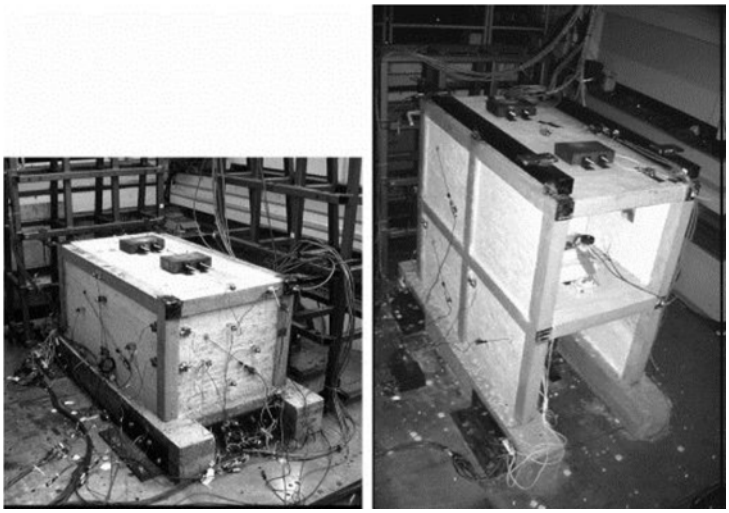

Figure 3. 6 Overall view of instrumented specimens, (Zarnic, 2001)

Their model responses also showed that buildings designed according to Eurocodes are able to sustain relatively high dynamic excitation due to the significant level of structural over strength. Lee and Woo (2001) present shake table test results of a 1/5 scale, two-bay three-storey masonry-infilled RC frame (Figure 3.7) designed according to the Korean practice and similitude law. It can be recognized that the masonry infills contribute to the large increase in the stiffness and strength of the global structure whereas they also accompany the increase of earthquake inertia forces. The failure mode of the masonry-infilled frame was shear failure due to the bed-joint sliding of the masonry infills while that of the bare frame appeared to be the soft-storey plastic mechanism at the first storey.

Heshemi and Mosalam (2006) report a shake-table experiment conducted on a one storey middle bay substructure taken from one hypothetical 5-storey prototype structure, as shown in Figure 3.8. They found that the infill panel makes the test structure stiffer by a factor of 3.8, shortens the natural period of the test structure by 50%, increases the damping coefficient depending on the level of shaking from about 4.5-12% and increases the dissipated energy in the system. Such changes significantly affect the shear force demand of structures and generally reduce the displacement demand. Quantitatively, the URM infill wall causes about a 30% increase in the demand forces in the test structure.

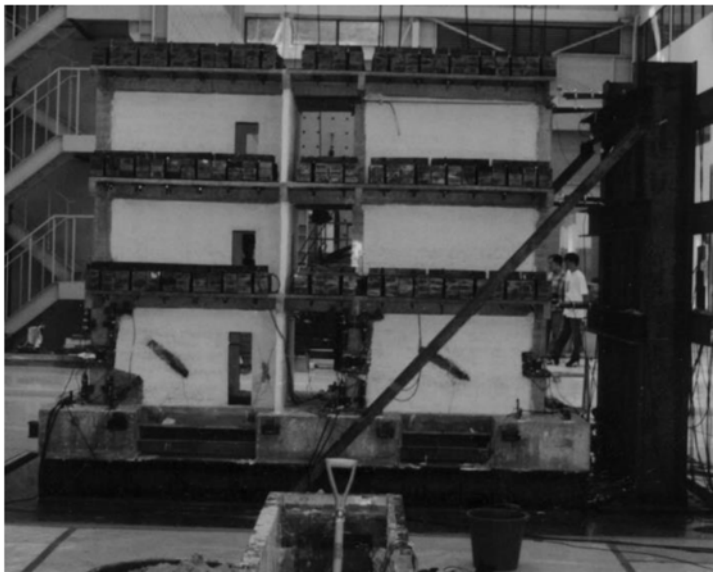

Figure 3. 7 Experimental set-up for shake-table tests, (Lee and Woo, 2001)

Figure 3. 8 Test structure and failure mode of infill panels after shake-table tests (Heshemi and Mosalam, 2006)

Stavridis and Shing (2012) present shake-table results of a 2/3-scale, three-storey, two-bay, reinforced concrete frame infilled with unreinforced masonry walls. The tested specimen is representative of the construction practice in California in the 1920s. As shown in Figure 3.9, the specimen has one bay fully infilled with solid unreinforced brick masonry infill walls and window openings in the other. The results demonstrated that infill RC frames can behave in a safe manner during strong earthquakes provided that sufficient infill walls are present, and openings are much more vulnerable to collapse than solid walls. The tested structure appeared to be more ductile than what is anticipated in ASCE 41, even though the final failure mechanism beyond the peak drift was brittle and undesirable (Stavridis and Shing, 2012).

Figure 3. 9 Pictures of damaged specimen and column failure in the first storey after tests (Stavridis and Shing, 2012)

For out-of-plane investigation, Tu et al. (2010) present shake-table test results of four full-scale single-storey RC frames infilled with unreinforced masonry panels. The four specimens include one bare frame, two frames with confined masonry panels (pre-laid unreinforced masonry (URM) panels surrounded by cast-in-place reinforced concrete (RC) boundary frames) of different thickness and one infilled frame. The test results indicate that confined masonry panels exhibited notable resistance to out-of-plane inertial force via the arching mechanism. Infill panels also showed arching at low motion intensity, but separated from bounding frames at higher intensity and collapsed under the inertial force caused by the self-weight of the infill panel (Tu et al., 2010). The test specimen is demonstrated in Figure 3.10.

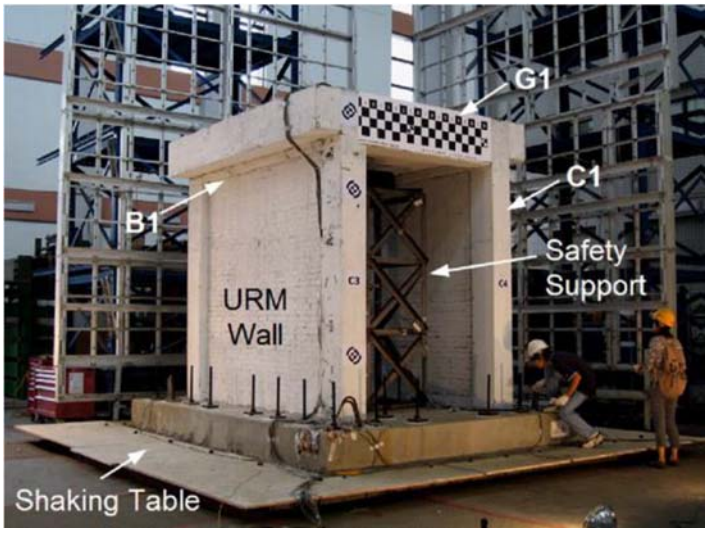

Figure 3. 10 Test setup for out-of-plane vulnerability investigation, (Tu, et al., 2010)

Zhang (2015) proposed and tested an innovative flexible connection detailing method which could effectively mitigate undesirable interaction damage for infilled RC frame structures and minimize the life-safety hazard under potential earthquake excitation. This proposed strategy isolates the infill panel from bounding columns with finite width vertical gaps during the construction phase, and steel wire connections are deployed in mortar layers and anchored to columns. To evaluate the effectiveness and adaptability of the proposed seismic mitigation strategy, extensive shake-table tests and numerical investigations are conducted, based on which, the performance criteria and comprehensive design recommendations were proposed.

Taking into account the similitude requirements, a total of nine one-third scale, single-storey single-bay RC frames with different masonry configurations and flexible connection details were carefully designed and tested on a unilateral shake-table in Honk Kong University of Science and Technology HKUST (Figure 3.11). Three real earthquake records are selected and scaled to ascending intensity levels and used as input signals. A series of thorough investigations including dynamic characteristics, hysteretic behaviour, failure mechanism, out-of-plane vulnerabilities, the effect of connection length, and the effect of different gap filling materials and load transfer mechanisms are rigorously studied. A discrete modelling approach employing a surfaced-based interaction modelling technique to simulate fracture, crack propagation, sliding and separation, and post-fracture behaviour of mortar joints is also developed and verified by finite element software ABAQUS. Dynamic and monotonic push simulations are carried out and compared with the experimental observations. The numerical and experimental results indicated that the proposed seismic damage mitigation concept could considerably reduce undesirable interaction between infill panels and bounding frame, protect the columns from direct shear failure at an early stage, and provide structural redundancy at high levels of excitation. Globally, the structural stability and integrity, displacement ductility, and energy dissipation capacity of infilled RC frame are remarkably improved.

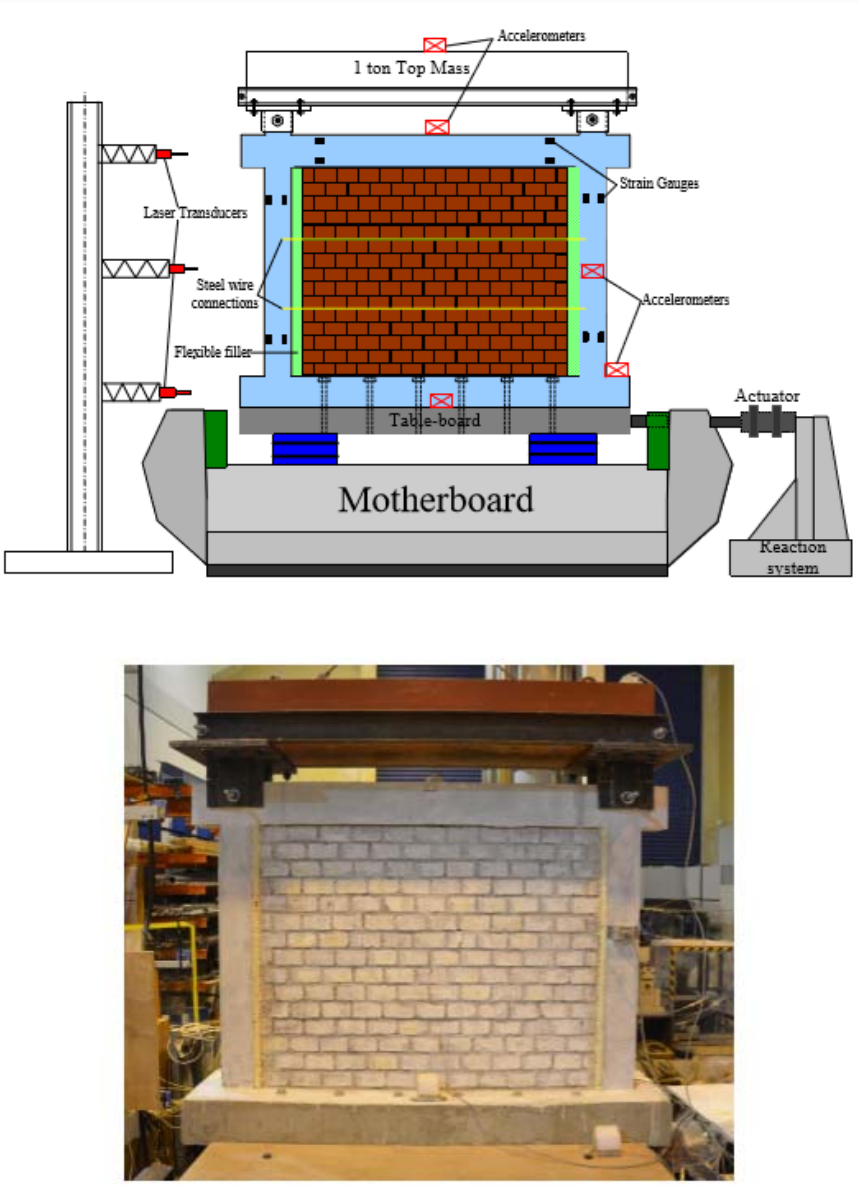

Figure 3. 11 Shaking table tests performed by Zhang (2015)

3.4. Analytical models for masonry infill panels

The analytical modelling of the infilled frame system is a challenging issue since these structures exhibit a highly nonlinear inelastic behaviour due to the interaction between infilled panels and surrounding frames. Since the first attempt to estimate the performance of composite infilled frame structures, it has been concluded from experimental and analytical observations that a diagonal strut with appropriate geometrical and mechanical properties could be a suitable candidate for modelling walls.

3.4.1. Macro analytical models for infilled frames

a. Single diagonal strut model

Polyakov (1960) conducted one of the first analytical studies based on elastic theory, and suggested the possibility of considering an infill panel as one equivalent diagonal strut.

Holmes (1961) followed this idea and suggested replacing the infill wall with an equivalent pin-jointed diagonal strut which has the same material and stiffness as the infill wall. The width of this diagonal strut was defined by:

$$\frac{w}{d} = \frac{1}{3}$$

where d is the diagonal length of a masonry panel, as shown in Figure 3.12.

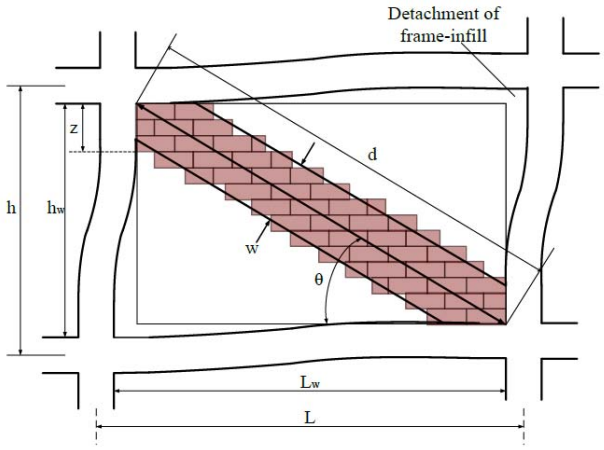

Figure 3. 12 Diagonal strut model for infilled frames

In order to investigate more precisely the width of the diagonal strut, Smith (1962) conducted a series of tests on masonry infilled steel frames and found that the ratio varied from 0.1 to 0.25. This concept was widely accepted as a simple and rational way to describe infill panels and continued to be studied by other researchers. Smith (1966, 1967; Smith and Carter, 1969) used additional experimental data to relate the width of an equivalent strut to the contact length of an infill/frame. The equivalent width λ_h was then defined as a function of the relative panel-to-frame stiffness parameter:

$$\lambda_h = h \sqrt[4]{\frac{E_w t_w sin2\theta}{4EIh_w}}$$

where E_w is the modulus of elasticity of the masonry panel; E_I is the flexible rigidity of the columns; t_w is the thickness of the infill panel and equivalent strut; w_h is the height of the infill panel and h is the

height of the column between center lines in beams; θ is the angle between the diagonal strut and beam, the tangent of which is equal to:

$$\theta = tan^{-1}\left(\frac{h_w}{L_w}\right)$$

The mathematical expression of equivalent width was improved by different researchers to provide preliminary analysis; the developments are summarized in Table 3.2. Lately, there are some additional model proposed but in general they are based on the presented ones.

Table 3. 2 Mathematical expressions of equivalent strut width proposed by different researchers

Year	Researcher	Formulas
1961	Holmes, 1960	$w = \frac{1}{3}d$
1969	Stafford-Smith, 1969	$w = \frac{\pi}{2\lambda} \quad \lambda = [\frac{E_w t_w \sin 2\theta}{4E_c I_c h_w}]^{\frac{1}{4}}$
1972	Mainstone, 1972	$4 < \lambda h < 5$ masonry infills, $\frac{w}{d} = 0.175(\lambda h)^{-0.4}$ Concrete blocks infills, $\frac{w}{d} = 0.115(\lambda h)^{-0.4}$ $\lambda h > 5$ masonry infills, $\frac{w}{d} = 0.16(\lambda h)^{-0.3}$ Concrete blocks infills, $\frac{w}{d} = 0.1(\lambda h)^{-0.3}$
1984	Liauw and Kwan, 1984	$w/d = 0.95\sin 2\theta / (2\sqrt{\lambda_h})$
1987	Decanini and Fantin, 1987	Uncracked panel: $w = \left(\frac{0.748}{\lambda_h} + 0.085\right)d$ if $\lambda_h \le 7.85$ $w = \left(\frac{0.393}{\lambda_h} + 0.130\right)d$ if $\lambda_h > 7.85$ Cracked panel: $w = \left(\frac{0.707}{\lambda_h} + 0.010\right)d$ if $\lambda_h \le 7.85$ $w = \left(\frac{0.470}{\lambda_h} + 0.040\right)d$ if $\lambda_h > 7.85$
1988	Eurocode 8	$w = 0.15d$
1992	Paulay and Priestley, 1992	$w/d = 1/4$
1999	Flanagan and Bennet, 1999	$w = \frac{\pi}{C\lambda\cos\theta}$ *

* C is an empirical constant varying with the in-plane drift displacement

b. Multiple strut models

Thiruvengadam (1985) first proposed replacing the infill panel with a multiple-strut to model the seismic performance of infilled frames. This model consists of a moment-resistant frame with a large number of pin-jointed diagonal and vertical struts. The lateral stiffness of infill and its shear deformation is modelled by a set of pin-ended diagonal struts that run in both directions, while the vertical truss provides vertical stiffness. The main purpose of this model is to evaluate the natural frequency and mode of vibration, and the nonlinear behaviour of the frame and infill was not generally considered. Later in 1986, Syrmakezis and Vratsanou (1986) recommended five parallel struts in each diagonal direction. They concluded that the contact length has a significant influence on the bending moment distribution in the frame members.

Despite increasing the complexity, the multiple-strut model is more rational and can represent the actions of infill panels more accurately.

Aiming to estimate the response of infilled frames under earthquake excitation taking into account of the stiffness and strength degradation in infill panels, Chrysostomou (1991, 2002) proposed six compression only struts model as shown in Figure 3.13. Three parallel struts were used in each diagonal direction and at any point during the analysis of nonlinear response, only three of the six struts were active, and when their compressive force reduced to zero, switching to the opposite direction took place. The location of off-diagonal struts is defined by parameters, which represents a fraction of the length or height of a panel and is associated with the position of the formation of a plastic hinge in a beam or column. The theoretical values of this parameter were also suggested by Liauw and Kwan (1983a, b).

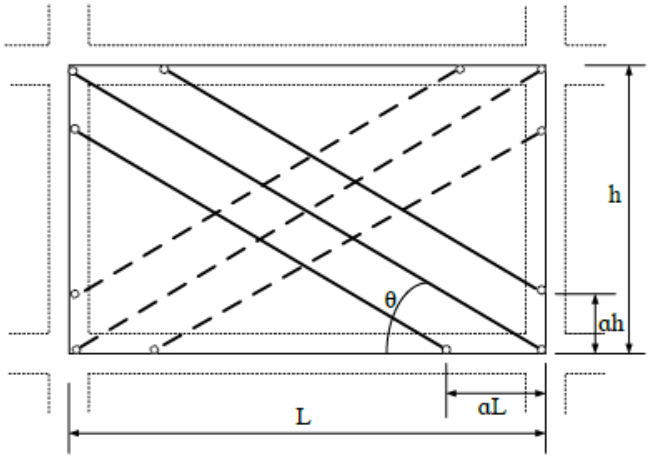

Figure 3. 13 Illustration of six-strut model for infilled RC frame

Crisafulli (2007) investigated the influence of different multi-strut models on the seismic performance of infilled frames, and according to the numerical results obtained from single-, two-, and three-strut

models, the researcher found that the single-strut model underestimates the bending moment of the surrounding frames because the lateral forces are primarily resisted by the truss mechanism of the infill panel. On the other hand, the two-strut model leads to larger values than those corresponding to the finite element model. Three strut-model, as shown in Figure 3.14 (c), can give better approximation although some differences arise at the ends of column elements. Although the single-strut model constitutes a sufficient tool for the prediction of the full response, the triple-strut model is superior in precision, Crisafulli adopted the double-strut model which is accurate enough and less complicated compared to other models.

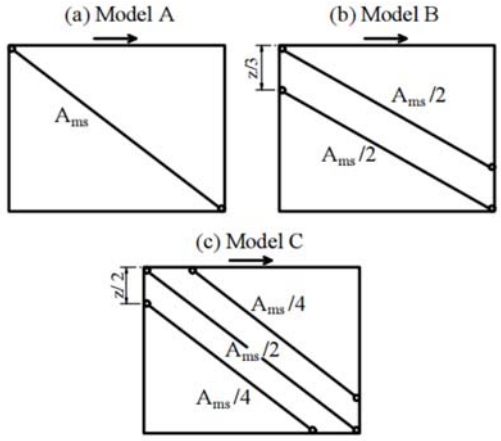

Figure 3. 14 Strut models considered in the preliminary study (Crisafulli, 2007)

EI-Dakhakhni (2003) suggested that in order to produce bending moments in frame members as shown in Figure 3.15, at least two additional off-diagonal struts at the points of maximum field moments are needed. This technique makes use of the orthotropic behaviour of masonry walls. The experimental observation and numerical simulation on steel frames with masonry infills showed that the three-strut model can simplify the nonlinear modelling of infilled frame structures.

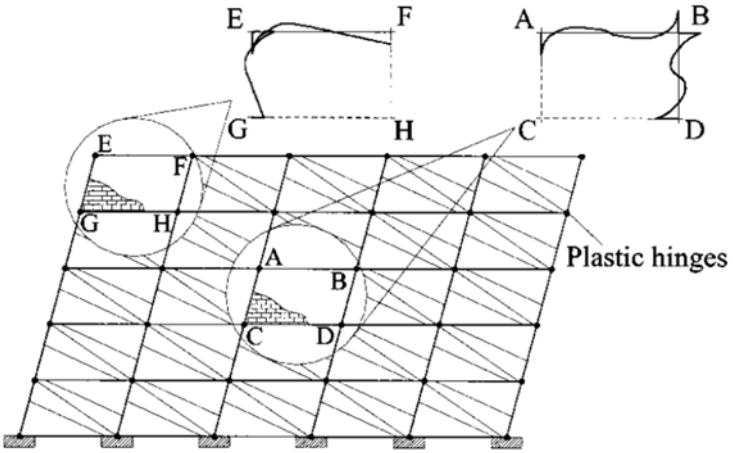

Figure 3. 15 Bending moment diagrams for different bays in a multi-storey infilled frame building (EI-Dakhakhni 2003)

Crisafulli and Carr (2007) proposed a new macro model, in which a four-node panel element is connected to the frame at beam-column joints, and internally, the panel element accounts separately for the compressive and shear behaviour of the masonry panel using two parallel struts and a shear spring in each direction, as shown in Figure 3.16. The advantage of this model is that it allows adequate consideration of lateral stiffness and strength of the masonry panel, particularly when shear failure along mortar joints or diagonal tension failure happens. Furthermore, the model is easy to apply in the analysis of large infilled frame structures and can be implemented in commercial finite element software.

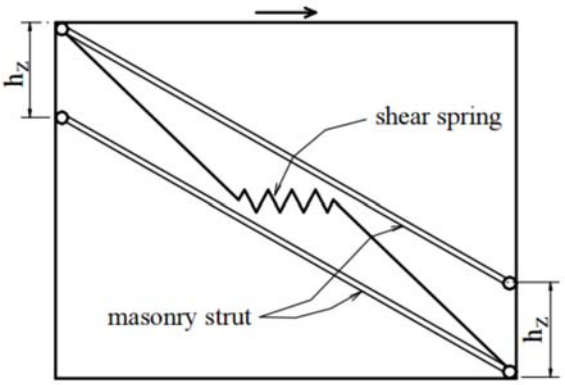

Figure 3. 16 Multi-strut model proposed by Crisafulli and Carr (2007) for masonry-infilled panels (only the struts and the shear spring active in one direction are represented)

c. Out of plane analytical model

Out-of-plane collapse is a kind of typically observed failure mode of infill walls; however, most of the aforementioned research focused on the in-plane seismic performance of masonry infill frames, and the combined loading effect has not been reflected in most of the analytical models in the literature. It has been indicated that under the in-plane damage of infills, the out-of-plane capacity of unreinforced masonry (URM) brick infill walls can be reduced by as much as a factor of 2.0, and sometimes weak out-of-plane resistance of the infill walls can be prone to damage during a strong earthquake motion (Angel, 1994).

The out-of-plane strength of unreinforced or partially reinforced infilled walls can be enhanced by a relatively weak arching action; such extra out-of-plane capacity depends on the masonry's compressive strength rather than tensile strength (McDowell et al., 1956; Klingner et al., 1996; Shing and Mehrabi, 2002). Some researchers indicate that the out-of-plane strength of a masonry infill is mainly dependent on its slenderness (Flanagan, 1999). In 1994, Angel and Abrams proposed an analytical model to determine the out-of-plane resistance of an infill wall based on the arching action of an infill strip spanning two rigid supports, as shown in Figure 3.17. The infill wall is idealized as a

strip with unit width that spans two fully restrained supports against translation and rotation. Under the lateral load, the largest compressive strain in the masonry is introduced at the support and the centre of the panel by the rotation of the segments. The out-of-plane strength deterioration may reach as much as 50% for infill panels with a high slenderness ratio when in-plane cracking has already occurred.

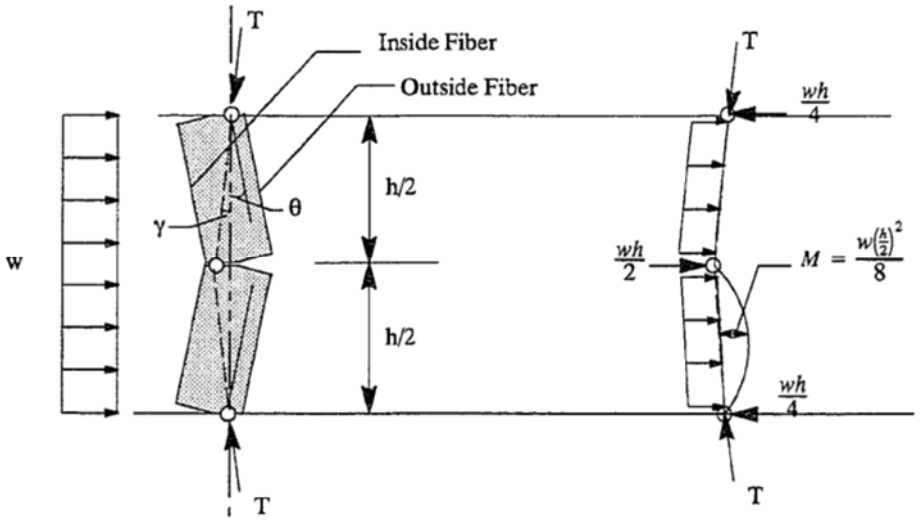

Figure 3. 17 Idealized loading and behaviour of a unit strip and infill panel (Angel, 1994)

3.4.2. Micro modelling for masonry infill panels

The large number of factors influencing the properties of infill panels, such as joint width and running bond, dimension and anisotropy of the bricks, material properties of both bricks and mortar, and workmanship quality, make the simulation of masonry panels extremely difficult. Depending on the orientation of mortar joints relative to the stress direction and the normal stress level, failure can occur in the mortar joints only (shear sliding failure) or simultaneously in the joints and brick blocks. Cracking of mortar joints results in strength and stiffness degradation of infill panels which significantly influences the contacting force transmitted at infill-frame interfaces. According to Lourenco and Rots (1997), Lourenco (1996), Mehrabi and Shing (1997), Asteris (2013), Yuen (2012) and Kuang & Yuen (2013), three different levels of idealization may be considered for analytical models of masonry panels, as shown in Figure 3.18.

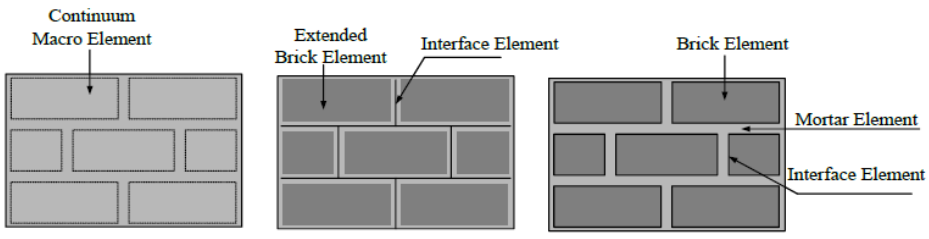

Figure 3. 18 Different masonry modelling strategies recognized by Lourenco (1996)

a. Homogenization modelling of masonry infills

The periodic arrangement of masonry units allows one to exact a repetitive unit cell or representative volume element (RVE) from the composite masonry panel and formulate a homogenization problem to determine the equivalent and macroscopic mechanical behavior of the homogenized continuum (Yuen, 2012). In this approach, the masonry units and mortar are modelled together as a continuum either isotropically or anisotropically. While saving considerable computational intensiveness, and simplifying the model assembly and meshing, the continuum modelling strategy still has drawbacks in that it is not suitable for detailed stress analysis of small panels and cannot capture all the failure mechanisms.

b. Modelling of infills as two phase material

The second method uses the lumped-interface strategy in which two sets of element are developed. One set of elements is expanded units represented by a continuum element, while in the other set, the properties of mortar and unit/mortar interface are lumped into a zero length joint element. When cohesive interactions which can simulate the macroscopic traction separation and fracture behaviour of mortar joints are adopted for interface elements, the crack propagation together with pre- and post-fracture behaviour of mortar joints can be accurately simulated. This approach leads to a reduction in computational intensiveness and yields the most suitable method applicable to a wide range of structures.

c. Modelling of infills as a three phase material

The most detailed model approach considers all the infill components including bricks, mortar joints, and the interface between them separately (Lofti & Shing, 1994; Mehrabi et al., 1997; Lourenco & Rots, 1997; Mosalam et al., 1997c; Yuen and Kuang, 2011a, 2011b). In this approach, the units and mortar are represented by continuum elements whereas the unit-mortar interface is represented by dis-continuum elements. While leading to the most accurate results and better simulating the macroscopic traction-separation of mortar joints, this discrete approach is computationally intensive and may limit its applications to small specimens.

3.5. Previous studies on RC structures with masonry infill performed at IZIIS

A large number of experimental and analytical investigations related to this problem have been carried out at the Institute of Earthquake Engineering and Engineering Seismology – Skopje. To analyze the spreading of damage to nonstructural elements (the infill) and their nonlinear response under the effect of simulated vertical and reverse cyclic horizontal loads, investigations entitled “Behaviour of

Infill in Iron Concrete Frame Systems Under Seismic Effect" were performed under the leadership of Prof. Dr. Gavrilovic, (1992) (Figure 3.19).

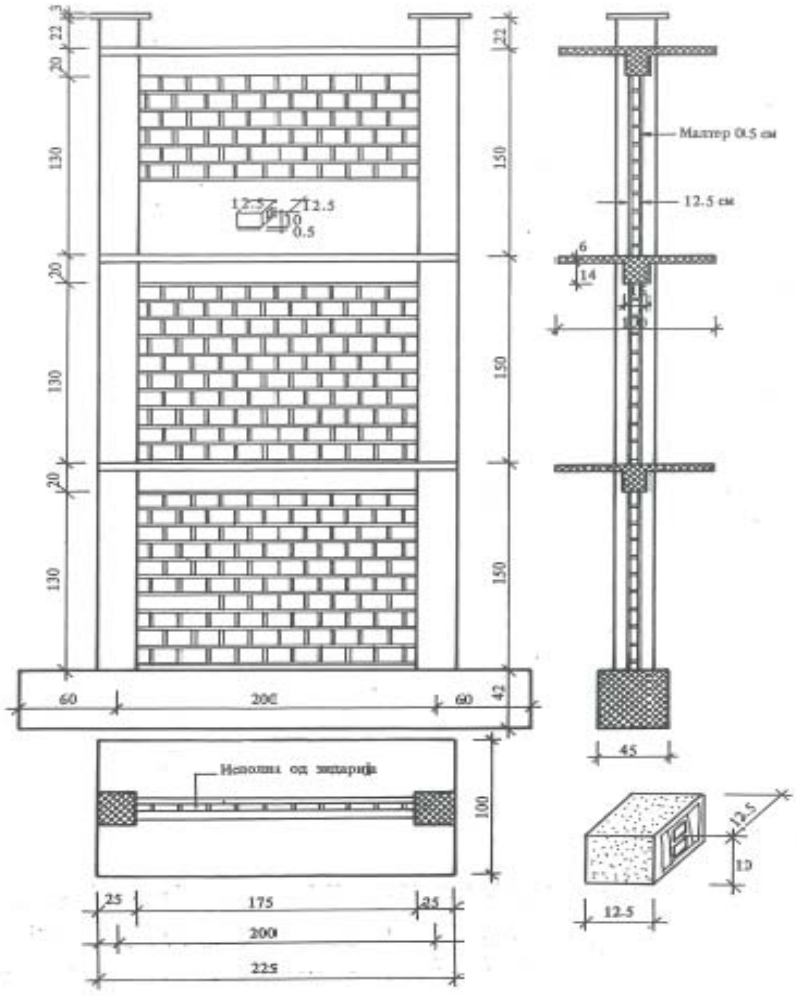

Figure 3. 19 Model of a single bay three-storey reinforced concrete frame with masonry infill

Five experimental models of three storey frame structures, one without an infill and four with different infill, were constructed to the scale of 1 : 2, namely 2- masonry infill (hollow ceramic blocks), 3-infill of siporex plates, 4-gypsum plate infill, 5-ertozol Infill.

All models were tested to details, particularly their nonlinear behavior, obtaining thus the bearing and deformability capacities expressed through the hysteretic relationships (P-Δ diagrams) and stiffness deterioration until the occurrence of the failure mechanism (Figure 3.20).

The quasi-static tests were carried out at the Dynamic Testing Laboratory of IZIIS by simulation of simultaneous axial and cyclic transverse loads by gradual increase of intensity and control of displacements at the top (the third storey) and summary of the test results are given in table

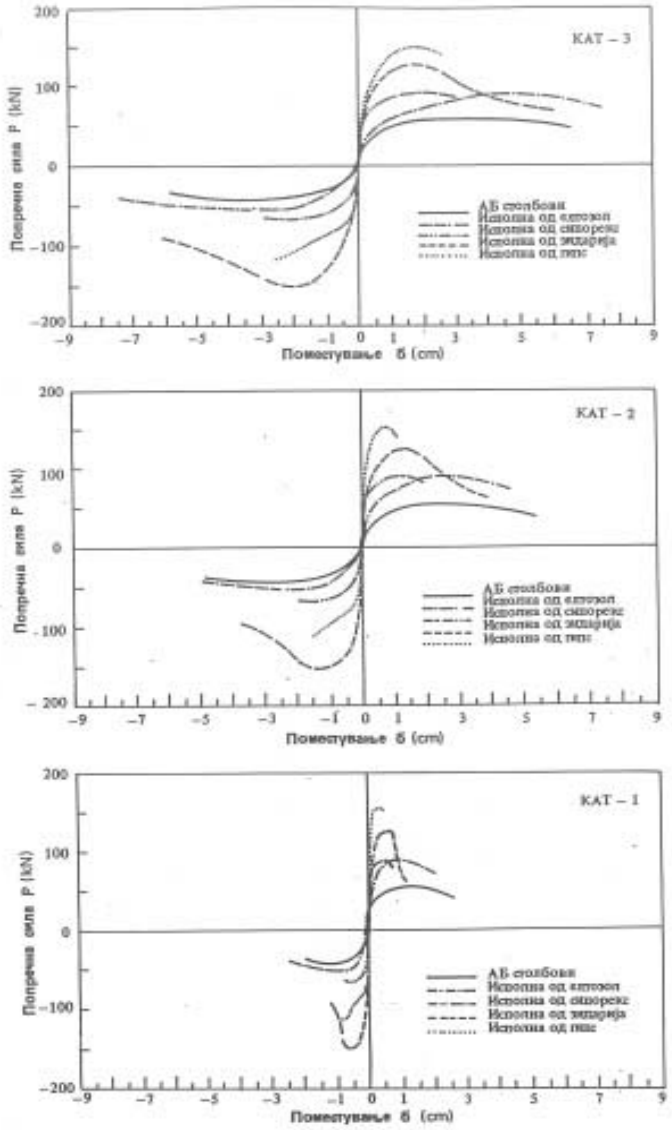

Figure 3. 20 Comparative presentation of cumulative envelope curves (P-Δ diagrams) obtained from experimental tests on the frame model with and without an infill

Table 3. 3 Results from the tests from Gavrilovic et al. (1992)

Exp.	Structural system	Fc [kN]	Dc [cm]	Fy [kN]	Dy [cm]	Fu [kN]	Du [cm]
1	Bare frame model	14	0.029	42	0.43	48.5	1.73
2	Frame model with masonry infill (hollow ceramic blocks)	/	/	80	0.192	92.7	0.67
3	Frame model with infill of siporex plates	/	/	35	0.11	41.3	0.34
4	Frame model with infill of gypsum plates	/	/	69.7	0.139	82.8	0.47
5	Frame model with eltozol infill	/	/	18	0.5	23.3	1.83

The first experiment showed nonlinear behavior with slight deterioration of stiffness and ductility of D=4. The presented results from the second experiment showed nonlinear behavior of masonry characterized by more intensive deterioration of stiffness-deformability characteristics once the infill reaches the ultimate point. In this case, considerable increase of initial stiffness and strength of the model is observed.

-The third experimental test was performed on the same frame model with infill of siporex plates. The initial stiffness and strength were higher compared to the pure frame model, but as in the previous case, there was an abrupt deterioration after the reaching of the ultimate point.

The fourth experimental test was performed with infill of gypsum plates. Also, in this case, the initial stiffness and the achieved strength were considerably higher than those in the case of the pure frame model, but with great and fast deterioration after the reaching of the ultimate point.

-The fifth experimental test was carried out with eltozole infill. In its nonlinear behavior, eltozole as an infill within a frame structure mainly follows the strength and deformability characteristics of the pure frame model.

So, based on these experimental investigations, an analytical “infill” model for simulation of the nonlinear response of the infill was developed. The parameters that define this model directly control the spreading of the damage in the tested model. Figure 3.21 and Figure 3.22 present the F-D relationship and loading and unloading laws for the INFILL model.

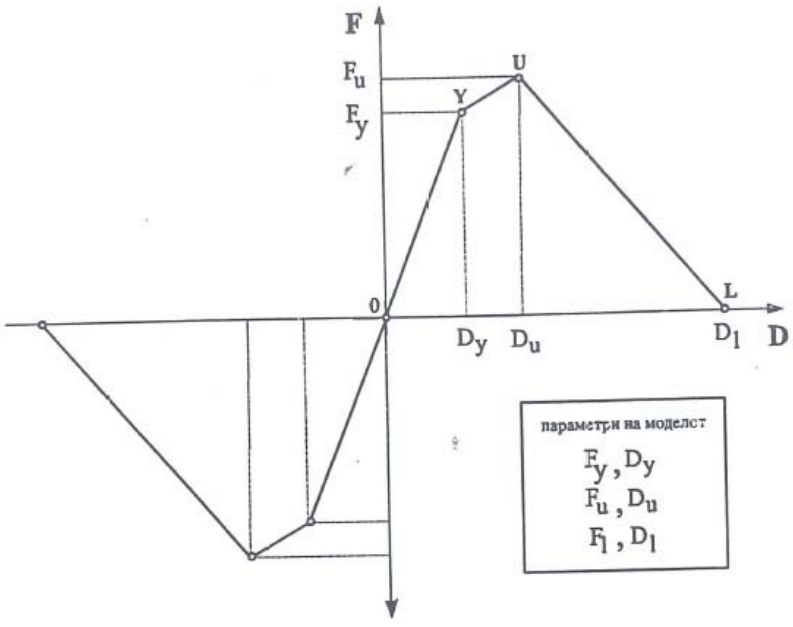

Figure 3. 21 Principal envelope of F-D relationship for the axial elements of the INFILL model

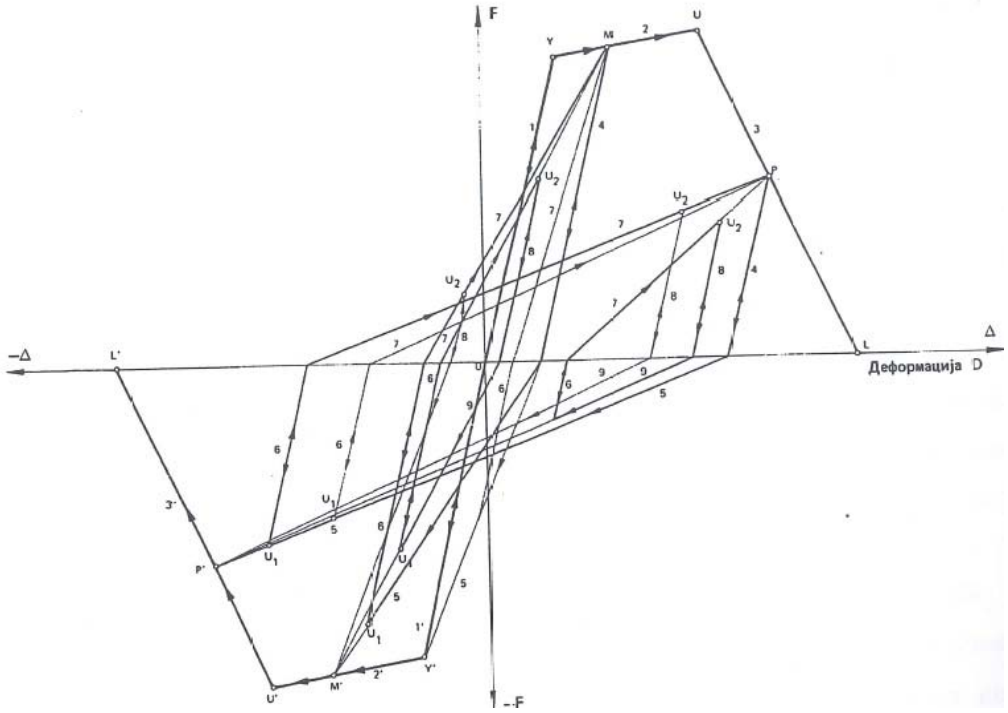

Figure 3. 22 Loading and unloading laws for the "infill" model in simulation of force-deformation relationship

Within the doctoral dissertation entitled "Definition of Empirical and Theoretical Models for Definition of Vulnerability level of High Rises" elaborated by Nikola K. Nochevski in 1993, the afore mentioned experimental investigations and the obtained analytical models for simulation of nonlinear behavior of RC structural (Takeda –model) and nonstructural elements (Infill-model) were used. These were further used for verification of the proposed vulnerability models in which the infill elements had an important role. In the initial chapters, damages to a large number of structures due to occurred earthquakes are analyzed, with a special emphasis on the Montenegro earthquake of 15.04.1979. Presented are empirical vulnerability functions representing relationship between the inflicted damages and the earthquake intensity. In addition, the damages incurred by the Skopje earthquake of 26.07.1963 are considered and analyzed and classification is made depending on the structural system, the extent of damage, the position, orientation and alike.

Based on bearing and deformability capacity of elements, damage criteria for structural and nonstructural elements were defined for estimation of the so called "degrees of damage" ranked from DD=1 (undamaged elements) to DD=5 (completely collapsed elements). Damage functions were also analyzed from the aspect of cost of repair and their economic justification. Applied in the analysis for definition of theoretical vulnerability functions was a complex integral procedure based on a certain number of parametric nonlinear structural response analysis, separately for each building and each structural and nonstructural element. A large number of nonlinear dynamic analyses on 11 structures

were performed in a total of 18 orthogonal directions. In the presented conclusions on the experimentally tested five models, it is clearly pointed out that the effect of the nonstructural elements can be very important and must be always taken into account in the formulation of mathematical models for nonlinear analyses.

In the doctoral dissertation entitled “Development and Application of Nonlinear Micromodels for Evaluation of Seismic Behaviour of Reinforced Concrete Frame Structures with Infill of Unreinforced and Reinforced Masonry”, elaborated by Lidija Krstevska, (2002), a concept was developed for a nonlinear micro-analysis of reinforced concrete frame structures with infill of plain and reinforced masonry and it was verified through results from laboratory tests. Within this dissertation, ample analytical and experimental investigations were performed by following contemporary scientific-research trends in Europe and worldwide.

According to this concept of micro-modeling, there were developed corresponding models of nonlinear discrete components by which were presented the specific nonlinear characteristics of different elements and materials in the system. There were developed four types of models for modeling beam elements, infill, mortar and behavior of reinforcement, respectively. These were implemented in the proposed concept. Figure 3.23 shows the model for infill modeling.

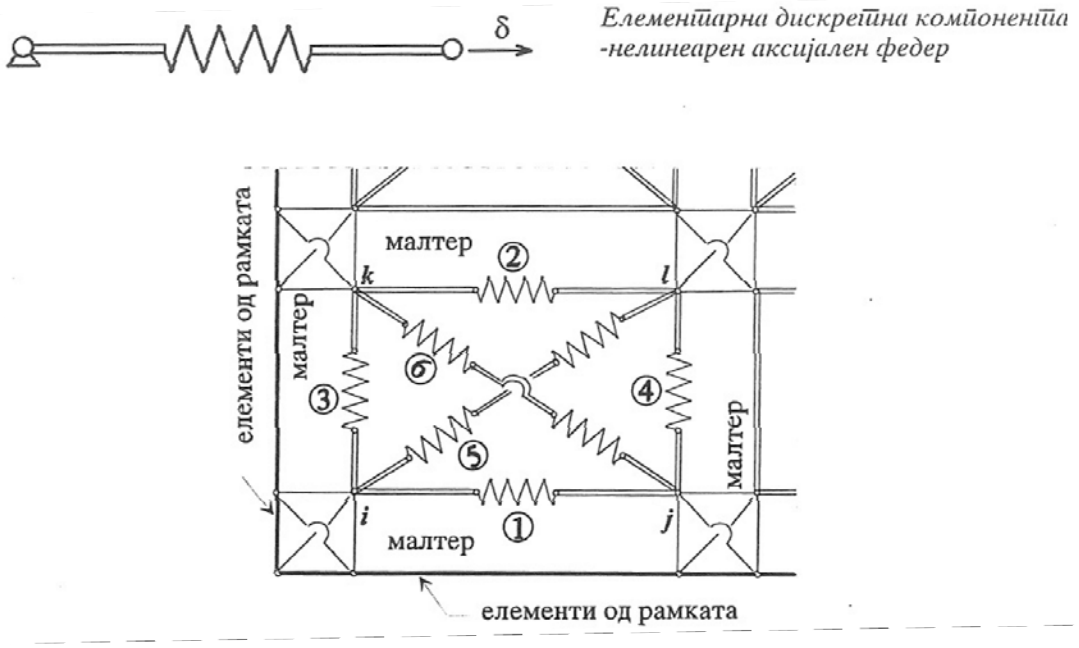

Figure 3. 23 NDC-INFILL model (Krstevska, 2002)

In the IZIIS laboratory, 12 models were tested to obtain their mechanical characteristics.

The verification of the applied analytical procedure through definition of the nonlinear response to earthquake effect showed that the new proposed concept of nonlinear micro-modeling could successfully simulate the nonlinear response of systems constructed as frames with masonry infill.

Although results from the analyzed concept for nonlinear micro modelling showed good correlation, their application in every day design practice is not convenient since it is demanding a lot fo time and powerful computer calculations. For practical application more simplified macro-models should be used.

Presented briefly in the subsequent text will be only a small part of the analytical and experimental investigations carried out in the IZIIS laboratory within the doctoral dissertation entitled "Innovative HD Systems with Infill as a Way of Reduction of Seismic Risk for Reinforced Concrete Buildings" – 2013 elaborated by Isak S. Idrizi (Fig. 3.24) . The results obtained for a plain RC frame, frame with masonry infill and frame with the innovative HD system were compared.

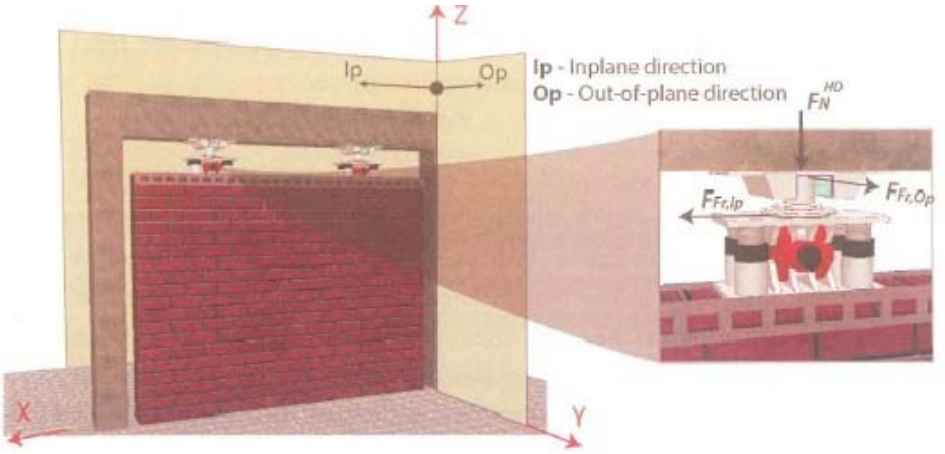

Figure 3. 24 View of RC frame with masonry infill and applied HD system.

Analytically analyzed further by macro modeling was the nonlinear behavior of a 4 storey 2D frame without infill at the first story that was compared to the HD system. Micro modeling of the infill of a model to the scale of 50% and 100% was presented with previously experimentally obtained mechanical characteristics of the infill.

Through numerous analytical and experimental experiments, the effects of the infill as a material within RC frames were analyzes and compared to the results obtained by application of the HD system.

4. INNOVATIVE METHOD FOR IMPROVEMENT OF THE SEISMIC RESISTANCE OF THE MASONRY INFILL WALLS IN RC FRAME STRUCTURES – EXPERIMENTAL PROGRAM

4.1. Background of research - FRAMA project

As mentioned in Chapter 3 observations from the recent major earthquakes have shown that the structural interaction between columns and infill walls of RC frames under seismic excitation can significantly alter the structural behaviour, thus causing catastrophic consequences. To improve the understanding of this problem, a research project "Frame – masonry composites for modeling and standardizations (**FRA**med-**MA**sonry)" was started at the Faculty of Civil Engineering and Architecture, Josip Juraj Strossmayer University of Osijek, Croatia (2014-2017). The principal investigator from Croatia was Prof. Dr. Vladimir Sigmund and the funding was provided by the Croatian Science Foundation. The main objective was to investigate the safety and behavior of buildings with masonry-infilled RC frames through near full-scale dynamic earthquake-simulation tests accompanied by supporting pseudo-dynamic tests of structural assemblies and components and by calibrated analytical solutions.

The Institute of Earthquake Engineering and Engineering Seismology, UKIM-IZIIS from Skopje was partner in the realization of the experimental investigations which were carried out at the IZIIS Dynamic Testing Laboratory in the period of June, 2015-August, 2015, (Necevska-Cvetanovska et al., 2015).

The complete experimental programme of the project consists of:

- laboratory tests of concrete, steel, masonry unit (bricks) and mortar specimens for definition of their strength characteristics;
- quasi-static tests of 2 series (each consisting of 6 elements) of masonry wall samples in cement-lime mortar; the first one of hollow-clay masonry and the second one of solid-clay masonry bricks, for definition of their mechanical characteristics and failure mechanism and
- shaking-table tests of the two models of three story RC building with hollow-clay masonry infill (MODEL 1) and solid-clay masonry infill (MODEL 2), to a scale 1:2.5.

Detailed information regarding complete experimental programme are given in Necevska-Cvetanovska et al., (2015).

In order to meet the PhD goals additional third Model IW-SB was designed and tested, which is out of the objectives of the FRAMA project. This Model used the same bare reinforced concrete structure, but with proposed innovative connection of the masonry infill to the RC frame.

Further on some brief introduction details are given regarding the two models testes in FRAMA project in order to have possibility to correlate the obtained results from the shake table tests between Model IW-SB and these two models. Results were mainly focused on comparison with Model 1 which is referent model in the investigations.

4.1.1 Similitude requirements of the experimental model

The geometrical scale of the model was selected on the basis of the characteristics of the seismic shake table and the precisely defined objectives of testing, i.e., based on the following criteria:

K1 - proportions of the shaking table (4.5 m x 4.5 m)
K2 - allowed total height of the model (10m)
K3 - allowed total weight of the model (400 kN)
K4 - realistic reproduction of nonlinear behaviour
K5 - realistic reproduction of the failure mechanisms

The reinforced concrete frames abutting the infill walls were designed in compliance with Eurocode 2 and 8 provisions (CEN, 2004a; CEN, 2004b) as medium-ductility moment resisting frames. They were constructed in the Dynamic Testing Laboratory of IZIIS using a traditional technology of construction of RC frames with masonry infill. The construction was carried out by Construction Company GOLDEN-ART from Skopje. Shake table tests were performed in the Dynamic Testing Laboratory of IZIIS. The artificial mass simulation law was applied to account for the models scaling.

The following materials have been used for construction of the models:

- Concrete class C25/30 XC1
- Reinforcement class B500B
- Hollow clay infill walls for Model 1
- Solid-clay masonry units called “GITER” were used for construction of the Model 2.
- Lime-cement mortar prepared with lime : cement : sand ratio equal to 1:1:5 and target compressive strength of M5

The shake table constraints have resulted in the design of a three-story test structure with two bays in the assumed N-S direction and one bay in the E-W direction (Figure 4.1). The height of the model is 3.9m. The Model 1 structure has hollow-clay infill walls and MODEL 2 structure has solid-clay infill walls. The total weight of the Model 1 was 29 200 kg and of the Model 2 was 30 600 kg (Guljas et a. 2018).

Figure 4.1 3D view of Model 1 and Model 2 to a scale of 1:2.5 (Report IZIIS 2015-31)

The specimens were built at a geometric scale of 1:2.5 scale. The maximum aggregate size in the test specimens was 8 mm, compared with a typical size of approximately 20 mm for full-scale RC construction. The masonry units were cut from full-scale masonry units to preserve the relative area of voids. Mortar thicknesses also were reduced and were sized for compliance with Eurocode 6, which governs the design of masonry structures in Europe (EN 1996–1). Eurocode 6 Section 8.1.5 requires joints to be between 6 and 15 mm, corresponding to 2.4–6 mm for a scale factor of 2.5. For these tests, a joint thickness of 6 mm was chosen for compliance with provisions and to improve constructability, as thin joints would have been difficult to construct and could have led to issues with uneven joint thickness. Similitude practices commonly used in reduced-scale earthquake simulation tests were followed. Cauchy-Froude similitude was satisfied, which involved scaling mass and the duration of the ground motion such that gm/EL2 in the prototype

and the model were equal (g = gravitational acceleration, m = mass, E = elastic modulus, and L = length). This meant: (1) adding mass to the system and (2) reducing the time step of the full-scale ground motion record. The first is done to increase the period of the system and to produce meaningful axial stresses in the vertical elements. The second is done with the intent of matching dominant frequencies in the ground motion and test specimen. The addition of mass and compression of records has been a common practice in earthquake simulation tests of RC structures since they became more common in the 1970s [Gulkan and Sozen, 1971; Otani and Sozen, 1972; Hidalgo and Clough, 1974; Aristizabal and Sozen 1976] and is frequently used in IZIIS laboratory (Sendova et al. 2013).

Computed were the scales of all the remaining physical quantities in model analysis of problems in dynamics of structures (Table 4.1). The considered structures have relatively low levels of axial stresses at the base which justifies the adoption of a model with neglected gravity forces ($g_r \neq a_r$, gravity acceleration cannot be simulated). In such a case, the scales of all the quantities of interest are expressed only in relation to the geometrical scale l_r adopting a material identical to that of the prototype.

Table 4. 1 Scaling factors for the parameters of the model used for dynamic analysis (expressed via l_r, ρ_r, σ_r) (Sendova et al. 2013)

Physical quantity	*Scale*
Length, displacement	l_r
Acceleration	$a_r = \sigma_r / l_r \rho_r = 1/ l_r$
Time	$t_r = l_r / (\rho/ \sigma)_r^{0.5} = l_r$
Frequency	$f_r = (\sigma/\rho)_r^{0.5} / l_r = 1/ l_r$
Mass	$m_r = l_r^3 \rho_r = l_r^3$
Force, weight	$P_r = l_r^2 \sigma_r = l_r^2$
Stress	$\sigma_r = 1$
Mass density	$\rho_r = 1$
Deformation	$\varepsilon_r = 1$
Modulus of elasticity, shear modulus	$E_r = \sigma_r = 1$
Poisson's coefficient	$\nu_r = 1$
Damping coefficient	$\mu_r = 1$

The comparison between the characteristics of the models and the hypothetical prototype, i.e., the comparison of the designed and the obtained scales can be explained as follows:

- **Geometrical scale**

The geometrical scale of the model is determined considering the first three criteria. The proportions of the model are obtained for an assumed scale of l_r = 1:2.5.

- **Density**

From condition k4 and considering the specific behaviour of masonry as a non-homogeneous material, it follows that the masonry have to be constructed from natural material (brick, limecement mortar). Hence, the scale of the density of material is defined as $\rho_r = 1$.

- **Stress**

Considering condition k5 and the fact that the failure mechanism depends mostly on the stress states of certain walls, the scale for normal stresses is $\sigma_r=1$. In the considered case it is:

$$\sigma_{0r} = \frac{m_r g_r}{Fr} = \frac{1}{2}$$

The required additional normal stresses are provided by adding the required load level representing the floor and roof structure, so the resulting $\sigma_{0r}=0.94$.

- **Elasticity Modulus**

From the condition for realistic simulation of the failure mechanism, i.e., stress scale $\sigma_r = 1$, it follows that the scale of the elasticity modulus and the shear modulus has to be $E_r=1$. Taking into account the usage of natural materials, it is possible to obtain very similar values for E_m and E_p.

- **Mass**

Starting with relation $m_r = l_r^3 \rho_r$, for the mass scale it is obtained:

$$m_r = \left(\frac{1}{2.5}\right)^3$$

Hence, satisfying the geometrical and the density scale, it follows that the mass of the model has to be 15.6 times less than the mass of the prototype.

- **Frequency**

The frequency notation is given a significant importance in dynamics of structures. The natural frequencies are the main dynamic characteristic of structures. Their relation with the frequency content of excitation has a significant effect upon dynamic response, inducing either amplification or attenuation of the seismic effect (resonance is the ultimate case of this phenomenon). Starting

with the relation $f_r = (\sigma_r / \rho_r)^{0.5} / l_r$, it follows that the natural frequency of the model should be 2.5 times greater than that of the prototype.

$$f_r = \frac{\left(\frac{\sigma_r}{\rho_r}\right)^{0.5}}{l_r} = 2.5$$

- **Time**

The time is the very important quantity in dynamic analysis. All the terms of the equations of motion represent, in fact, functions of time. The time scale is inversely proportional to the frequency scale which, in the considered case means that the whole time scale has to be reduced, i.e., the scale of the input excitations is reduced 2.5 times.

- **Acceleration**

Starting with expression $a_r = \sigma_r / l_r \rho_r$, the scale of $a_r = 2.5$ is obtained. Considering the obtained scales for f_r and t_r, the acceleration values should be reduced 2.5 times when interpreting the results of the shaking table testing of the model.

- **Forces**

Important elements in dynamics of structures are also the forces, i.e., the dead weight $Q = m \cdot g$ for obtaining the normal stresses, and inertial forces $P_i = m \cdot a$. The force scale is defined by the expression: $P_r = l_r^2 \sigma_r = (1 / 2.5)^2$.

- **Damping coefficient**

The damping coefficient μ is a nondimensional quantity which is expressed as percentage of critical damping. The values of this coefficient depend on many factors (geometry, material, mass, stiffness) and are usually experimentally determined. In the considered case (a model designed according to the proportions of the prototype), $\mu_r = 1$ is adopted.

- **Poisson's coefficient**

The Poisson's coefficient n is a nondimensional characteristic of the material. If $\nu_r = 1$, which is quite realistic considering the selected material, the sliding modulus will be $G_r = E_r = 1$.

- **Deformation**

Deformations are nondimensional quantities that are directly used in the analysis. Their scale can be arbitrarily selected, independently from the other parameters. For the model with neglected

gravity forces $\varepsilon_r = 1$, i.e., $\varepsilon_m = \varepsilon_p$. By satisfying the scale for the bulk density in constructing the model to a scale of 1:2.5, used were original construction materials with physical-mechanical characteristics of material almost equal to those of the prototype that were prepared according to the designed proportions. Looking over the main characteristics, it is clear that almost ideal similarity between the model and the prototype has been achieved by modeling. Thus, conditions were created to interpret the results obtained from testing of the dynamic response of the models relating them directly to the prototype. The way in which the prototype is selected enables application of the acquired knowledge in seismic analysis of a large number of such buildings in the Balkan which is the main purpose of the performed investigations.

4.1.2 Description of the Models

3D frame model (MODEL 1) consists of two planar RC frames (axes A and B) infilled with hollow-brick masonry walls which are interconnected with perpendicular girders in the axes 1, 2 and 3. The frame in direction of axes 2 is infilled with the same masonry units, (Fig. 4.1-left). The mortar joints were 10 mm thick and they were fully mortared (for both horizontal and vertical joints). The scale of the Models comparing the real structure was selected 1:2.5.

3D frame model (MODEL 2), similar as MODEL 1, consists of two planar RC frames (axes A and B) infilled with solid-brick masonry walls which are interconnected with perpendicular girders in the axes 1, 2 and 3. The frame in direction of axes 2 is infilled with the same masonry units. The same bare RC frame structure was used for construction of MODEL 2. First, the damaged infill from the first and second story was demolished and removed from the structure. The next step was insertion of solid-clay masonry infill and vertical RC ties around the openings, (Fig. 4.1 right).

The models proportions were 2.78 x 4.66 x 3.90 m. The model structure is designed according to EN 1998-1:2004 thus satisfies the current requirement for seismic zone IX. (Guljas et al., 2018). The formwork and reinforcement details are given in the Necevska-Cvetanovska at el. (2015).

Various aspects were investigated based on the obtained results from shake table tests on the two models investigated in the FRAMA project, which are valuable contribution to the knowledge of masonry infill behaviour in general (Guljas et al., 2018; Burilo et. al, 2018 etc.)

4.2 Design and shake table tests of model with innovative infill connection (Model IW-SB)

For the purpose of this PhD research, a third model IW-SB (Infill Wall – Steel Bars) was designed and tested. The third model is built using the same reinforced concrete frame structure of Model

1 and Model 2, and innovative method was introduced for the connection of the masonry infill to the structure (Figure 4.2.). The anchor in the ends of the ties were placed at the distance of 6.9 cm and in the middle of the ties, the distance was doubled.

While the first two Models, Model 1 and Model 2, were fully infilled by masonry wall, in the third Model IW-SB, an innovative connection between columns and infill walls is introduced. They are connected by spaced mild steel bars, and two variant solutions are analyzed:

a) the first one without gap between infill and frame and using steel reinforcement and

b) the second one where the infill panel is separated from columns with two finite width vertical gaps filled with polystyrene foam (Figure 4.3).

Tailored-made experimental program is performed to investigate whether proposed column-infill connection details can effectively improve the seismic performance of masonry-infilled RC frame structures. In addition, the displacement ductility and energy dispassion capacity of the RC frame system with masonry infill was taken into consideration.

Figure 4.2 Construction of Model IW-SB

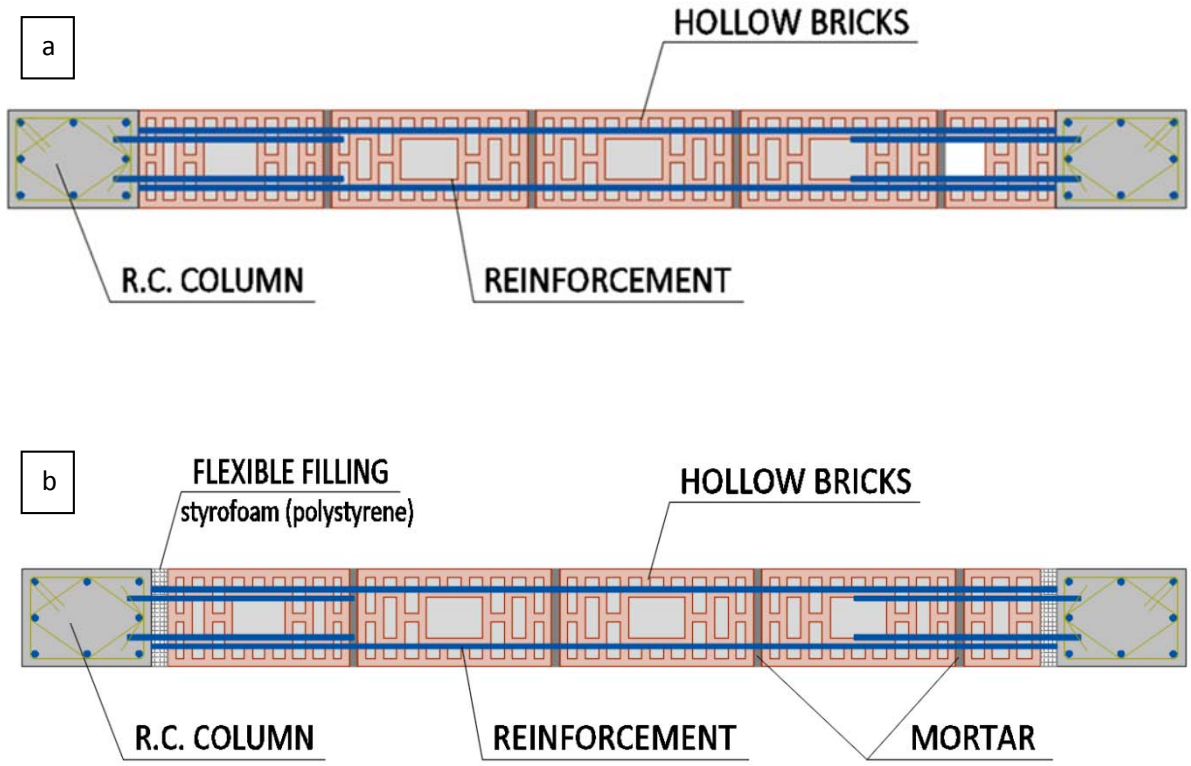

Figure 4.3 Masonry infill configuration and layout of proposed connection of Model IW-SB a) variant solution –without vertical gap b) variant solution with vertical gap filled by flexible filling

Further on in this chapter detailed description of the test setup, built-in materials, instrumentation and shake table tests results are given for Model IW-SB.

4.2.1. Laboratory testing of built-in materials

In accordance with the proposed programme, a series of laboratory static tests on prepared concrete, steel and mortar samples, as well as on brick units were performed for the needs of subsequent constructing the scaled model. The same materials are used for design and construction of all three models (Model 1, Model 2 and Model IW-SB). The responsible for realization of the above tests was GOLDEN ART Construction Company from Skopje. Selected results are presented in the following sections of the Chapter 4 in order to get insight into the obtained results from laboratory tests of built-in materials for better understanding of performance of the models. The complete results in the integral form can be find in Sigmund at al.

a. Mechanical properties of concrete

Laboratory testing of concrete samples (13 in total) to define concrete compressive strength and modulus of elasticity were performed.

The compressive strength of concrete samples was determined using the procedure established on the EN 12390–3:2011 standard. The concrete samples had proportion 150 x 150 x 150 mm and were taken from the different part of the structures e.g. foundation (1 specimen at the age of 7 days) and story levels (9 specimens at the age of 28 days). The characteristics value of the concrete compressive strength was 39.1MPa, 42.8 MPa and 27.6 MPa, accordingly for each story, (Fig. 4.4).

The modulus of elasticity of concrete samples was determined using the procedure established on the EN 12390–13:2013 standard. The concrete cylinders had proportion 150 x 300 mm and were taken from the different story levels (3 specimens). The average characteristics value of the modulus of elasticity was 38 838 MPa, (Fig. 4.4).

Figure 4.4 Experimental determination of concrete compressive strength and modulus of elasticity (Report IZIIS 2015-31)

b. Mechanical properties of steel

Reinforcing steel bars of three different diameters were tested under tensile loading using the procedure established on the EN ISO 15630–1:2010 standard and the results obtained are presented in Table 4.2. Indexes "*y*", "*max*" and "*ult*" stands for yielding, maximum stresses and strains at the failure point, respectively.

Table 4. 2 Physical properties of steel reinforcement samples (Report IZIIS 2015-31)

Rebar diameter	Date	f_y [MPa]	f_{max} [MPa]	f_{ult} [MPa]	E_s [GPa]	e_y [%]	e_{max} [%]	e_{ult} [%]
Ø4	5.7.2015	753.50	780.40	500.00	204.25	0.555	1.122	2.780
Ø6	4.9.2015	563.50	588.92	350.00	188.12	0.499	2.378	5.988
Ø8	4.9.2015	590.50	620.75	400.00	198.62	0.498	2.846	7.786

c. Mechanical properties of mortar sample

In accordance with the proposed programme, laboratory testing of mortar samples proportioned 160 x 40 x 40 mm, taken during the construction of the wall elements and model, were realized for definition of their strength characteristics.

The flexural and compressive strength of mortar samples was determined using the procedure established on the EN 1015-11:2008 standard. Three samples were taken from each of the phases of construction of wall elements at three different story levels and tested after 28 days (9 samples in total) for building MODEL 1. For the MODEL 2, six specimens were taken from the first and the second story. The results of testing of characteristics flexural and compressive strength of mortar samples are presented on Table 4.3.

Table 4. 3 Characteristics value of the flexural and compressive strength of mortar samples (Report IZIIS 2015-31)

		Flexural strength [MPa]	Compressive strength [MPa]
MODEL 1	1 storey	2.5	9.1
	2 storey	3.1	10.4
	3 storey	4.3	12.2
MODEL 2	1 storey	3.7	11.3
	2 storey	2.3	8.7
	3 storey	/	/

d. Mechanical properties of masonry units-testing of hollow-clay masonry units

Having in mind that for Model IW-SB hollow clay was used as infill, only results for hollow clay are given. Hollow-clay masonry units are manufactured by MLADOST TMP from Mala Plana, Serbia. They units were cut from the standard units that are commonly used for infill masonry walls. From the standard units' dimensions of 120 x 250 x 190 cm they were cut twice along the height and brick unit has dimensions 250 x 120 x 65 mm (Figure. 4.5).

Figure 4.5 Experimental determination of compression strength of hollow-clay masonry units (Report IZIIS 2015-31)

Specification of hollow-clay masonry units was determined using procedure established on the EN 771-1:2011 and the compressive strength EN 772-1:2011 standard. In order to obtain compressive strength of the brick units, six specimens were tested in horizontal and six in vertical position (Figure 4.5). The characteristics value of the compressive strength from vertical tests is 14.59 MPa and from horizontal ones, 3.43 MPa.

4.2.2. Quasi-static tests on masonry panels

To define the mechanical characteristics of masonry, the bearing capacity and the failure mechanisms, quasi-static tests on two series, each consisting of six elements of masonry wall samples in cement-lime mortar; the first one of hollow-clay masonry and the second one of solid-clay masonry bricks were performed. For that purpose, before starting with the models construction, total of 12 wall elements were constructed in the IZIIS' Dynamic Testing Laboratory, (Figure 4.6).

The advantage of these tests is the possibility of precise control during the experiment and detailed monitoring of different phenomena. The only shortcoming is the absence of dynamic effects.

Based on the carried out experimental quasi-static tests on wall elements performed at IZIIS Lab, the following is concluded:

- The average characteristics compressive strength of the hollow-clay masonry units was 1.50 MPa and average characteristics tensile and shear strength were 0.05 MPa and 0.08 MPa, accordingly.

These results from these quasi-static tests are prerequisite for correct further analysis of the scaled model as well as for interpretation of the model behaviour.

Figure 4.6 Wall elements for quasi-static testing (Report IZIIS 2015-31)

a. Characteristics of masonry panels

Two basic types of wall element built from hollow-clay were tested in the considered case (Table 4.4). The first type was wall elements subjected to axial compression test, (Figure 4.7), while diagonal compression test was performed for the second type of wall elements, (Figure 4.8). The tests were performed up to initial occurrence of cracks or up to failure of the elements. Apart from the total force, recorded was also the total displacement of the actuator in the direction of force application as well as other quantities of interest which was done by a corresponding instrumentation.

Table 4. 4 Proportions and type of tests (Report IZIIS 2015-31)

	Proportions of the wall elements [mm]	
	Axial compression test	**Diagonal compression test**
Hollow-clay		
W1	510 x 120 x 550	
W2	510 x 120 x 550	
W3	510 x 120 x 550	

W4	640 x 220 x 640
W5	640 x 220 x 640
W6	640 x 220 x 640

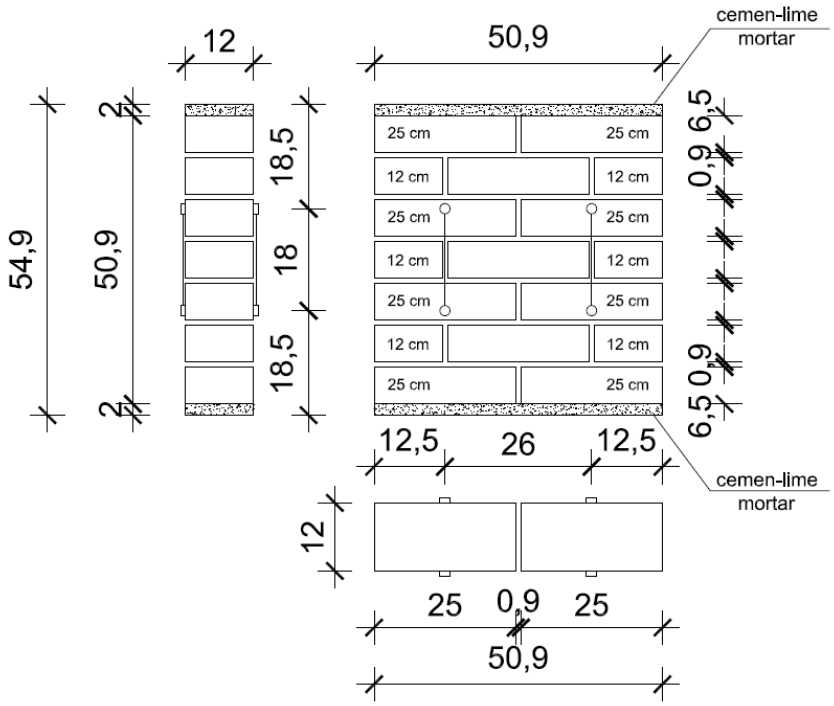

Figure 4.7 Proportion of the wall elements for axial compression tests (FRAMA - Model 1 and Model IW-SB)

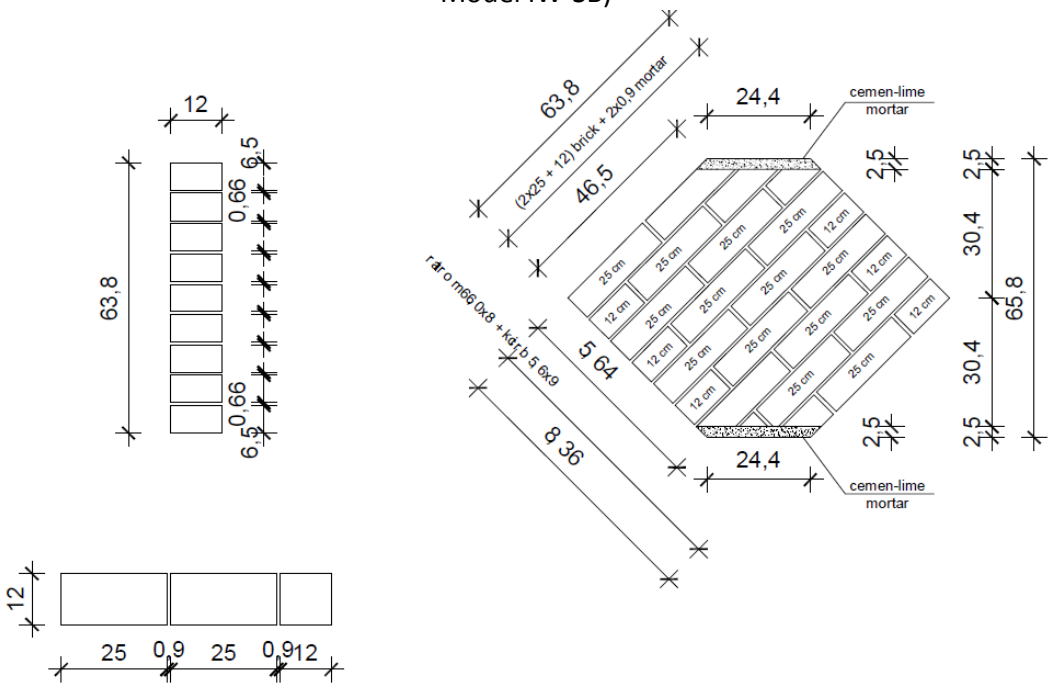

Figure 4.8 Proportion of the wall elements for diagonal compression tests (FRAMA - Model 1 and Model IW-SB)

b. Instrumentation

The instrumentation of the wall elements was done by use of corresponding types of instruments in accordance with the programme and the objectives of the tests. One channel was used to measure the size of the applied force, while the other channels were used to measure relative displacements (LVDT-s). In that way, information on the behaviour of the elements was obtained through the relative displacements at characteristic points and experimental values of strength characteristics were obtained.

The subsequent sections show selected results of the tested wall elements.

c. Tests on panels from hollow-clay masonry units

Within this testing programme six wall elements were subjected to monotonous increase of the force amplitude up to total failure of the elements. The compressive strength of hollow-clay masonry wall samples (W1, W2 and W3) was determined using the procedure established on the EN 1052-1:2004 standard and the referent tensile strength of hollow-clay masonry walls (W4, W5 and W6) was determined using the procedure established on the American ASTM E519/E519M-10 standard. The average characteristics compressive strength was 1.50 MPa (Figure 4.9) and average characteristics tensile and shear strength were 0.05 MPa and 0.08 MPa, accordingly, (Figure 4.10).

Figure 4.9 Experimental determination of compressive strength of hollow-clay masonry walls (Report IZIIS 2015-31)

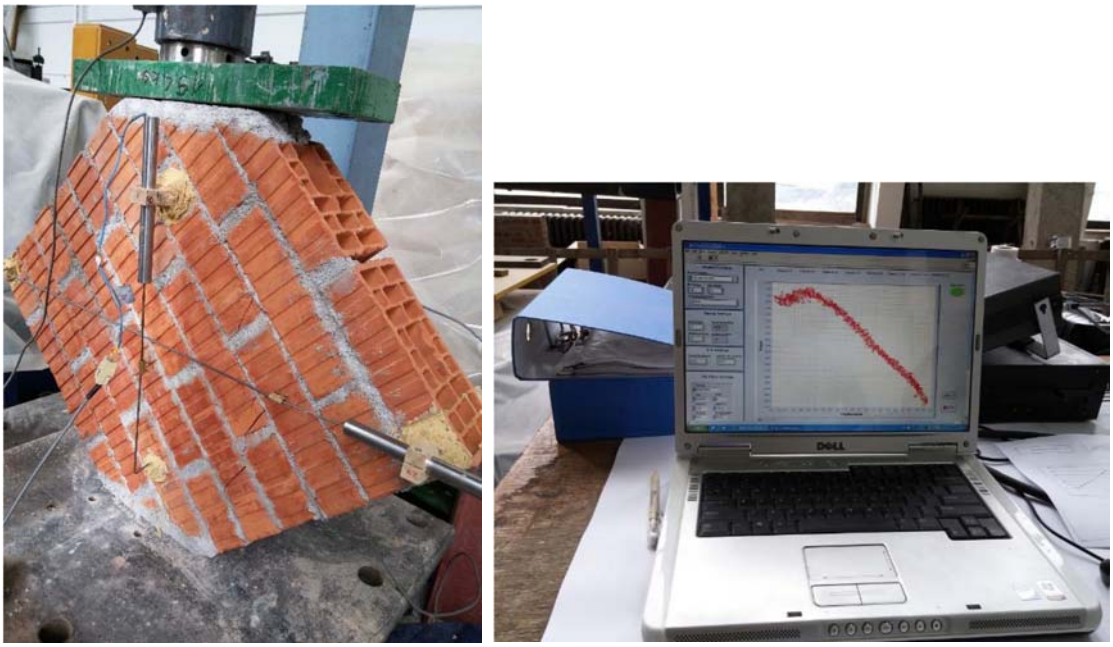

Figure 4.10 Experimental determination of referent tensile and shear strength of hollow-clay masonry walls (Report IZIIS 2015-31)

4.2.3. Design and construction of Model IW-SB - test-set up, instrumentation and experimental programme

a. Testing equipment at IZIIS

A biaxial shake table is a key facility for generation of earthquake motions (Figures 4.11, 4.12, Table 4.5). It is a complex integral electro-hydraulic system which enables programmed generation of translational vibrations in both horizontal and vertical direction. The model tested on this system was supported by a 5 m x 5 m x 0.8 m slab, which is a rigid body of ideal symmetry in respect to its center. The shake table is supported by four vertical hydraulic actuators which enable a motion in vertical direction. Two horizontal actuators enable motion in horizontal direction.

Figure 4.11 IZIIS' seismic shake table – top view (left), below the table (right)

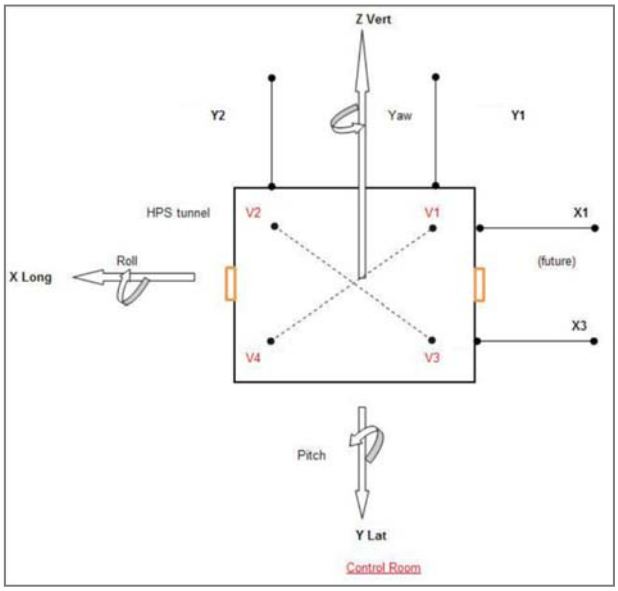

Figure 4.12 Degrees of freedom (actuators in X-longitudinal direction are not installed)

The seismic shake table has the following characteristics:

- size in plane 5.0 x 5.0 m.
- shaking table mass is 33.0 t
- pay load 40.0 t
- 5 degree-of-freedom (DOF)
  2 lateral (Y1-Y2) and 4 vertical actuators (V1-V4)
- MTS Digital Controller 469D
  Total mass of the supporting structure - 1200 t
  3 hydraulic power supplies with a maximum flow of 1,250l/min
  The required electric power to feed the three pumps is 1,020 A
- Operational since 1980MTS Digital Controller 469D:
- Data acquisition system (DAS)
  - National Instruments (NI) PXI modular system:

Table 4. 5 Kinematic quantities for zero pay load

Direction	displacement	velocity	acceleration
Y	±125 mm	±1.0 m/s	±3.0 g
Z	±60 mm	±0.5 m/s	±1.5 g
Roll	±2.0 deg	±13 deg/s	±200 deg/s2
Pitch	±2.0 deg	±13 deg/s	±200 deg/s2
Yaw	±2.0 deg	±26 deg/s	±200 deg/s2

b. Design of Model IW-SB

3D frame model (Model IW-SB) consists of two planar RC frames (axes A and B) infilled with hollow-brick masonry walls which are interconnected with perpendicular girders in the axes 1, 2 and 3. The frame in direction of axes 2 is infilled with the same masonry units, (Figures 4.13, 4.14 and 4.15). The proposed innovative method for the connection is presented. The mortar joints were 10 mm thick and they were fully mortared (for both horizontal and vertical joints). The model proportions were 2.78 x 4.66 x 3.90 m.

All columns dimensions are 12 x 16 cm and there are three schemes of reinforcement – columns along the axes 1 contain 8ϕ6, columns along the axes 2 contain 8ϕ8 and columns along the axes 3 contain 4ϕ8 + 4ϕ6, with transverse reinforcement ϕ6/5 (10) cm. The cross-section of all beams are 12 x 16 cm and reinforced with 3ϕ8, in both, lower and upper zone. RC slab is 8cm thick and reinforced with steel mesh Q139 (ϕ4/10) for bidirectional bearing capacity. The model has a rigid foundation which is fixed to the shake table thus preventing any sliding, displacements and rotations. The model structure is designed according to EN 1998-1:2004 thus satisfies the current requirement for seismic intensity of ag $\geq$ 0.3 g. Selected drawings of the formwork and reinforcement details are given in the Figures 4.16 and 4.17.

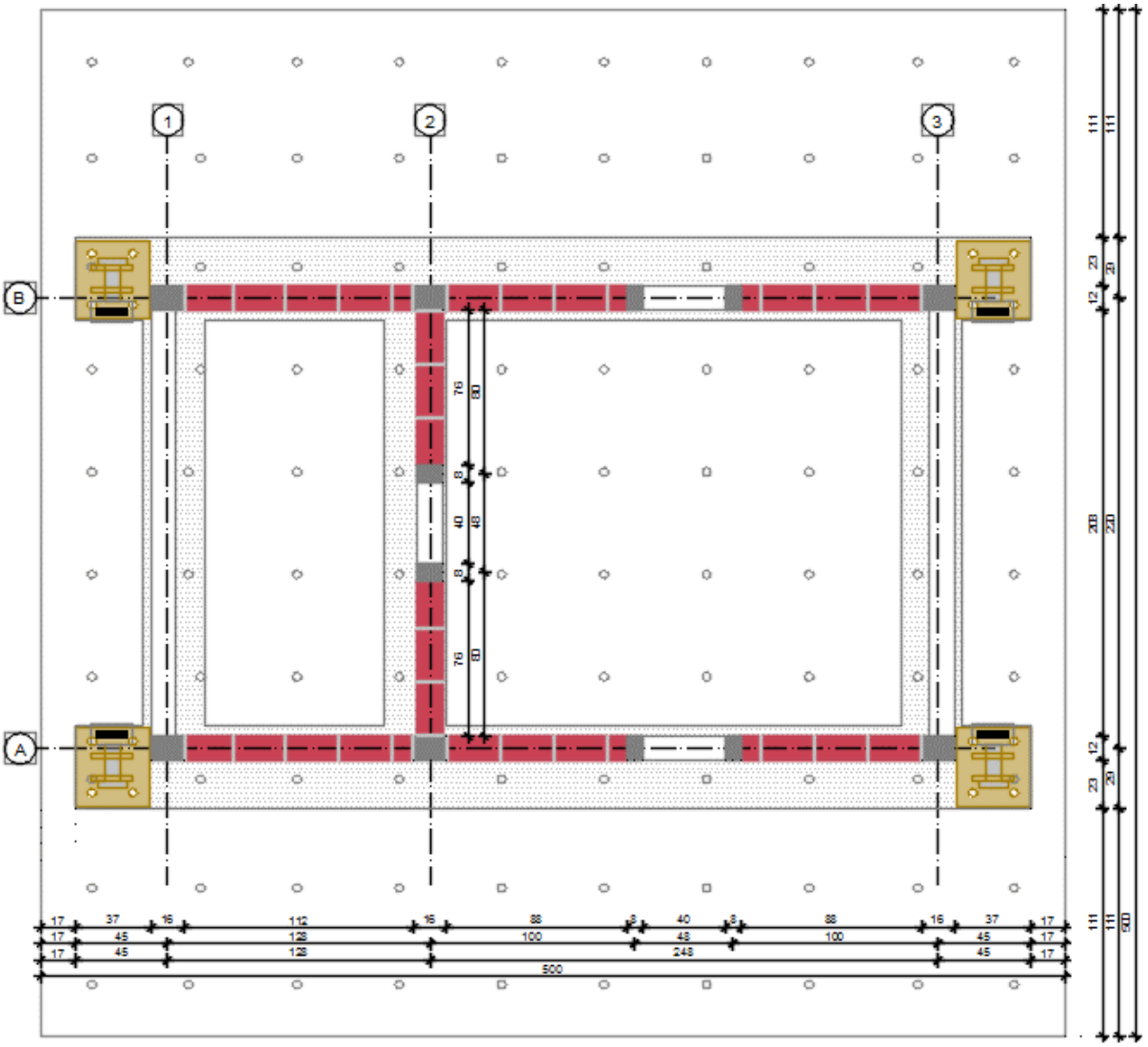

Figure 4.13 Layout of the Model IW-SB over the shake table

Figure 4.14 Infill wall sequence in frames A and B – Model IW-SB

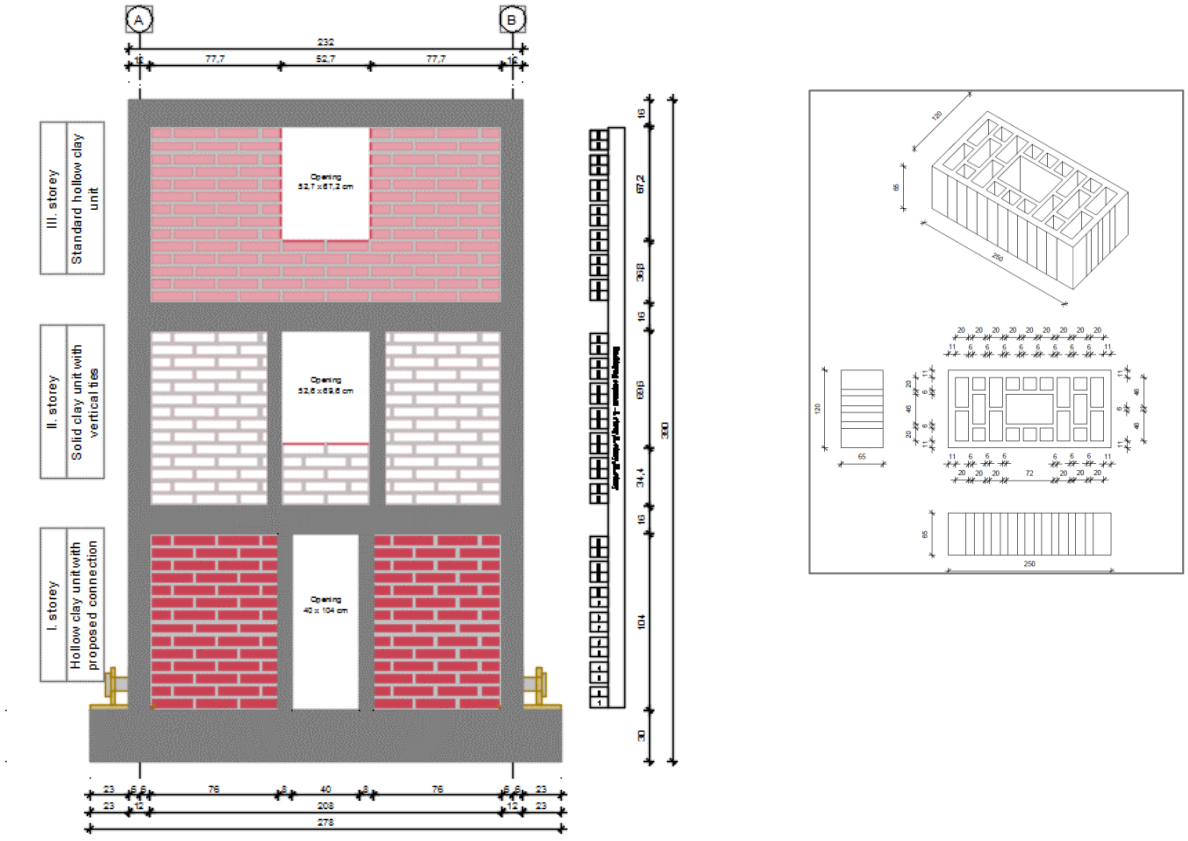

Figure 4.15 Infill wall sequence in frame 2 – Model IW-SB and hollow-brick unit

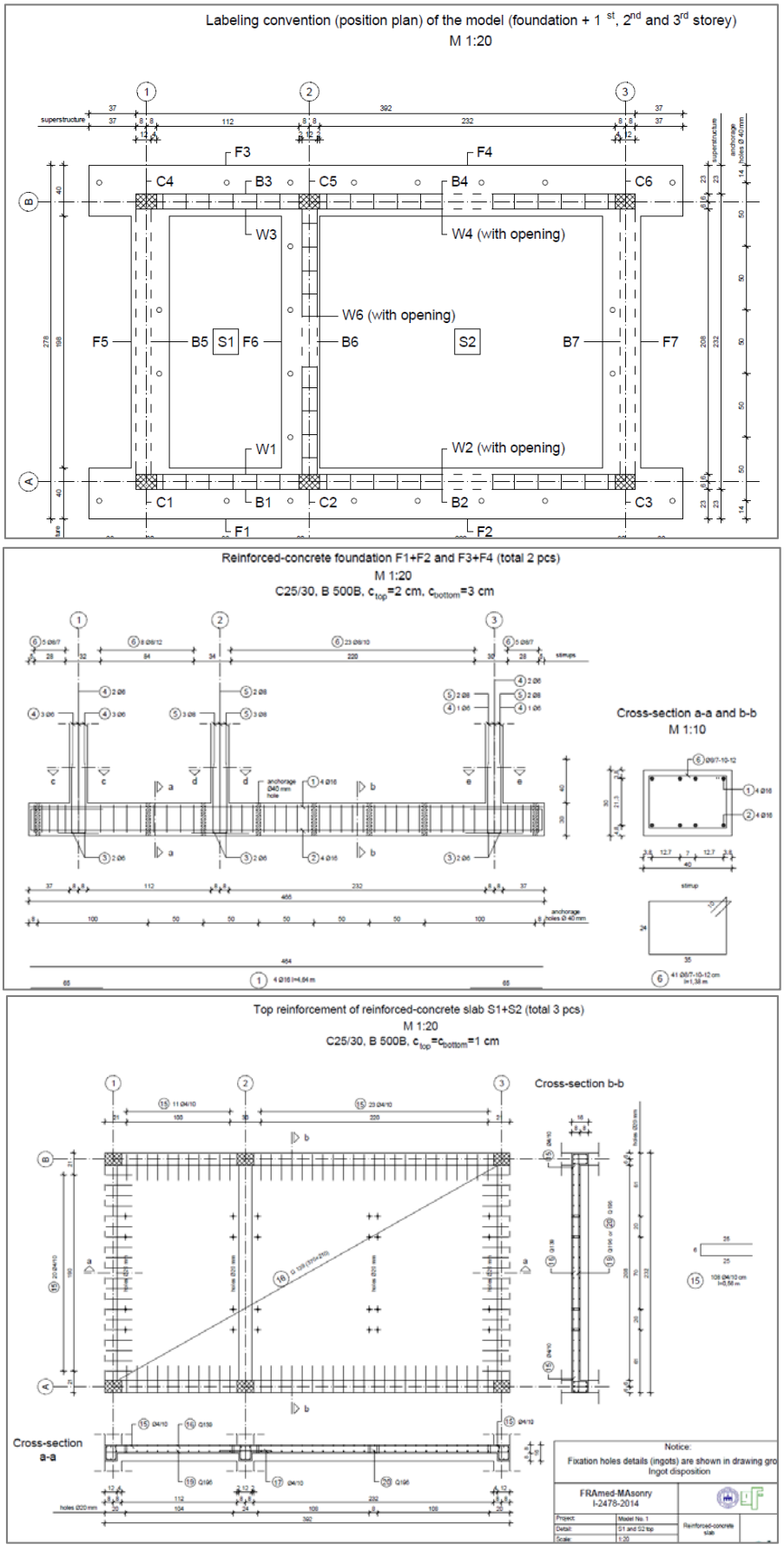

Figure 4.16 Formwork and reinforcement details – Model IW-SB

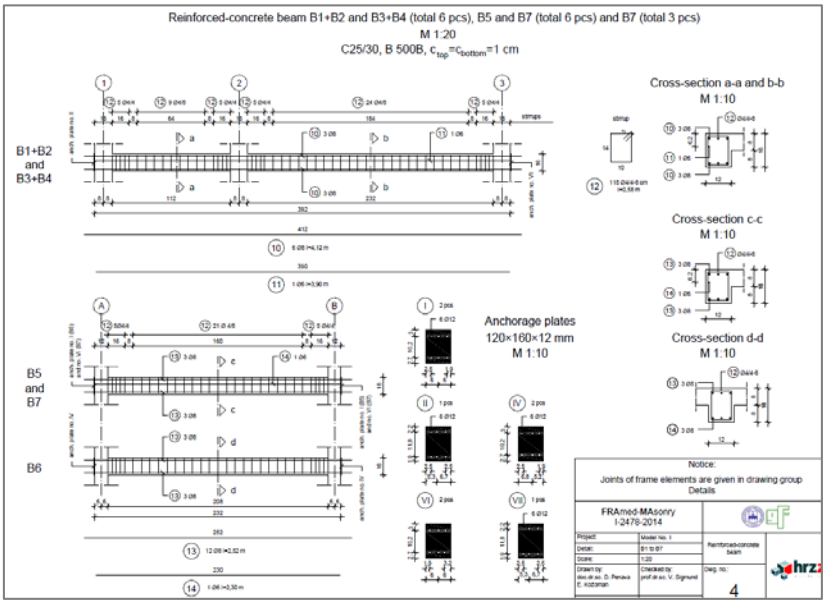

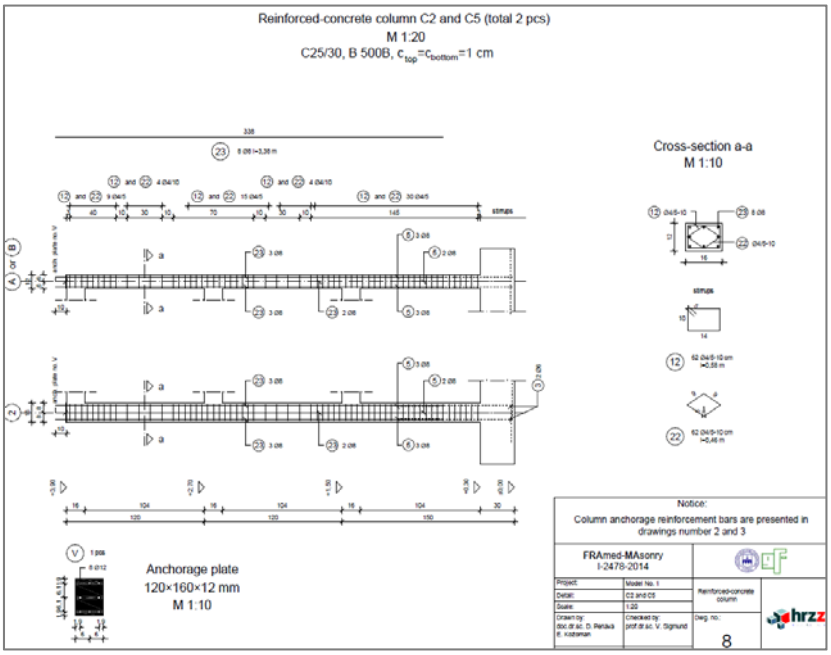

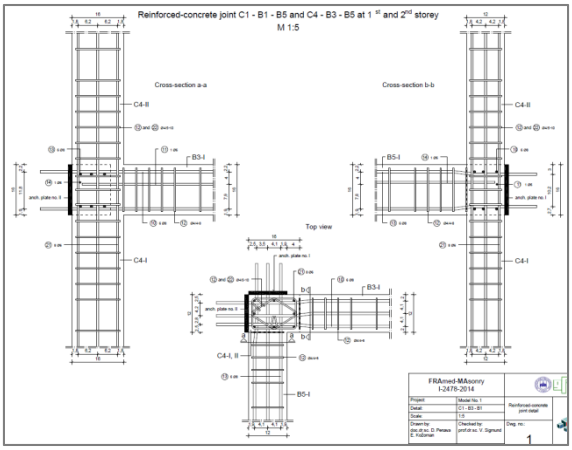

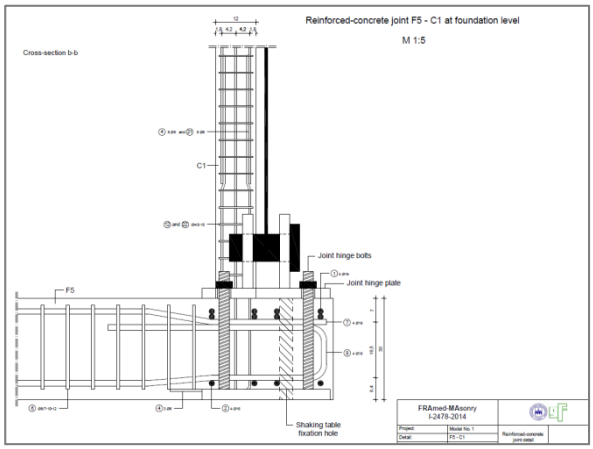

Figure 4.17 Formwork and reinforcement details – Model IW-SB, (*contd.*)

c. Construction of the Model IW-SB

In accordance with the designed proportions, the model was constructed in the Dynamic Testing Laboratory of IZIIS using a traditional technology of construction of RC frames with masonry infill. The construction was carried out by Construction Company GOLDEN-ART from Skopje.

The following materials have been used for construction of the model:

- Concrete class C25/30 XC1
- Reinforcement class B500B
- Hollow-bricks with proportion 250 x 120 x 65 mm manufactured by MLADOST TMP, Mala Plana
- Lime-cement mortar prepared with lime : cement : sand ratio equal to 1:1:5 and target compressive strength of M5

A reinforced concrete platform with proportions of 2.78 m x 4.66 m and a thickness of 0.30m was constructed as a foundation for the model for the purpose of its construction and transport, (Figure 4.18).

Figure 4.18 Construction of RC foundation of the scaled model

The construction of model was finished in three weeks. After being completed and dried for a period of 30 days on the place where it was constructed, the model was transported and mounted to the shake table by 90-tons auto crane. A total of 20 anchors were used for anchoring the model with the shake table.

Presented further are several pictures of construction of the model and its mounting on the shake table (Fig. 4.19).

Figure 4.19 Construction of the RC frame of Model IW-SB

The construction of the infill was performed directly on the RC structure, previously mounted on the shaking table. The technology of the construction is presented in subsequent steps in Figure 4.20. The building of the infill was done in every bay of the frame, at the beginning at frame A. In each bay there are 14 layers of bricks. According the design of the innovative connection in this research, at each second layer of bricks starting from up and down two steel reinforcement bars with ø6 mm, while in the middle part the distance between the bars was three layers of bricks. The procedure of the construction was the following: First two layers of bricks were set, on which above the mortar was installed. After that in both frames, at the columns, anchors with length of 5cm were installed. In the middle, additional reinforcement bar was inserted which was connected with small wires to the reinforcement anchored in the columns from left and right in order to have continuous length of the reinforcement installed in the infill. Above the reinforcement another layer of mortar with same depth is installed. The procedure is repeated with all other layers above in the infill panel. At the bays where there were no columns, the anchorage was performed in the vertical RC belts. At frame B, the second variant of the proposed solution for connection was installed, with vertical gaps 2.5cm width and filled with polysterene foam (Figure 4.21).

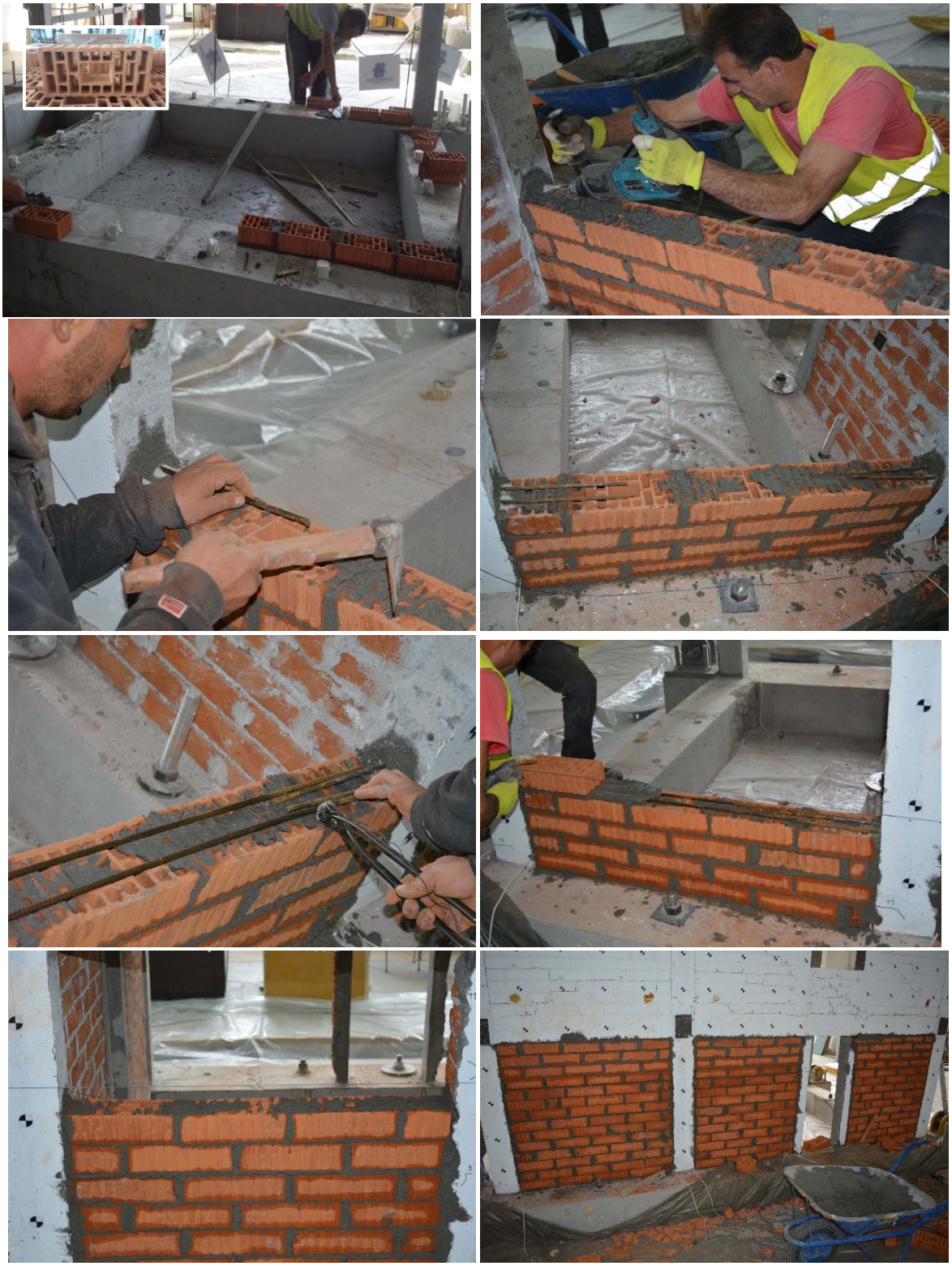

Figure 4.20 Construction of the Model IW-SB – variant solution a)

Figure 4.21 Construction of the Model IW-SB – variant solution b)

d. Instrumentation set-up

The model response was monitored by high speed data acquisition system consisting of 20 accelerometers (ACC), channels 1-20; 20 displacement transducers (LVDT), channels 25-44; 4 linear potentiometers (LP), channels 21-24 and 12 strain gages (SG), channels 45-56, providing information about accelerations at different levels and points, relative displacements, deformations and strains at selected points. The complete instrumentation set-up is presented in Figures 4.22 – 4.25.

The characteristics of used transducers for measuring points are as follows:

- KYOWA MCD-8A AND MCD-16A - Multi conditioner system for stain gage and accelerometers (ACC):
    - KYOWA AS-5GB
      Sensitivity 1V/g full range ± 5.0g frequency response DC to 100 Hz
    - KYOWA AS-20GB
      Sensitivity 1V/g full range ± 20g frequency response DC to 250 Hz
    - KISTLER 8712A5M1
      Sensitivity 1V/g full range ± 5.0g frequency response 0.5 Hz to 8000 Hz
    - PCB 333B50
      ceramic shear ICP® accel, 1000 mV/g, 0.5 to 3k Hz, full range ± 5.0g
- Linear Potentiometers (LP):
    - HSI Model 1850
    - Sensitivity 0.13mV/V/inch full range 15 inch
- LVDT's
    - Macro Sensors Model DS750

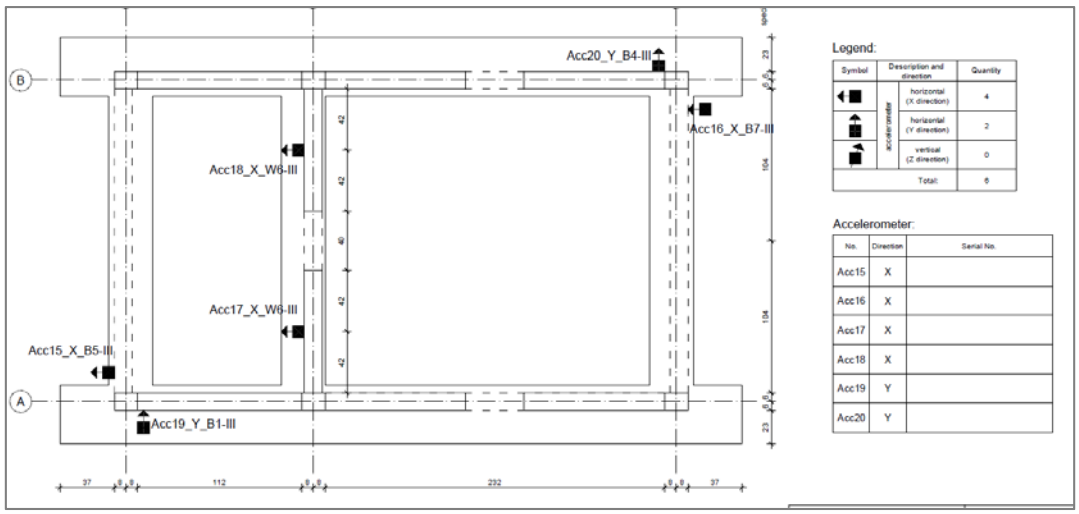

Figure 4.22 Instrumentation of the Model IW-SB - accelerometers (roof level)

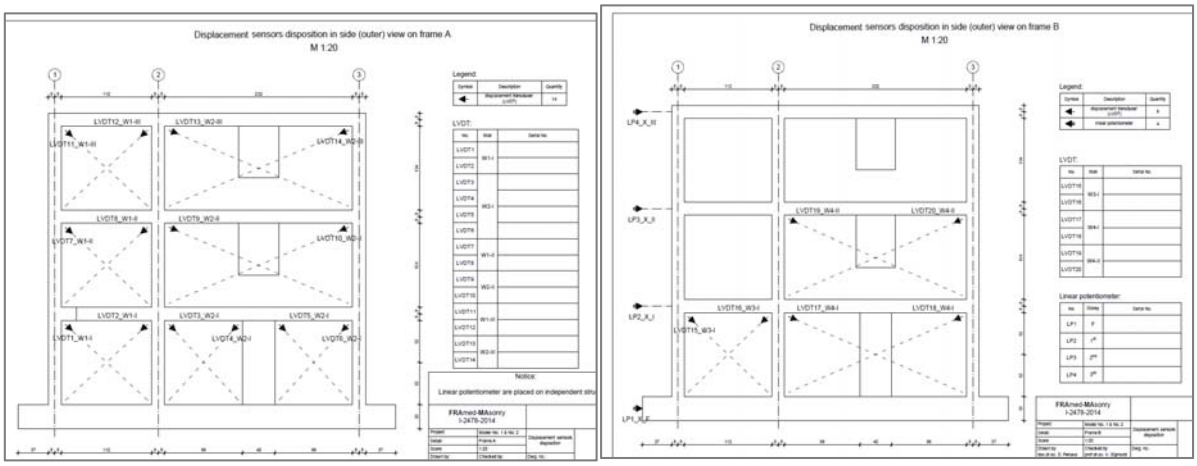

Figure 4. 23 Instrumentation of the Model IW-SB – LVDT and LPs (frame RA and RB)

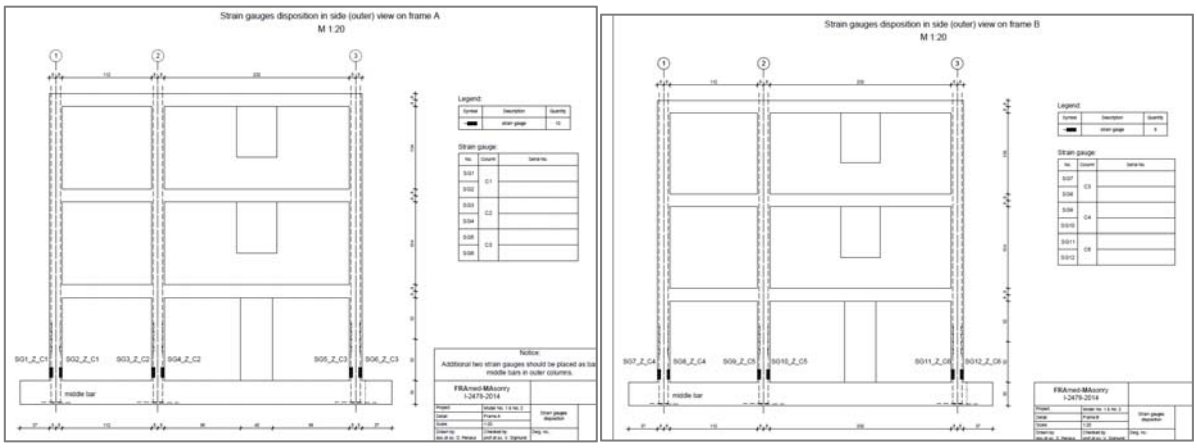

Figure 4.24 Instrumentation of the Model IW-SB – strain gages (frame RA and RB)

Figure 4.25 Instrumentation of the Model IW-SB – view on the shake table

e. Testing protocol and scaling of the earthquake record

The shake table tests of 1:2.5 scaled **Model IW-SB** required tailor-made testing protocol consists of several test phases, in order to investigate the safety and performance of RC frame system with hollow-clay masonry infill walls, in linear and nonlinear range. The testing protocol was consisting of two main phases:

1. Tests for definition of dynamic characteristics of the model, before and at the end of the seismic tests (Table 4.6 - tests 01 and test 14), in order to check stiffness degradation of the model produced by micro or macro cracks developed during the tests – ***resonant frequency search tests***

2. Seismic testing by selected earthquake record until heavy damage. The tests are performed in several steps, increasing the input intensity of the earthquake, (Table 4.6 – tests 02-13), in order to obtain the response in linear range, as well as to define the initial crack state, development of failure mechanism and possible collapse of the model – ***seismic response tests***

After the mounting of the model on the shake table, random excitation test was applied in Y direction of the model. This testing method is based on the concept of white noise input excitation when multi-frequency components uniformly participate in the Fourier amplitude spectrum of input motion within the selected frequency range. Consequently, the model response contains natural frequencies as dominant in Fourier amplitude spectra. In this case, a frequency range from 0.5 - 35 Hz has been selected and has been simulated by the shake table.

Table 4. 6 Sequential order of performed tests - Model IW-SB

Test ID	Test type	Axis	Test parameters
Test01	Sine sweep test	Y	f: 0.5÷35 Hz, a=0.02 g sweep rate: 1 oct/min
Test02_HN5	Time History Seismic test Herceg Novi	Y	Ref. peak acc.: 0.05 g (Y)
Test03_HN10	Time History Seismic test Herceg Novi	Y	Ref. peak acc.: 0.1 g (Y)
Test04_HN20	Time History Seismic test Herceg Novi	Y	Ref. peak acc.: 0.2 g (Y)
Test05_HN30	Time History Seismic test Herceg Novi	Y	Ref. peak acc.: 0.3 g (Y)
Test06_HN40	Time History Seismic test Herceg Novi	Y	Ref. peak acc.: 0.4 g (Y)
Test07_HN60	Time History Seismic test Herceg Novi	Y	Ref. peak acc.: 0.6 g (Y)
Test08_HN70	Time History Seismic test Herceg Novi	Y	Ref. peak acc.: 0.7 g (Y)
Test09_HN80	Time History Seismic test Herceg Novi	Y	Ref. peak acc.: 0.8 g (Y)
Test10_HN100	Time History Seismic test Herceg Novi	Y	Ref. peak acc.: 1.0 g (Y)
Test11_HN120	Time History Seismic test Herceg Novi	Y	Ref. peak acc.: 1.2 g (Y)
Test12_HN140	Time History Seismic test Herceg Novi	Y	Ref. peak acc.: 1.4 g (Y)
Test13_HN160	Time History Seismic test Herceg Novi	Y	Ref. peak acc.: 1.6 g (Y)
Test14	Sine sweep test	Y	f: 0.5÷35 Hz, a=0.02 g sweep rate: 1 oct/min

The ground motion record used for the shake table tests is the ground motion recorded at the Herceg - Novi station during the 15th April 1979 Montenegro earthquake, (Figure 4.26). The earthquake had a moment magnitude of 6.9 and a hypocentral depth of 12 km. To account for the fact that the structure is constructed at 1:2.5 scale, the record was scaled in time by reducing the duration by a factor √2.5. The record was base line corrected and then scaled to match the different levels of peak

ground acceleration (PGA) that were used as input signals for the shake table test, (Table 4.6). In total, 14 tests were performed among which 12 were seismic response tests with PGA increased from 0.05 g up to 1. 6 g. In such a way the complete seismic performance of the structure starting from linear range, appearing of first cracks in the walls up to developing of the failure mechanisms in infill was captured.

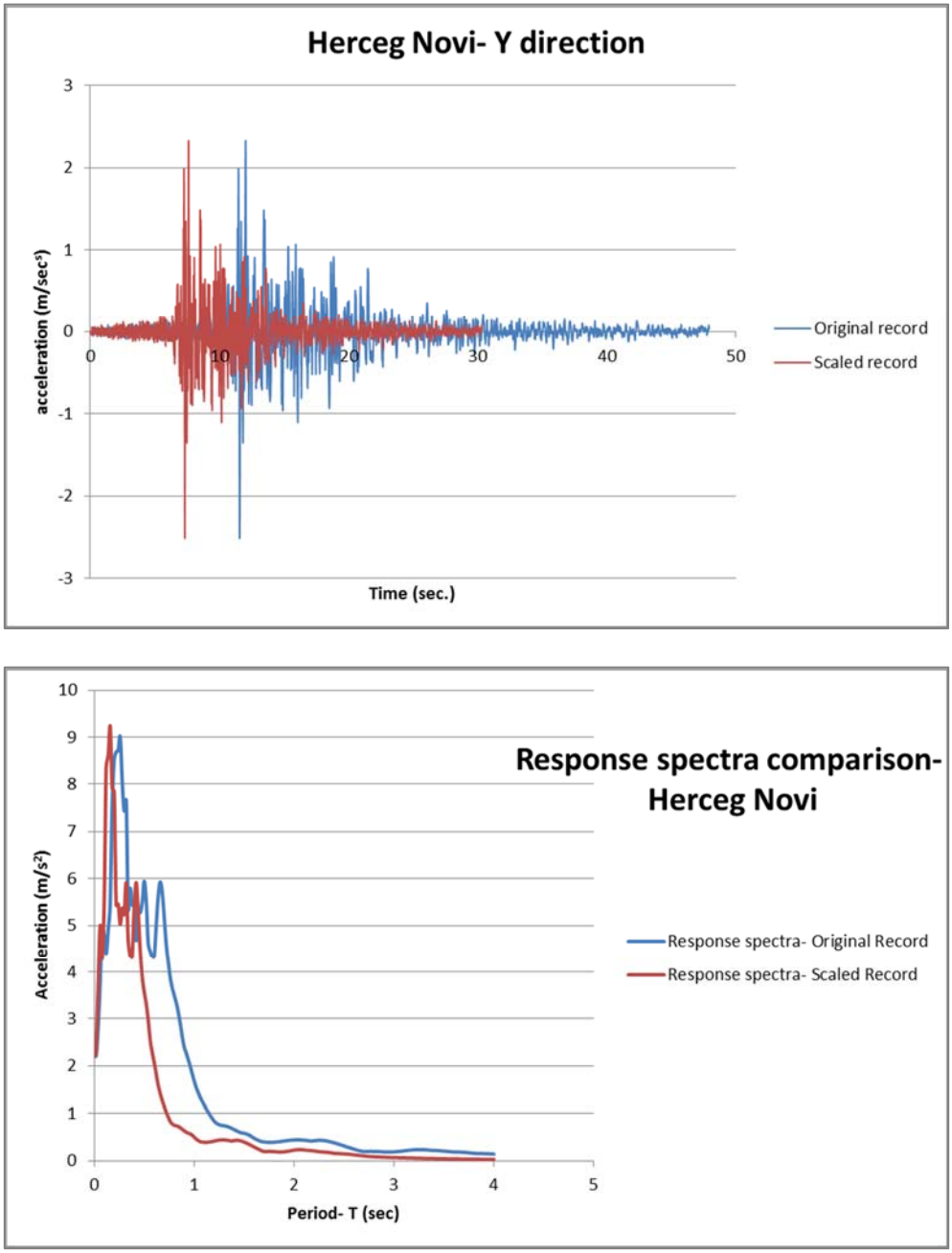

Figure 4.26 Acceleration time histories and frequency content of applied earthquake

4.2.4. Shake table tests and results

It is important to note that all of the measured results which are presented in this section, should be accepted along with the simulated law requirements presented in Table 4.1.

4.2.4.1 Sine sweep tests

Testing of the 1:2.5 scaled Model IW-SB was carried out using equipment which, operating as an integral system, had to provide the following functions:

- generation of programmed motions;
- measurement and recording of the characteristic values of input excitation and of the dynamic performance of the model;
- data processing and presentation.

Testing of the Model IW-SB was performed considering the procedure described in previous section. The selected results obtained from experimental testing are presented further.

Definition of dynamic properties of the Model IW-SB was first step of experimental testing, which enabled acquiring of important information about the stiffness (natural frequencies) of the model. Natural frequency was defined in Y direction of the model, by applying resonant frequency search tests. Frequencies obtained at the test 01 (before starting of the seismic response tests) and at the test 14 (after finishing the last seismic response test with PGA = 1.6 g) are presented in Figure 4.27.

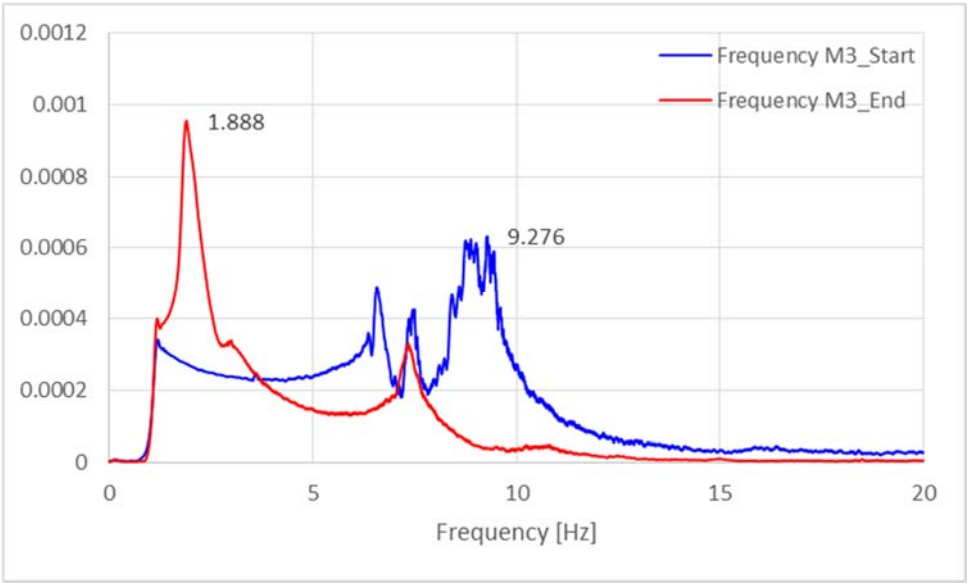

Figure 4.27 Obtained frequencies of the Model IW-SB, before and at the end of the seismic response tests

Table 4.7 represents the frequencies of Model IW-SB. From the results analysis it can be concluded that the frequency of 9.276 Hz at the beginning of tests, after performing all twelve series of seismic

response tests decreases to value of 1.888 Hz. Or, the period of the structure T=0.108 sec increases to a value of T=0.530 sec, which is 4.91 times higher period comparing to the one at the begging of the tests. This emphasizes the reduction of the initial stiffness of the model due to the occurrence of damages, especially in the masonry infill.

Table 4.7 Frequencies of Model IW-SB before and after seismic tests

Model	First Frequency before testing	First frequency after testing
Model IW-SB	9.276 Hz	1.888 Hz (after 1.6g)

Time history of the input motion recorded by the acceleration at the level of the foundation (acc0_System sensor), at the PGA = 1.6 g is given in Figure 4.28.

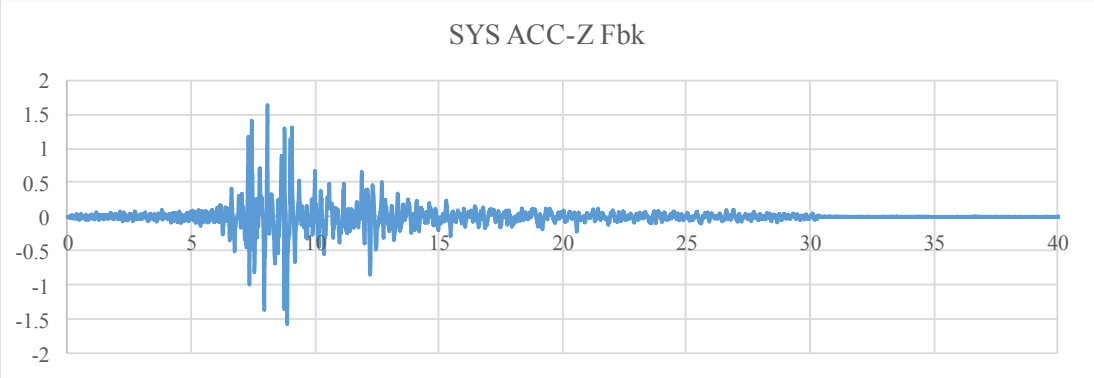

Figure 4.28 Acceleration time history at the level of the platform, (PGA = 1.6 g)

4.2.4.2. Results from shake table tests of Model IW-SB

a. Visual observations of damage of the infill

After each seismic test with different level of excitation, visual observation and marking of the appeared cracks in the infill is performed. Visual observations of the damage in the infill of the frame A where variant solution a), connection with reinforcement bars installed, is given in the Figure 4.29. Until 0.4g no visible cracks could be detected on both the infill panel and bounding frame. This observation coincides with conclusions from researchers that column-to-panel ties could be effective in increasing the ultimate strength and initial stiffness of infilled RC frame structures. It is necessary to point out that minor cracks mainly concentrated on the contact between infill and RC frame appeared around 0.5g.

The high amplitude excitations which were further applied on the model, with peak acceleration ranged from 0.6g up to 1.6g, caused further damage to the infilled frame structure but did not cause collapse neither of the infill panel or RC frame.

This failure mechanism demonstrates that full length steel bars strengthened the infill panel and improved its integrity. The infill panel kept stable because of the six layers of full-length connection bars anchored to columns. Full-length connection bars did improve the in-plane stability of the infill panel under earthquake excitation; however, the deployed steel bars may also change the crack propagation in the infill panel. For PGA =1.6 g, flexural cracks developed in the plastic hinge regions of columns, and the maximum first storey drift ratio reached 2.89%.

It should be pointed out that a reliable connection detailing method could provide stable out-of-plane capacity of infill panels. The infilled frame experienced favorable seismic performance with no damage observed on RC frame members.

Selected results showing damage distribution in the model are presented in the Figure 4.29. Similar conclusions apply for the second variant solution in frame B, which are presented in Figure 4.30).

Figure 4.29 Damage to infill of the Model IW-SB, frame A – infill connection - first variant solution

Figure 4.30 Damage to infill of the Model IW-SB -frame B- infill connection - second variant solution

b. Results from the transducers measurements

Data from acceleration and displacement transducers (Figures 4.31 to 4.38), as well as strain gauges (Figure 4.40) from the reinforcement in the columns are analyzed and results are further presented for three selected PGAs: 0.1g – as low amplitude excitation, 0.6g -as medium amplitude excitation and 1.2 and 1.6g as high amplitude excitation. The original recorded values were double filtered with frequencies 0.3 Hz as lower bandpass and 44 Hz as higher bandpass.

It is important to note that before analyzing the data, the displacement time histories of the linear potentiometer transducers (LP1-LP4) were compared to the displacement time histories obtained from double integration of the acceleration records. Both graphs fitted very well and in further analysis the linear potentiometers measurements were used.

Maximum displacements on the top as well measured maximum interstory drifts for the selected excitations and presented in Table 4.8. From the presented graphs it can be concluded that displacements values are in the range of 2 mm at the top of the structure for 0.1g, 7 mm for 0.6g, 38 mm for 1.2g and 52 mm for 1.6g.

Further on, base shear vs top displacement diagrams are elaborated (Figs 4.45 – 4.49). It is noted that the displacement time histories for LP-01 are in fact the referent displacements at the structure foundation, which represent the referent point for calculation the floor displacements from other channels (LP-02 – LP04).

-low excitation (0.1g)

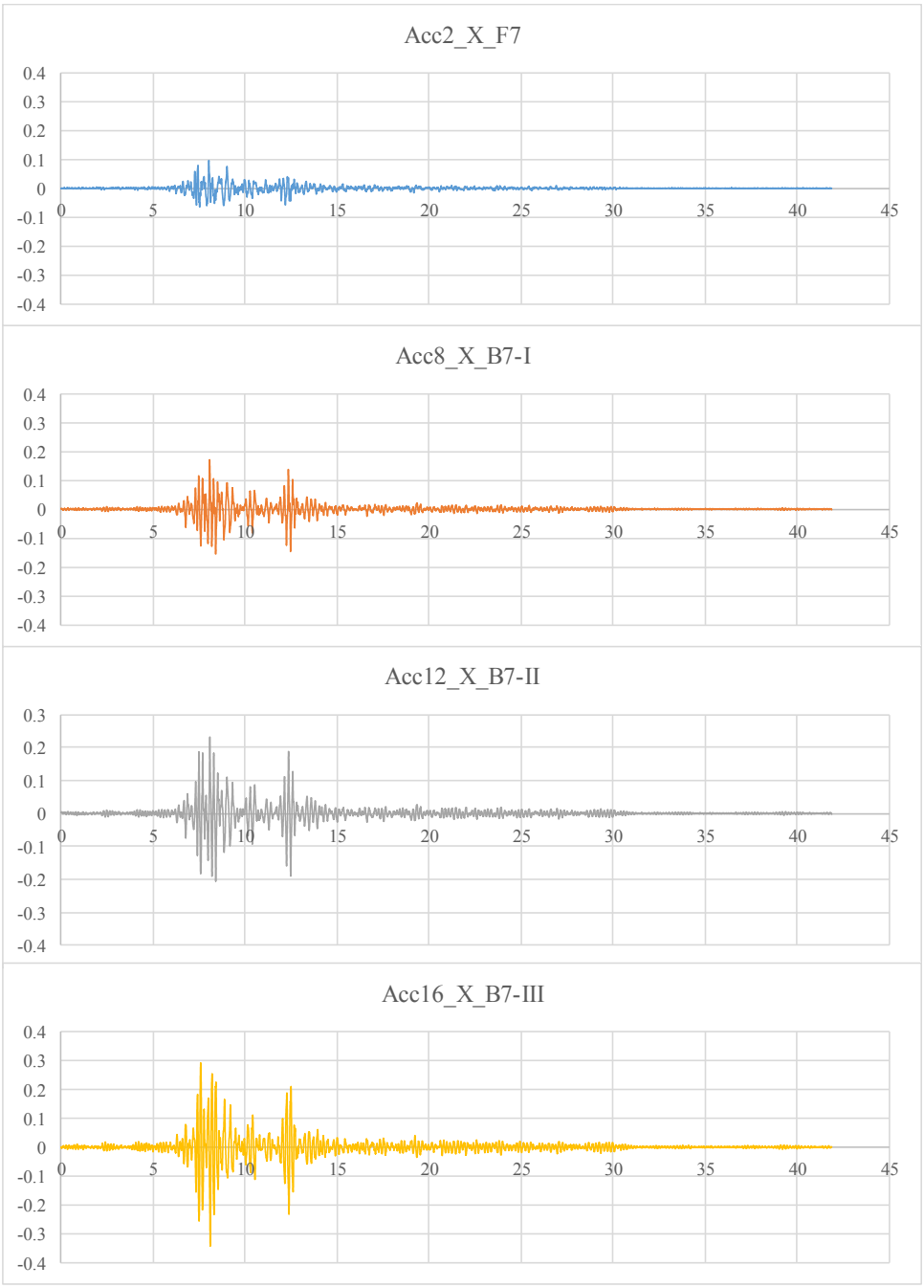

Figure 4.31 Acceleration time histories at each floor level for test No03_HN10 (0.1g)

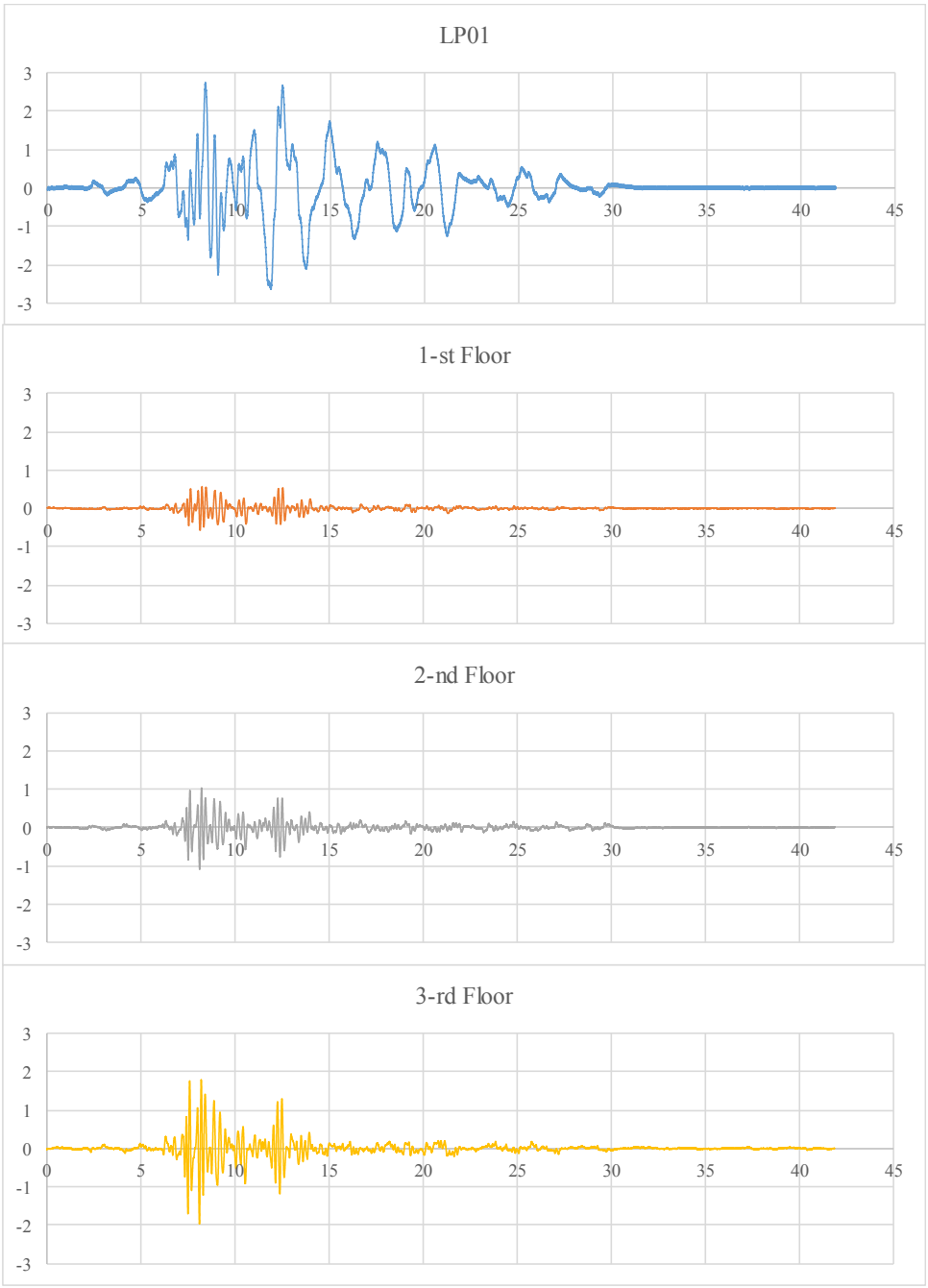

Figure 4.32 Displacement time histories at each floor level for test No03_HN10 (0.1g)

-medium excitation 0.6g

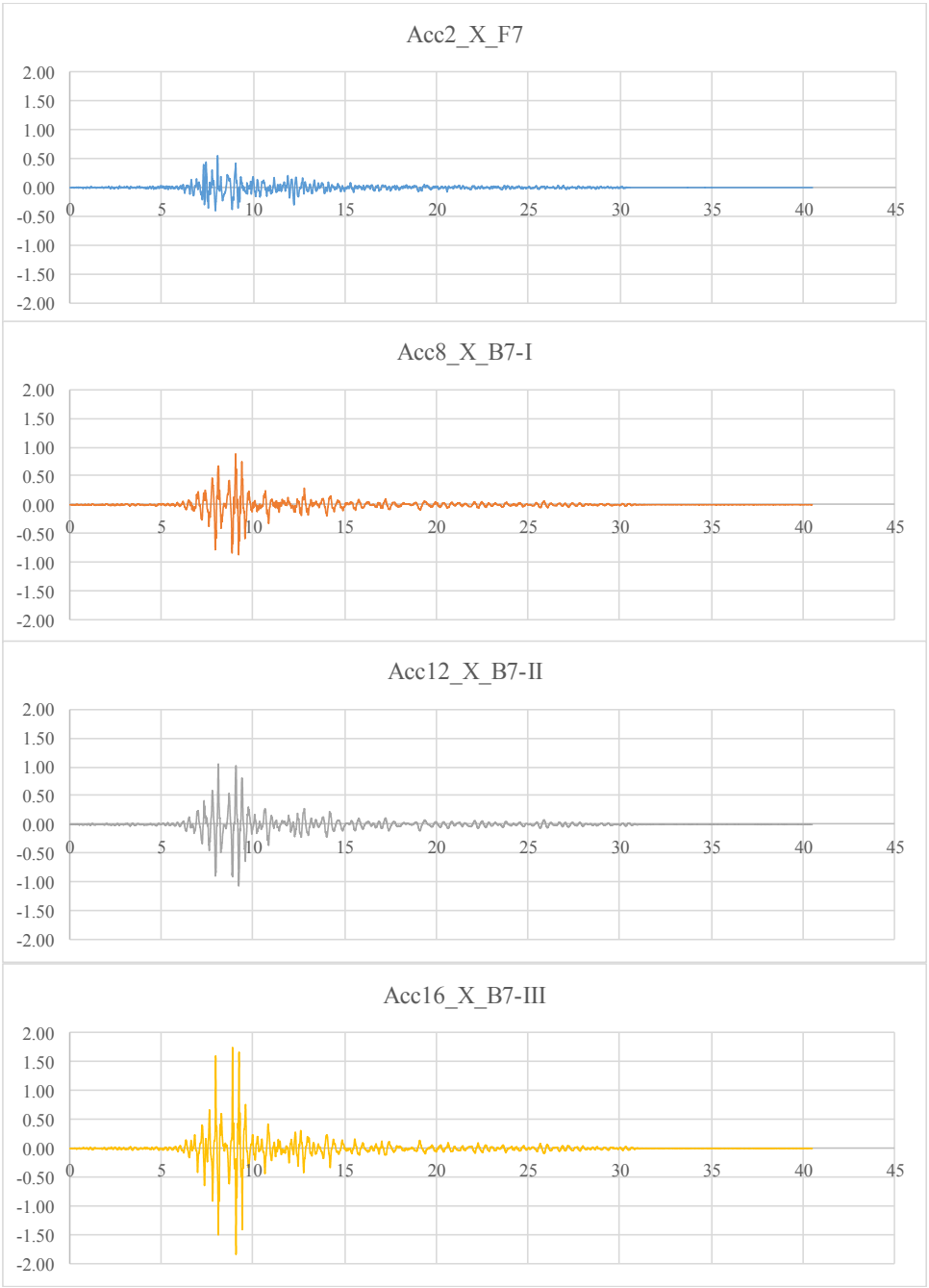

Figure 4.33 Acceleration time histories at each floor level for test No07_HN60 (0.6g)

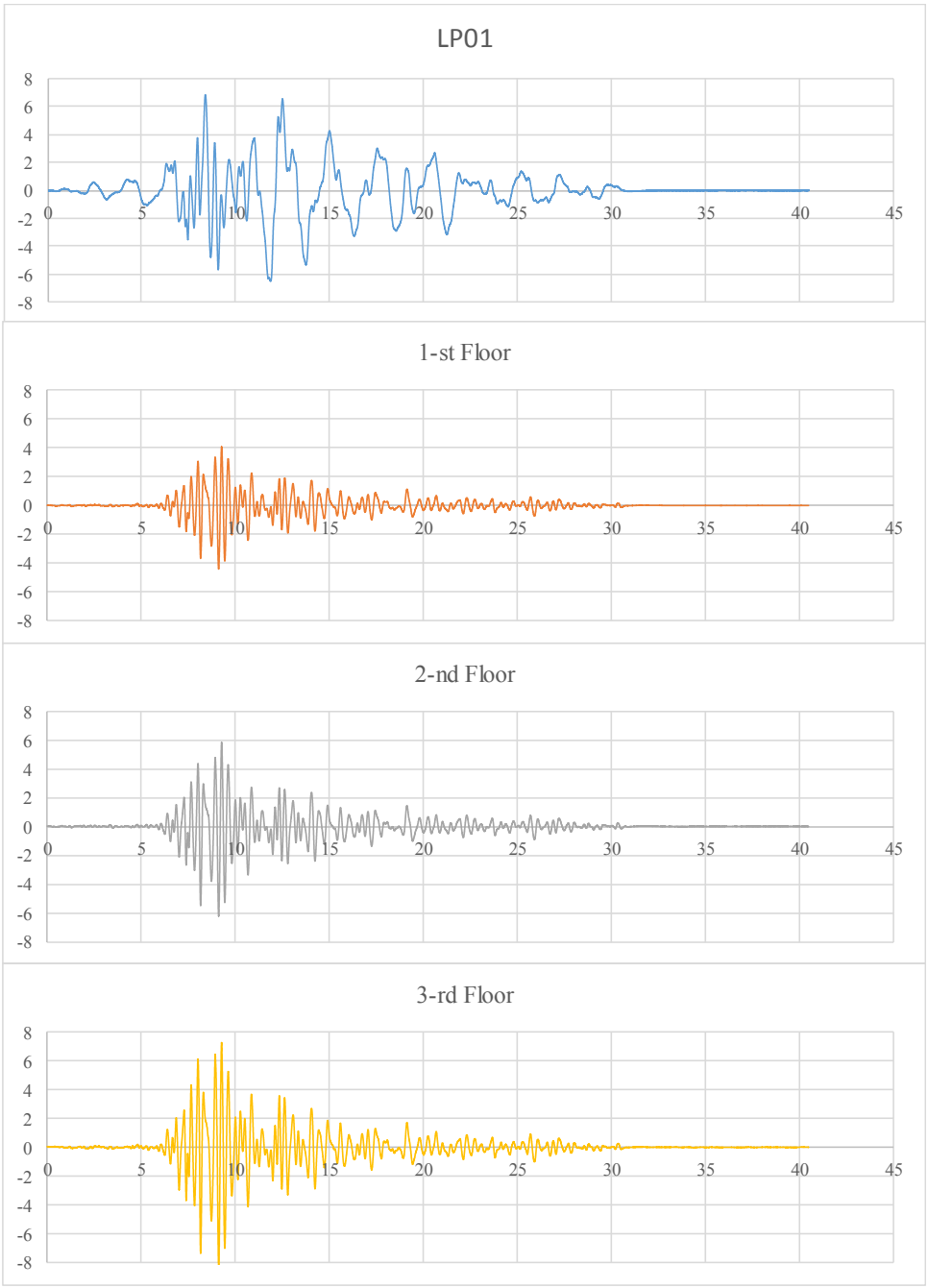

Figure 4.34 Displacement time histories at each floor level for test No07_HN60 (0.6g)

-high excitation 1.2g

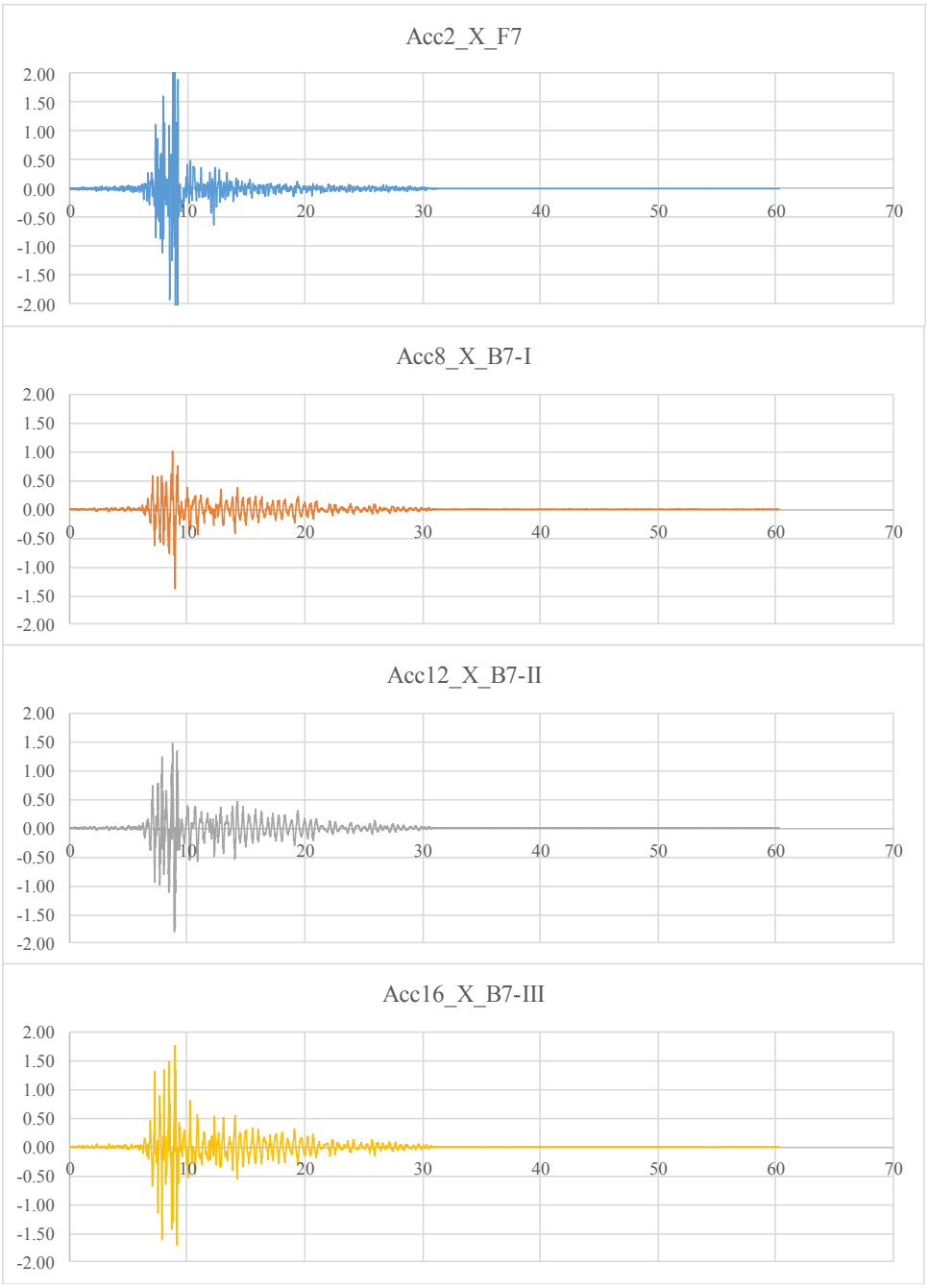

Figure 4.35 Acceleration time histories at each floor level for No11_HN120 (1.2g)

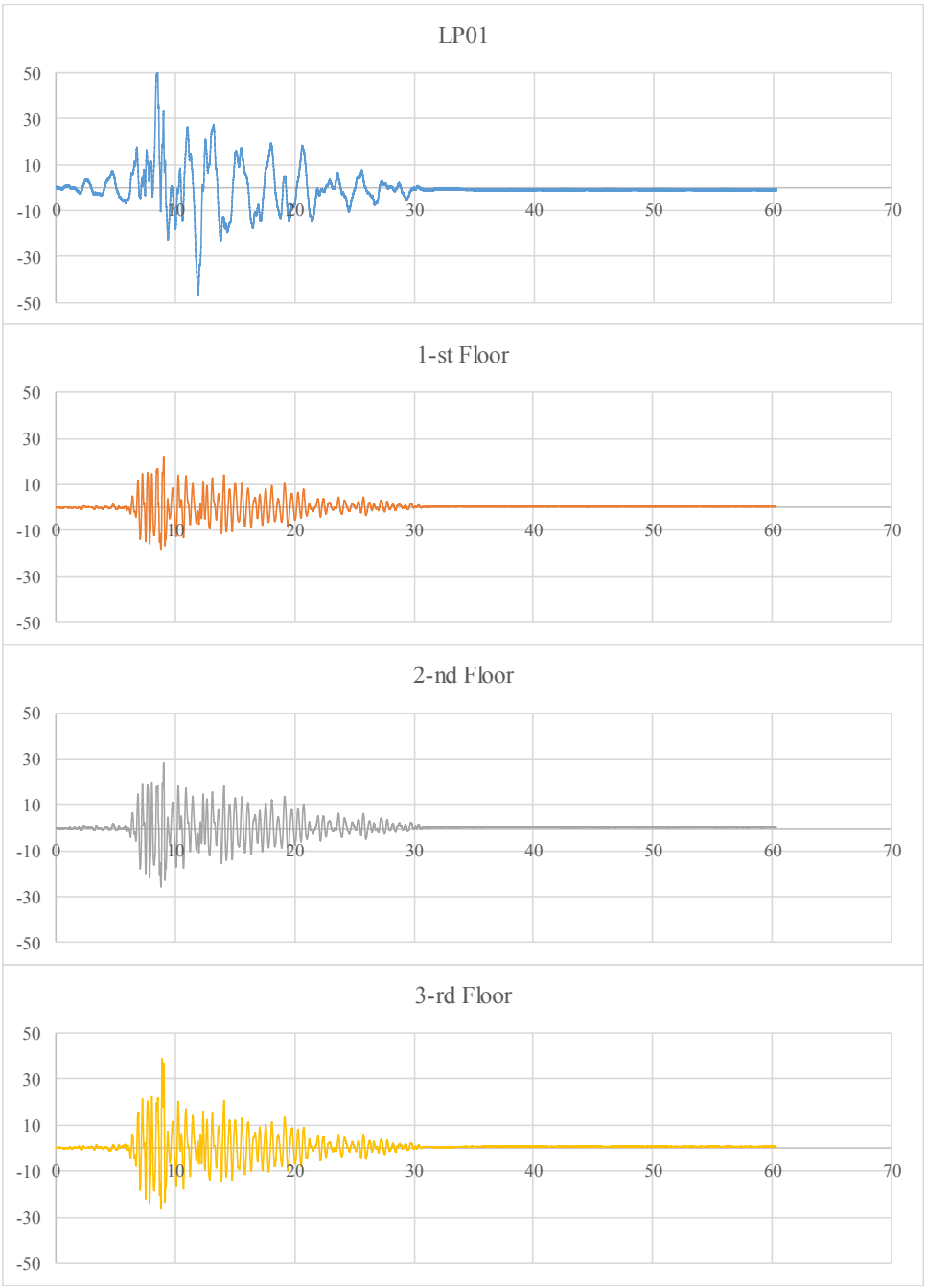

Figure 4.36 Measured maximum and minimum displacements at each floor level for test No11_HN120 (1.2g)

-maximum excitation 1.6g

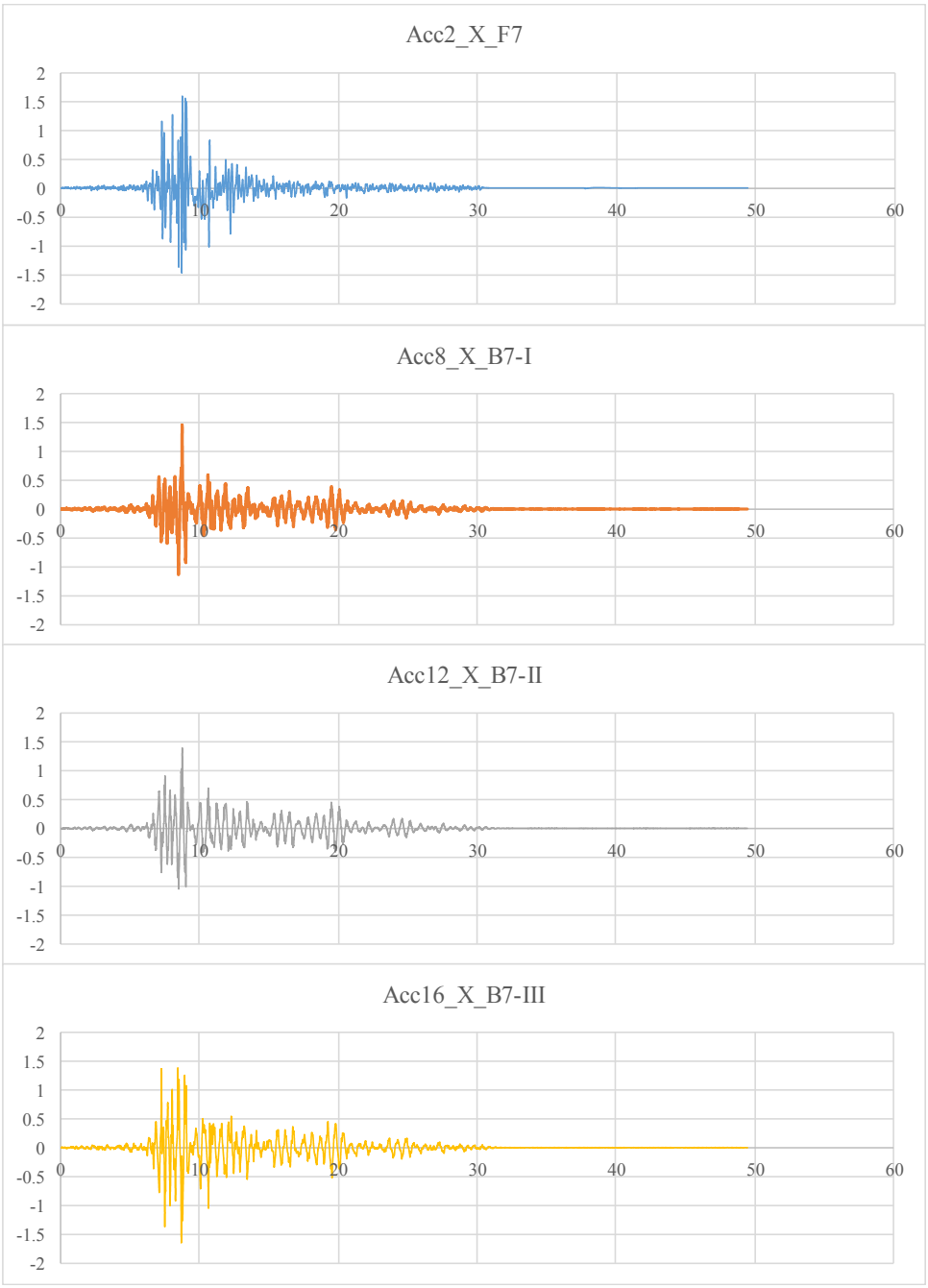

Figure 4.37 Acceleration time histories at each floor level for test No13_HN160 (1.6g)

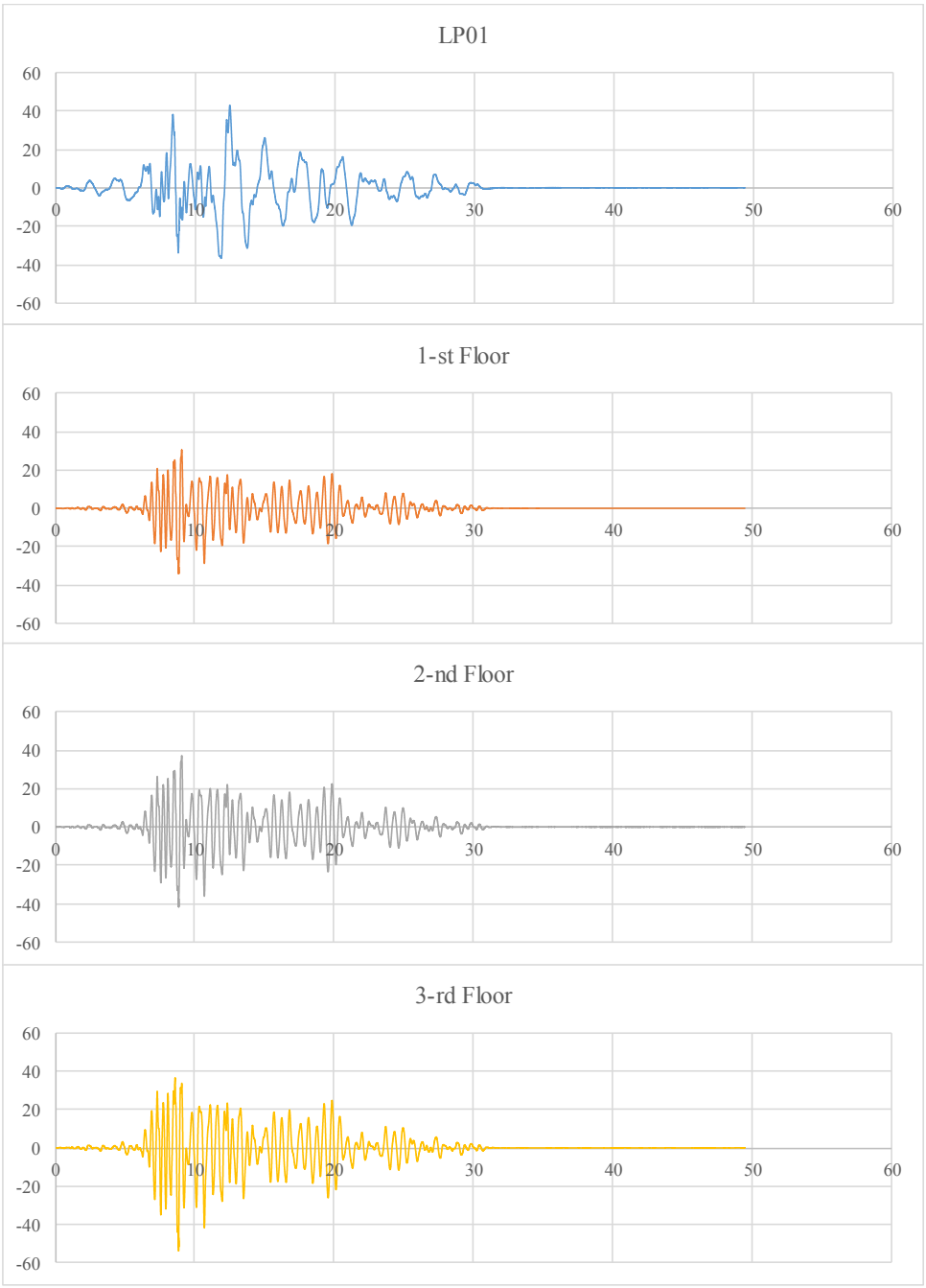

Figure 4.38 Displacement time histories at each floor level for test No13_HN160 (1.6g)

- strain gauges results

Figure 4.39 represents the maximum measured strain time histories for the 0.05g, 0.6g. 1.2g and 1.6 g. Analyzing the strain gauges measurement it was observed that for level 0.6g there is yielding of the reinforcement only at one column with value of the strain of 2.5 ‰. For 1.20g the maximum value of the strain is 3.9 ‰, and for the 1.60g is 4.41 ‰.

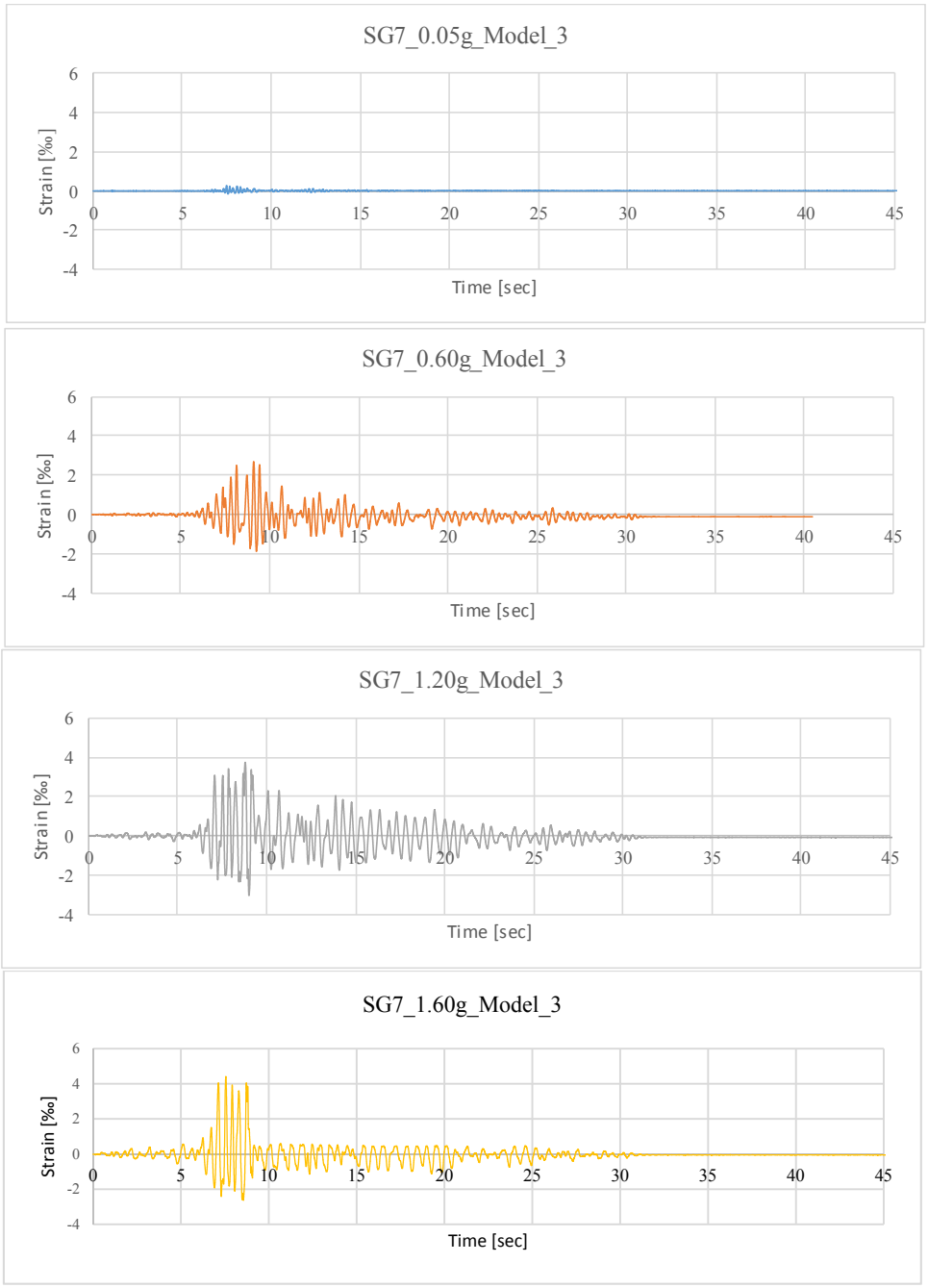

Figure 4.39 Measured strains for test No02_HN005 (0.05g), No07_HN060 (0.60g), No11_HN120 (1.2g), No13_HN160 (1.6g)

-maximum floor displacements

For the selected earthquake excitation measured maximum and minimum displacements on floors are presented on the further graphs (Figure 4.40-4.43). It is important to note that these values are absolute maximum values and does not mean that they are necessary occurred at the same time. From the presented graphs it can be concluded that the values of the maximum displacements increase with the extension of the input motion.

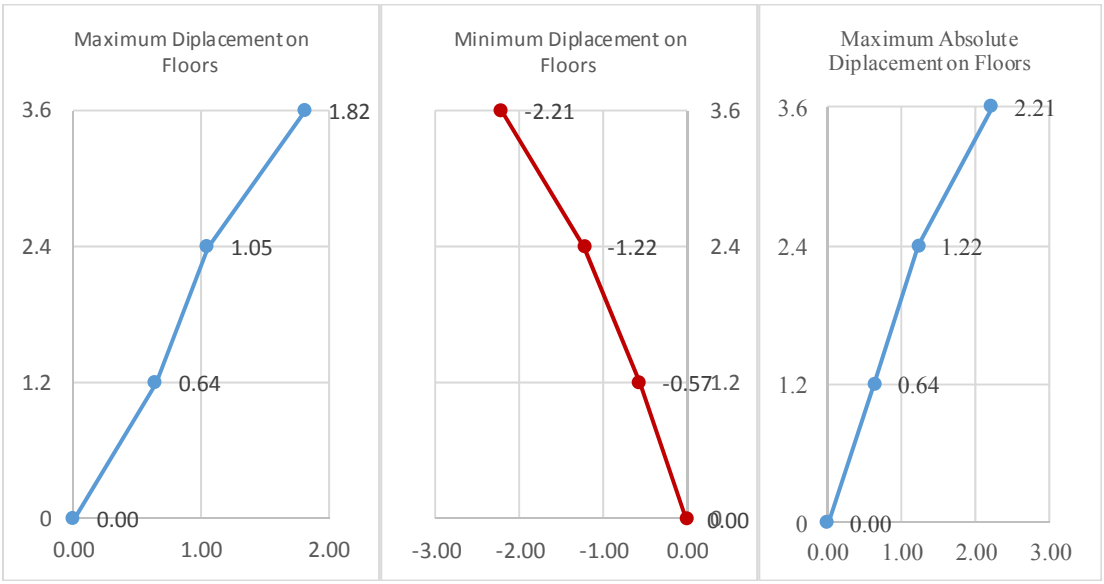

Figure 4.40 Measured maximum and minimum displacements at each floor level for test No03_HN10 (0.1g)

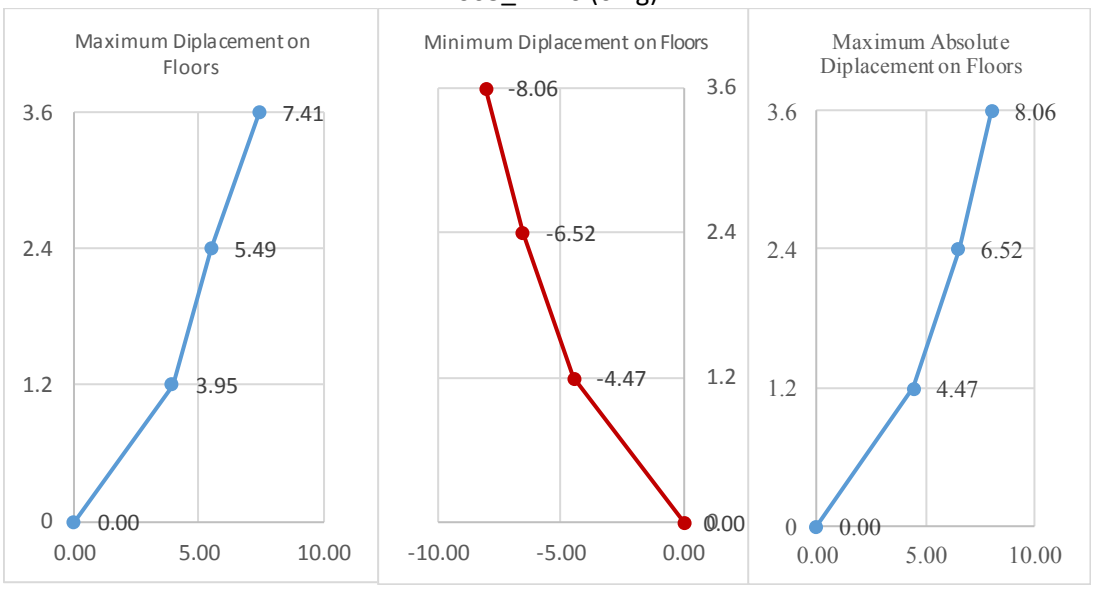

Figure 4.41 Measured maximum and minimum displacements at each floor level for test No07_HN60 (0.6g)

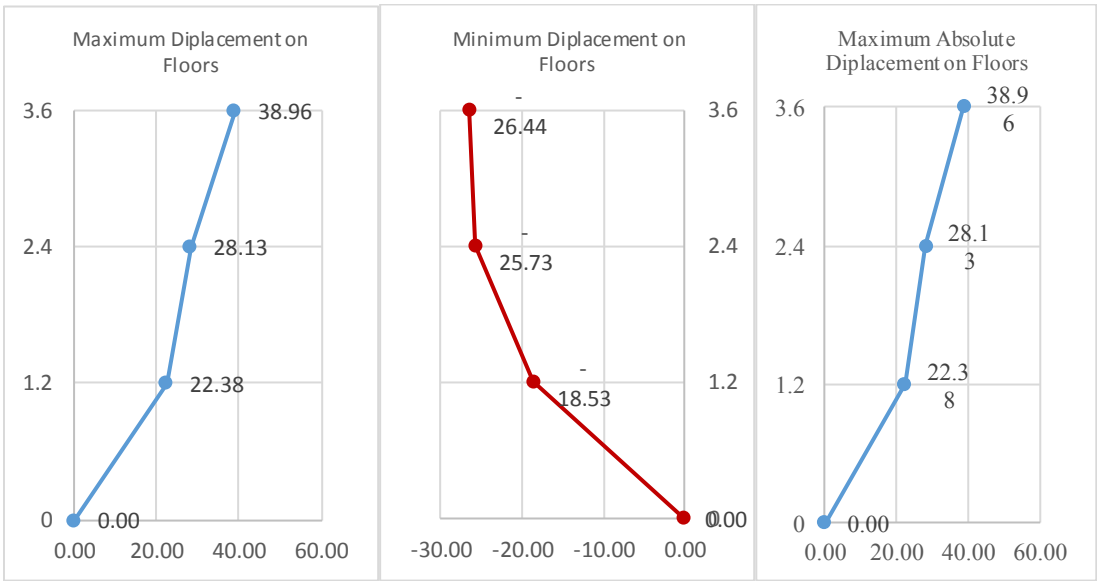

Figure 4.42 Measured maximum and minimum displacements at each floor level for test No11_HN120 (1.2g)

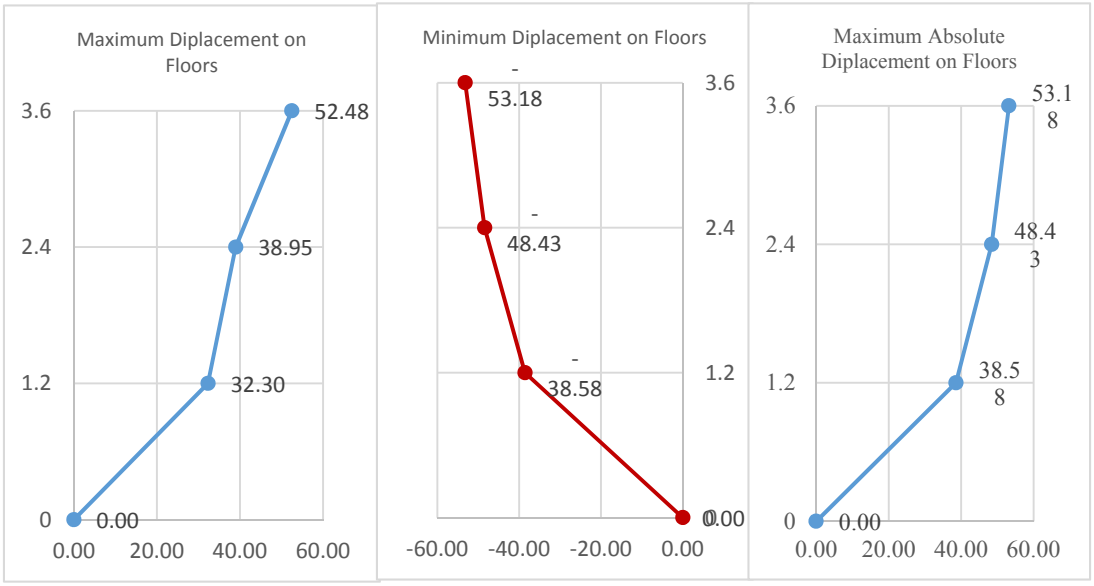

Figure 4.43 Measured maximum and minimum displacements at each floor level for test No13_HN160 (1.6g)

-interstory drifts

Interstory drifts are more valuable parameter for the performance of the structure. They are calculated based on the LP measurement on each floor and are presented in Table 4.8 in percentage for each level of excitation.

Table 4. 8 Maximum measured interstory drift ratio for each level of seismic intensity.

PGA	Interstory drift ratio [%]		
	1st floor	2nd floor	3rd floor
5%	0.02	0.02	0.03
10%	0.05	0.05	0.09
20%	0.10	0.10	0.10
30%	0.18	0.16	0.16
40%	0.23	0.16	0.15
60%	0.37	0.17	0.13
70%	0.67	0.29	0.20
80%	0.77	0.45	0.38
100%	1.43	0.39	0.44
120%	1.86	0.48	0.69
140%	2.59	0.48	0.67
160%	2.89	0.82	0.44

- base shear vs top displacement

In order to represent the seismic performance of the Model IW-SB under shake table tests, base shear vs top displacement graphs are plotted in Figures 4.44-4.48. Base shear force is calculated from the accelerometers measurement at the ground level multiplied by the mass of the model. The graphs clearly represent the seismic performance of the structure, the degradation of the stiffness and nonlinear behavior of the structure.

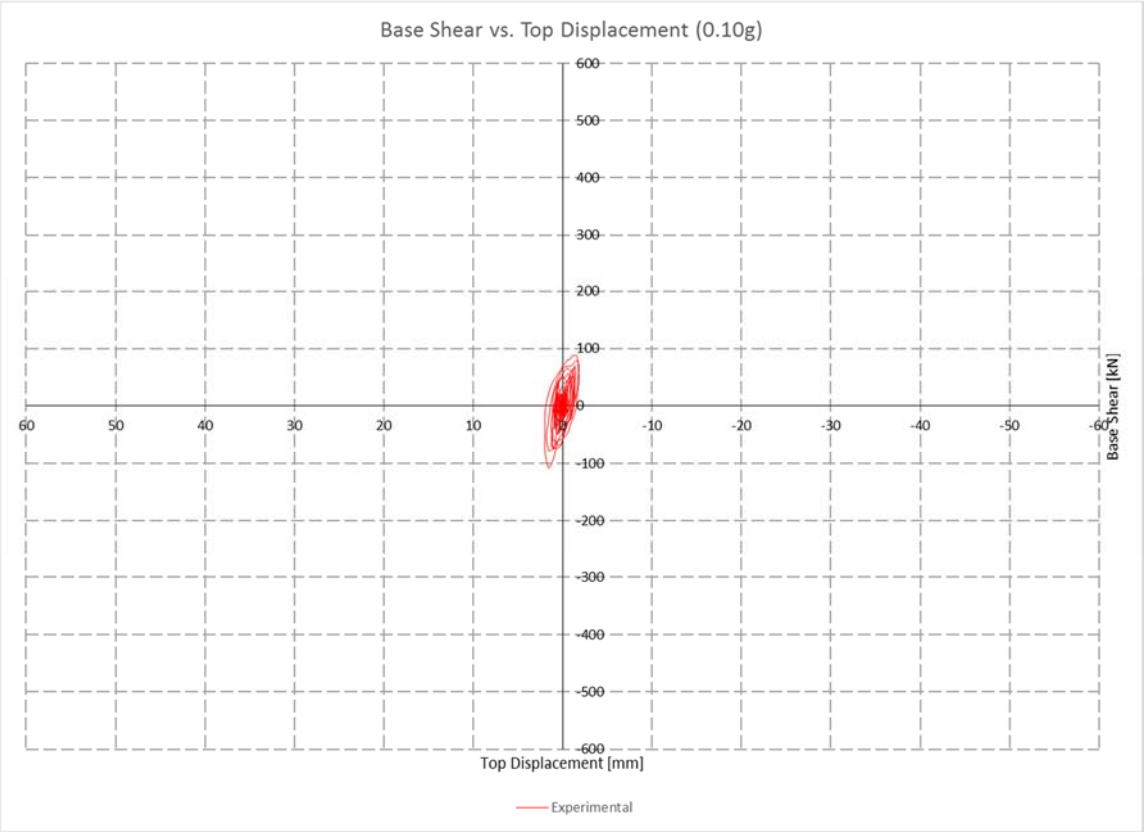

Figure 4.44 Experimental Base shear vs. top displacement for 0.10g

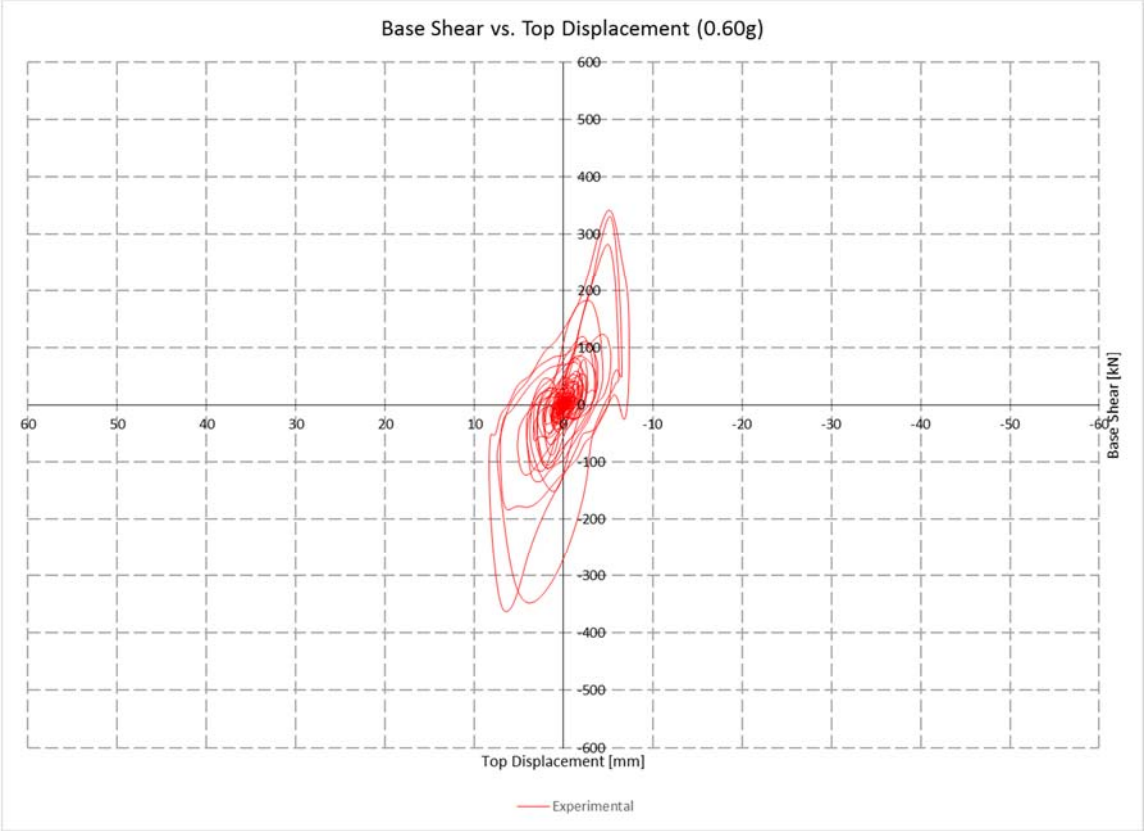

Figure 4.45 Experimental Base shear vs. top displacement for 0.60g

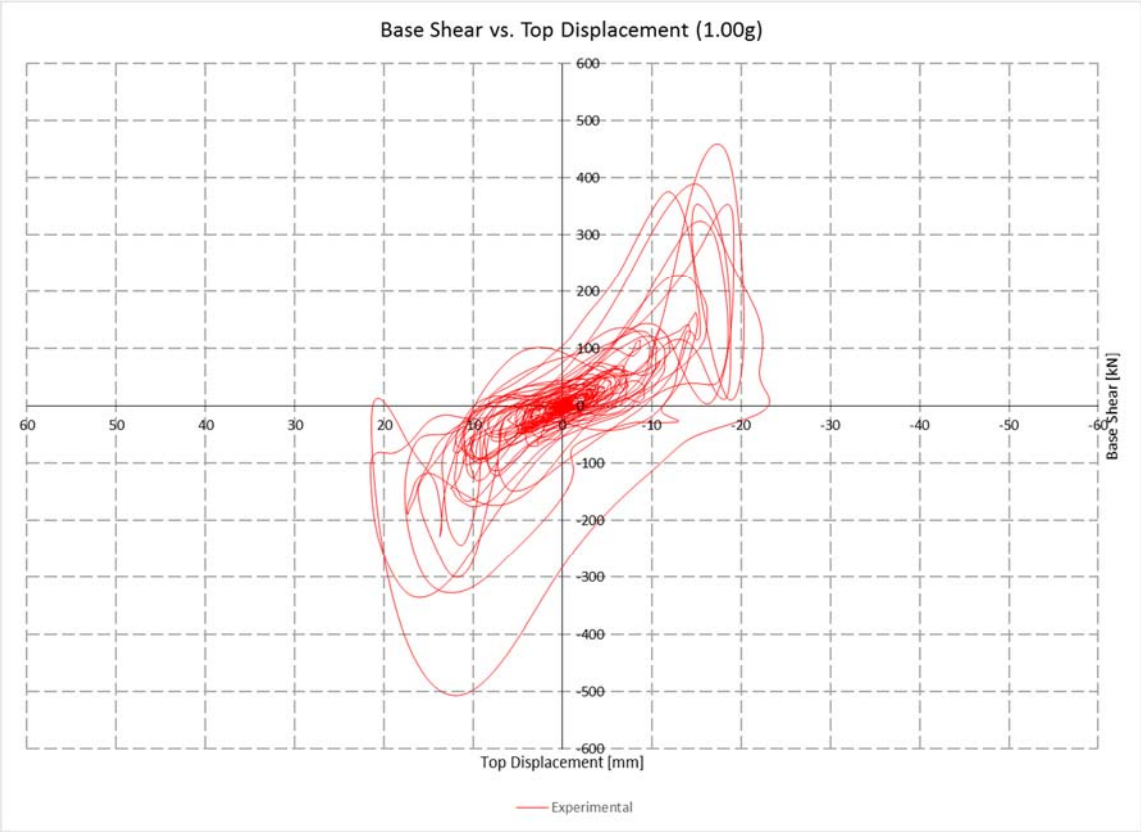

Figure 4.46 Experimental Base shear vs. top displacement for 1.00g

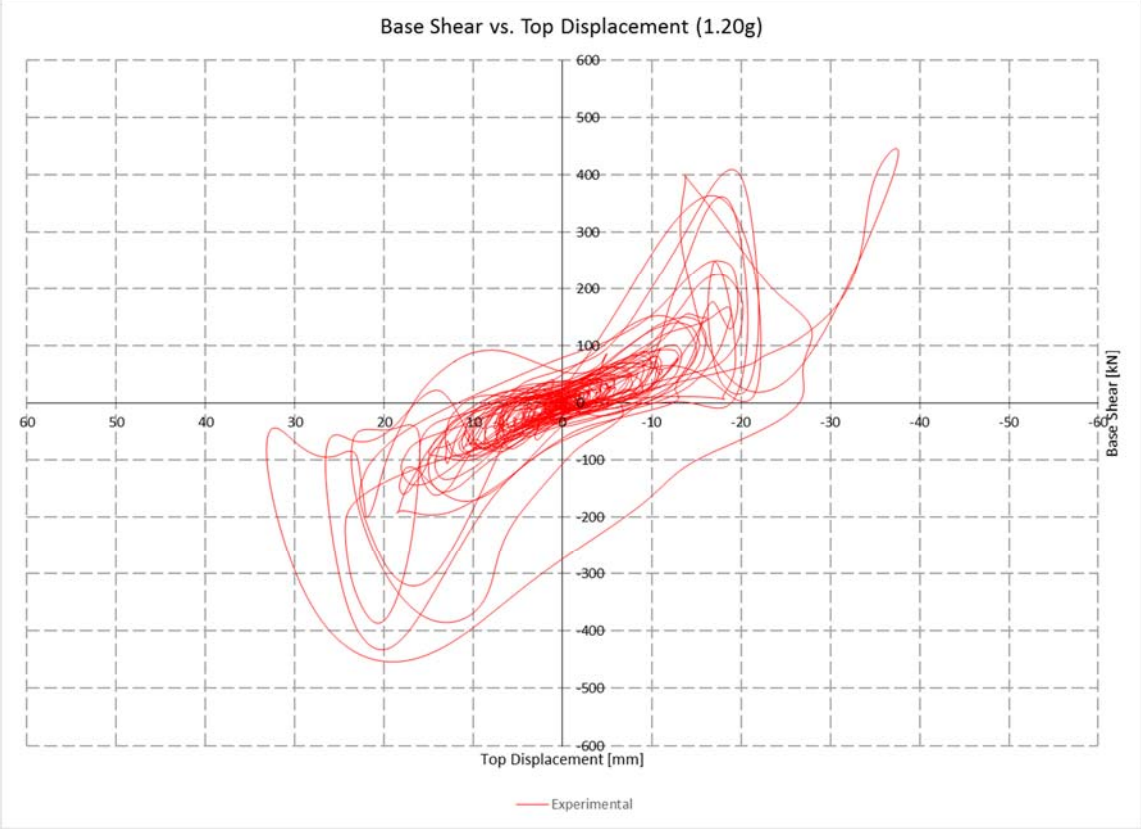

Figure 4.47 Experimental Base shear vs. top displacement for 1.20g

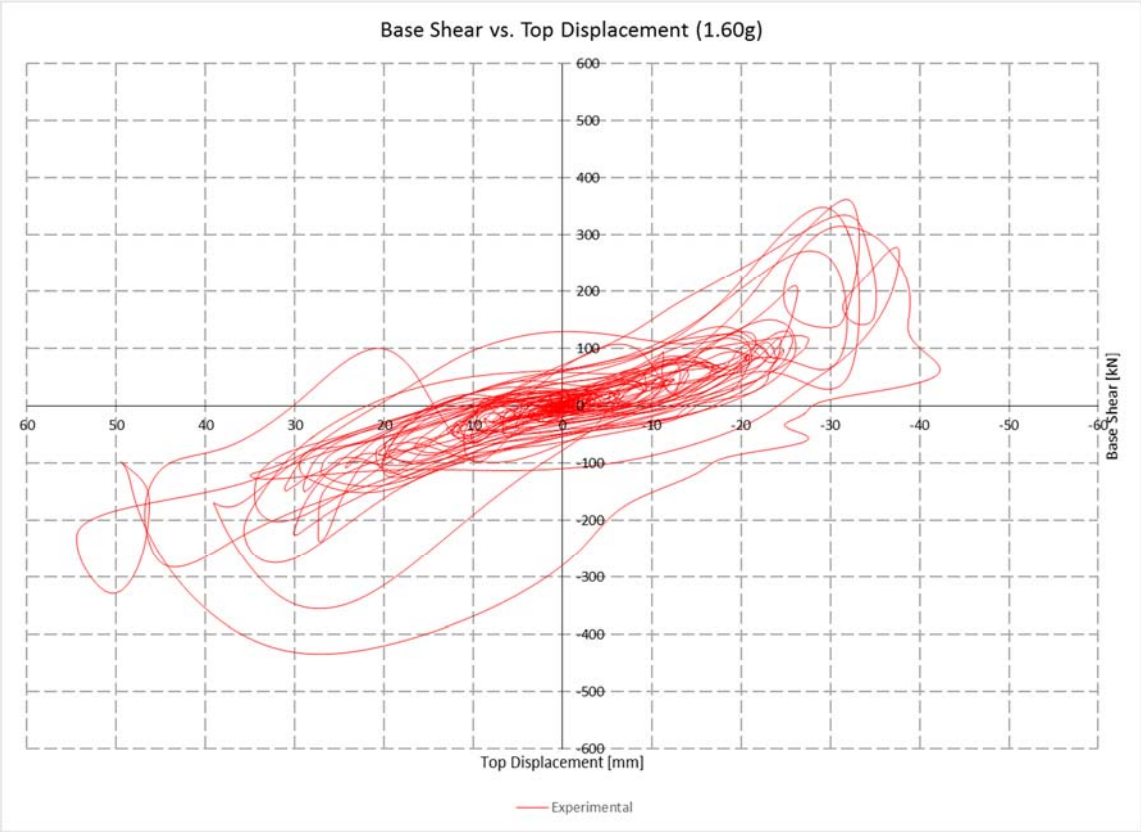

Figure 4.48 Experimental Base shear vs. top displacement for 1.60g

4.2.4.3 Comparison of shake table tests results – Model IW-SB with innovative infill connections versus Model 1 (referent model)

-sine sweep tests - natural frequencies

For Model 1 (as a referent model for comparison) sine sweep tests are performed at the beginning and after the test with earthquake excitation of 0.60g. The values of the frequency of the model were 8.785 Hz and 3.047 Hz respectively, or the frequency is decreased for 2.90 times. For this model, sine sweep test aren't performed after the last series of seismic test of 1.20g earthquake excitation.

It can be seen that the frequency of the Model IW-SB, at the start of the testing, is around 5.6% bigger than for Model 1 (Figure 4.49, Table 4.9), which is expected having in mind the implemented (proposed) connection of the infill walls.

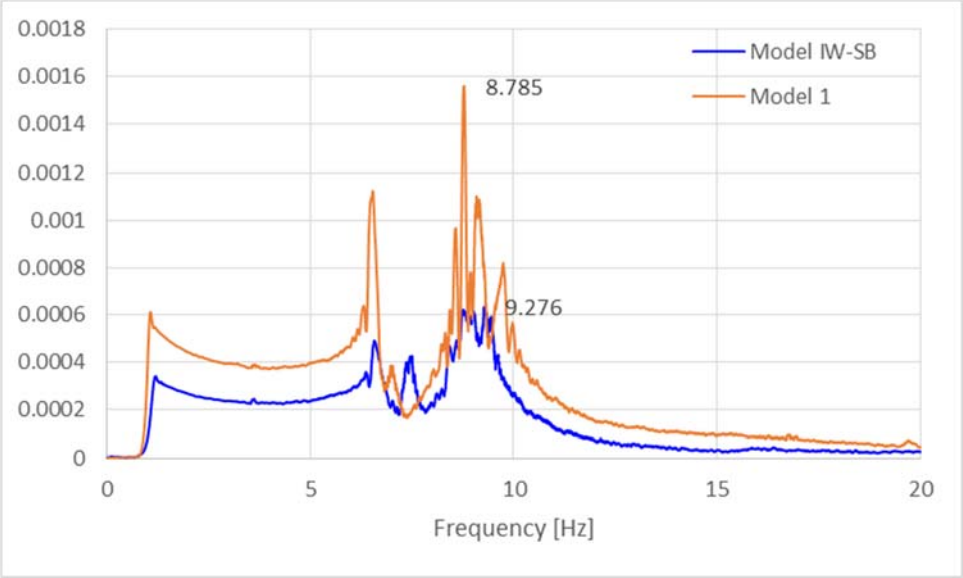

Figure 4. 49 Comparison of the obtained frequencies of the Model IW-SB and Model 1, before testing

Table 4. 9 Frequencies of Model IW-SB and Model 1 before and after seismic tests

Model	Natural Frequency before testing	Natural frequency after testing
Model IW-SB	9.276 Hz	1.888 Hz (after 1.6g)
Model 1	8.785 Hz	3.047 Hz (after 0.6g)

-visual observation of the damages

Presented further are the photos of damage in the infill during shake table tests in both models, (Fig. 4.50). For input acceleration less than 0.4 g, the structure experienced negligible-

to-slight damage in the first story walls (based on the definitions in (ATC, 1998; Grünthal et al., 1998). At the level of 0.4 g in both test series, cracks began to form around the perimeter of the infill walls with some crushing at the corners, (Figure 4.50a).

Model 1	***Model IW-SB***
a 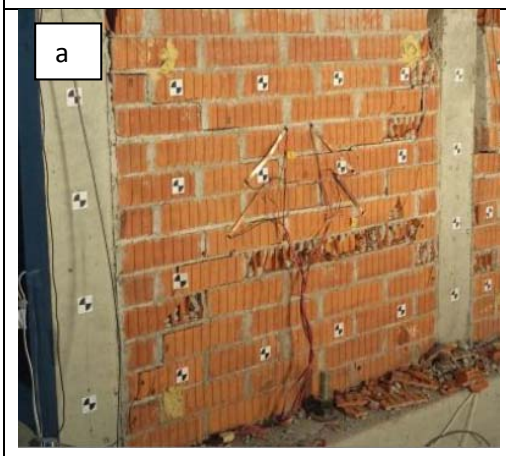	
b 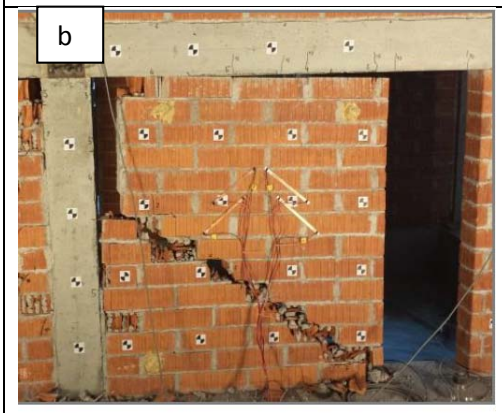	

Figure 4.50 Observed in-plane damage a) after 0.4g and b) after the final tests of 1.2 g/1.6g, for Model 1 and Model IW-SB

At 0.8 g in Model 1, the first and second story infill walls began to develop inclined cracks at isolated locations. These cracks formed in both directions. At the end of testing of Model 1 (PGA=1.2g), the infill wall adjacent to the door opening had collapsed, and significant diagonal cracks occurred in the infill panels, (Figure 4.50b, left).

In contrast, infill damage at the end of the testing of Model IW-SB was only concentrated on the connections of the panel to the RC frame. The infill panels in Model IW-SB were being

engaged more effectively in resisting the lateral demands, and kept their integrity until the last level of excitation of 1.6g. This observation contributed to the statement that with reinforcement bars the seismic capacity and in plane and out of plane stability of the infill is significantly improved, (Figure 4.50b, right).

-interstory drifts

As mentioned in previous sections, interstory drift ratio were calculated for each level of seismic excitation based on the LP measurements from the tests. These drifts were compared with results obtained for Model 1 and Model 2, published by Guljas et al. (2018). The numerical values of all drifts are given in the Table 4.9 and illustrated in the Figs 4.51-4.56. It can be observed that the interstory drifts at Model IW-SB are lower than that of Model 1 which indicates to the conclusion that the proposed method for connection between the infill and the RC frame significantly improves the seismic performance of the overall structure. Regarding Model 2, which is built with solid clay infill, for lower and intermediate amplitude excitation, Model IW-SB has higher values of drifts which is expected having in mind the higher stiffness of solid clay masonry in general. Yet, for the highest amplitude excitation, Model 2 in some cases goes beyond Model IW-SB with the interstory drifts, which means that the new proposed Model IW-SB can sustain very high level of excitation without causing significant damage and large plastic deformation.

Table 4.10 Maximum interstory drifts for Model IW-SB compared with Model 1 and Model 2, (Guljas et al, 2018)

Model IW-SB	Interstory drift ratio [%]			Model 1	Interstory drift ratio [%]			Model 2	Interstory drift ratio [%]		
	1st floor	2nd floor	3rd floor		1st floor	2nd floor	3rd floor		1st floor	2nd floor	3rd floor
5%	0.02	0.02	0.03	5%	0.04	0.05	0.05	5%	0.03	0.04	0.03
10%	0.05	0.05	0.09	10%	0.07	0.09	0.08	10%	0.05	0.07	0.06
20%	0.10	0.10	0.10	20%	0.10	0.09	0.08	20%	0.10	0.09	0.06
30%	0.18	0.16	0.16	30%	0.21	0.15	0.23	30%	0.08	0.11	0.08
40%	0.23	0.16	0.15	40%	0.28	0.26	0.26	40%	0.12	0.14	0.13
60%	0.37	0.17	0.13	60%	0.43	0.26	0.28	60%	0.14	0.14	0.12
70%	0.67	0.29	0.20	70%	0.73	0.37	0.33	70%	0.20	0.17	0.17
80%	0.77	0.45	0.38	80%	0.93	0.47	0.41	80%	0.30	0.26	0.26
100%	1.43	0.39	0.44	100%	1.66	0.72	0.45	100%	0.93	0.50	0.93
120%	1.86	0.48	0.69	120%	2.55	0.84	0.78	120%	1.25	0.63	1.22
140%	2.59	0.48	0.67	140%	/	/	/	140%	1.63	0.76	1.50
160%	2.89	0.82	0.44	160%	/	/	/	160%	/	/	/

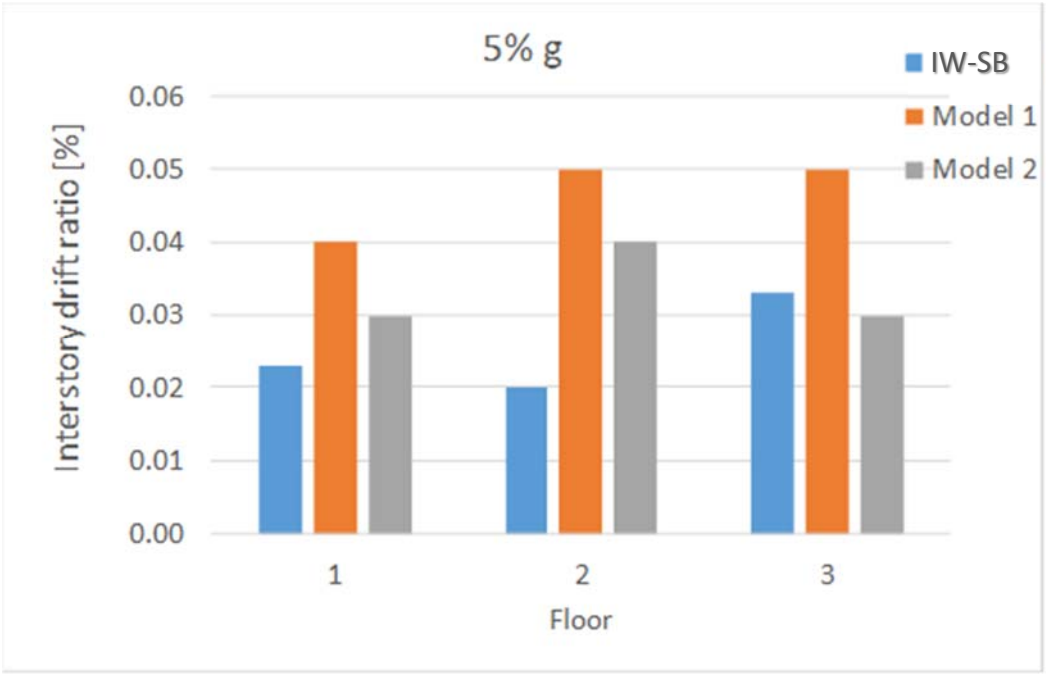

Figure 4.51 Interstory drift comparison of Model IW-SB (this study) with Model 1 and Model 2 from FRAMA project (Guljas et al. 2018) for 5 % g

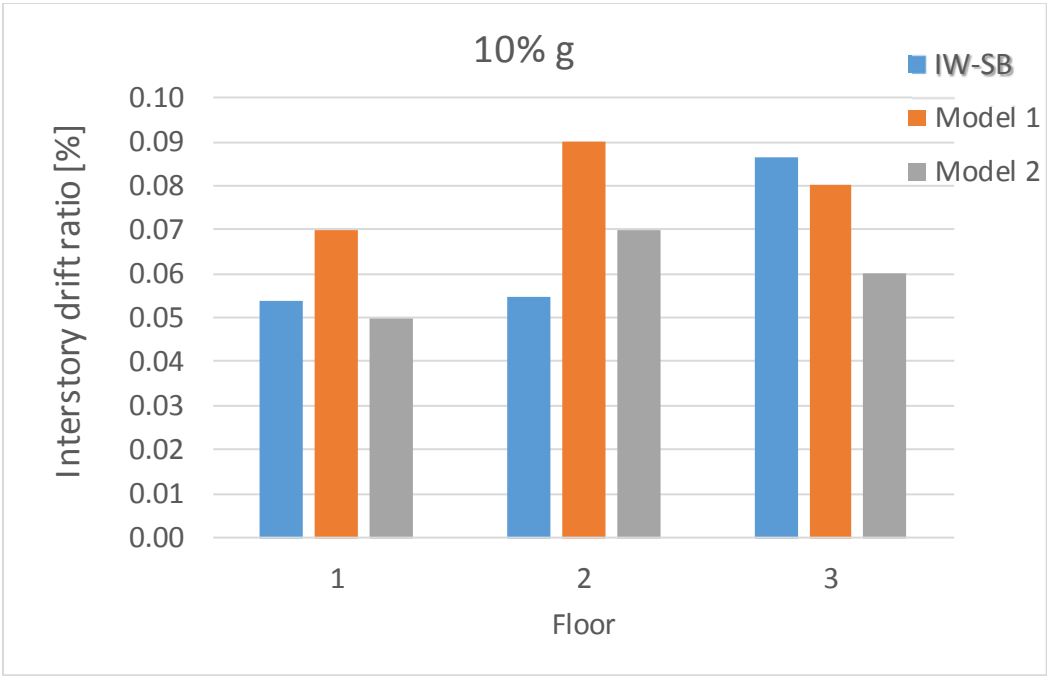

Figure 4.52 Interstory drift comparison of Model IW-SB (this study) with Model 1 and Model 2 from FRAMA project (Guljas et al. 2018) for 10 % g

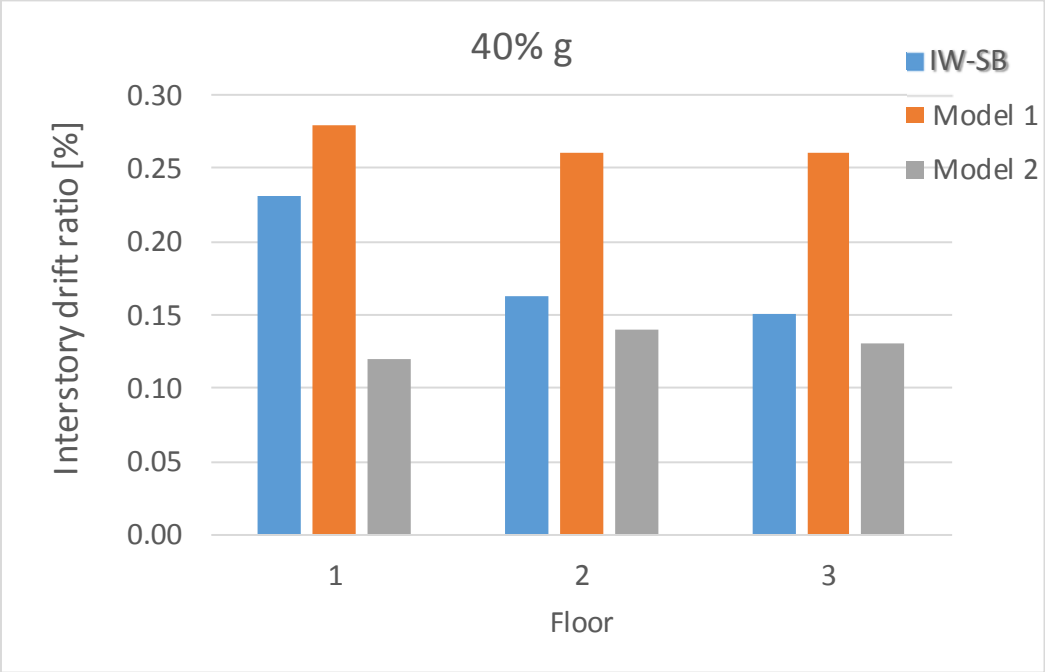

Figure 4.53 Interstory drift comparison of Model IW-SB (this study) with Model 1 and Model 2 from FRAMA project (Guljas et al. 2018) for 40 % g

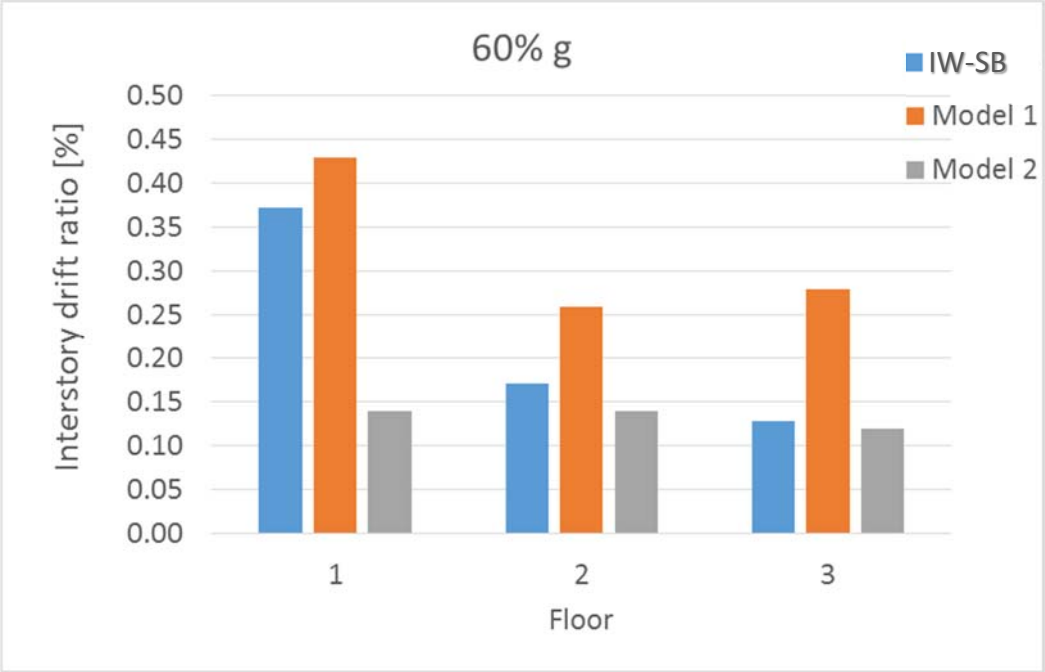

Figure 4.54 Interstory drift comparison of Model IW-SB (this study) with Model 1 and Model 2 from FRAMA project (Guljas et al. 2018) for 60 % g

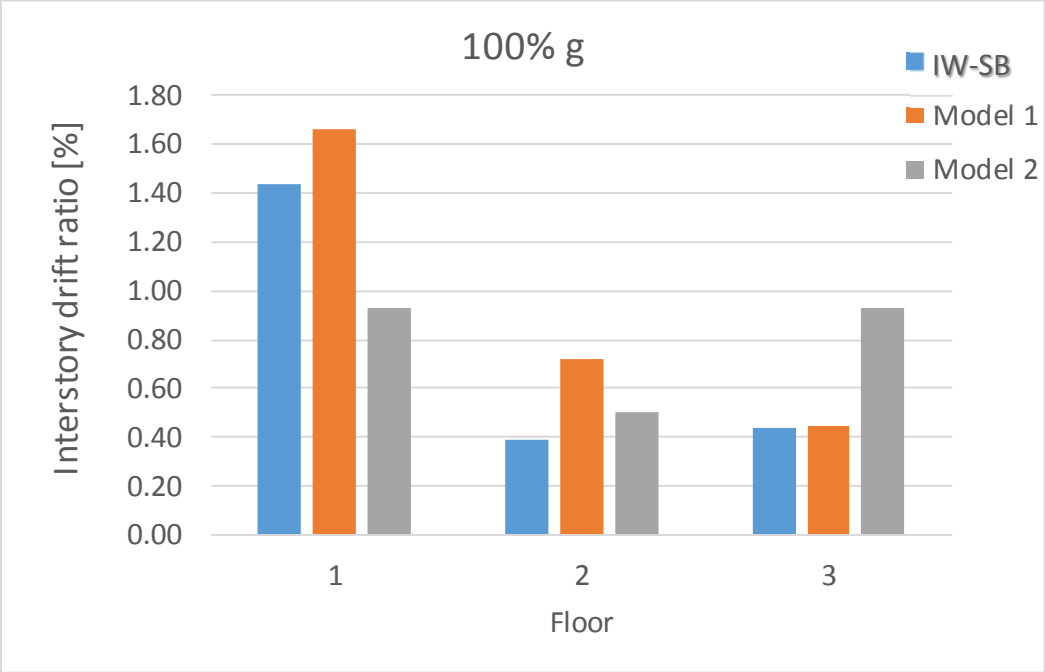

Figure 4.55 Interstory drift comparison of Model IW-SB (this study) with Model 1 and Model 2 from FRAMA project (Guljas et al. 2018) for 100 % g

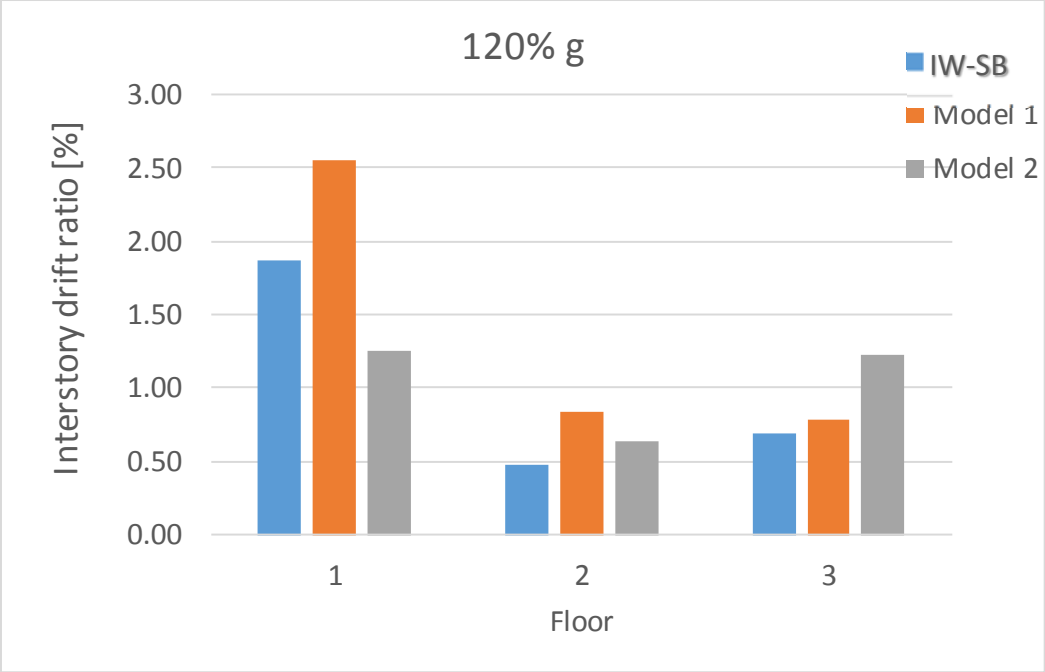

Figure 4.56 Interstory drift comparison of Model IW-SB (this study) with Model 1 and Model 2 from FRAMA project (Guljas et al. 2018) for 120 % g

-comparison of strain in the reinforcement of the columns

Results from comparison of the strain measurements with the referent Model 1 show that maximum values measured for strain for Model 1 are higher that the values measured for Model IW-SB, (Fig. 4.57). This statement also contributes to the fact of better seismic performance of Model IW-SB.

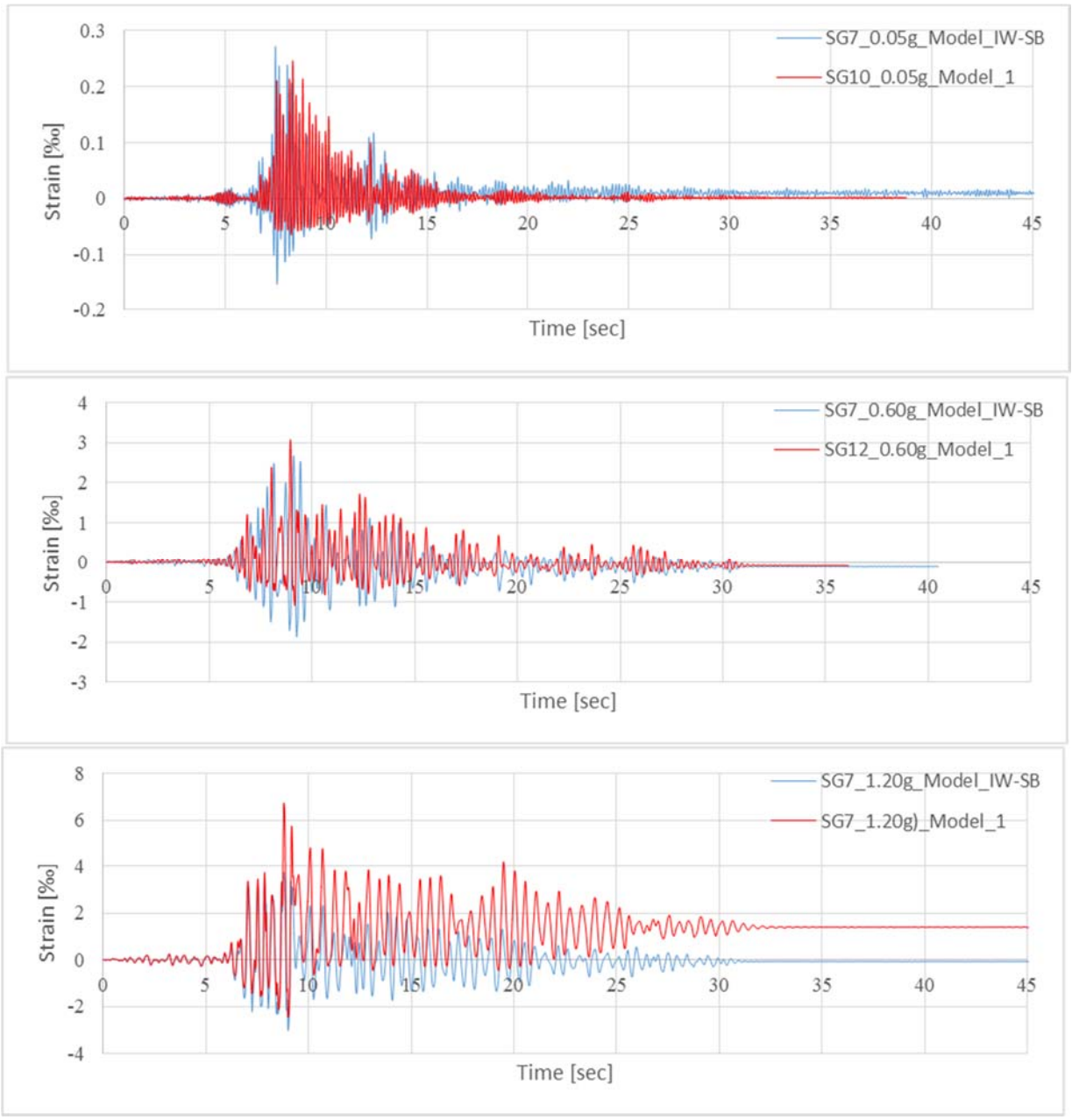

Figure 4.57 Comparison of the measured strains for Model 1 and Model IW-SB

-comparison of base shear - top displacements diagrams

Base shear vs top displacements graphs are compared to the referent Model 1 and presented on the following graphs (Figures 4.58-4.61). From the results it can be observed, that for higher excitation the Model IW-SB is slightly stiffer than Model 1 and thus has better seismic performance in the nonlinear zone of structural behavior.

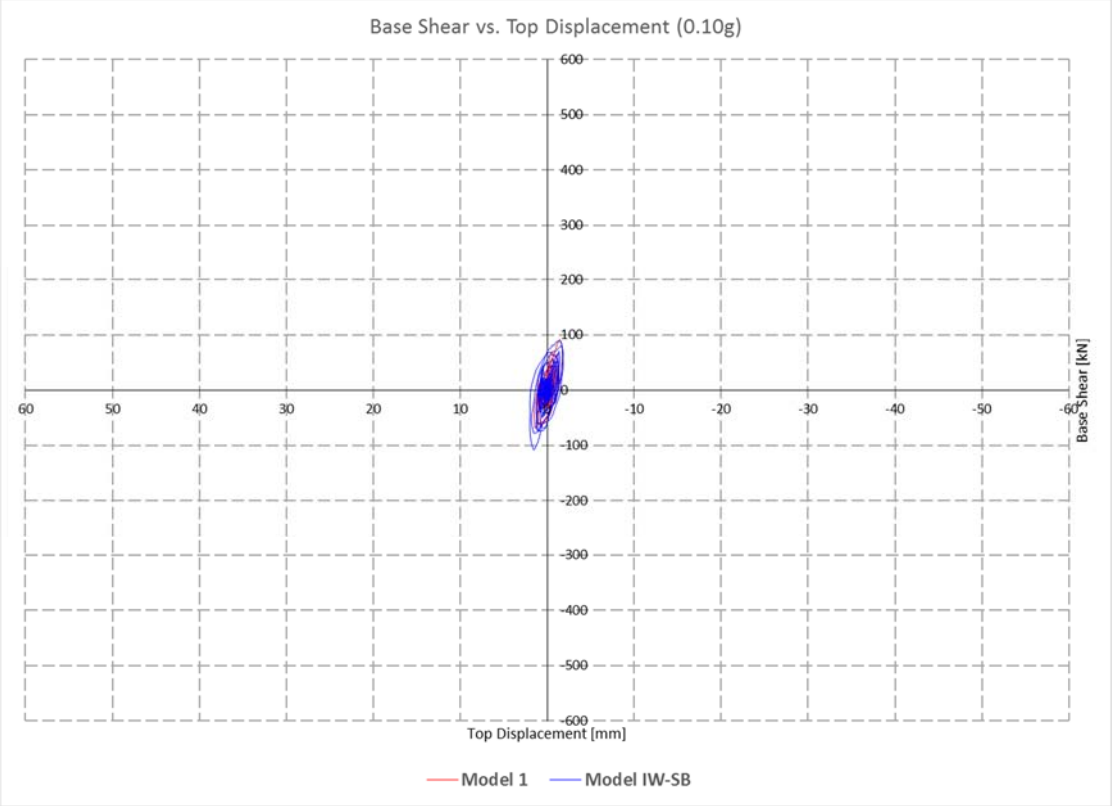

Figure 4.58 Experimental Base shear vs. top displacement comparison for Model 1 & Model IW-SB for 0.10g

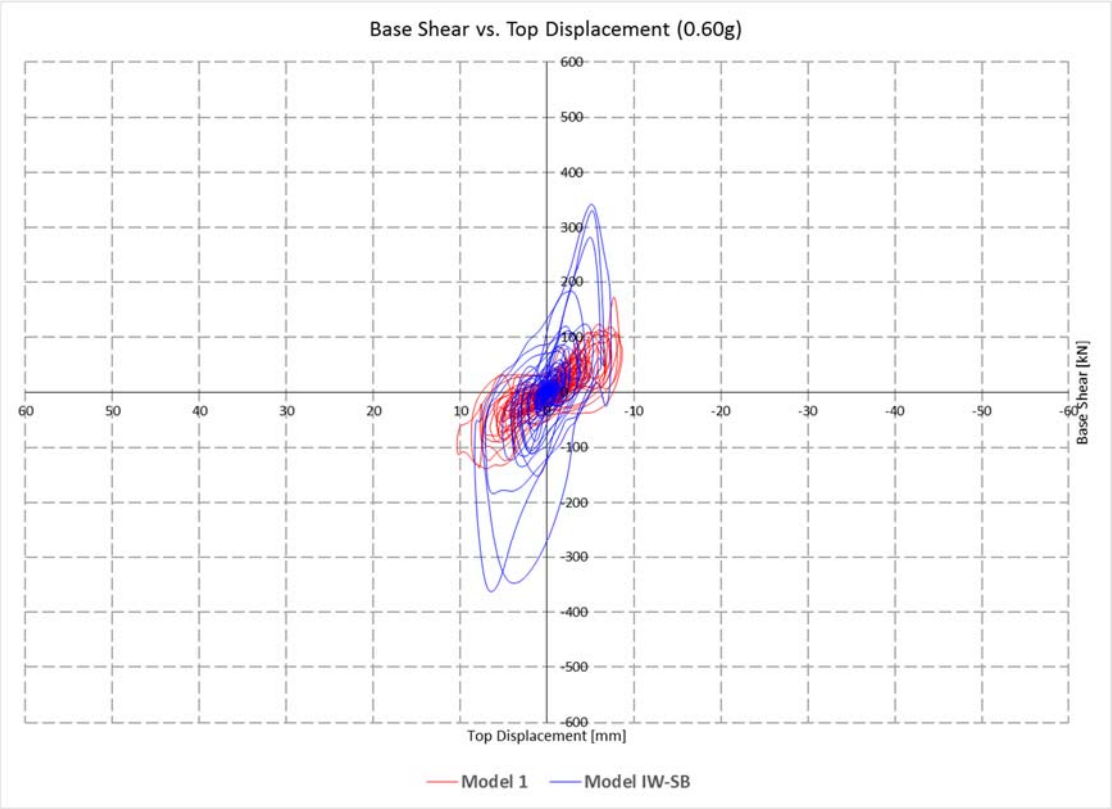

Figure 4.59 Experimental Base shear vs. top displacement comparison for Model 1 & Model IW-SB for 0.60g

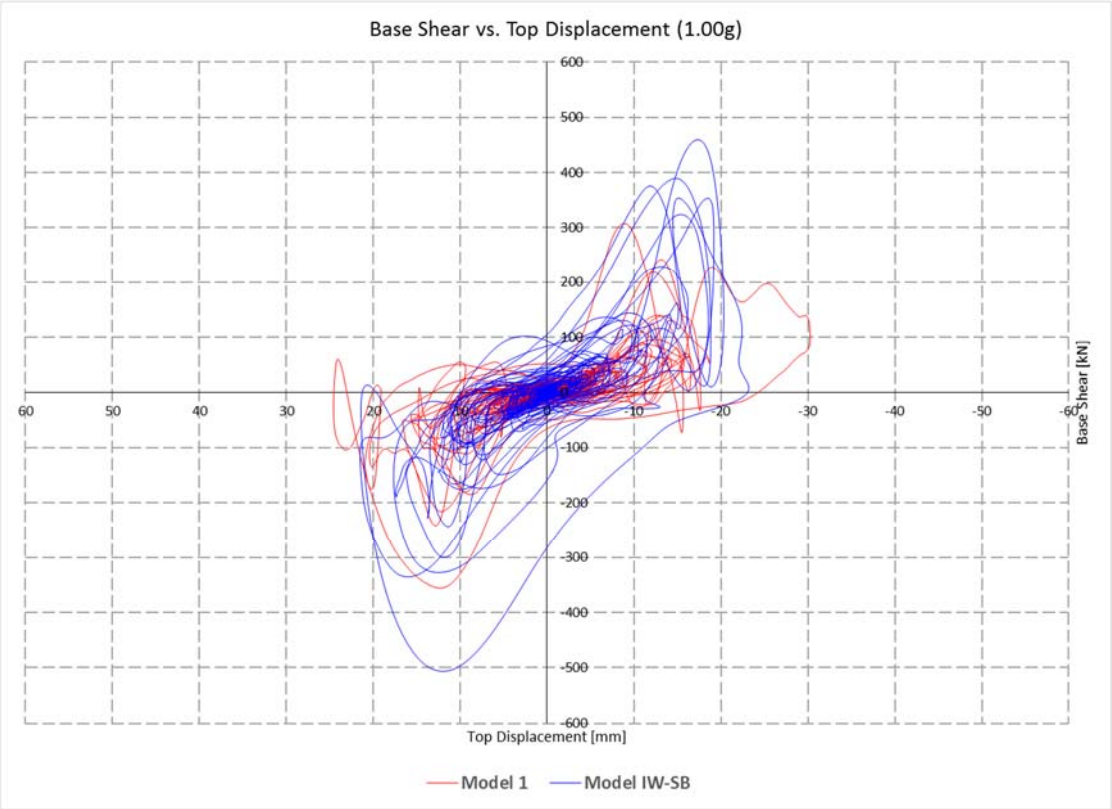

Figure 4.60 Experimental Base shear vs. top displacement comparison for Model 1 & Model IW-SB for 1.00g

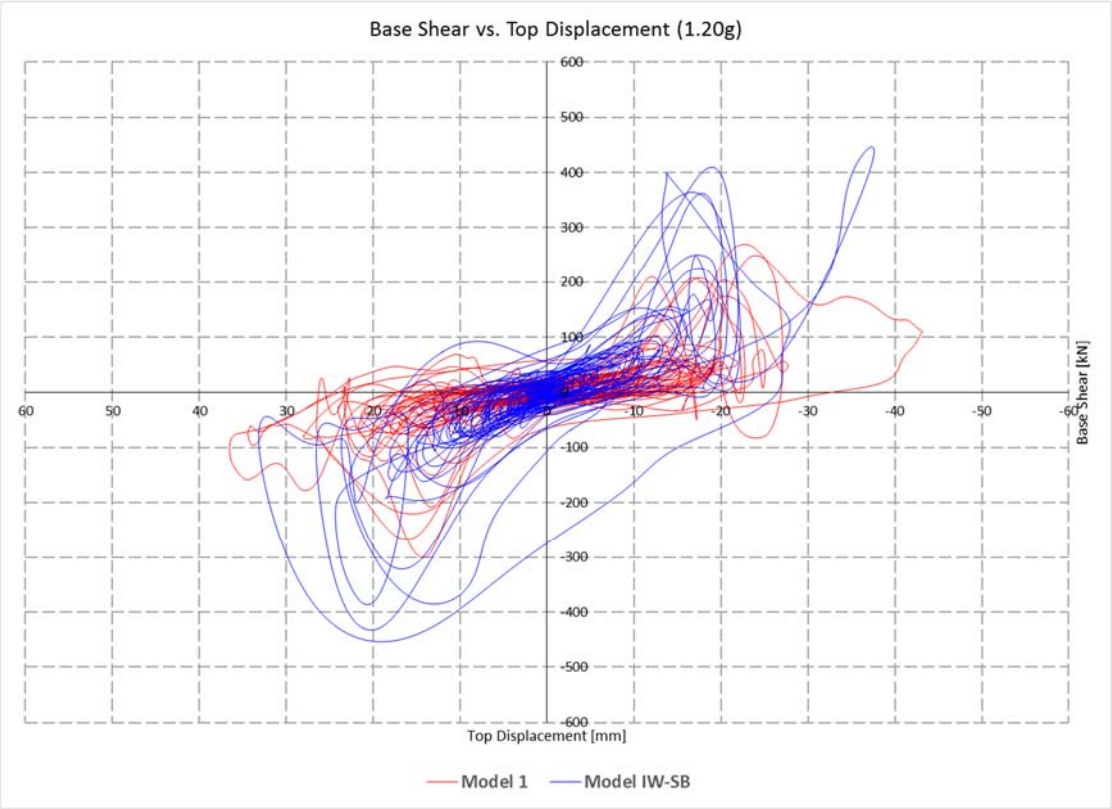

Figure 4.61 Experimental Base shear vs. top displacement comparison for Model 1 & Model IW-SB for 1.20g

4.3 General conclusions

- *3D frame model (Model IW-SB) consists of two planar RC frames (axes A and B) infilled with hollow-brick masonry walls which are interconnected with perpendicular girders in the axes 1, 2 and 3.* The frame in direction of axes 2 is infilled with hollow masonry units, (Figures 4.13, 4.14 and 4.15). The proposed innovative method for the connection is presented. The mortar joints were 10 mm thick and they were fully mortared (for both horizontal and vertical joints). The model proportions were 2.78 x 4.66 x 3.90 m.

- *The shake table tests of 1:2.5 scaled Model IW-SB required tailor-made testing protocol consists of several test phases, in order to investigate the safety and performance of RC frame system with hollow-clay masonry infill walls, in linear and nonlinear range*. The testing protocol was consisting of two main phases: Tests for definition of dynamic characteristics of the model, before and at the end of the seismic tests – resonant frequency search tests; and Seismic testing by selected earthquake

record until heavy damage – seismic response tests, which were performed in several steps, increasing the input intensity of the earthquake, in order to obtain the response in linear range, as well as to define the initial crack state, development of failure mechanism and possible collapse of the model

- *Visual observations of damage after the final tests in Model IW-SB and Model 1 from FRAMA project.* Before the test at 0.4 g, in both test series the structure experienced negligible-to-slight damage in the first story walls. At 0.4 g in both test series, cracks began to form around the perimeter of the infill walls with some crushing at the corners.

  At 0.8 g in Model 1, the first and second story infill walls began to develop inclined cracks at isolated locations. These cracks formed in both directions. At the end of Model 1 (1.2g), the infill wall adjacent to the door opening had collapsed, and significant diagonal cracks occurred in the infill panels. In contrast, infill damage at the end of Model IW-SB was only concentrated on the connections of the panel to the RC frame. The infill panels in Model IW-SB were being engaged more effectively in resisting the lateral demands, and kept their integrity until the last level of excitation of 1.6g. This observation contributed to the statement that with reinforcement bars the seismic capacity and in plane and out of plane stability of the infill is significantly improved.

- *Acceleration and displacement time histories.* From the presented graphs it can be concluded that displacements values are in the range of 2 mm at the top of the structure for 0.1g, 7 mm for 0.6g, 38 mm for 1.2g and 52 mm for 1.6g. The peak values of the Model IW-SB comparing to Model 1 has lower values almost for excitation level which also contributes to better seismic performance of Model IW-SB.

- -*Strain in the reinforcement of the column of RC frame.* Results from comparison of the strain measurements with the referent model 1 from FRAMA project show that maximum values measured for strain for Model 1 are higher that the values measured for Model IW-SB. This statement also contributes to the fact of better seismic performance of Model IW-SB.

- -*Interstory drifts.* Integratory drift ratio were calculated for each level of seismic excitation. These obtained drifts were compared from results obtained for Model 1 and Model2 from FRAMA project published in the paper given by Guljas et al. (2018). Results pointed out that Model IW-SB is having lower values than Model 1 which indicates to the conclusion that the proposed method for connection between the infill and the RC frame significantly improves the seismic behaviour of the overall structure in general. Regarding Model 2, which is built with hollow clay infill, for lower and intermediate amplitude excitation Model IW-SB has higher values of drifts which is considerably expected. Yet for the highest amplitude excitation Model 2 in some cases goes beyond Model IW-SB with the interstory drifts, which means that the new proposed Model IW-SB can sustain very high level of excitation without causing significant damage and large plastic deformation. The values of the drifts of Model IW-SB 3 are 0.02% for 0.1g, 0.37% for 0.6g, 1.86% for 1.2g and 2.89% for 1.6g.

5. NUMERICAL SIMULATION AND VERIFICATION OF THE SHAKE TABLE TESTS

5.1. Choosing the right modeling approach

The complex nature of the interaction between concrete frames and masonry infill wall panels is reflected perhaps in the large number of experimental studies conducted on this topic (Table 5.1), (Griffith et al, 2008) The need to predict the cyclic behaviour of infilled frames becomes fundamental when the nonlinearity of the materials are taken into consideration. There has been much work conducted in the topic of the seismic performance of infilled frame buildings from various researchers. Some experimental and analytical investigations in this topic have been carried out by Klingner and Bertero (1978) who studied the effects of cyclic loads by testing portions of multi-storey buildings, also providing a first hysteretic model. Doudoumis and Mitsopoulou (1986) introduced in their hysteretic model an initial non-loading branch due to shrinkage of contact zones between masonry infill walls and integral RC structure. Experimental pseudo-dynamic tests on masonry infilled RC frames were carried out by Mander et al. (1993, 1994) and Mehrabi et al. (1996) who also provided a cyclic law based on the results of tested infilled frames specimens. Other hysteretic models were further proposed, each of them based on different assumptions.

The results of these and other previous studies suggest that the brickwork can be accurately modelled using “equivalent struts”. However, the most significant outcome is perhaps the general consensus that brickwork infill can have a beneficial effect on the overall seismic performance of the building if it is properly tied into the rest of the building. Madan et al. (1997) proposed a hysteretic single-strut model taking into account strength and stiffness decay and pinching, Crisafulli (1997) investigated the influence of different multiple-strut models on structural response, Kappos et al. (1998) presented a hysteretic model based on shear strength of infills. In the last years Cavaleri et al. (2005) proposed a highly detailed constitutive law for cyclical or monotonic behaviour of an equivalent single strut and provided a first calibration of the parameters involved, while Crisafulli and Carr (2007) developed a new multi-strut macromodel including in addition to classical truss elements, governed by axial compressive laws, a special shear frictional strut. Among the above mentioned models, those including the cyclic behaviour often depend on a large number of parameters, making it difficult to use them for practical applications. The problem becomes more relevant in the case of multiple-strut configurations (double, triple pin jointed struts or mixed axial and shear struts) without considering the different possible infill/frame couplings, which introduce further uncertainties. However, the

necessity to assess the capacity of existing structures is increasing nowadays, and as several studies demonstrate (Dolšek and Fajfar (2008), Kakaletsis et. al (2009), Stavridis, Koutromanos and Shing (2012), Uva et al. (2012), Fiore et al. (2012)), the analyses should be adequately performed including infill panels to avoid underestimation or overestimation of building's effective capacities.

Table 5.11 Summary of infilled frame test results Griffith et al, 2008

Reference	δ_{cr} (%)	$\delta_{\max}$ (%)			Other Notes
	URM	URM	Frame + Infill	Bare Frame	
Mosalam et al (1998)	0.3	<0.8			
Negro & Verzeletti (1996)	<0.3		1.1	2.4	$V_{\max} = 0.4W$ for bare frame, $V_{\max} = 0.62W$ for infilled frame
Fardis and Calvi (1995)					$\delta_{\max}$ for URM is 0.1 $\delta_{\max}$ for frame
Schneider et al (1998)	0.1	1			$k < 0.3k_i$ by 0.2% drift
Kappos et al (1998)	0.07	0.2-0.4	0.4	0.7	Comparative drift values for structure subject to same input. $\tau_u \approx 0.35MPa$
Valiasis & Stylianidis (1989)			0.3		$V = 0.8V_{\max}$ at 3% drift
Zarnic (1995)	0.1	0.3	0.6	2	
Manos et al (1995)	0.15		0.3	1	$\tau_u \approx 0.3MPa$ $V = 0.8V_{\max}$ at 2% drift for infill frame
Michailidis et al (1995)	0.1	0.25-0.35			$\tau_{cr} \approx 0.25MPa$, $\tau_u \approx 0.32MPa$
Pires & Carvalho (1992)			0.5		$\tau_u \approx 0.27 - 0.51MPa$
Pires et al (1995)			0.3	2	$V = 0.8V_{\max}$ at 6% drift
Zarnic & Tomazevic (1984)	0.2		1	3	
Zarnic & Gostic (1997)		0.2	1	>1	
Valiasis & Stylianidis (1989)			0.6	1	$\tau_u \approx 0.25 - 0.3MPa$
Mehrabi et al (1996)	0.3		0.6	3.1	$\tau_u \approx 0.5MPa$, $V = 0.8V_{\max}$ at 1.5% drift for infilled frame, 6.8% for bare frame
Shing et al (1992)					$\tau_u \approx 0.34MPa$
Carydis et al (1992)					Good system behaviour up to 0.14% drift; steel frame with infill
Govindan et al (1986)			3	1.5	
Zarnic (1998)			0.3		$V = V_{\max}$ for $0.3\% < \delta < 2\%$ used in mathematical model of URM infill

1. δ_{cr} = is the lateral storey drift at which the masonry infill cracks.
2. $\delta_{\max}$ = the lateral storey drift at which the maximum force $V_{\max}$ is attained for the URM infill, infilled frame or bare frame, respectively.
3. W = weight of structure.
4. k = lateral in-plane stiffness of the URM, k_i = the initial stiffness.
5. τ_u = maximum shear strength of the URM, τ_{cr} = cracking strength of the URM.

The introduction of the infill panel contribution in the seismic performance of the integral structure thus appears absolutely necessary as does the adoption of simplified models, also not too heavy from the computational point of view.

This chapter of the thesis has the aim to discuss how the cyclic behaviour of infilled frames can be predicted with sufficient accuracy by a simple modelling in order to be implemented in the practical design and preliminary capacity check in the design / analysis process. There are two main different approaches on modelling infill walls. Micro model, based on the finite element techniques and macro model in terms of the equivalent strut method. The main difference between the two methods is the precision that micro modelling is dealing with all individual components brick, block unit and mortar while macro modelling consider the whole masonry as a composite unit. Micro-modeling is used generally to understand the local behavior of masonry infills. Inelastic properties of both unit and mortar and some mechanical properties as Young's modulus, Poisson's ratio are taken into account in detailed micro-modeling. This approach is highly time consuming and it is recommended to be used for single frame only. On the other hand, the macro modeling approach is generally used in order to capture the global performance and failure mechanism of the structure as a whole. As a conclusion, it can be said that the process of choosing the right modelling approach (the input) is connected with the results that are tried to be obtained and analyzed (the output).

The main goal of this chapter is to simulate the global performance of the structure for the proposed infill wall connection using the existing modeling techniques. Having in mind that macro modelling has been used widely due to simple and efficient computational process for obtaining the global structure performance, the logical modelling approach is modelling the infill walls with macro models proposed from various authors.

The modelling of the equivalent diagonal struts is performed by means of equivalent compression strut analogy according to ASCE/SEI 41-06 (FEMA 356) procedure, governed by the Pivot hysteretic law proposed by Dowell et al. (1998).

5.2. Numerical simulation of the experimental model

The numerical simulation of the seismic performance of the investigated model has been done using SAP 2000 integrated software for structural analysis and design. The SAP name has been synonymous with state-of-the-art analytical methods since its introduction over 30 years ago. SAP2000 follows in the same tradition featuring a very sophisticated, intuitive and versatile user interface powered by an unmatched analysis engine and design tools.

5.2.1. Material properties

The material properties and the stress-strain curve for the concrete, reinforcement and masonry materials are defined according to the obtained laboratory test results, previously shown in Chapter 4 (Fig. 5.1 & 5.2). Modulus of elasticity for masonry infill walls was accordingly 3800 MPa and the maximum force measured during the diagonal testing was around 20kN.

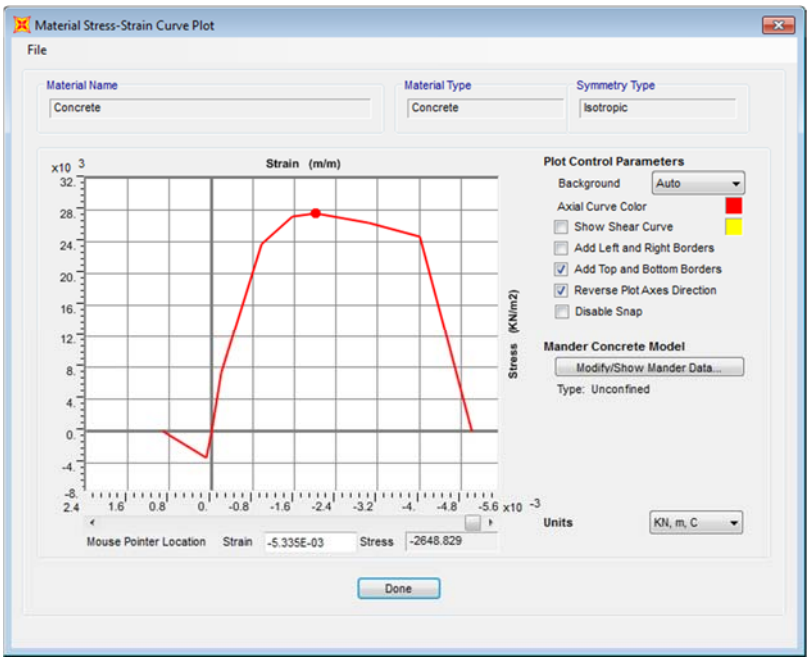

Figure 5.1 Stress - Strain Curve for Concrete

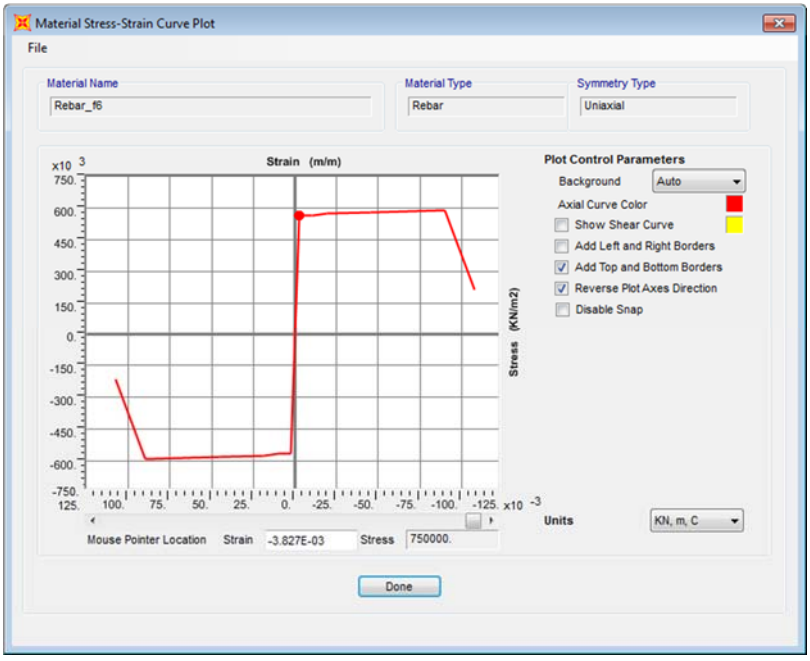

Figure 5.2 Stress - Strain Curve for Rebar Ø6

5.2.2. Nonlinear models for frame elements

The nonlinearity of the reinforced concrete structural elements (columns and beams) was achieved by assigning two plastic hinges per element (one at each end of the element) (Figure 5.3). The plastic hinge idealized model of beam-column elements is one of the simplest models which concentrates the inelastic deformations at the end of the element, such as through a rigid-plastic hinge. By concentrating the plasticity in zero-length hinges with moment-rotation model parameters, these elements have relatively condensed numerically efficient formulations. Hinge properties in SAP2000 define only the plastic behavior of the hinge. The elastic behavior of the frame element is determined by the frame section (and hence material properties) assigned to the element. Thus, the linear behavior of the structure is not changed by the assignment of hinges to the frame objects.

The portions of the hinge load-deformation curve from A to B and from A to B' are ignored by the program (Figure 5.4). After a hinge yields at point B, plastic deformation is determined by the curve B-C-D-E with all plastic deformation measured relative to B. Similarly, plastic deformation in the negative direction is measured relative to B'. The elastic slope of a hinge is actually given by the elastic stiffness of the element over the assumed length of the hinge. The strain-hardening slope is the slope of line BC.

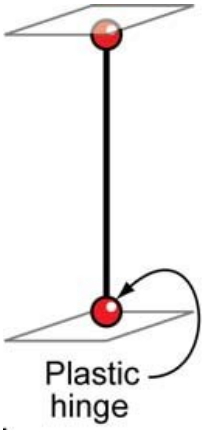

Figure 5.3 Plastic hinge idealized model of beam-column elements

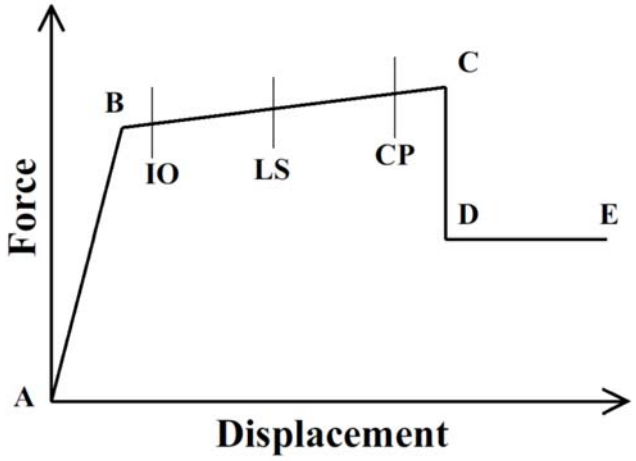

Figure 5.4 The A-B-C-D-E curve for Force vs. Displacement (SAP 2000 Reference Manual)

These plastic hinges represent points where the nonlinear material deformation occurs, being situated through elements' extremities because of higher bending forces. The plastic hinges behaviour is introduced by a moment versus curvature relation, inherent to each element. The ultimate deformation capacity depends on the ultimate curvature and plastic hinge length.

For beam's defined cross sections and material properties, (Fig. 5.5) the Moment-Curvature relationship is obtained (Fig. 5.6) and nonlinear plastic M3 hinges are applied at both ends of the elements at relative length of 0.05 and 0.95.

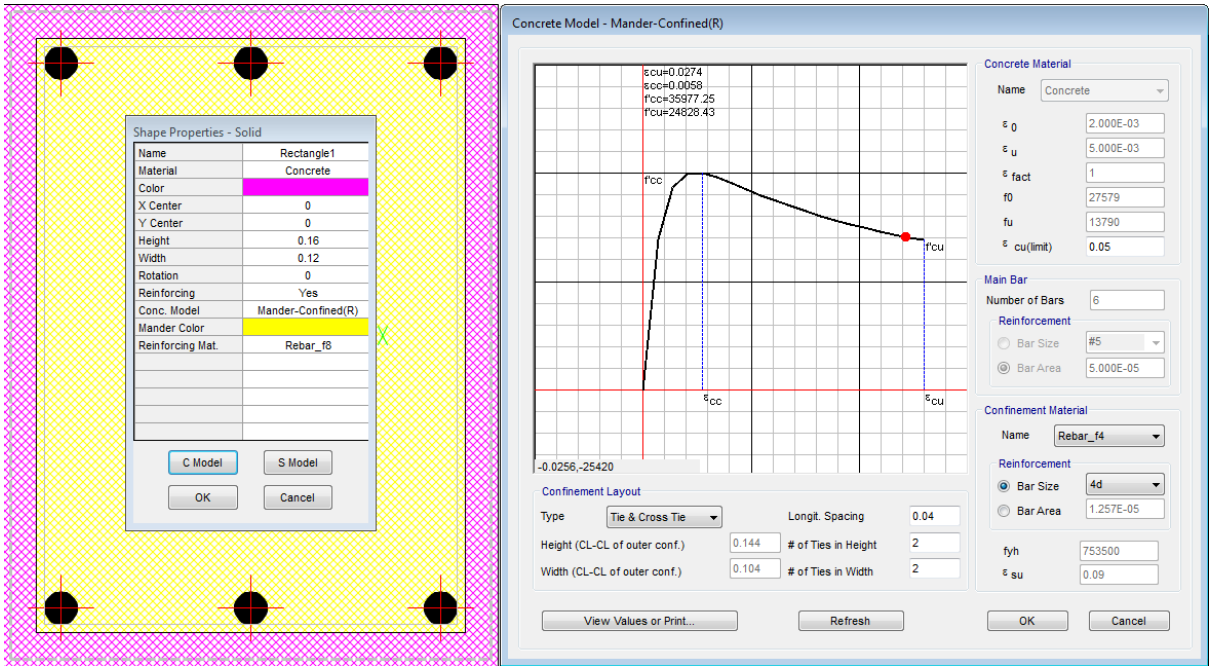

Figure 5.5 Defined Section Properties for Beams

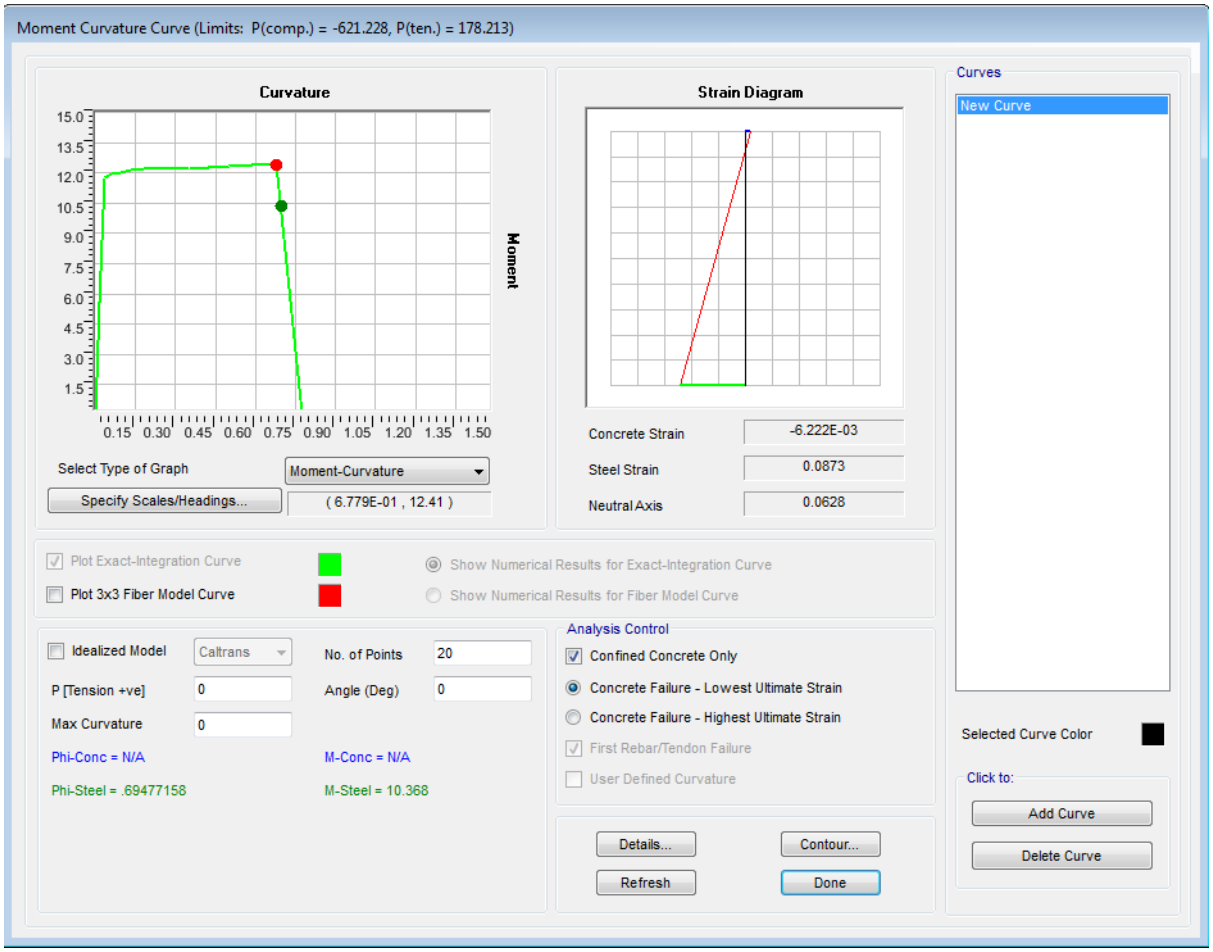

Figure 5.6 Moment Curvature Curve for Beams

Nonlinearity of the columns is modeled by deformation controlled P-M2-M3 hinge (Figure 5.7) for a different level of axial force, according to the column P-M diagram (Figure 5.8). The location of the hinges is the same as in the case of the beams (0.05 and 0.95 relative length respectively).

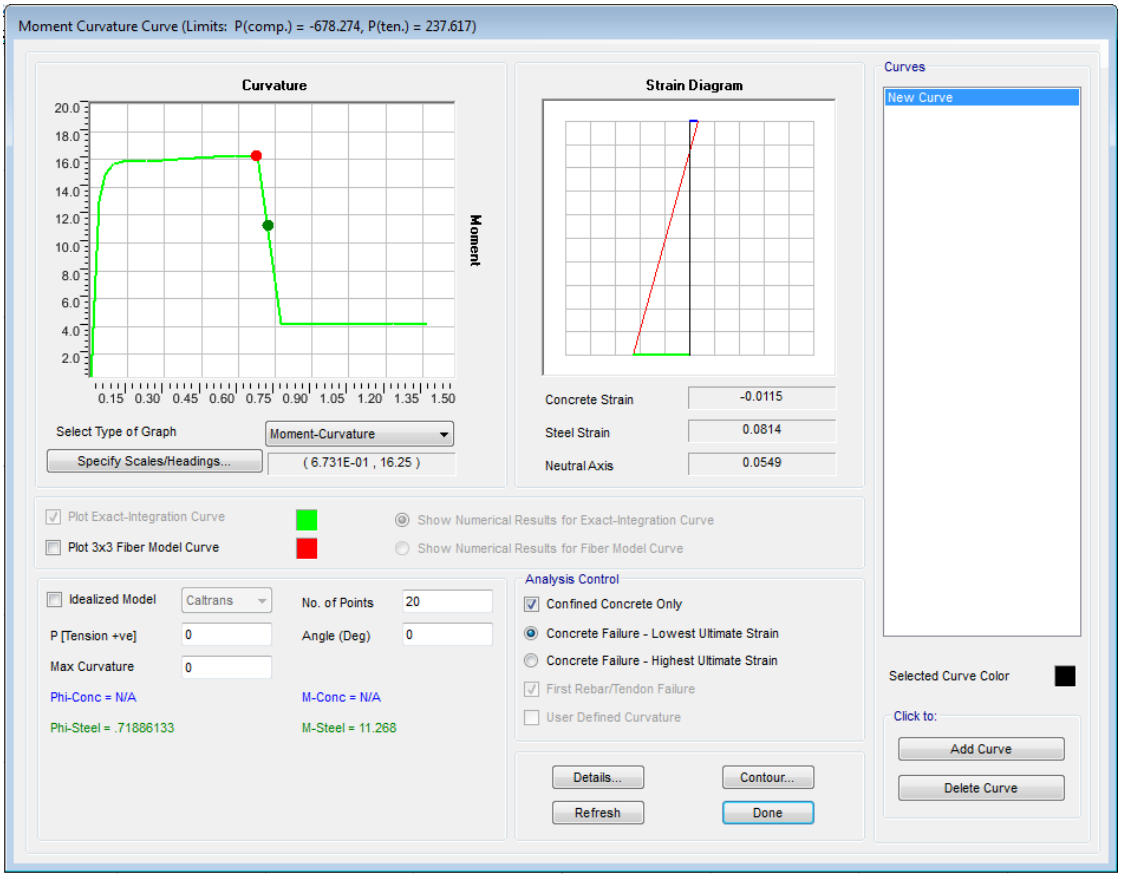

Figure 5.7 Moment Curvature Curve for Column C2

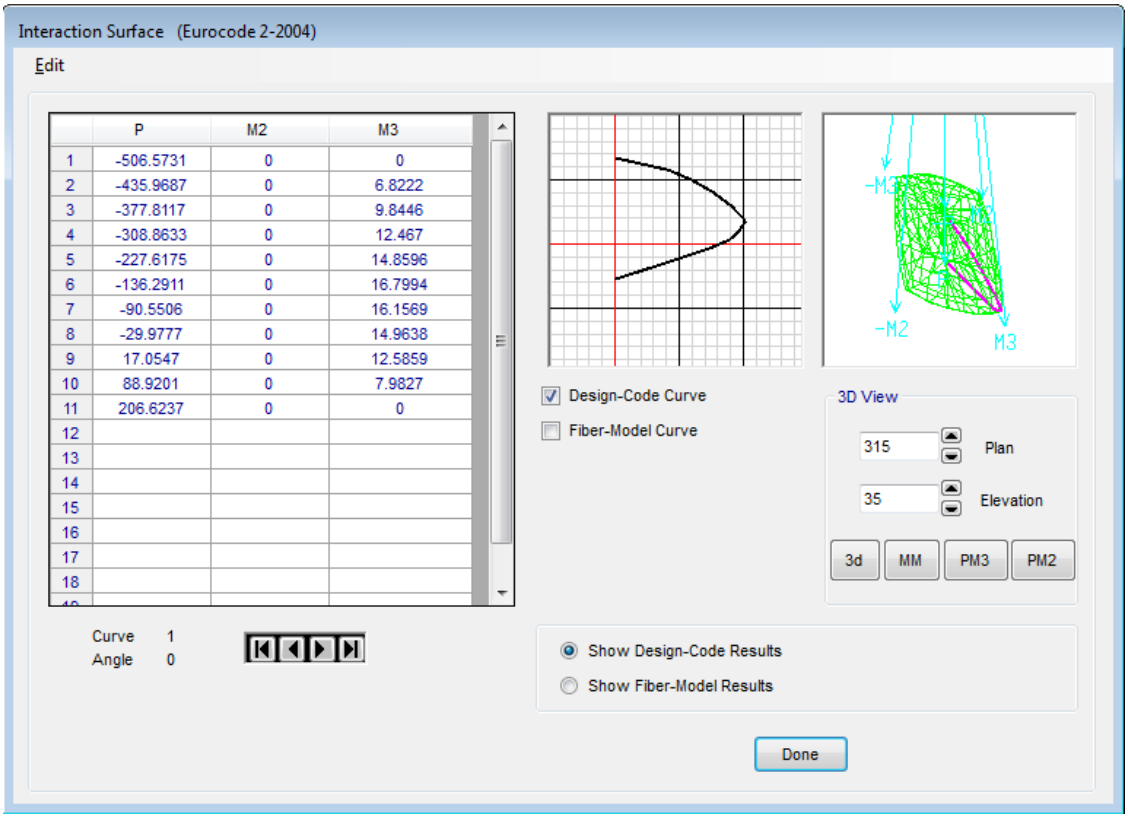

Figure 5.8 P-M2-M3 Curve for Column C2

5.2.3. Modelling of the infill walls using the equivalent diagonal struts according to ASCE/SEI 41-06 (FEMA 356) procedure

According to this procedure, in-plane lateral stiffness of an infilled frame system is not the same as the sum of the frame and infill stiffnesses because of the interaction of the infill with the surrounding frame. Experiments have shown that under lateral forces, the frame tends to separate from the infill near windward lower and leeward upper corners of the infill panels, causing compressive contact stresses to develop between the frame and the infill at the other diagonally opposite corners. Recognizing this behavior, the stiffness contribution of the infill is represented with an equivalent compression strut connecting windward upper and leeward lower corners of the infilled frame. In such an analytical model, if the thickness and modulus of elasticity of the strut are assumed to be the same as those of the infill, the problem is reduced to determining the effective width of the compression strut. Solidly infilled frames may be modeled with a single compression strut in this fashion.

For global building analysis purposes, the compression struts representing infill stiffness of solid infill panels may be placed concentrically across the diagonals of the frame, effectively forming a concentrically braced frame system (Figure 5.9).

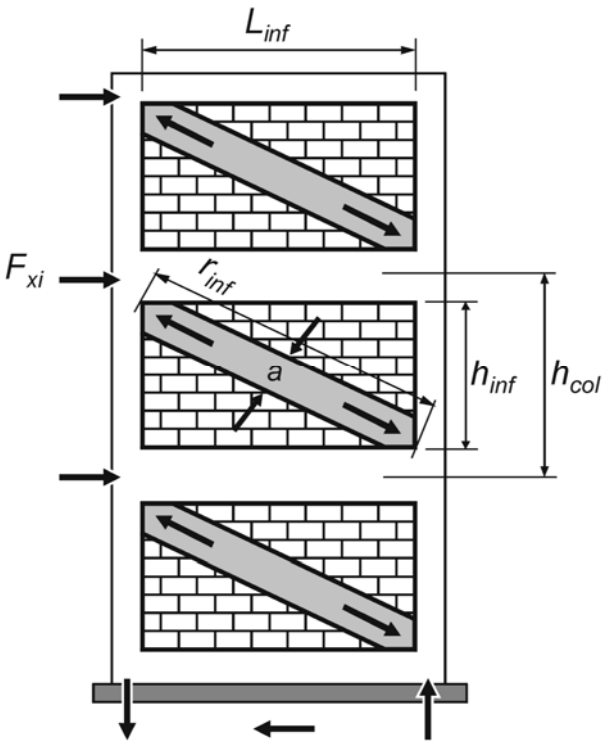

Figure 5.9 Compression Strut Analogy according to ASCE/SEI 41-06 (FEMA 356)

The elastic in-plane stiffness of a solid unreinforced masonry infill panel prior to cracking shall be represented with an equivalent diagonal compression strut of width, *a*, given by the following equation:

$$a = 0.175 \cdot (\lambda_t \cdot h_{col})^{-0.4} \cdot r_{inf}$$

where

$$\lambda_t = \left[\frac{E_{me} \cdot t_{inf} \cdot \sin 2\theta}{4E_f \cdot I_{col} \cdot h_{inf}}\right]^{\frac{1}{4}}$$

and

- h_{col} => Column height between centerlines of beams
- h_{inf} => Height of infill panel
- E_{fe} => Expected modulus of elasticity of frame material
- E_{me} => Expected modulus of elasticity of infill material
- I_{col} => Moment of inertia of column
- L_{inf} => Length of infill panel
- r_{inf} => Diagonal length of infill panel
- t_{inf} => Thickness of infill panel and equivalent strut
- θ => Angle whose tangent is the infill height-to length aspect ratio (radians)
- λ_t => Coefficient used to determine equivalent width of infill strut

The equivalent strut have the same thickness and modulus of elasticity as the infill panel it represents. Stiffness of cracked unreinforced masonry infill panels is represented with equivalent struts.

Having in mind that the infill walls of the selected model have certain amount of openings, it is expected that the strength of these infill walls will be considerably smaller. It depends of the location of the opening and the percentage of the space without infill. According to Al-Chaar, 2002:

$$R = 0.6 \cdot \left(\frac{A_{op}}{A_{infill}}\right)^2 - 1.6 \cdot \left(\frac{A_{op}}{A_{infill}}\right) + 1$$

where

- R => The Reduction Factor for ***a***

A separate calculation is made for each infill wall according to its geometric properties for both considered models (Model IW-SB & Model 1), which are presented in the following section 5.3.

5.2.4. Hysteresis Models for RC frame model

Hysteresis is the process of energy dissipation through deformation (displacement). Hysteretic behavior may affect nonlinear static and nonlinear time-history load cases that exhibit load reversals and cyclic loading. Monotonic loading is not affected.

Several different hysteresis models are available in the literature. Each one differs in the amount of energy they dissipate in a given cycle of deformation, and how the energy dissipation behavior changes with an increasing amount of deformation.

Typical for all models, cyclic loading behaves as follows:

- Initial loading in the positive or negative direction follows the back bone curve
- Upon reversal of deformation, unloading occurs along a different path, usually sharper than the loading path. This is often parallel or nearly parallel to the initial elastic slope.
- After the load level is reduced to zero, continued reversal of deformation causes reverse loading along a path that eventually joins the back bone curve on the opposite side, usually at a deformation equal to the maximum previous deformation in that direction or the opposite direction.
- The hysteretic behavior of the reinforced concrete under seismic loading is achieved by using Takeda model which is implemented in the computer software itself. This model is using a degrading hysteretic loop based on the Takeda model, as described in Takeda, Sozen, and Nielsen (1970). This simple model requires no additional parameters, and is more appropriate for reinforced concrete than for metals.
- Unloading is along the elastic segments. When reloading, the curve follows a secant line to the backbone curve for loading in the opposite direction. The target point for this secant is at the maximum deformation that occurred in that direction under previous load cycles. This results in a decreasing amount of energy dissipation with larger deformations. Unloading is along the elastic segments (Figure 5.10).

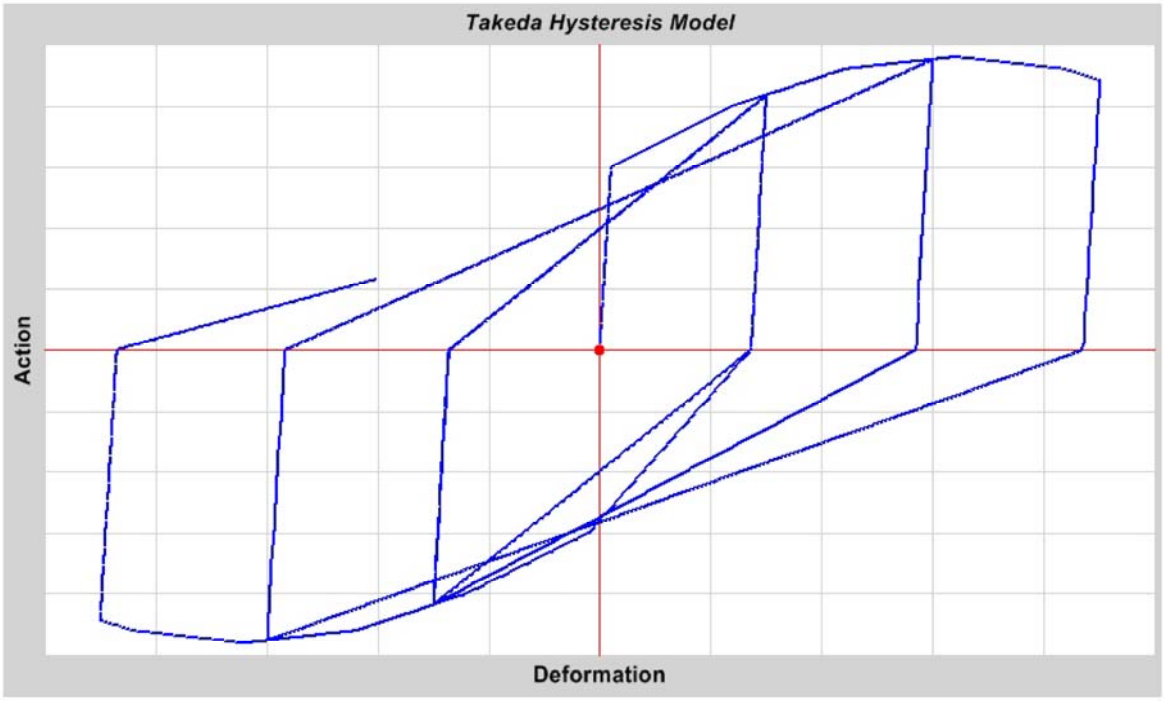

Figure 5.10 Takeda Hysteresis Model under Increasing Cyclic Load

5.2.5. Nonlinear Static Pushover Analysis

The recent advent of performance based design has brought the nonlinear static pushover analysis procedure to the forefront. Pushover analysis is a static, nonlinear procedure in which the magnitude of the structural loading is incrementally increased in accordance with a certain predefined pattern. With the increase in the magnitude of the loading, weak links and failure modes of the structure are found. The loading is monotonic with the effects of the cyclic behavior and load reversals being estimated by using a modified monotonic force-deformation criteria and with damping approximations. Static pushover analysis is an attempt by the structural engineering profession to evaluate the real strength of the structure, in a simplified manner comparing to nonlinear time history analysis and it promises to be a useful and effective tool for performance based design.

The ATC-40 and FEMA-273 documents have developed modeling procedures, acceptance criteria and analysis procedures for pushover analysis. These documents define force-deformation criteria for hinges used in pushover analysis. As shown in Figure 5.4, five points labeled A, B, C, D, and E are used to define the force deflection behavior of the hinge and three points labeled IO, LS and CP are used to define the acceptance criteria for the hinge (IO,

LS and CP stand for Immediate Occupancy, Life Safety and Collapse Prevention respectively.) The values assigned to each of these points vary depending primarily on the type of member as well as many other parameters defined in the ATC-40 and FEMA-273 documents.

In order to check the structure capacity and proposed infill connection effectiveness, a pushover analysis has been made for Model IW-SB, Model 1 and Bare-Frame Structure. The results and comments are shown in the following sections (5.3.4.; 5.3.6; 5.3.7 and 5.4.3).

5.2.6. Nonlinear Time-History Analysis

Time-history analysis is a step-by-step analysis of the dynamical response of a structure to a specified loading that may vary with time. It is used to determine the dynamic response of a structure to arbitrary loading. The dynamic equilibrium equations to be solved are given by:

$$K\,u(t) + C\,\dot{u}(t) + M\,\ddot{u}(t) = r(t)$$

where

- **K** is the stiffness matrix;
- **C** is the damping matrix;
- **M** is the diagonal mass matrix;
- **u**, **u̇**, and **ü** are the displacements, velocities, and accelerations of the structure; and
- **r** is the applied load.

If the load includes ground acceleration, the displacements, velocities, and accelerations are relative to this ground motion.

In a nonlinear analysis, the stiffness, damping, and load may all depend upon the displacements, velocities, and time. This requires an iterative solution to the equations of motion.

The load, **r**(t), applied in a given time-history case may be an arbitrary function of space and time. It can be written as a finite sum of spatial load vectors, $\mathbf{p}_i$, multiplied by time functions, $f_i(t)$, as:

$$r(t) = \sum_i f_i(t) p_i$$

When Acceleration Loads are used, the displacements, velocities, and accelerations are all measured relative to the ground. The time functions associated with the Acceleration Loads $\mathbf{m}_x$, $\mathbf{m}_y$, and $\mathbf{m}_z$ are the corresponding components of uniform ground acceleration, $\ddot{\mathbf{u}}_{gx}$, $\ddot{\mathbf{u}}_{gy}$ and $\ddot{\mathbf{u}}_{gz}$.

In order to get appropriate numerical results, a nonlinear direct-integration time-history analysis is performed for the model with the proposed infill wall connection (Model IW-SB) and Model 1 (Referent model). The results and observations are further presented in the following sections.

5.3. Capacity and damage (failure) mechanism of Model IW-SB

5.3.1. Mathematical model

A 3D mathematical macro model has been made in SAP 2000 in order to simulate the performance of the integral system for the proposed innovative infill wall connection using the properties and procedures described in chapter 5.2 (Figure 5.11). The frame was assumed to be fixed at the bottom, and columns and beams of the frame were modeled using two-nodded frame or beam elements. Masonry infill walls were modeled as equivalent diagonal compressive struts using two-nodded beam elements, according to ATC-40 (FEMA 356) procedure. Transfer of bending moments from RC frame to masonry was prevented by specifying moment releases at both ends of the struts. The specific modeling issues, the separate results and the discussion has been shown in the next few chapters.

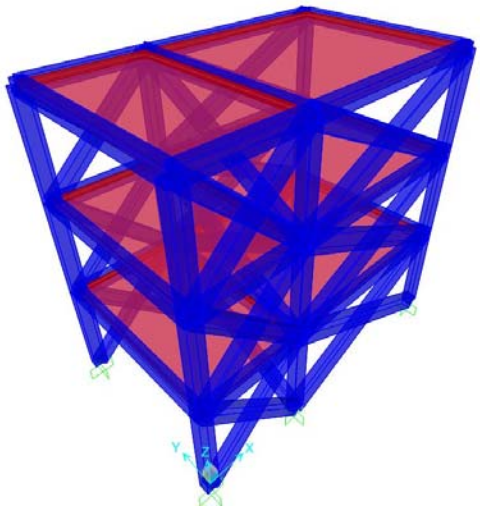

Figure 5.11 3D Isometric view of Model IW-SB

5.3.2. Specific modeling issues

From the analysis of the experimental results in Chapter 4, it can be concluded that with implementation of the proposed infill-bare frame connection, significant improvement of the seismic capacity and behavior of the structure has been made in comparison with the referent model (Model 1). Starting from the initial frequency of the structure, analysis of the structural and nonstructural element's cracks, through the acceleration and deformation time-histories, the proposed infill wall connection has improved the seismic performance of the structure as a whole. Having in mind that the purpose of Chapter 5 is to simulate the performance of the integral system using already well known and implemented procedures, the input parameters for the infill walls is quite an important issue. In this term, it was decided that the best alternative to simulated the experimentally captured behavior of the structure is to increase the strength of the infill walls (not the RC structural elements), considering that at some point it is expected that the infills will lose the bearing capacity and beyond that point the "defense" system will be composed of the reinforced concrete structure itself. According to the selected procedure, the infills are represented by the diagonal struts. Analyzing the formula for the calculation of the strut width, it is concluded that with the increase of the modulus of elasticity of the infill panel (E_{me}), the width of the diagonal strut (a_w) is increasing, so the strength of the wall itself will become bigger. Moreover, the increasing of the Modulus of elasticity of the masonry material will give bigger strength in the analysis of the structural system itself.

$$\lambda_t = \left[\frac{E_{me} \cdot t_{inf} \cdot \sin 2\theta}{4E_f \cdot I_{col} \cdot h_{inf}}\right]^{\frac{1}{4}}$$

After series of analysis in order to calibrate the value of the modulus of elasticity, certain observations can be highlighted:

- The initial value for the modulus of elasticity of standard infill panel (without using the proposed infill-bare frame connection) according to the experimental test data is 3.800.000,00 kN/m^2 (3.800,00 MPa).
- The initial value of the modulus of elasticity of the infill wall with implemented infill-bare frame connection is 9.280.00,00 kN/m^2 (9.280,00 MPa). This value gives best matches with the experimental results, comparing the deformation and total

displacements. This value is matching the mentioned values for the earthquake intensity from 0.05g up to 0.70g. Beyond this point the time-history patterns of displacements and acceleration, along with its intensities exhibits certain discrepancies.

- At certain point of increasing the intensity of the simulated earthquake (beyond acceleration of 0.80g), the value for the modulus of elasticity for the infill wall with implemented infill-bare frame connection is 5.900.00,00 kN/m^2 (5.900,00 MPa). With this value, both time-history pattern and intensities matched the experimental results.

The above mentioned observations are presented below (Table 5.2 and Figure 5.12).

Table 5.12 Infill panel modulus of elasticity for different level of earthquake for Model IW-SB (innovative model) and Model 1 (referent model)

Model	Earthquake Intensity											
	0.05g	0.10g	0.20g	0.30g	0.40g	0.60g	0.70g	0.80g	1.00g	1.20g	1.40g	1.60g
	E	E	E	E	E	E	E	E	E	E	E	E
	[Mpa]	[Mpa]	[Mpa]	[Mpa]	[Mpa]	[Mpa]	[Mpa]	[Mpa]	[Mpa]	[Mpa]	[Mpa]	[Mpa]
Model 3	9,280	9,280	9,280	9,280	9,280	9,280	9,280	5,900	5,900	5,900	5,900	5,900
Model 1	3,800	3,800	3,800	3,800	3,800	3,800	3,800	3,800	3,800	3,800	3,800	3,800

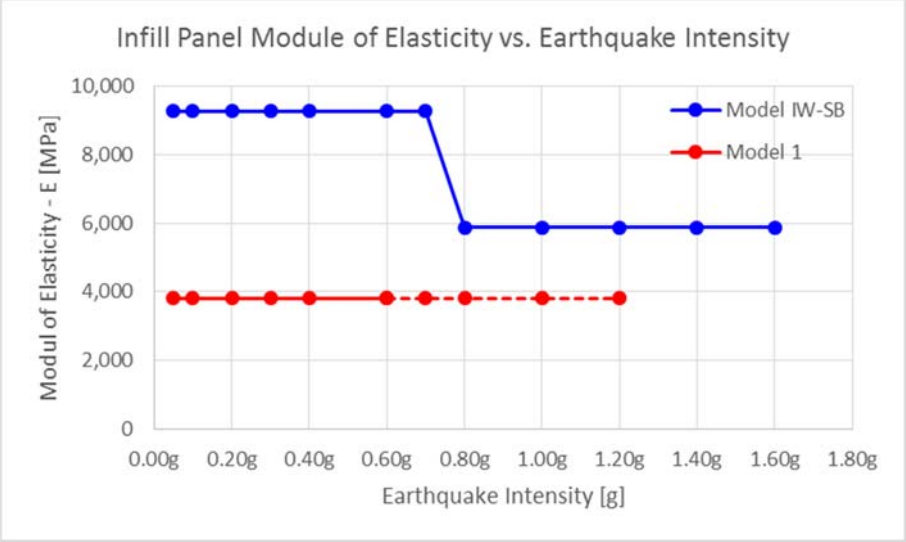

Figure 5.12 Infill panel module of elasticity vs. Earthquake intensity for Model IW-SB (innovative model) and Model 1 (referent model)

5.3.3. Assigning of frame hinges and modeling of diagonal compressive struts for infill walls

Plasticity in RC members was assumed to be lumped at probable locations. Plastic hinges were assumed at relative distance of 0.05 and 0.95 respectively as it is better described in section 5.2.2. Frame geometry and assigned frame hinges are shown on Figure 5.13 - 5.16.

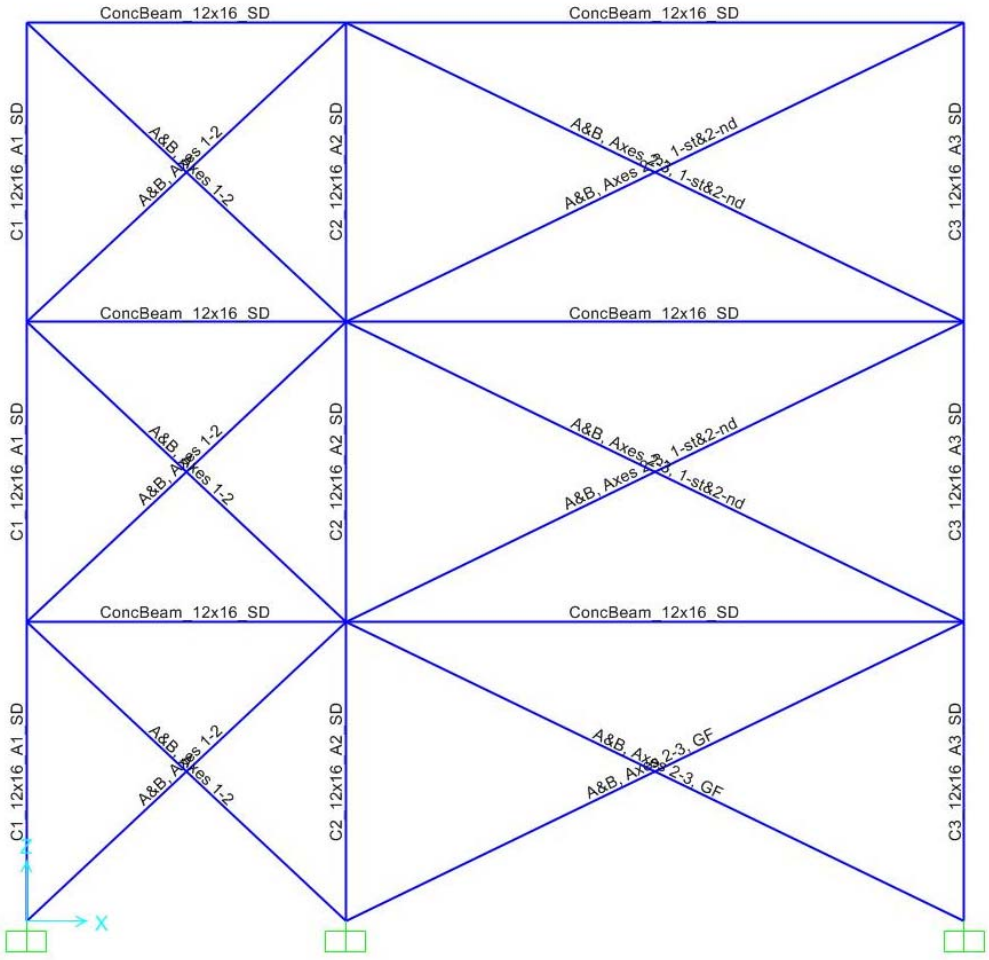

Figure 5.13 Assigned frame elements for Frame A and B

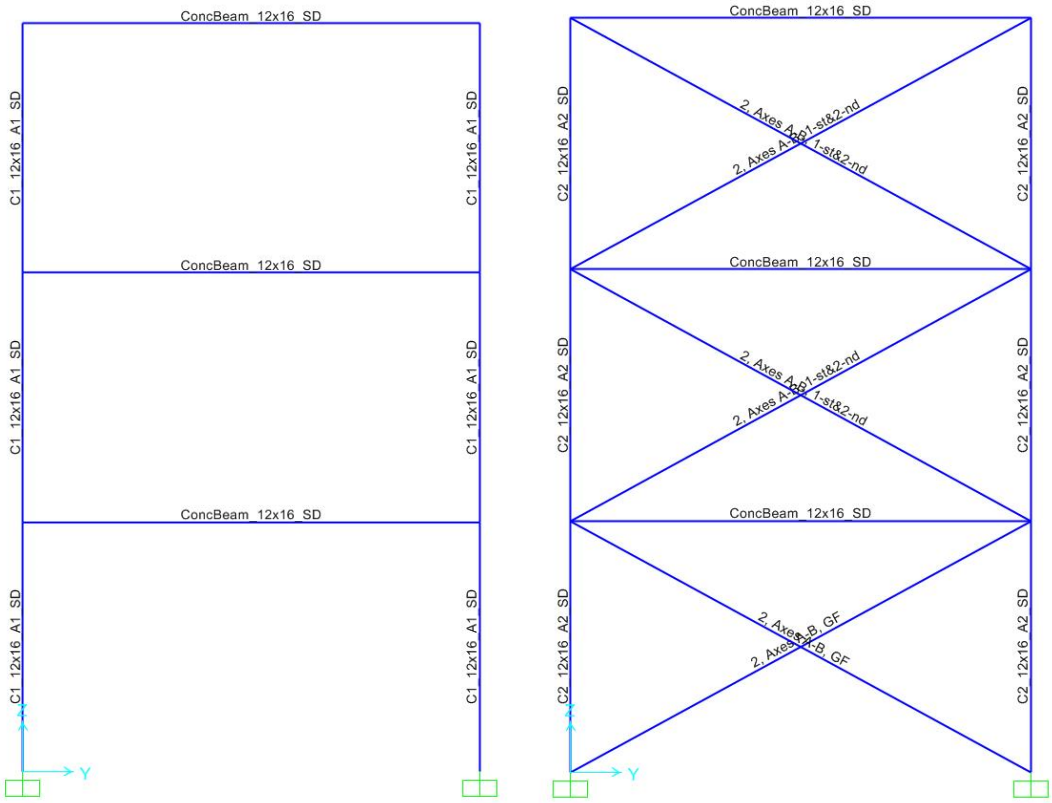

Figure 5.14 Assigned frame elements for Frame 1 and 3 (left) and Frame 2 (right)

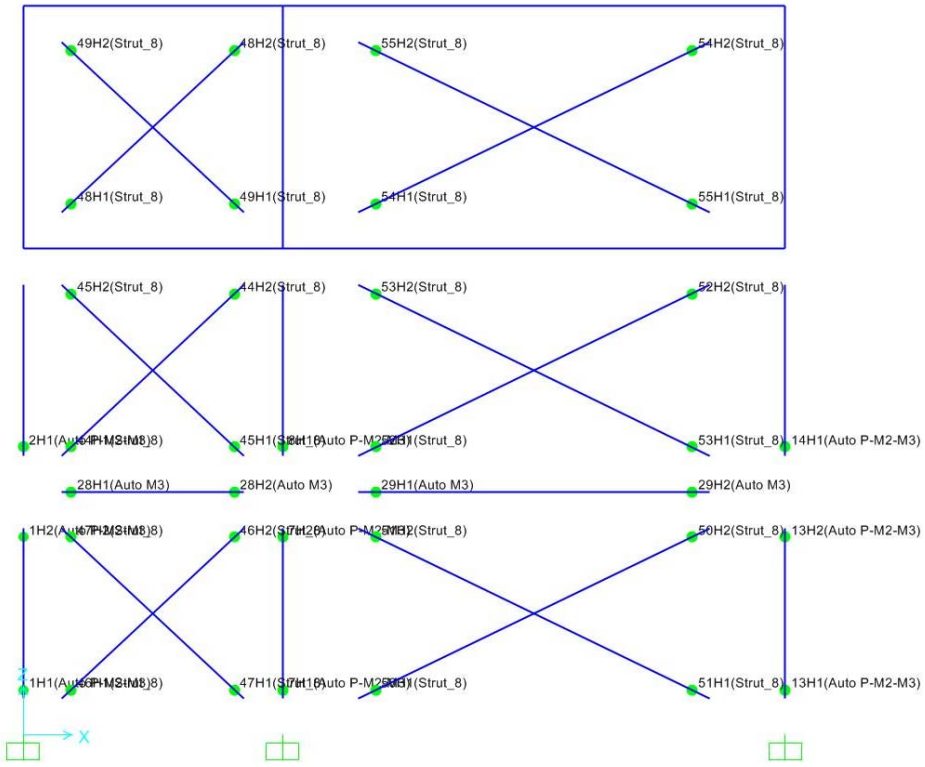

Figure 5.15 Assigned frame hinges for Frame A and B

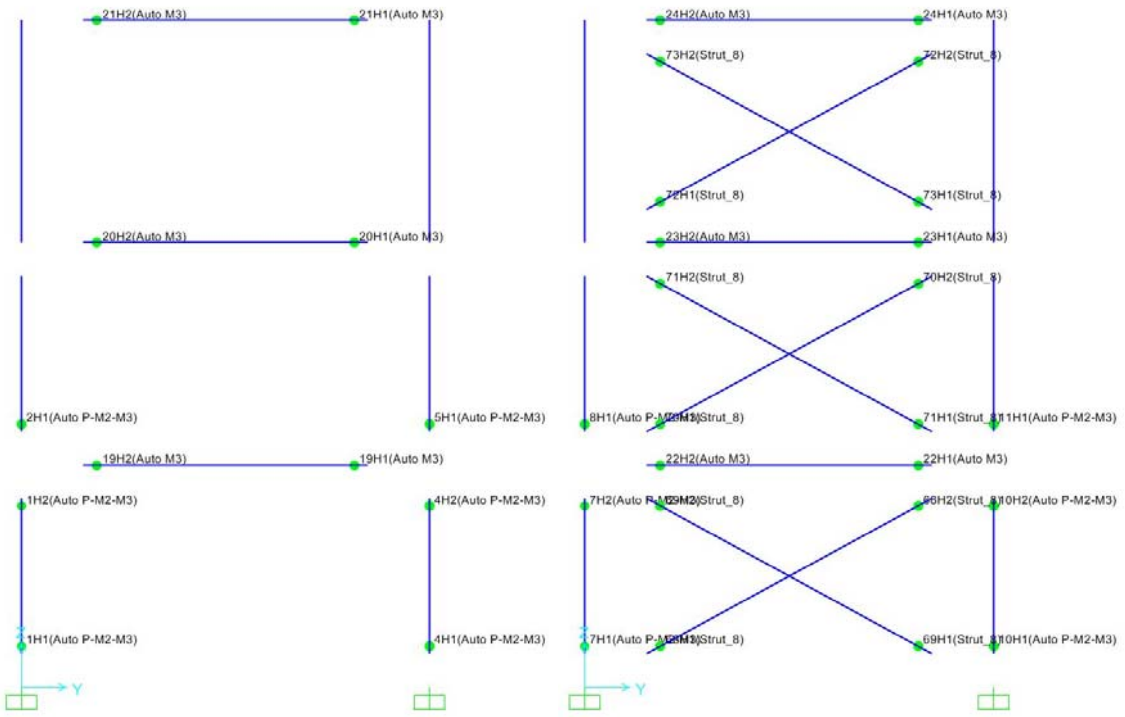

Figure 5.16 Assigned frame hinges for Frame 1 and 3 (left) and Frame 2 (right)

It can be observed that the nonlinear hinges are applied to the RC structural members on which a nonlinear behavior is expected. Members, like the second and the third floor beams and columns are expected to stay in an elastic range, so no nonlinear hinges are applied to those members.

For the purpose of infill wall modeling, a separate calculation has been made for each panel wall according to the procedure described in section 5.2.3 (Figure 5.17 and 5.18). Further on, an example of the calculation is presented.

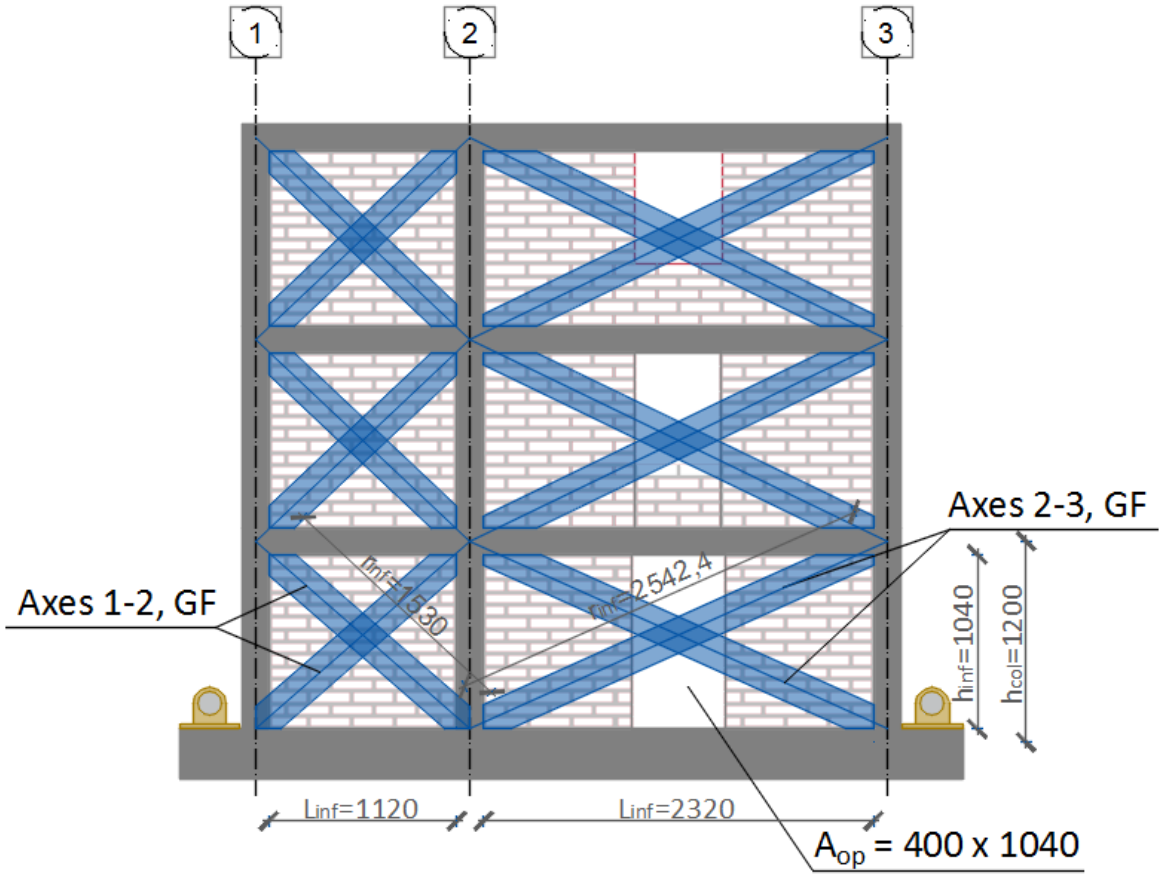

Figure 5.17 Diagonal strut properties for Ground floor of Frame 1 and 2

Frames A&B, Axes 1-2

h_{col} =	1200.00	[mm]	t_{inf} =	120.00	[mm]
h_{inf} =	1040.00	[mm]	θ =	0.74838	[rad] (42.88°)
E_{fe} =	38838	[N/mm2]	A_{op} =	0	[mm2]
E_{me} =	5900	[N/mm2]	A_{inf} =	1164800	[mm2]
I_{col} =	40960000	[mm4]			
L_{inf} =	1120.00	[mm]			
r_{inf} =	1530.00	[mm]			

R =	1.00	/
λ_t =	0.0032139	/
b_w =	156.04	[mm]

Frames A&B, Axes 2-3, GF

h_{col} =	1200.00	[mm]	t_{inf} =	120.00	[mm]	
h_{inf} =	1040.00	[mm]	θ =	0.47735	[rad]	(27.35°)
E_{fe} =	38838	[N/mm2]	A_{op} =	416000	[mm2]	
E_{me} =	5900	[N/mm2]	A_{inf} =	2412800	[mm2]	
I_{col} =	40960000	[mm4]				
L_{inf} =	2320.00	[mm]				
r_{inf} =	2542.00	[mm]				

R =	0.74	/
λ_t =	0.0030568	/
b_w =	196.26	[mm]

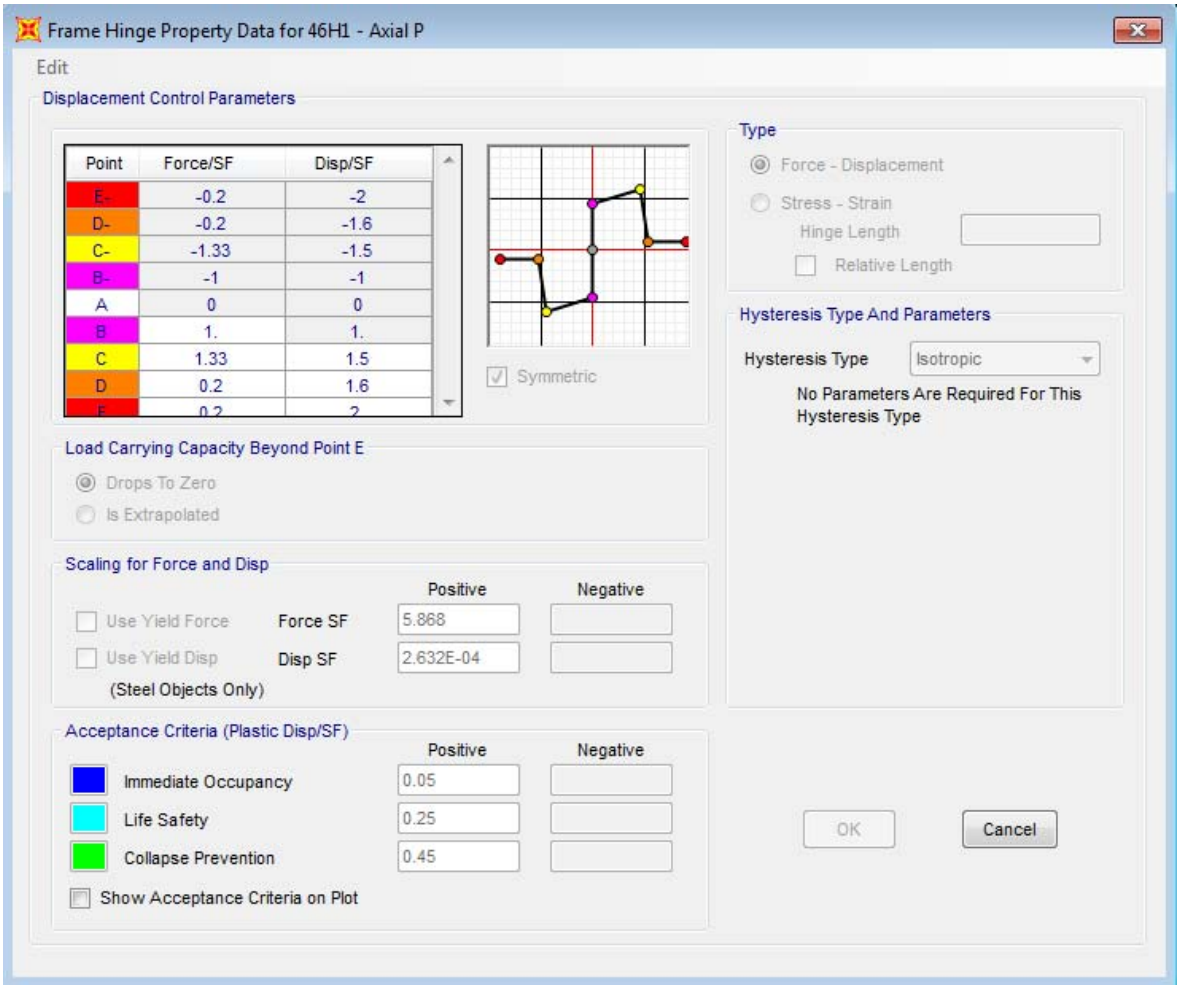

Figure 5.18 Force Displacement data for hinge 28H1 (Strut)

5.3.4. Results from nonlinear static (pushover) analysis

A nonlinear static (pushover) analysis has been performed for the 3D modeled structure as it was described in the previous sections. The analysis resulted in total of 67 steps, while the structure has been "pushed" for target displacement of 10cm. Plastic hinge formation and static pushover curve is presented in the Figs. 5.19-5.23.

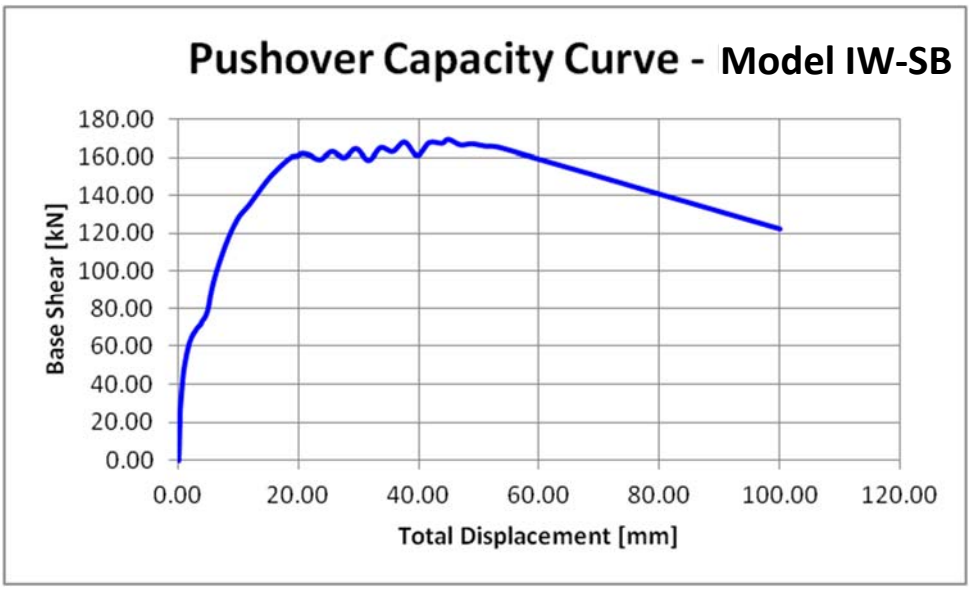

Figure 5.19 Pushover capacity curve for Model IW-SB

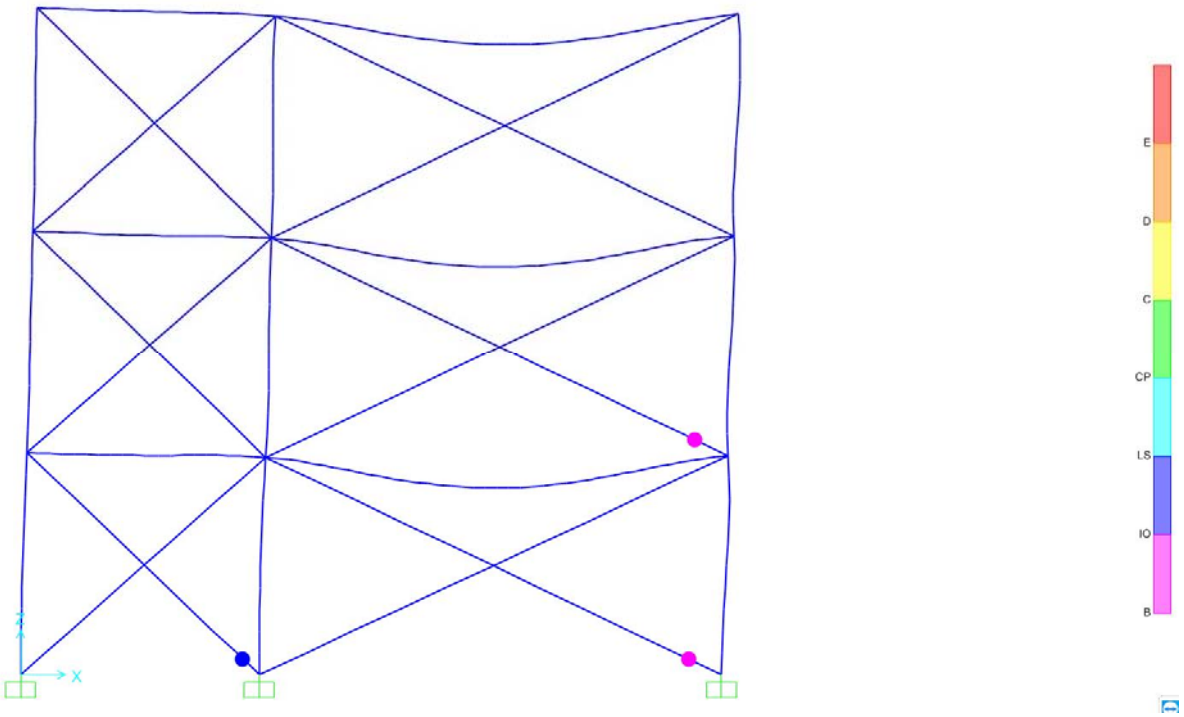

Figure 5.20 Plastic hinge formation in masonry at step 4 (δ= 1.85; F=62.35)

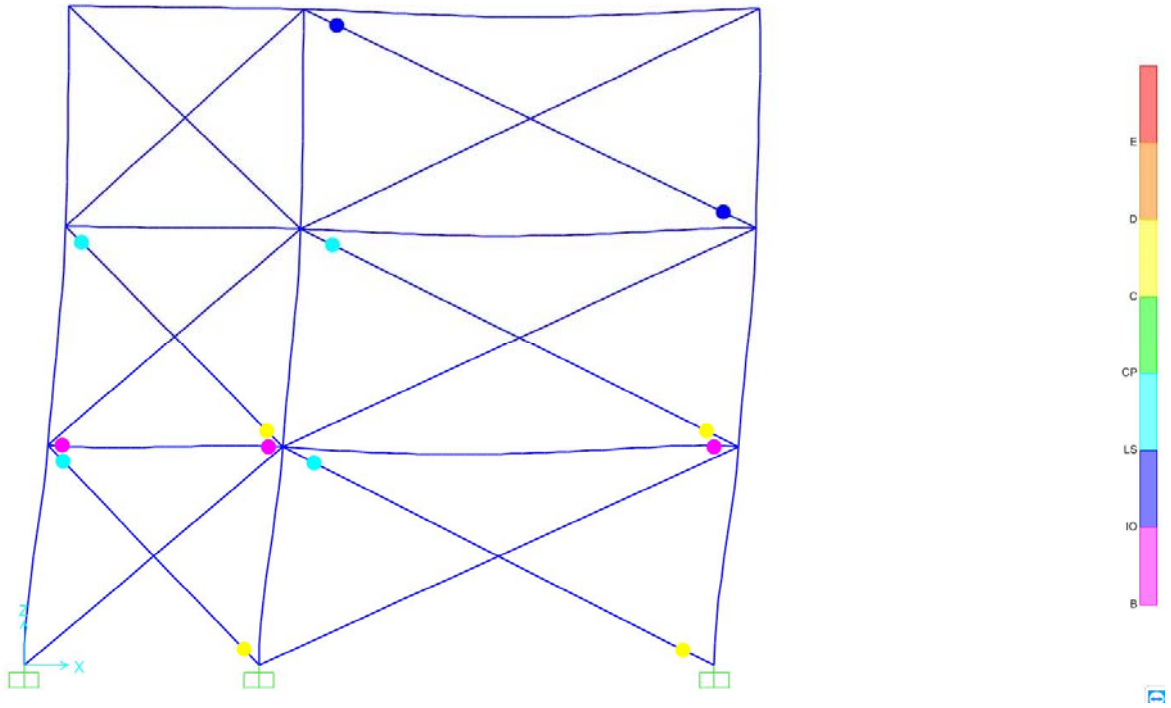

Figure 5.21 Plastic hinge formation at step 17 (δ= 4.79; F=78.35)

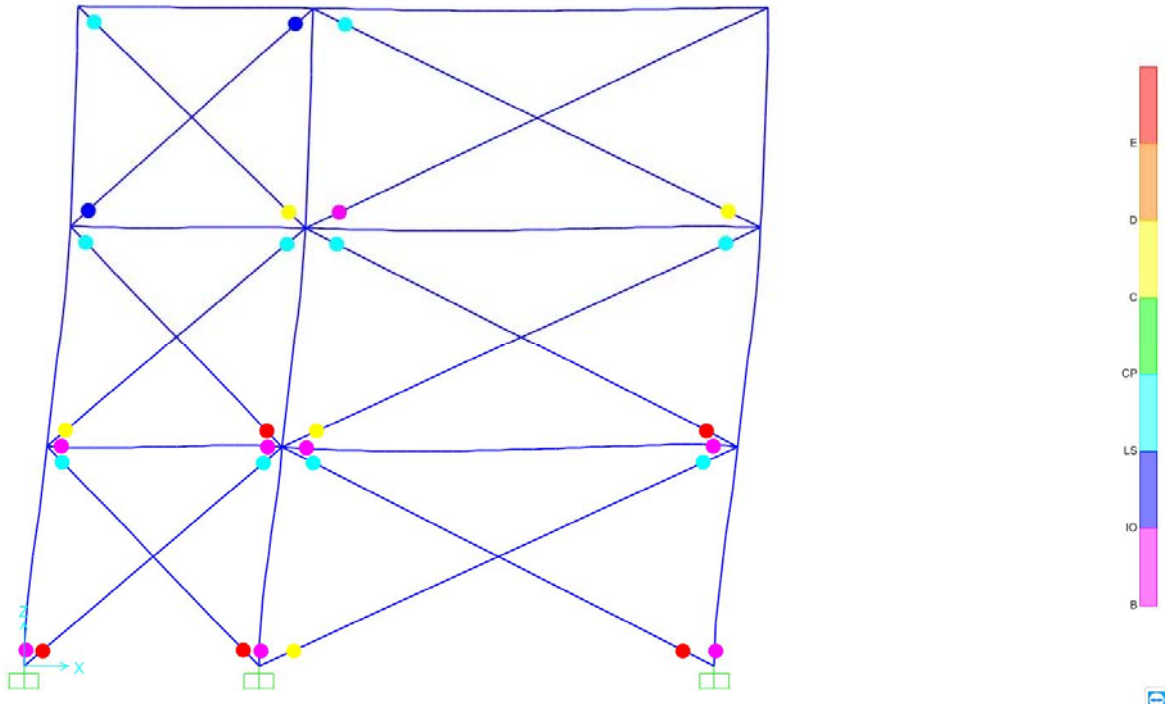

Figure 5.22 Plastic hinge formation at step 19 (δ= 7.78; F=113.74)

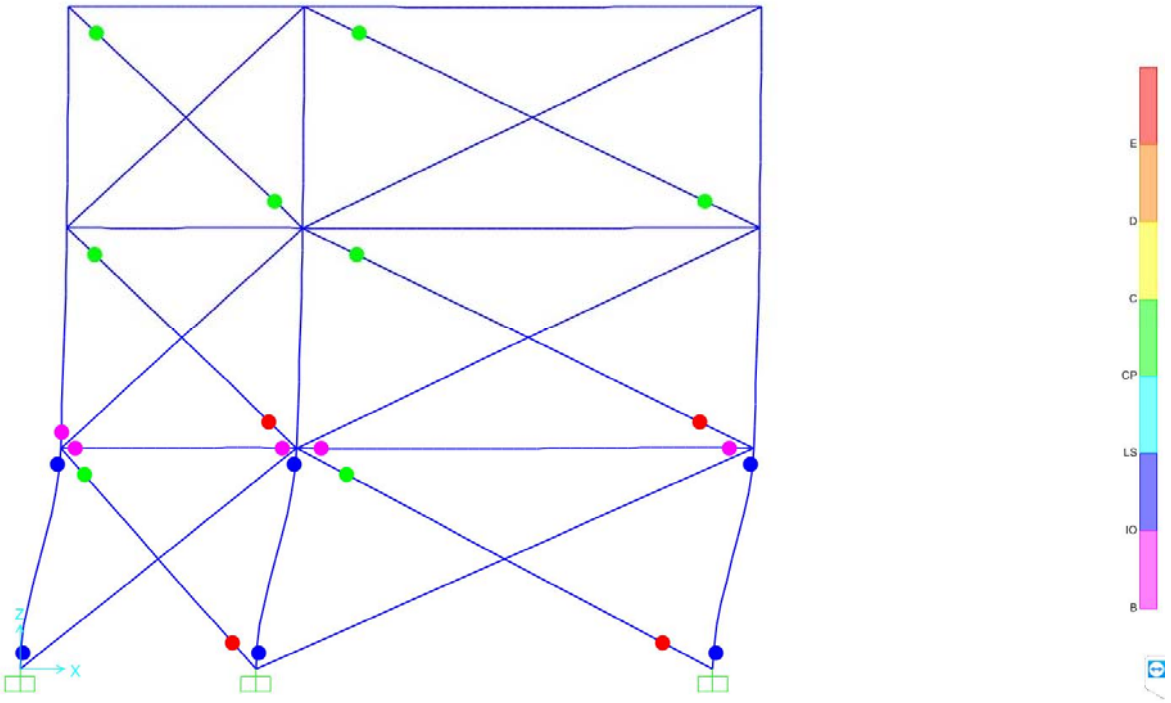

Figure 5.23 Plastic hinge formation at step 33 (δ= 31.61; F=158.57)

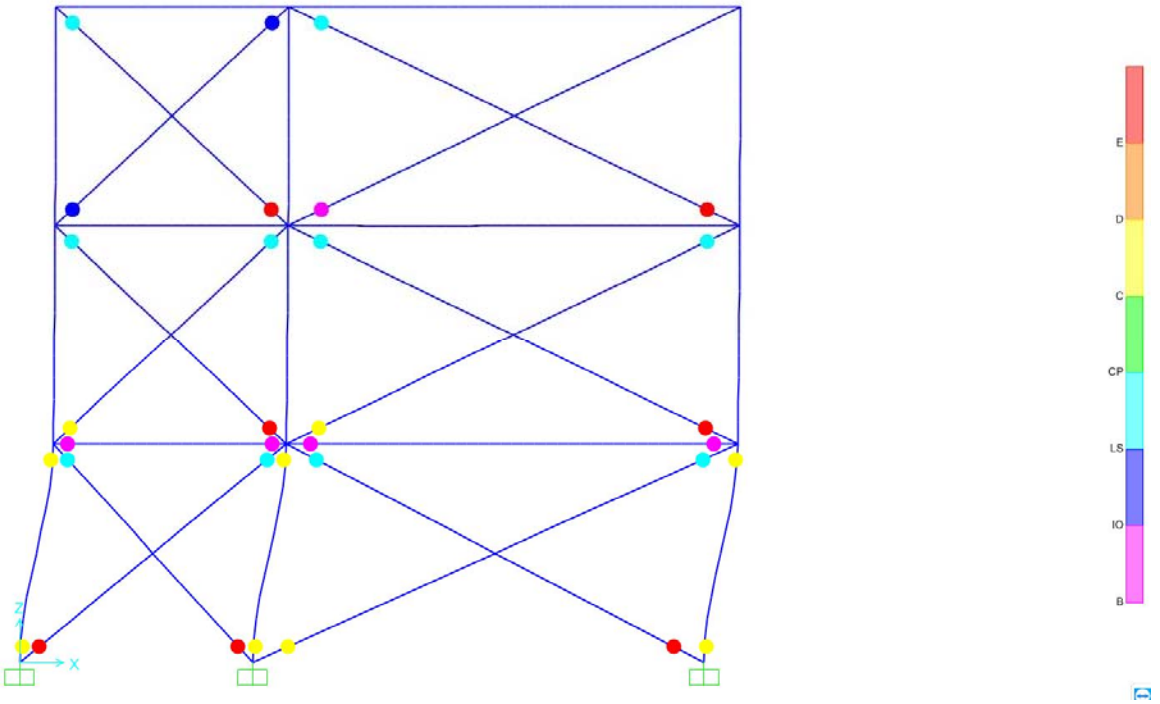

Figure 5.24 Plastic hinge formation at final step 67 (δ= 100.05; F=122.54)

From the results presented above, it can be concluded that the formation of the plastic hinge is firstly located at the masonry infill walls only, up to a Base Shear of around 75 kN and top displacement of 4.50 mm. The first plastic hinge in the RC structure is located in beams at the first floor at Step 17,

with a Base Shear of 78.35 kN and top displacement of 4.79 mm. First column hinge is happening at Step 19 with a Base Shear of 113.74 kN and top displacement of 7.78mm. The final step (Step 67) shows that the almost every infill wall lost its bearing capacity and the columns are actually collapsing.

5.3.5. Results from nonlinear direct integration time-history analysis

A nonlinear direct integration time-history analysis has been performed for the 3D modeled structure as it was described in the previous sections, from earthquake intensity from 0.05g and up to 1.60g. The time step for the time history analysis was as in the experiment, or 0.001 sec, which resulted with a total of more than 30.000 steps. In order to have more reliable performance of the structure, the first time-history load case (0.05g) has initial state with the load of the self-weight of the structure, infill walls and the ingots. Every next time-history load case (0.10g, 0.20g, 0.40g etc.) has initial state equal to the final step of the previous time-history load case. Top displacements, along with a Base Shear – Top displacement time-histories for selected earthquake intensities of 0.10g, 0.60g, 1.00g, 1.20 g and 1.60g are presented in the following figures (Figure 5.25-5.34).

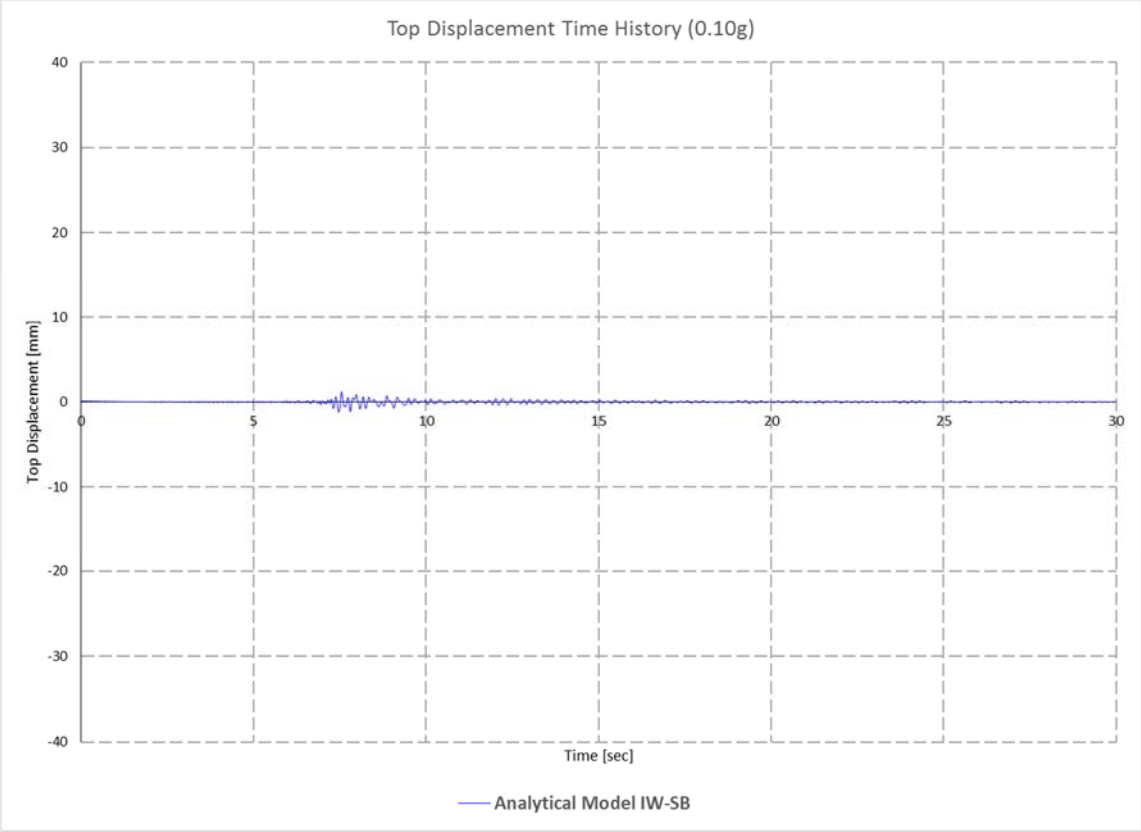

Figure 5.25 Top Displacement Time History for 0.10g

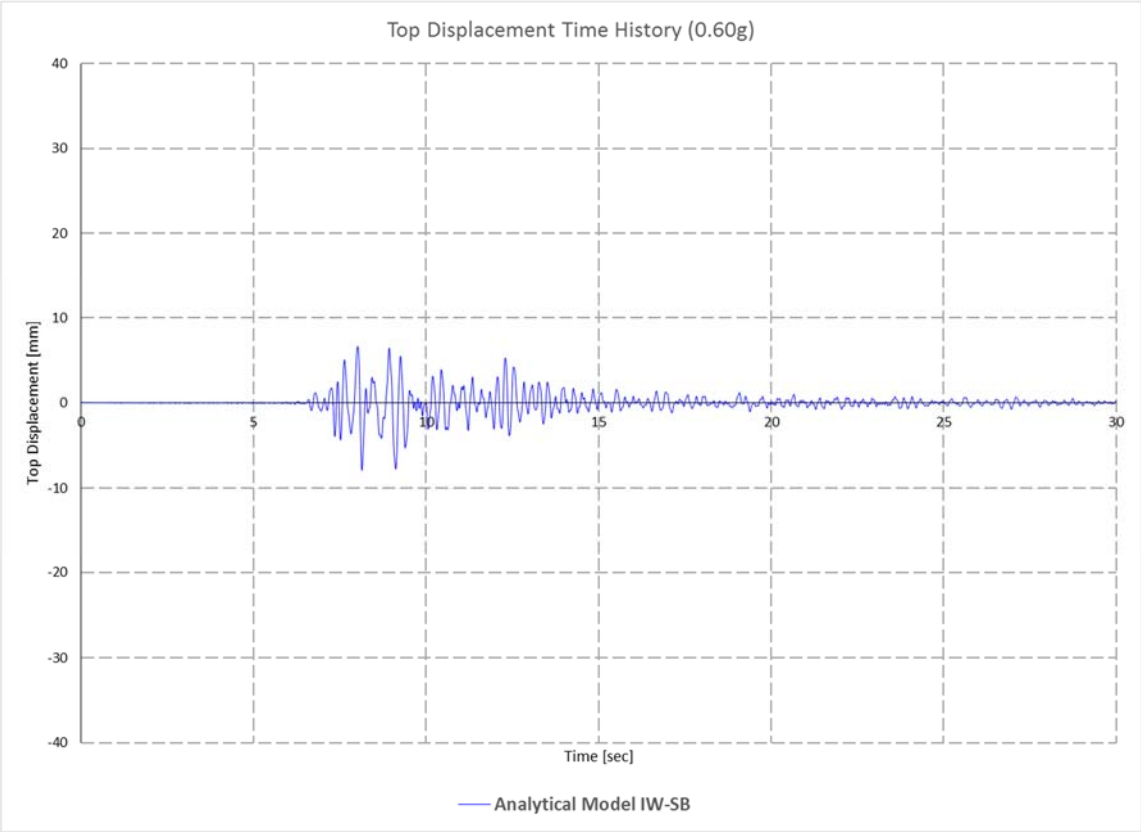

Figure 5.26 Top Displacement Time History for 0.60g

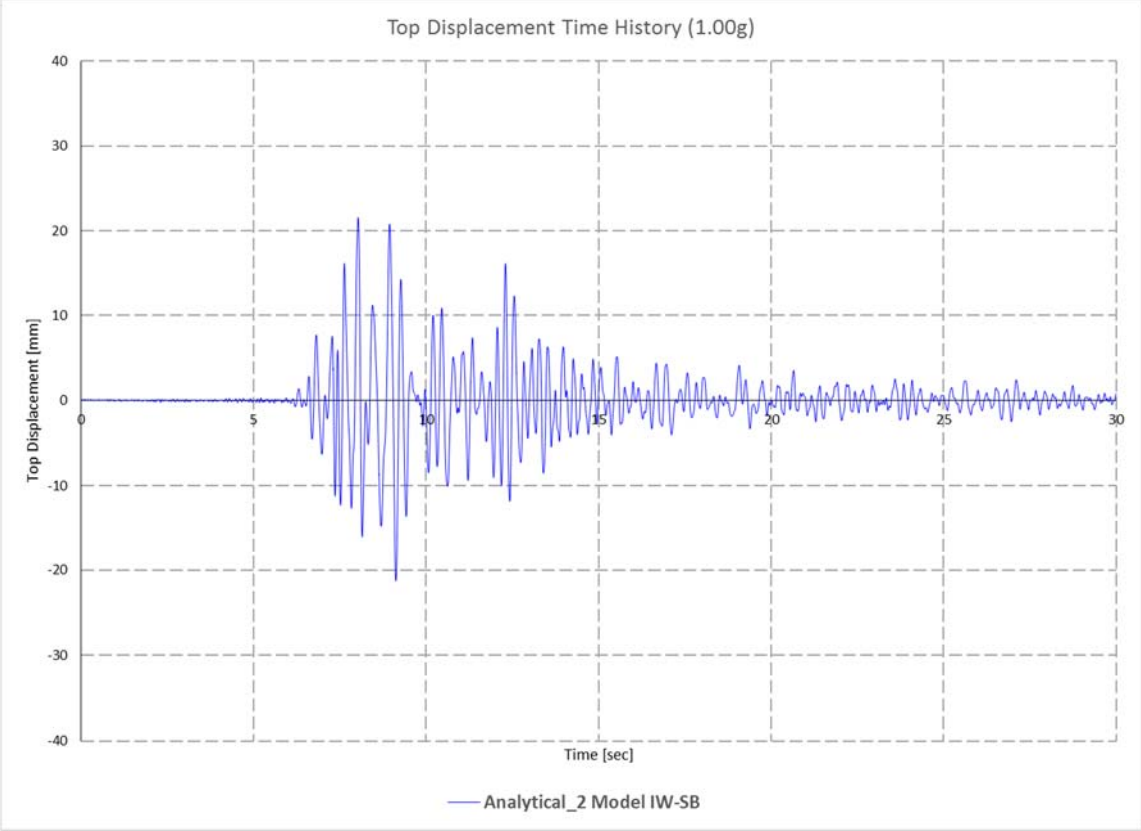

Figure 5.27 Top Displacement Time History for 1.00g

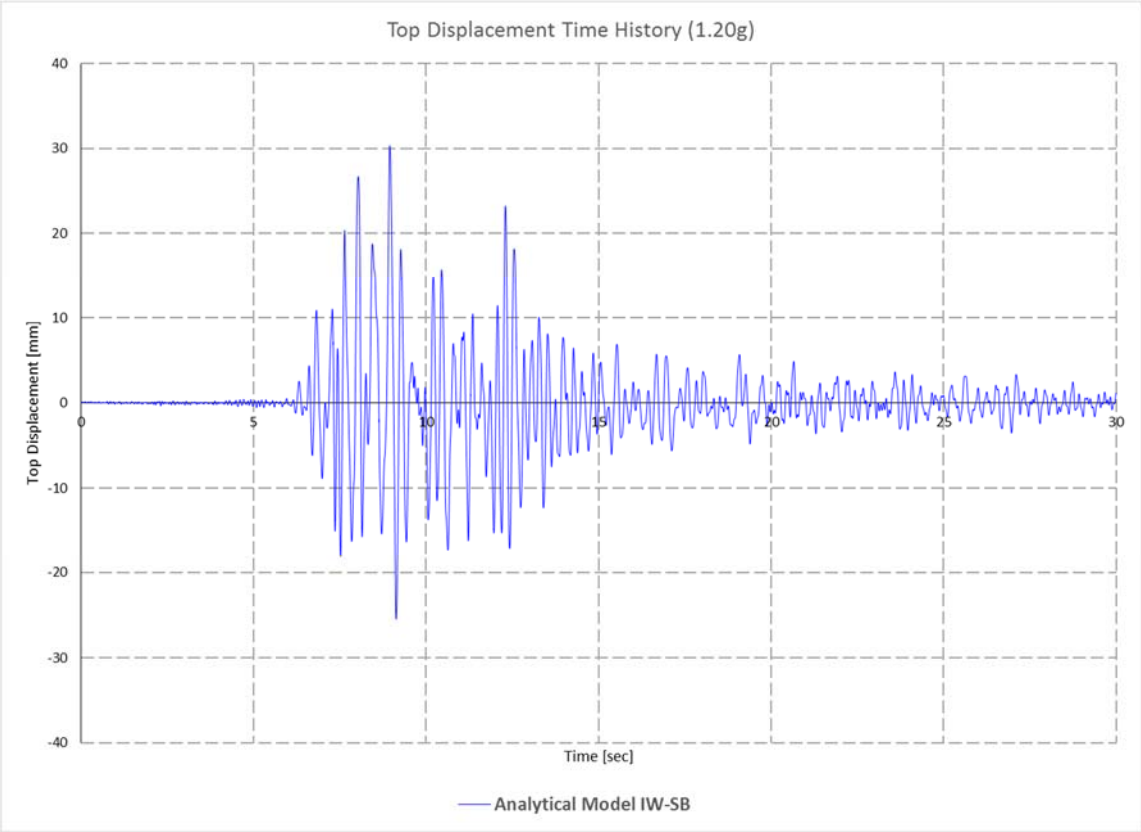

Figure 5.28 Top Displacement Time History for 1.20g

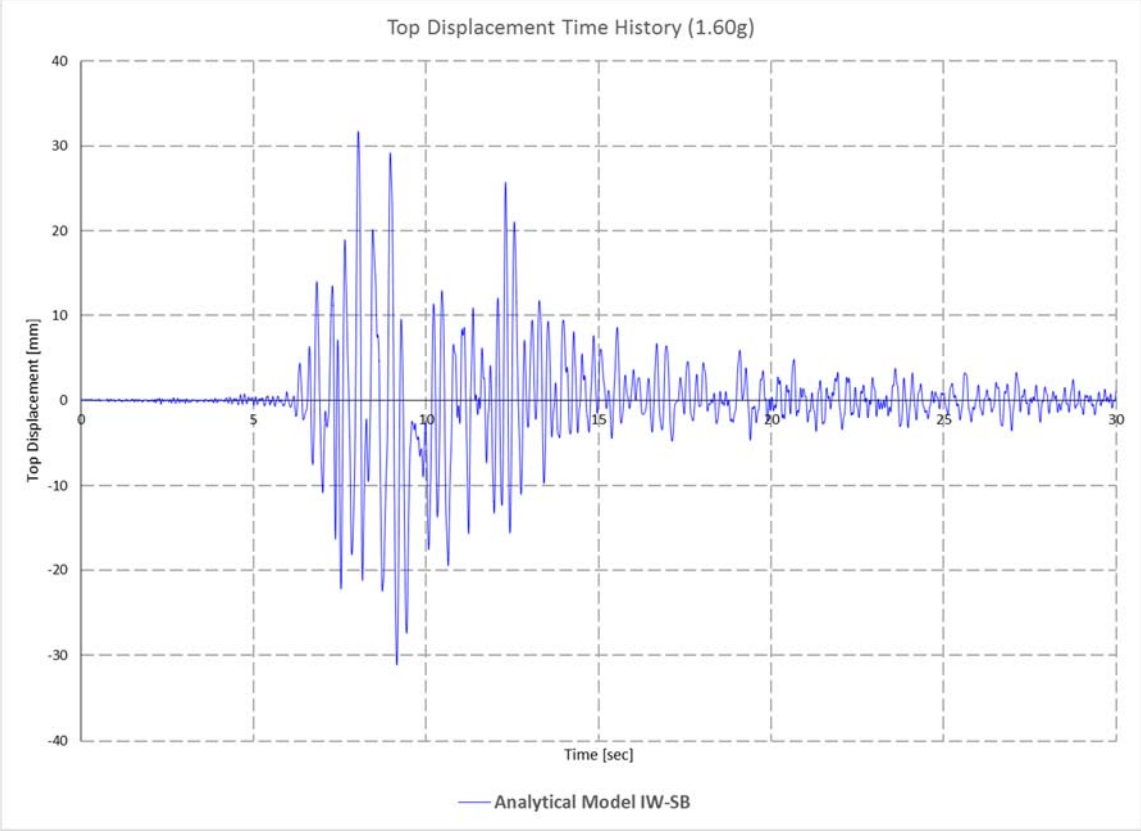

Figure 5.29 Top Displacement Time History for 1.60g

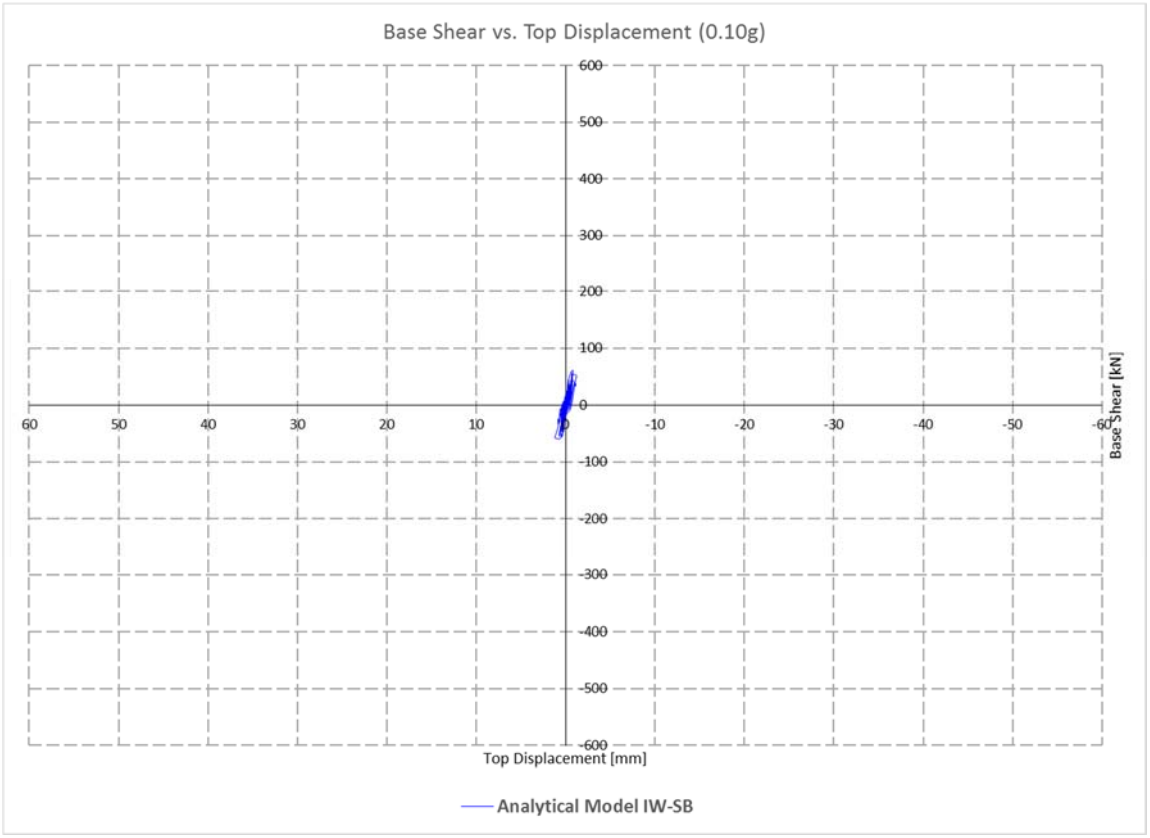

Figure 5.30 Base shear vs. top displacement for 0.10g

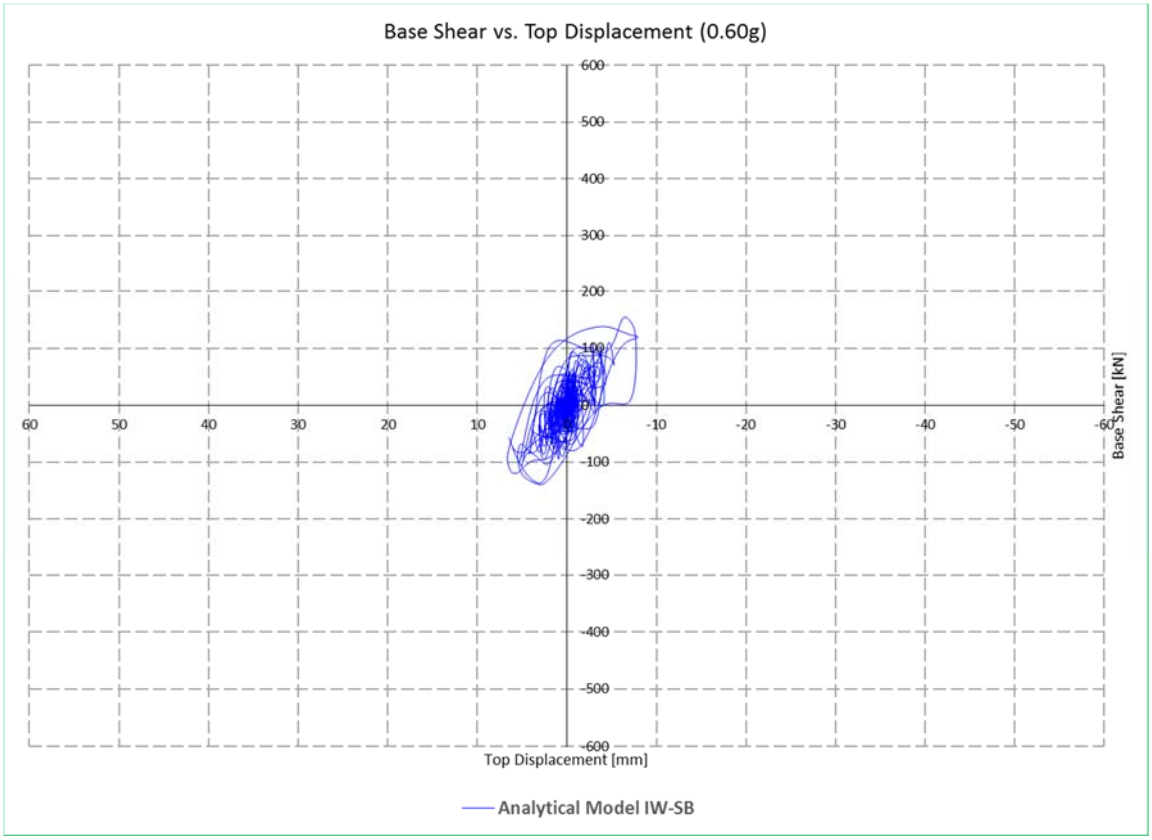

Figure 5.31 Base shear vs. top displacement for 0.60g

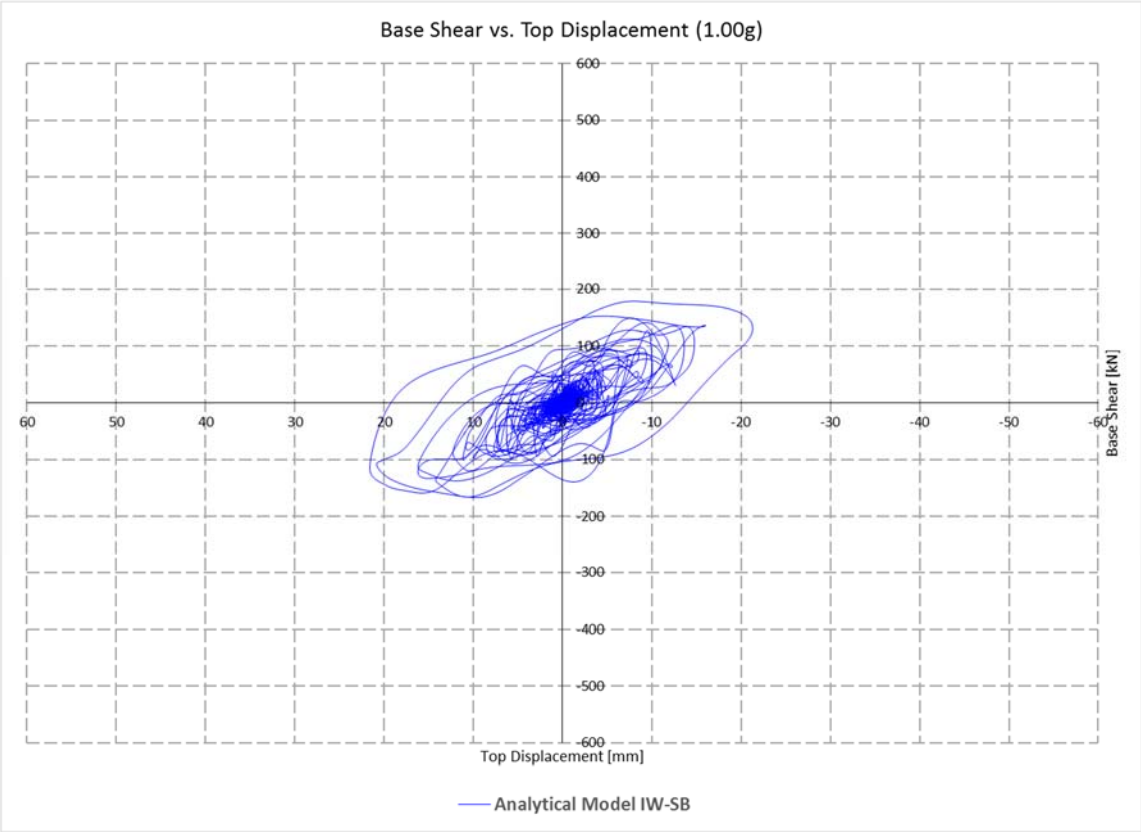

Figure 5.32 Base shear vs. top displacement for 1.00g

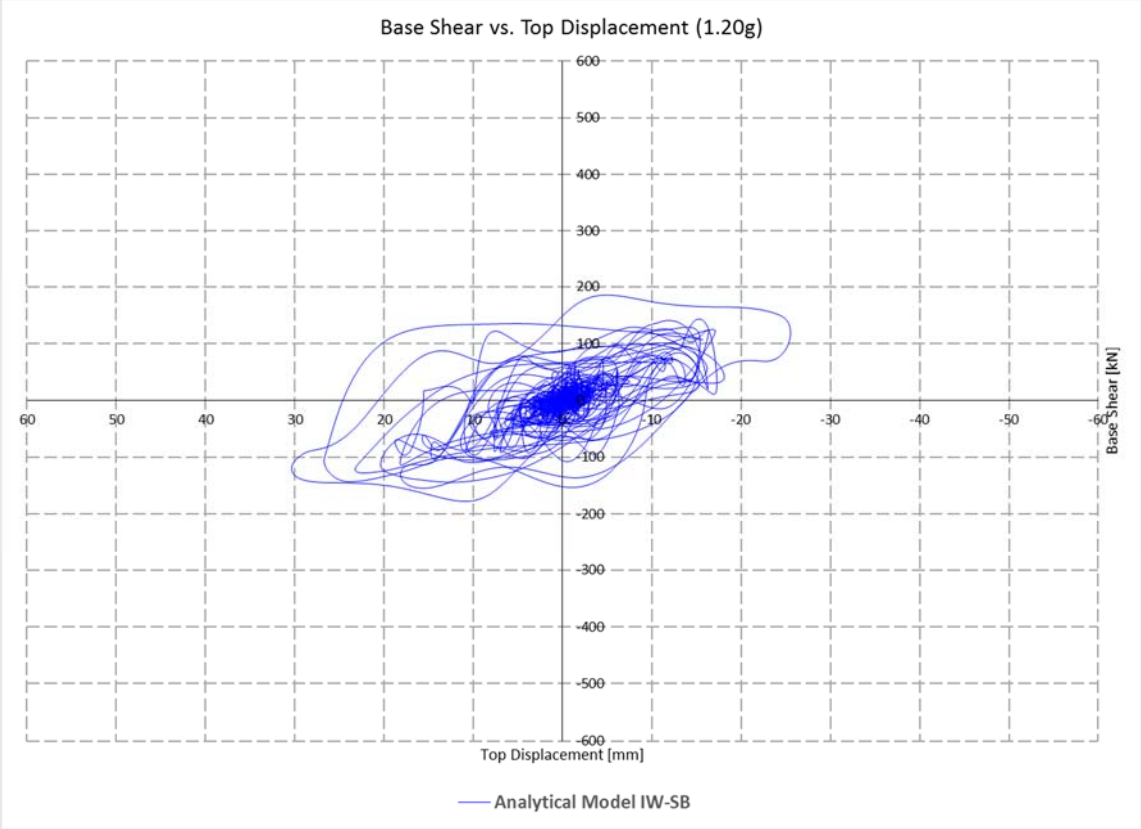

Figure 5.33 Base shear vs. top displacement for 1.20g

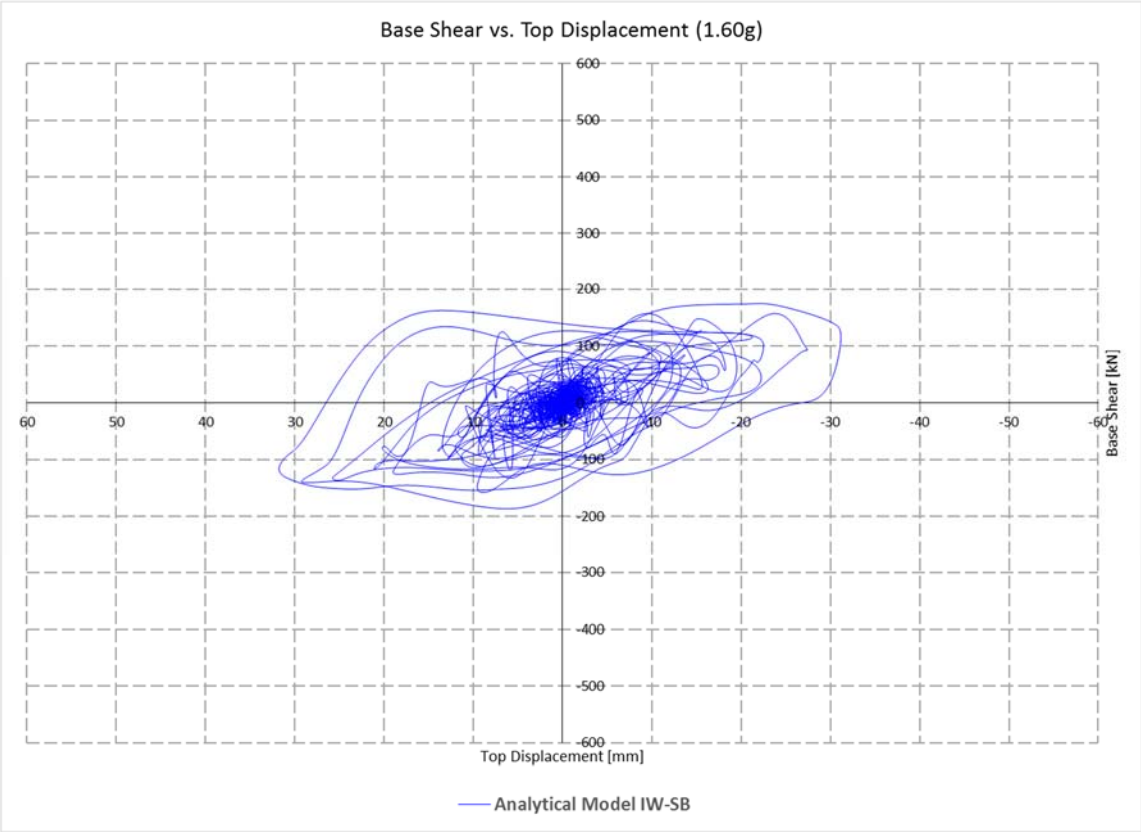

Figure 5.34 Base shear vs. top displacement for 1.60g

5.3.6. Capacity and damage mechanism of the referent Model 1

Model 1, as standard referent model for comparison, was also analyzed in the same manner as Model IW-SB. The goal here is to check the effectivity of the selected modeling approach for standard structure (as it is usually build on a construction site) by making a comparison of selected data with the experimental one and to make a comparison with the effectiveness of the proposed infill connection and modeling approach that is selected (previously described in Section 5.3.2).

The modeling approach was the same as in the case of analyzing Model IW-SB, except that in this case, a constant modulus of elasticity for masonry infill with a value of 3.800 MPa was used for every earthquake magnitude. In this manner, a nonlinear static (pushover) analysis along with direct integration time history analysis has been made and selected results are presented further on.

The pushover analysis resulted in total of 61 steps, while the structure has been “pushed” for target displacement of 10cm. Plastic hinge formation and static pushover curve is presented in the following figures (Figure 5.35-5.39).

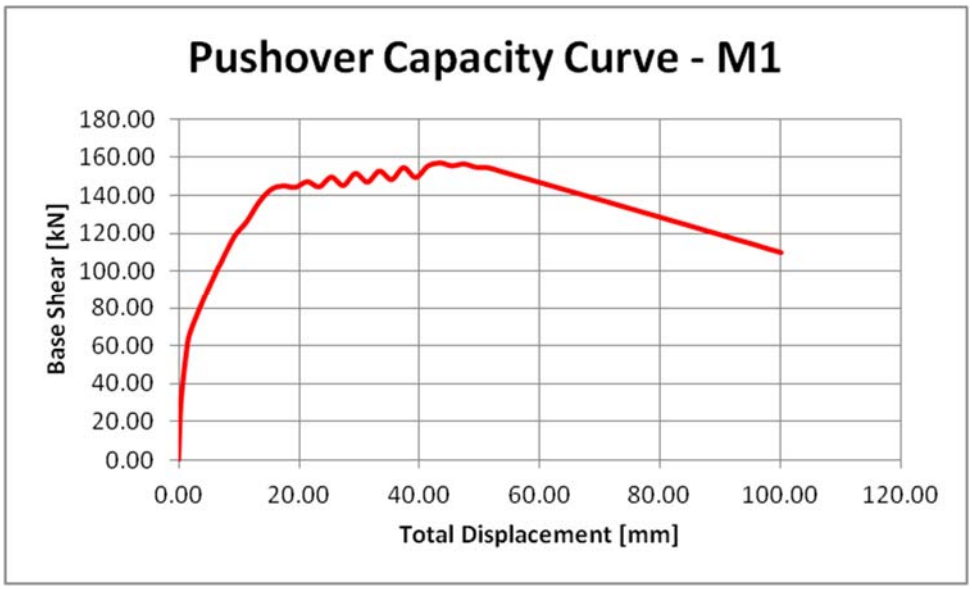

Figure 5.35 Pushover capacity curve for Model 1

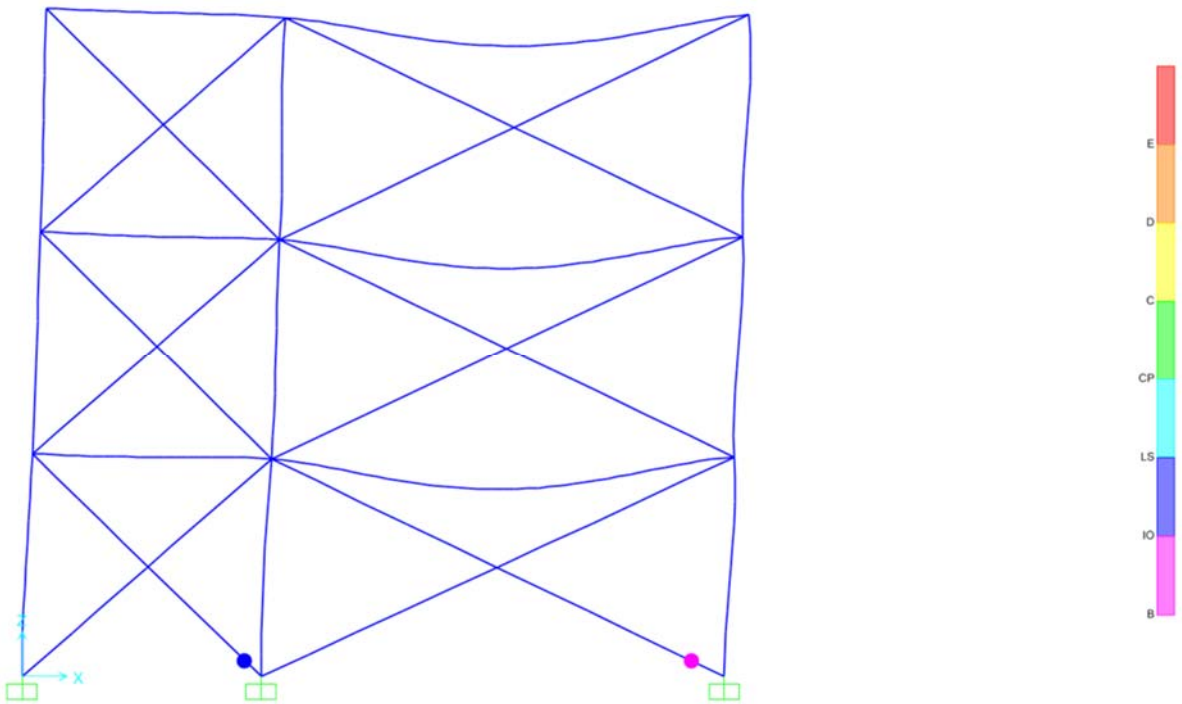

Figure 5.36 Plastic hinge formation in masonry at step 2 (δ= 1.27; F=54.71)

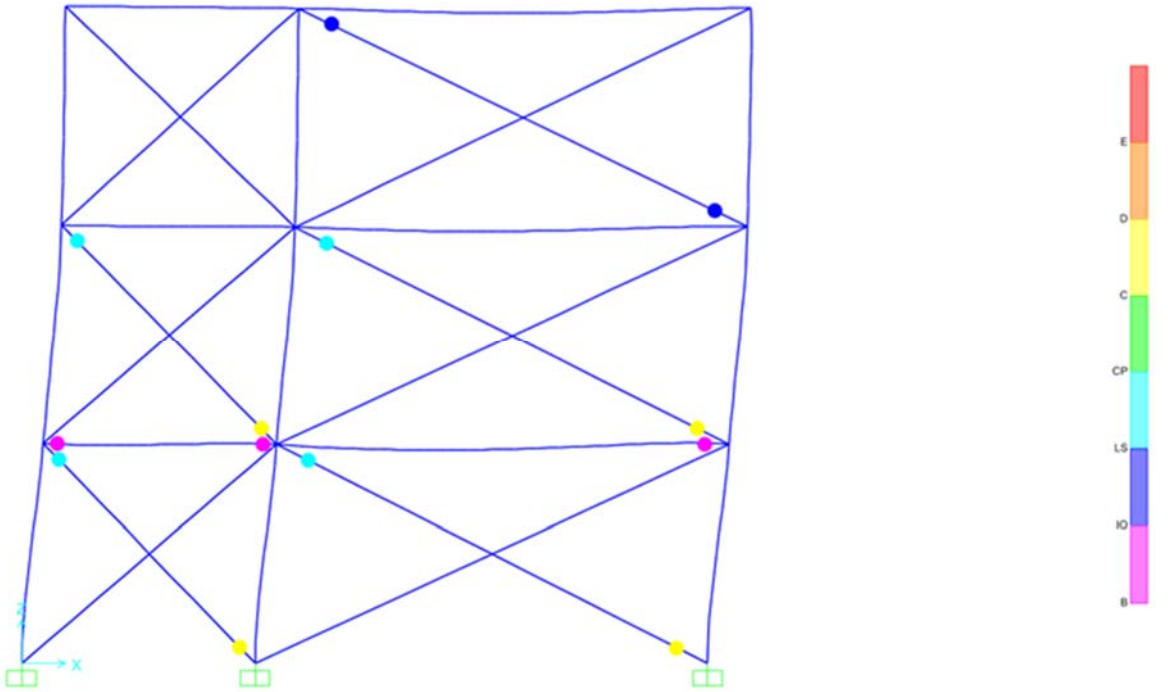

Figure 5.37 Plastic hinge formation at step 9 (δ= 6.53; F=101.10)

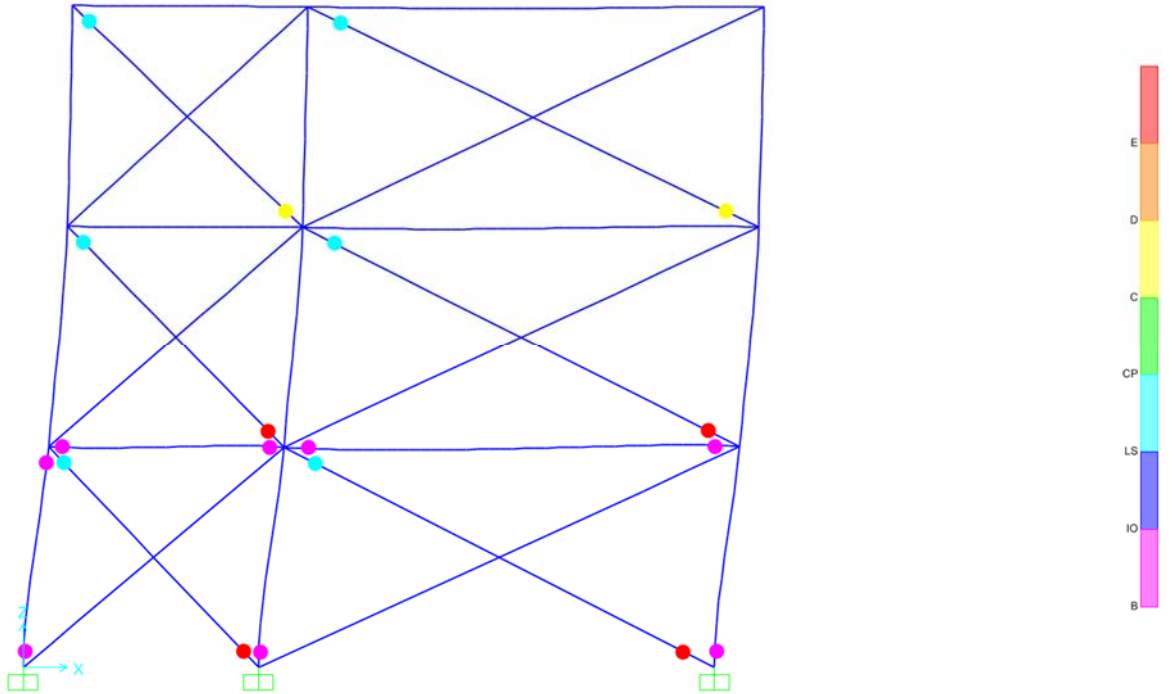

Figure 5.38 Plastic hinge formation at step 15 (δ= 9.39; F=118.59)

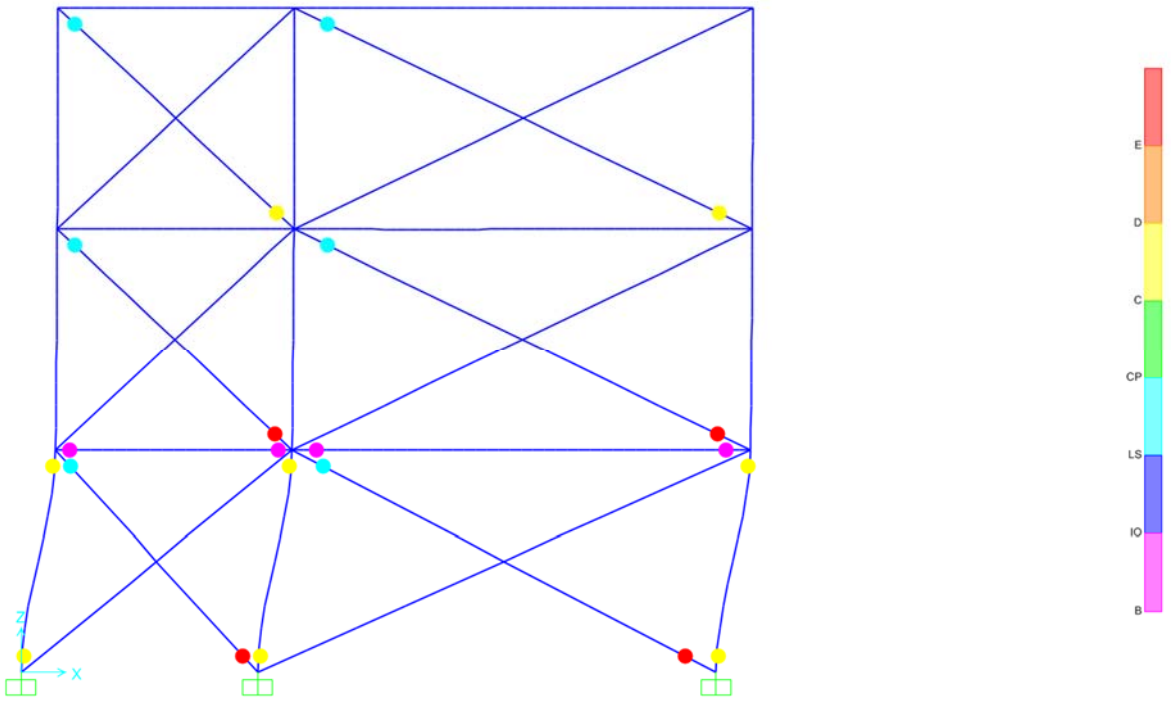

Figure 5.39 Plastic hinge formation at final step 67 (δ= 100.05; F=109.66)

From the results presented above, it can be concluded that the formation of the plastic hinge is firstly located at the masonry infill walls only, up to a Base Shear of around 65 kN. Beyond this value of Base Shear, plastic hinges started to form in the RC structure as well. The final step (Step 67) shows that almost every infill wall has lost its bearing capacity and the columns are actually collapsing.

Top displacements time-histories for selected earthquake intensities of 0.10g, 0.60g, 1.00g and 1.20g obtained from the nonlinear direct integration time-history analysis for the 3D modeled structure of Model 1 are presented in Figures 5.40-5.43.

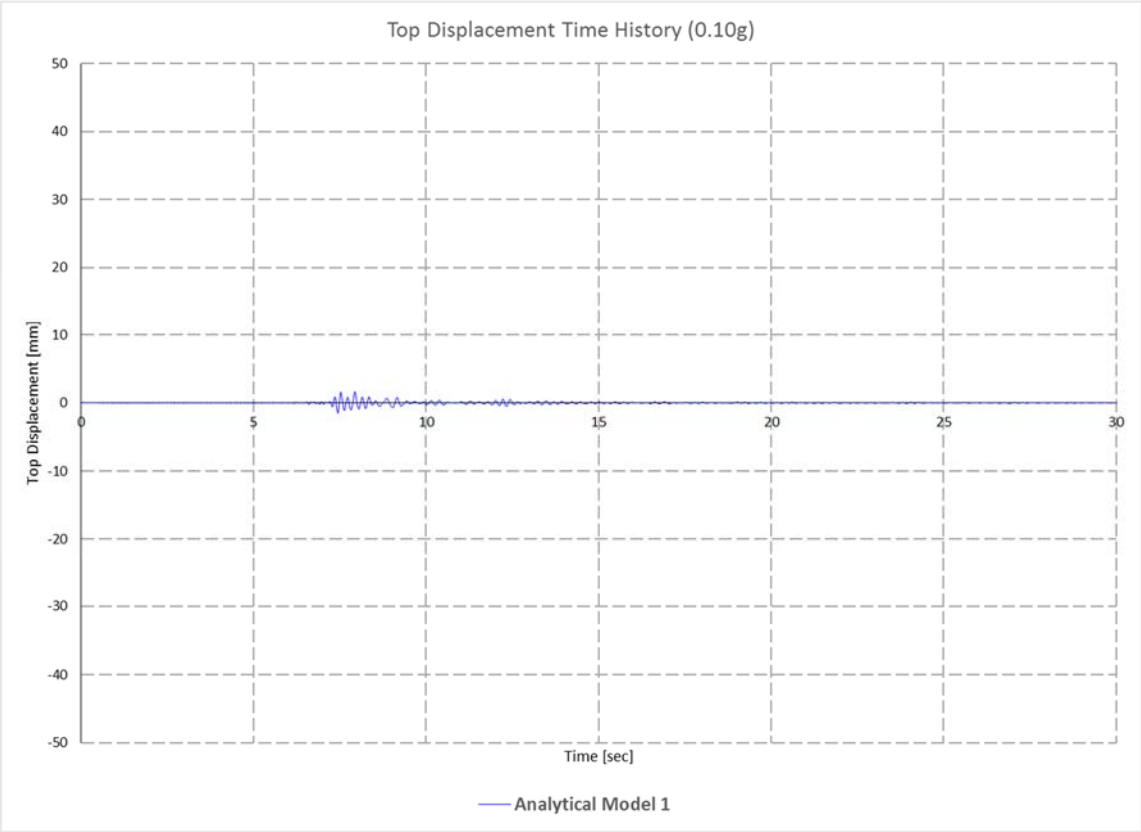

Figure 5.40 Top Displacement Time History for 0.10g

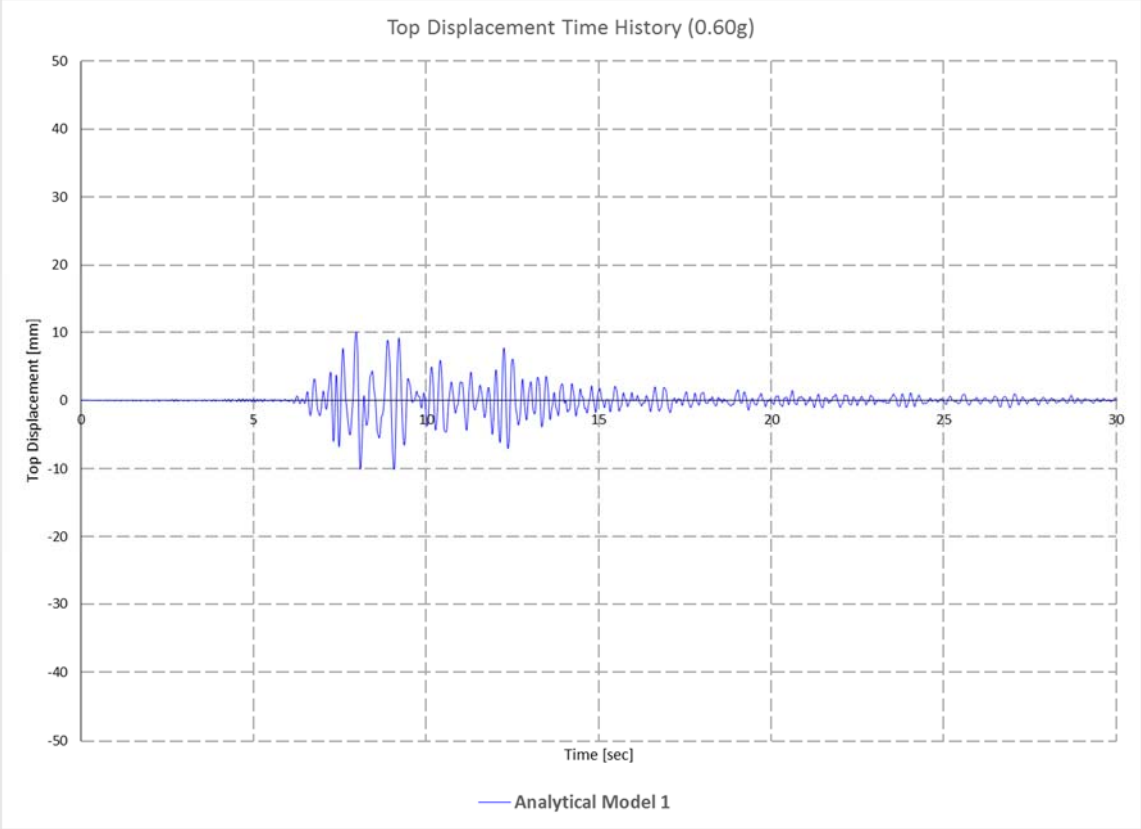

Figure 5.41 Top Displacement Time History for 0.60g

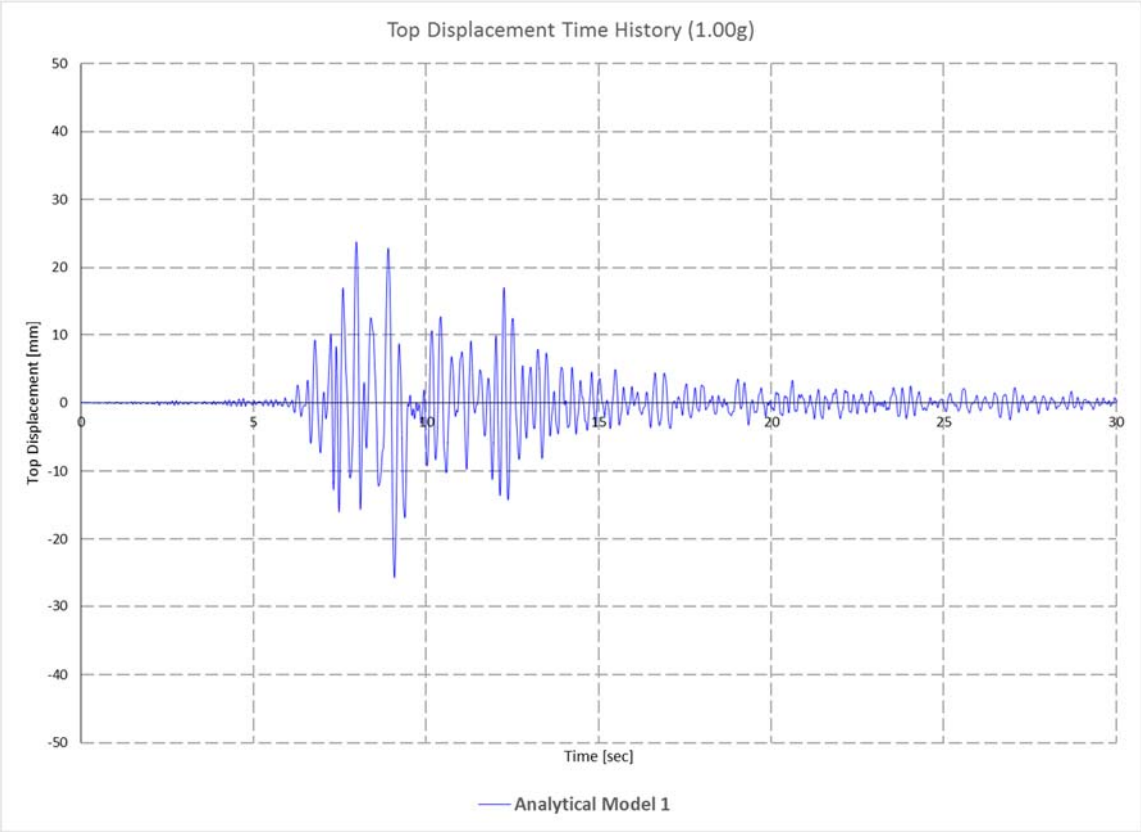

Figure 5.42 Top Displacement Time History for 1.00g

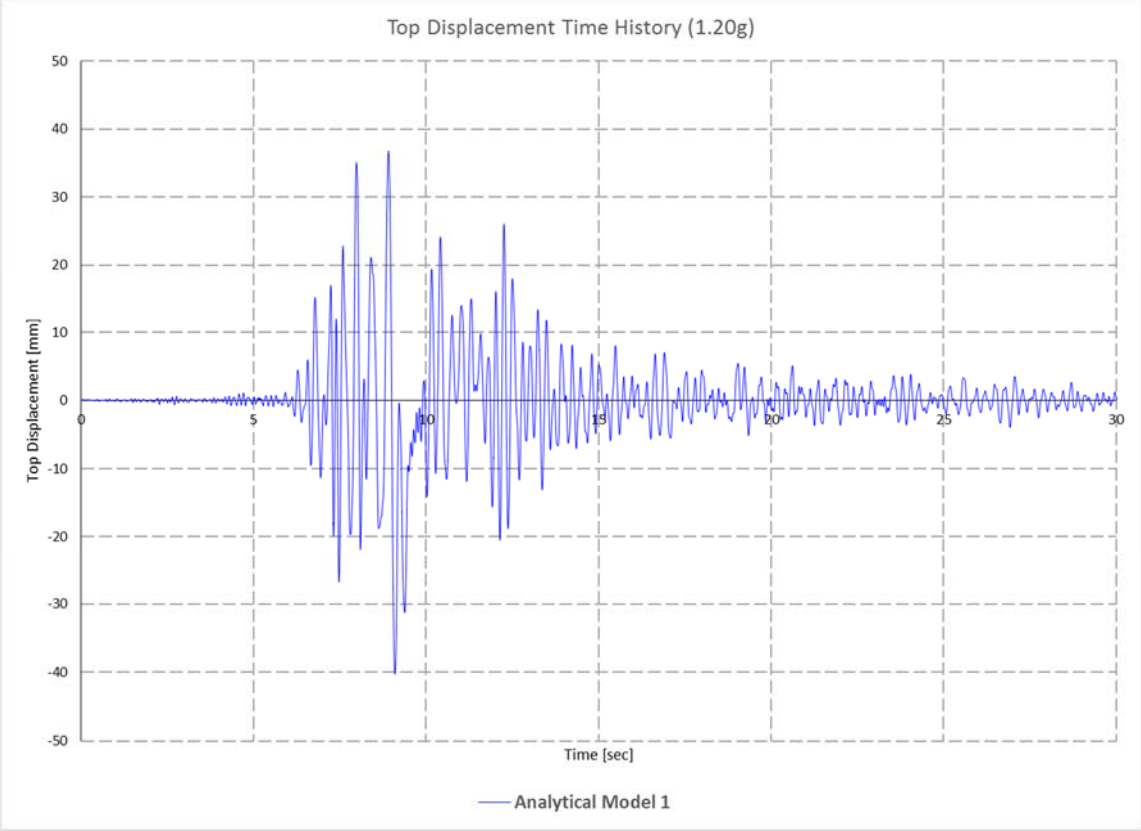

Figure 5.43 Top Displacement Time History for 1.20g

Base Shear – Top displacement time-histories for selected earthquake intensities of 0.10g, 0.60g, 1.00g and 1.20g obtained from the nonlinear direct integration time-history analysis for the 3D modeled structure of Model 1 are presented in the Figs. 5.44-5.47.

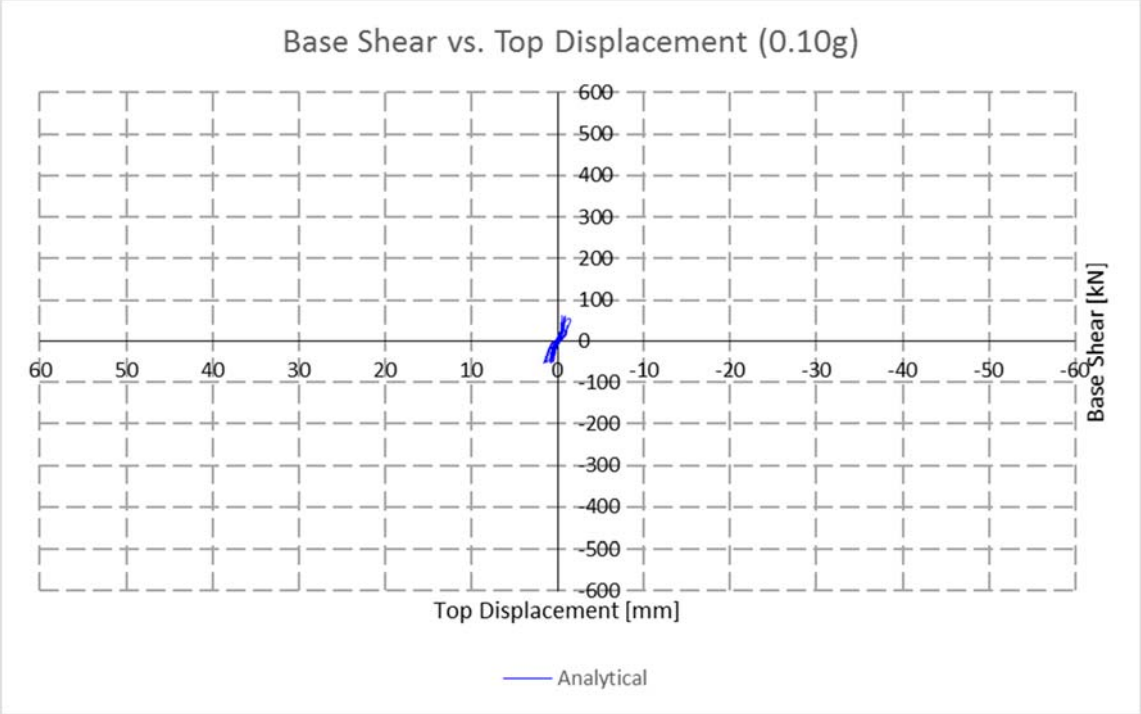

Figure 5.44 Base shear vs. top displacement for 0.10g

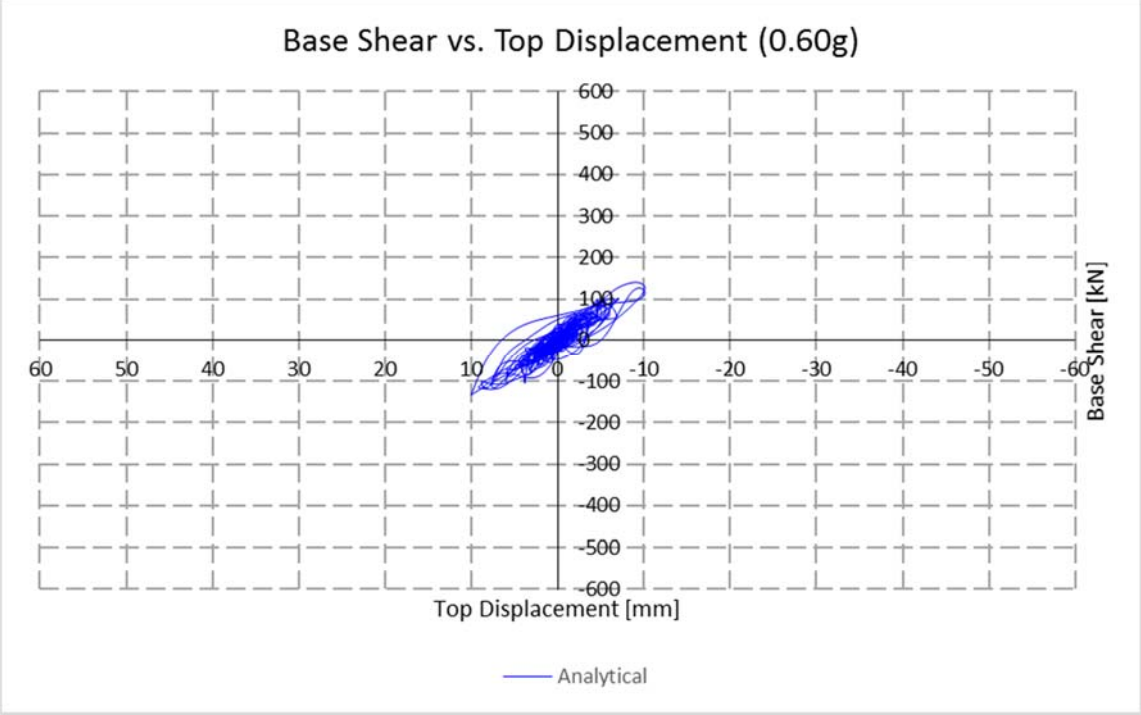

Figure 5.45 Base shear vs. top displacement for 0.60g

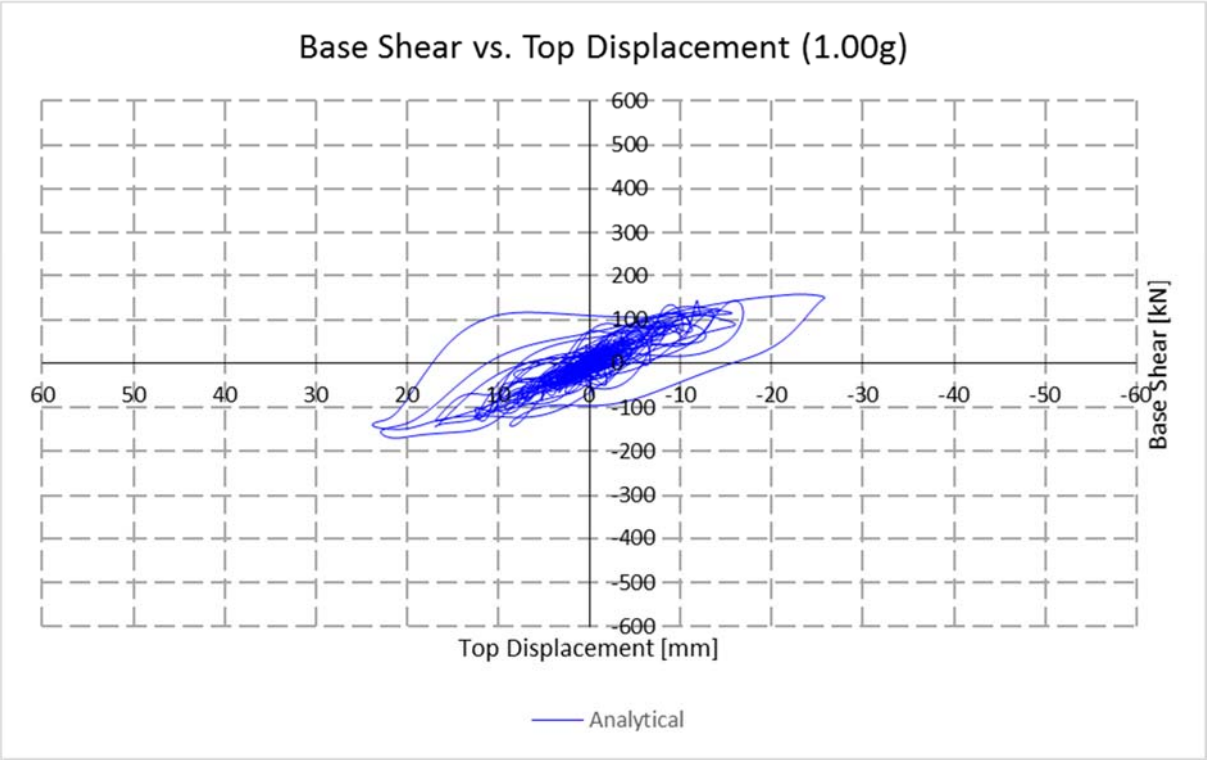

Figure 5.46 Base shear vs. top displacement for 1.00g

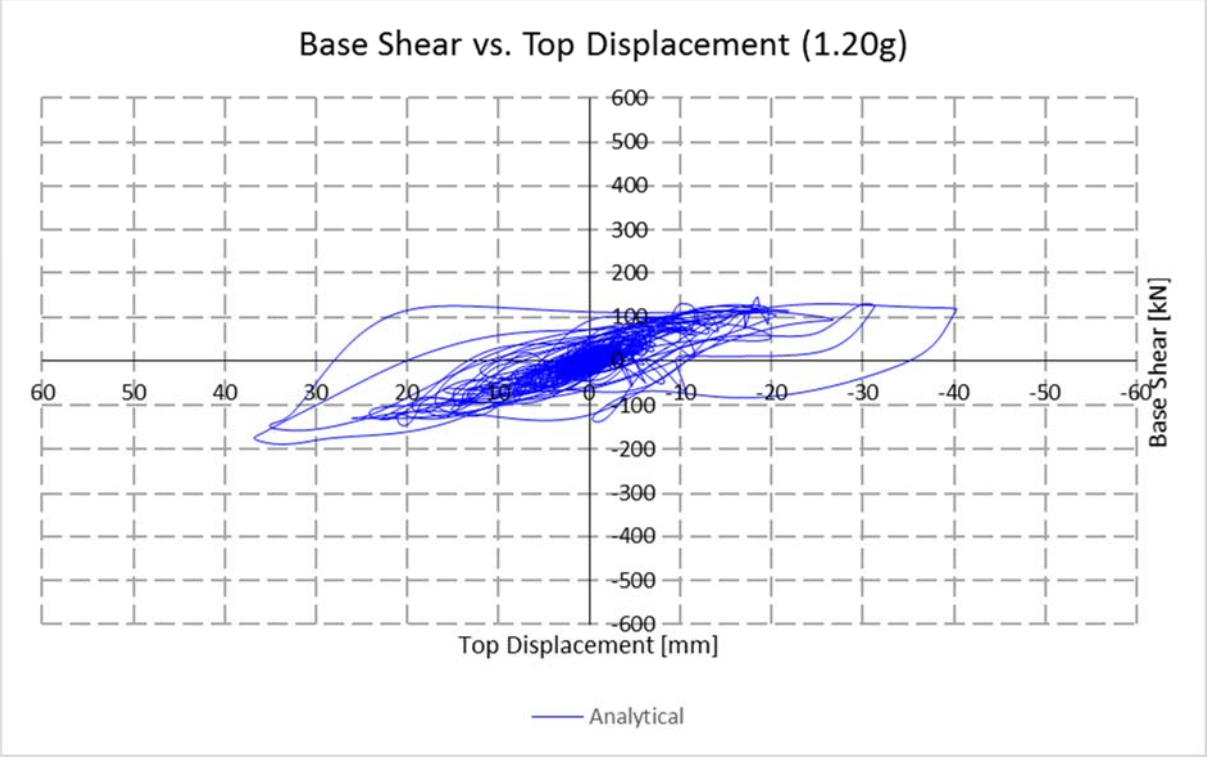

Figure 5.47 Base shear vs. top displacement for 1.20g

5.3.7. Capacity and damage mechanism of Bare Frame Structure

In order to get better visualization and chance for a comparison of the capacity and effectiveness of the proposed infill – bare frame connection, a nonlinear static (pushover) analysis has been performed for the structure without any infills. The time-history analysis is not carried out for this model, having in mind that the shake table tests weren't perform for the bare frame structure. The modeling of RC beams and columns nonlinearity is with the same procedure as for the previous models. In this manner, a nonlinear static (pushover) analysis has been made and selected results are presented further on.

The pushover analysis resulted in total of 78 steps, while the structure has been "pushed" for target displacement of 9cm. Plastic hinge formation and static pushover curve is presented in the following figures (Figure 5.48-5.52).

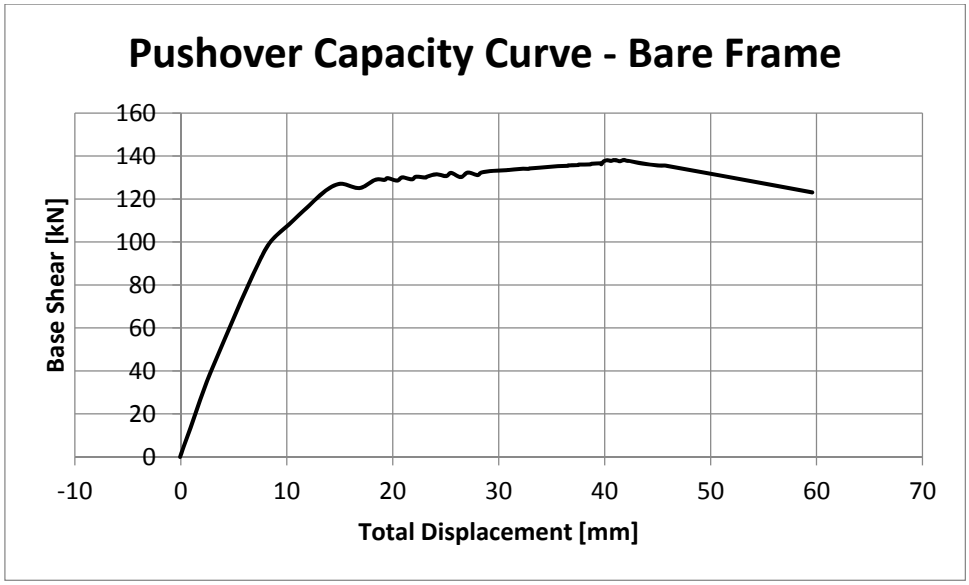

Figure 5.48 Pushover capacity curve for Bare Frame structure

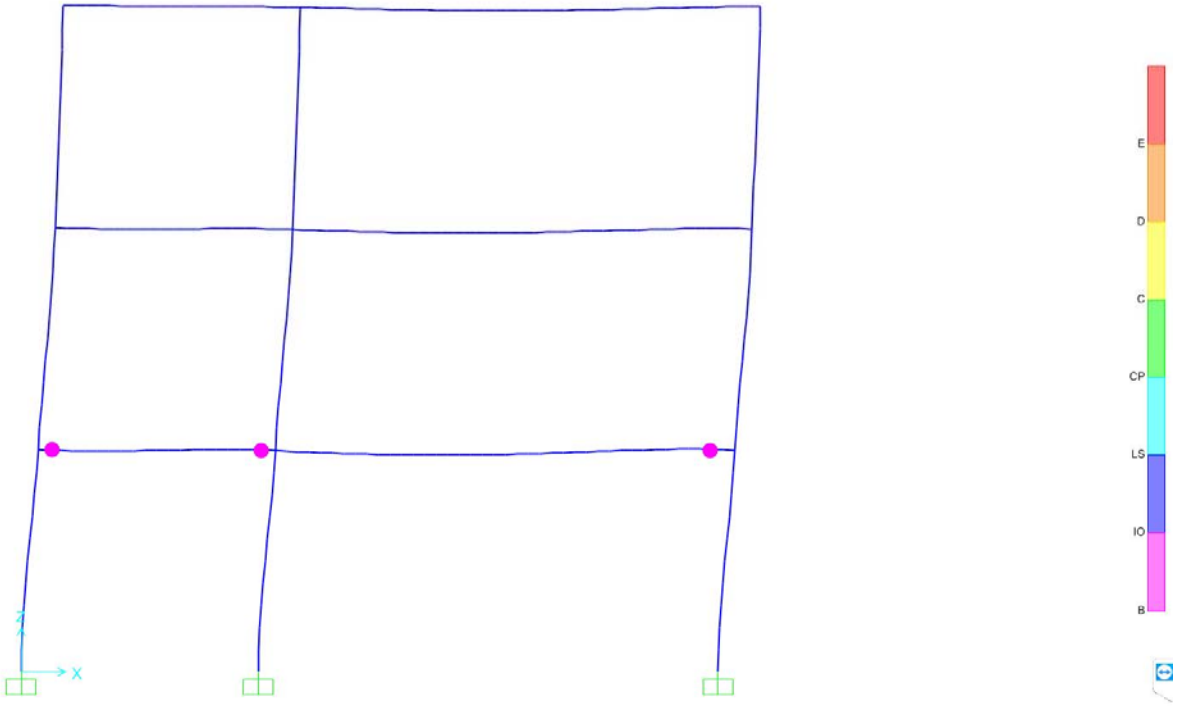

Figure 5.49 Plastic hinge formation in masonry at step 3 (δ= 5.10; F=65.82)

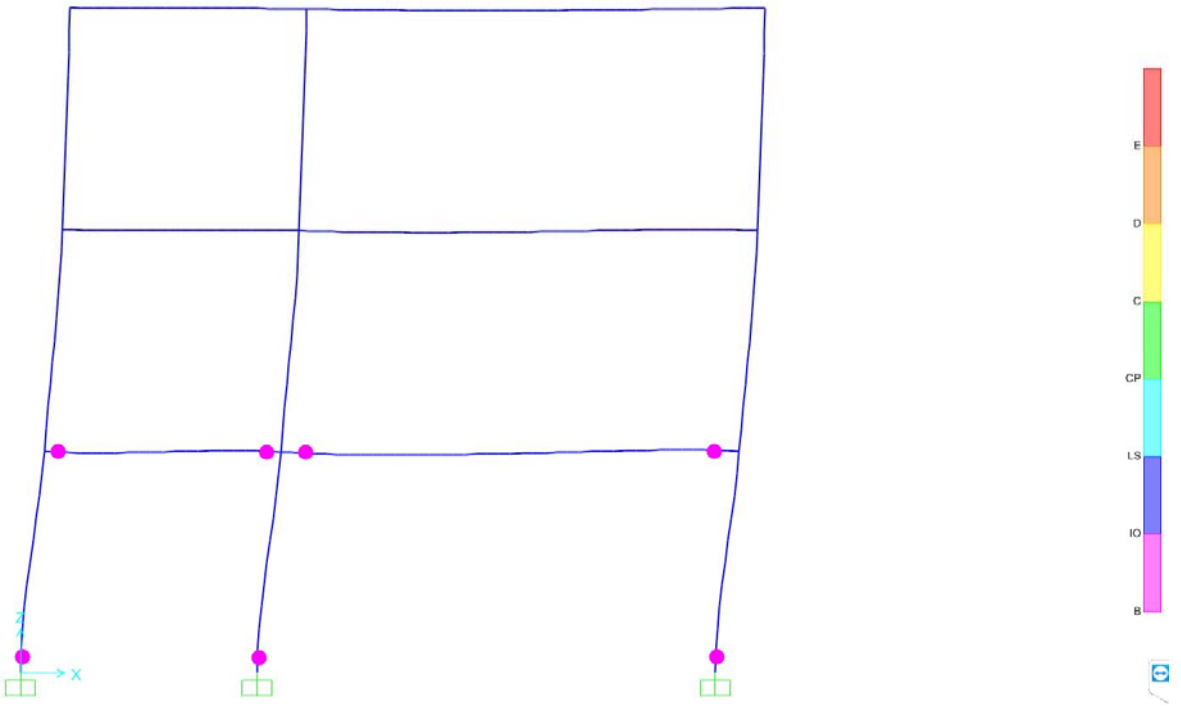

Figure 5.50 Plastic hinge formation at step 7 (δ= 12.04; F=116.65)

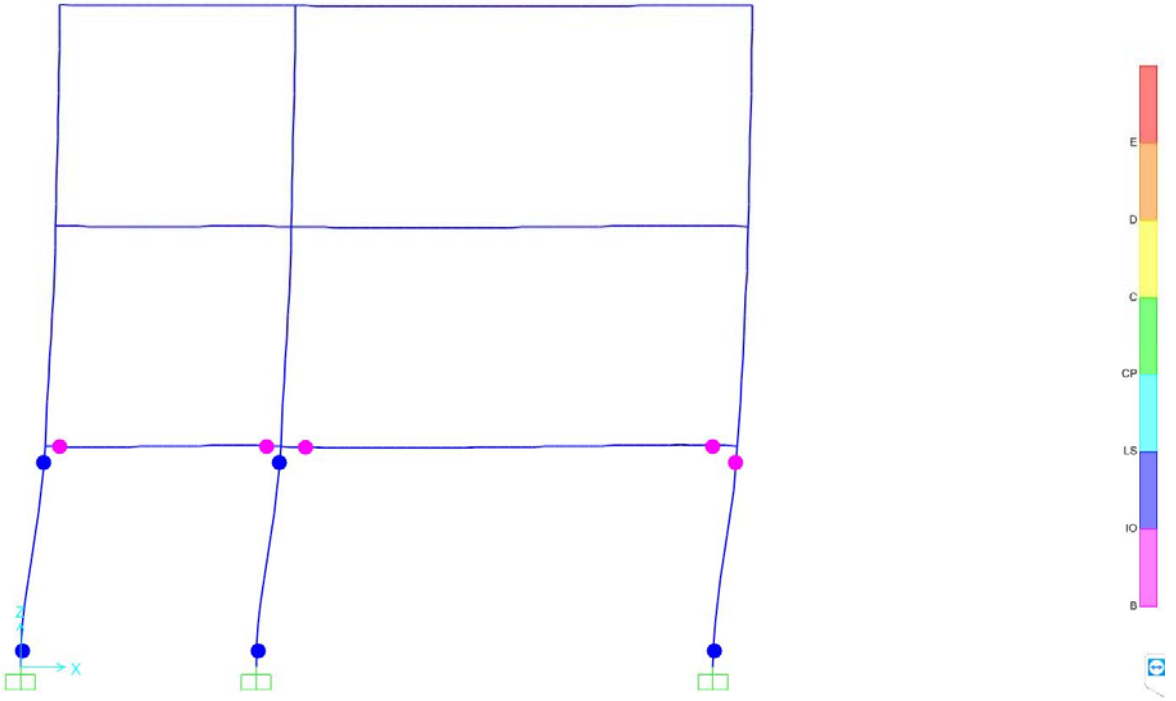

Figure 5.51 Plastic hinge formation at step 12 (δ= 19.23; F=128.91)

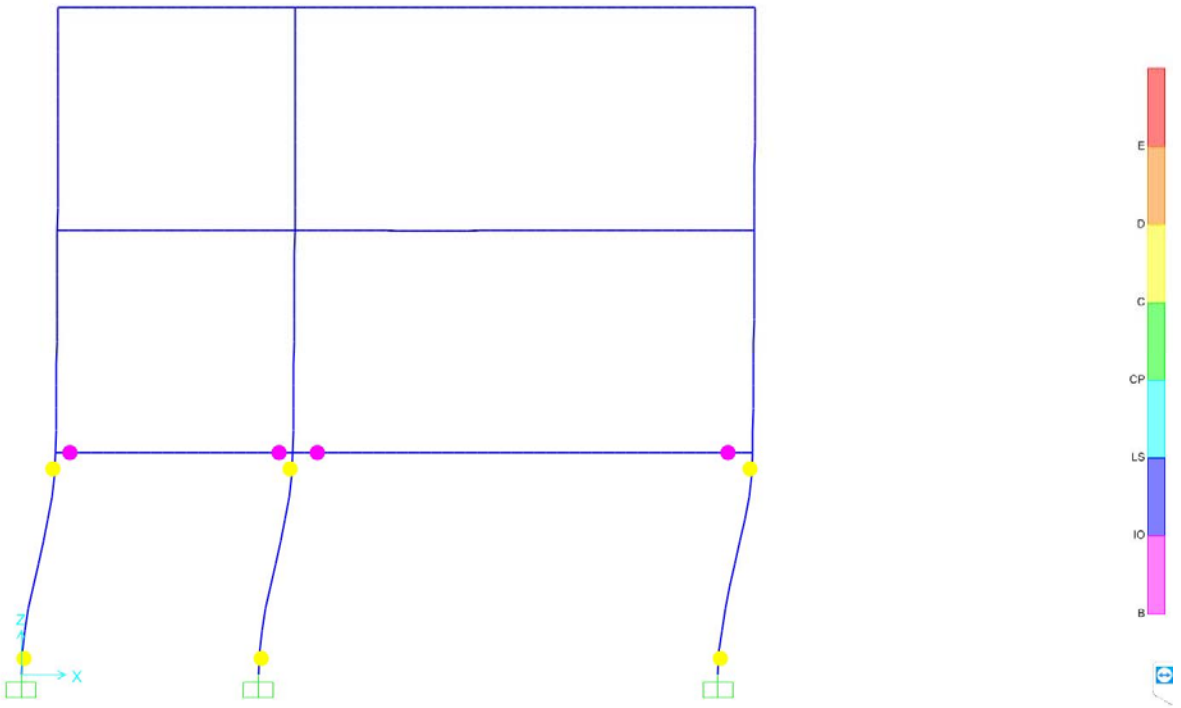

Figure 5.52 Plastic hinge formation at final step 78 (δ= 89.93; F=94.85)

From the results presented above, it can be concluded that the formation of the plastic hinge is firstly located in the beams, up to a Base Shear of around 110 kN. Beyond this value of Base Shear, plastic

hinges started to form in the RC columns as well. The final step (Step 78) shows that the beams are still at the start of the plastic zone, while the columns are actually collapsing.

5.4. Comparison and verification of selected results

5.4.1. Analytical vs. Experimental results comparison and verification for Model IW-SB

In order to check the effectiveness of the proposed procedure for analyzing the structure with the innovative infill wall connection, a comparison of selected analytical and experimental results for Model IW-SB has been done. Comparison of the top displacements time-histories for selected earthquake intensities of 0.10g, 0.60g, 1.00g, 1.20g and 1.60g, obtained from nonlinear direct integration time-history analysis for the 3D modeled structure for Model IW-SB and experimental shake table results of the considered model are presented in the Figures 5.53-5.57.

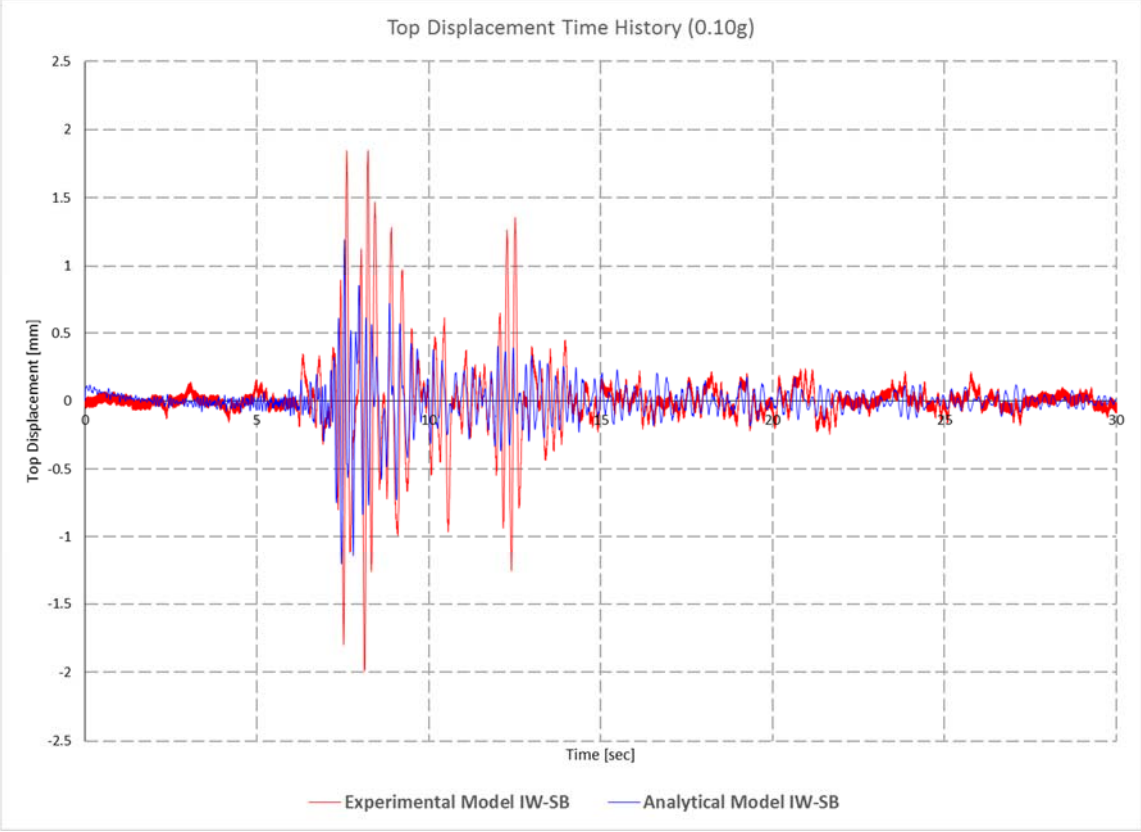

Figure 5.53 Comparison of Top Displacement Time Histories for 0.10g

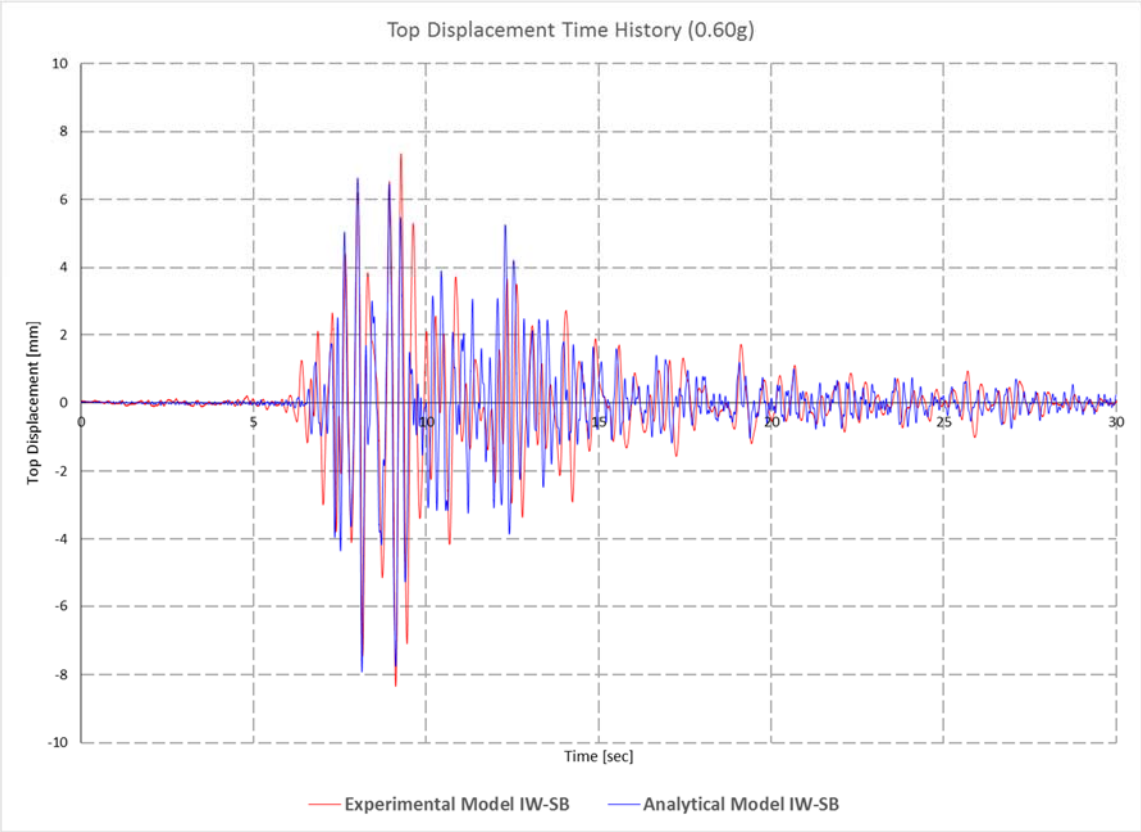

Figure 5.54 Comparison of Top Displacement Time Histories for 0.60g

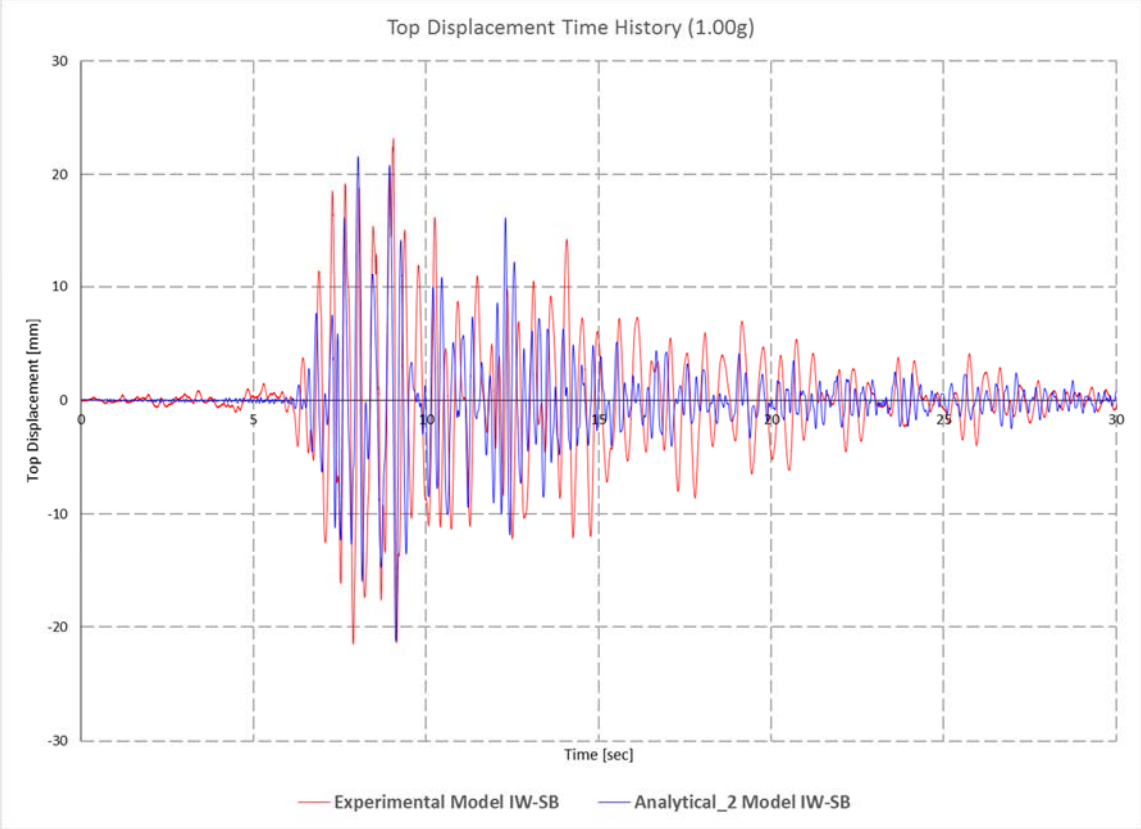

Figure 5.55 Comparison of Top Displacement Time Histories for 1.00g

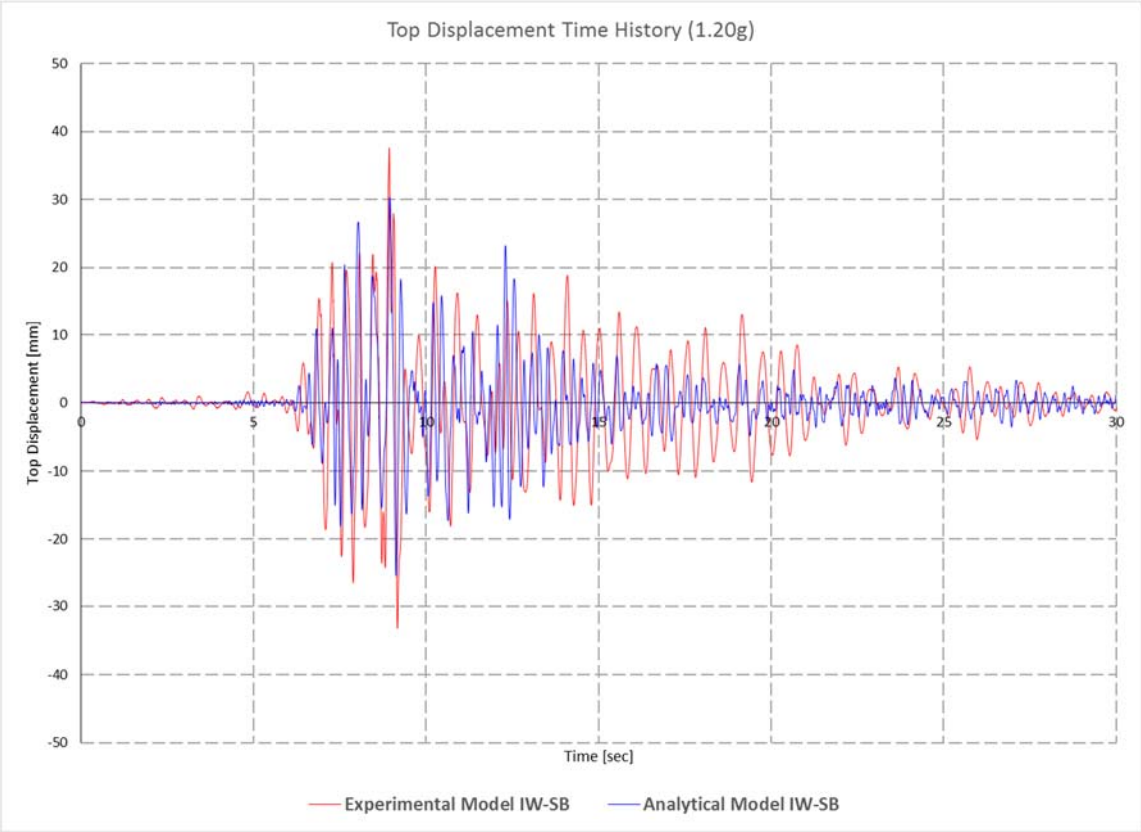

Figure 5.56 Comparison of Top Displacement Time Histories for 1.20g

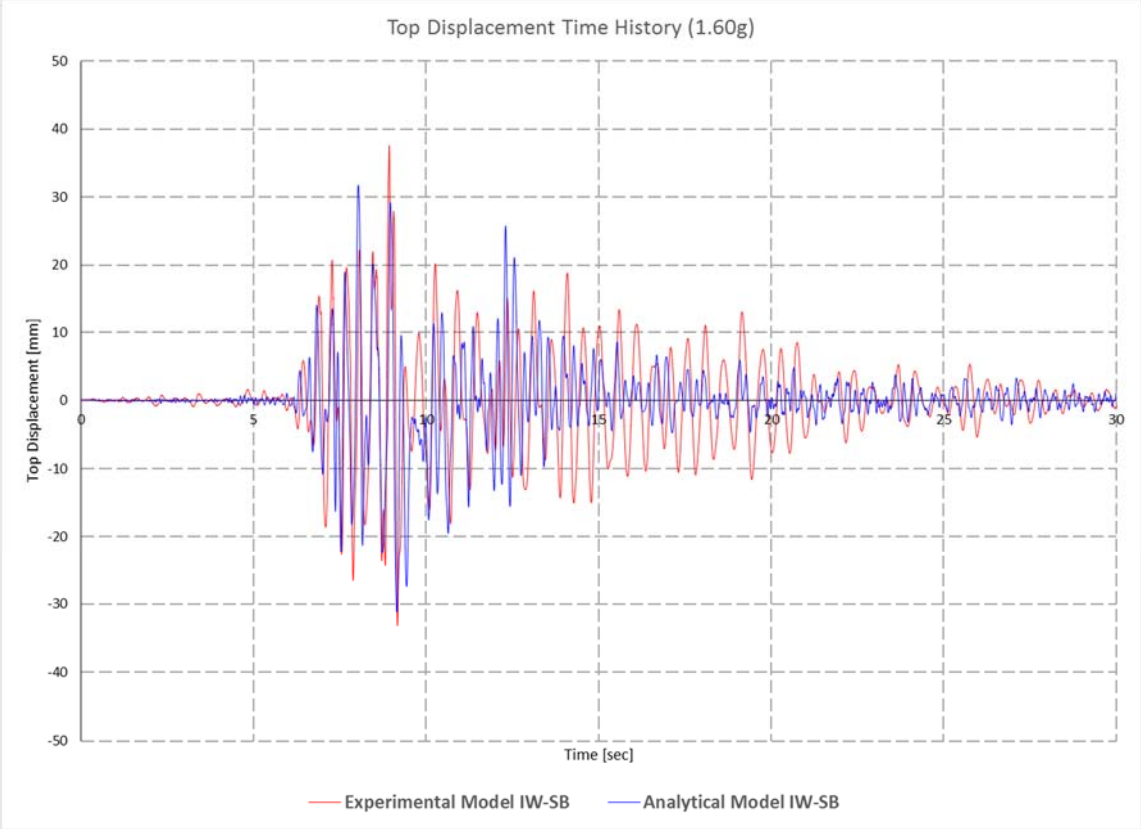

Figure 5.57 Comparison of Top Displacement Time Histories for 1.60g

Comparison of the Base Shear – Top displacement time-histories for selected earthquake intensities of 0.10g, 0.60g, 1.00g, 1.20g and 1.60g, obtained from nonlinear direct integration time-history analysis for the 3D modeled structure for Model IW-SB and experimental shake table results of the considered model are presented in the Figs. 5.58-5.62.

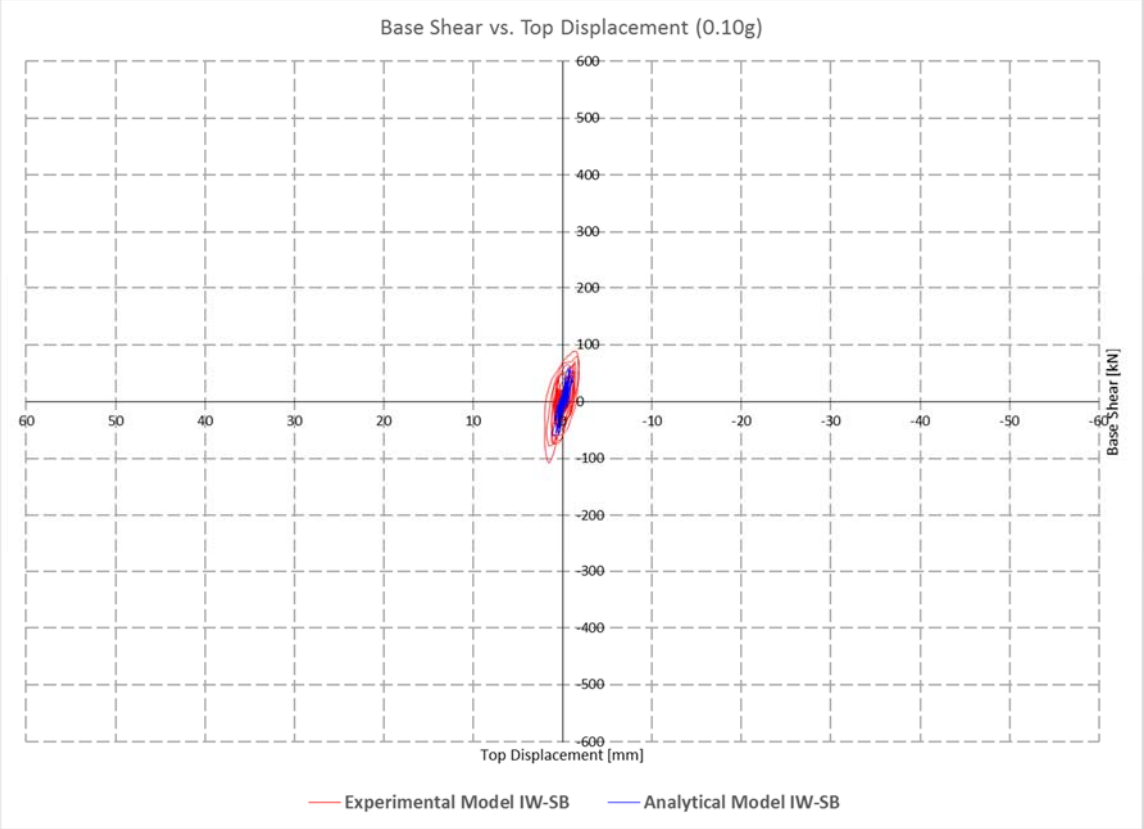

Figure 5.58 Experimental vs. Analytical [Base shear vs. top displacement for 0.10g]

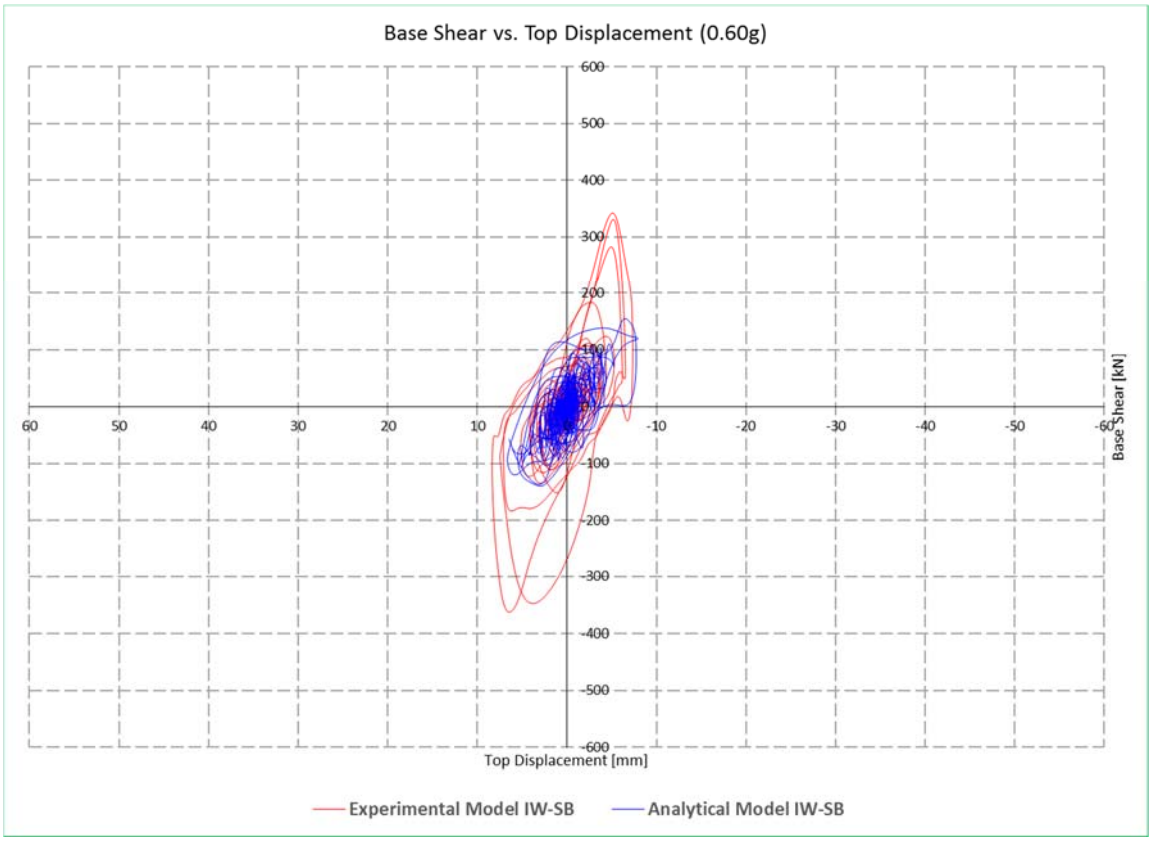

Figure 5.59 Experimental vs. Analytical [Base shear vs. top displacement for 0.60g]

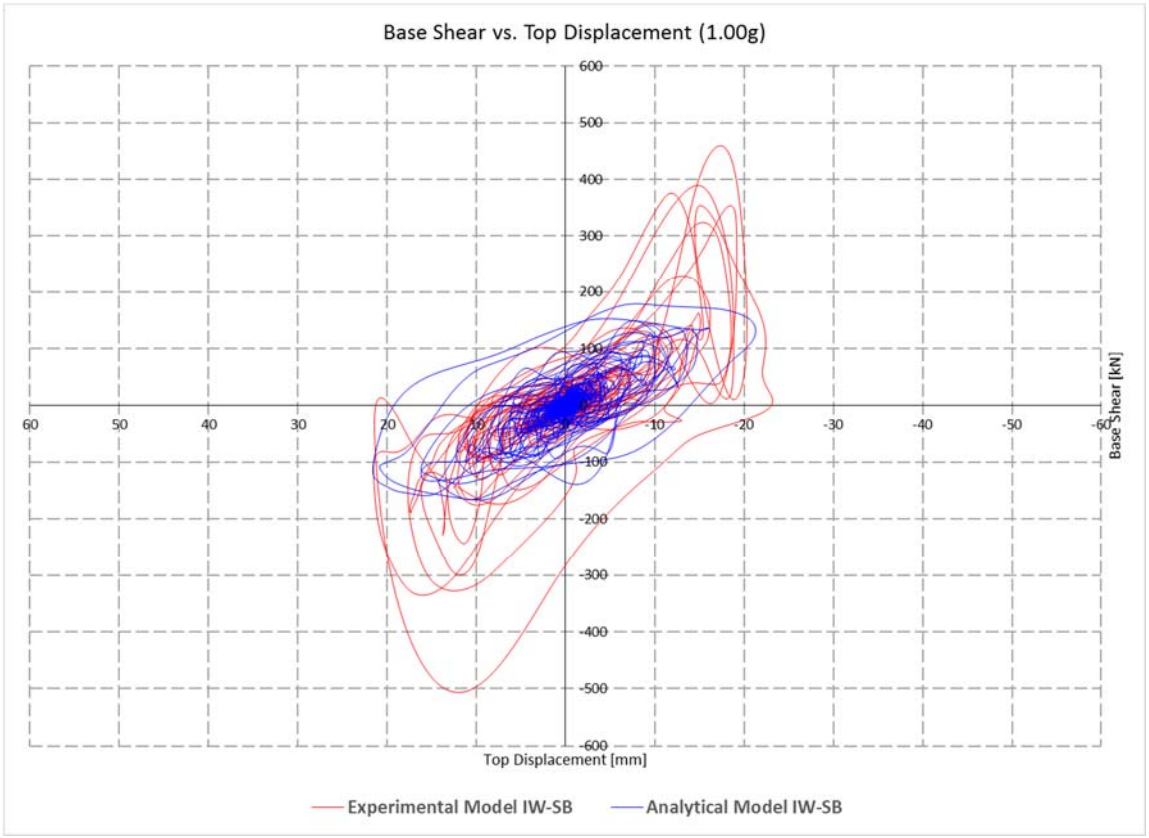

Figure 5.60 Experimental vs. Analytical [Base shear vs. top displacement for 1.00g]

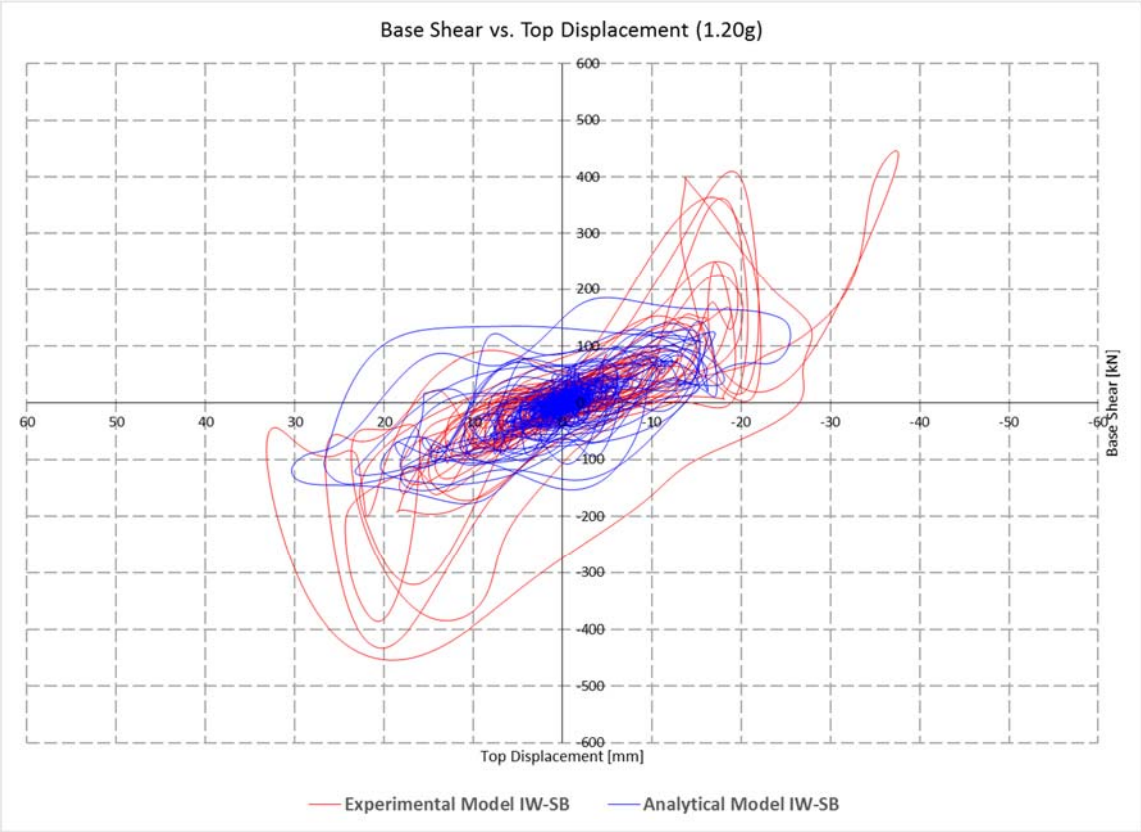

Figure 5.61 Experimental vs. Analytical [Base shear vs. top displacement for 1.20g]

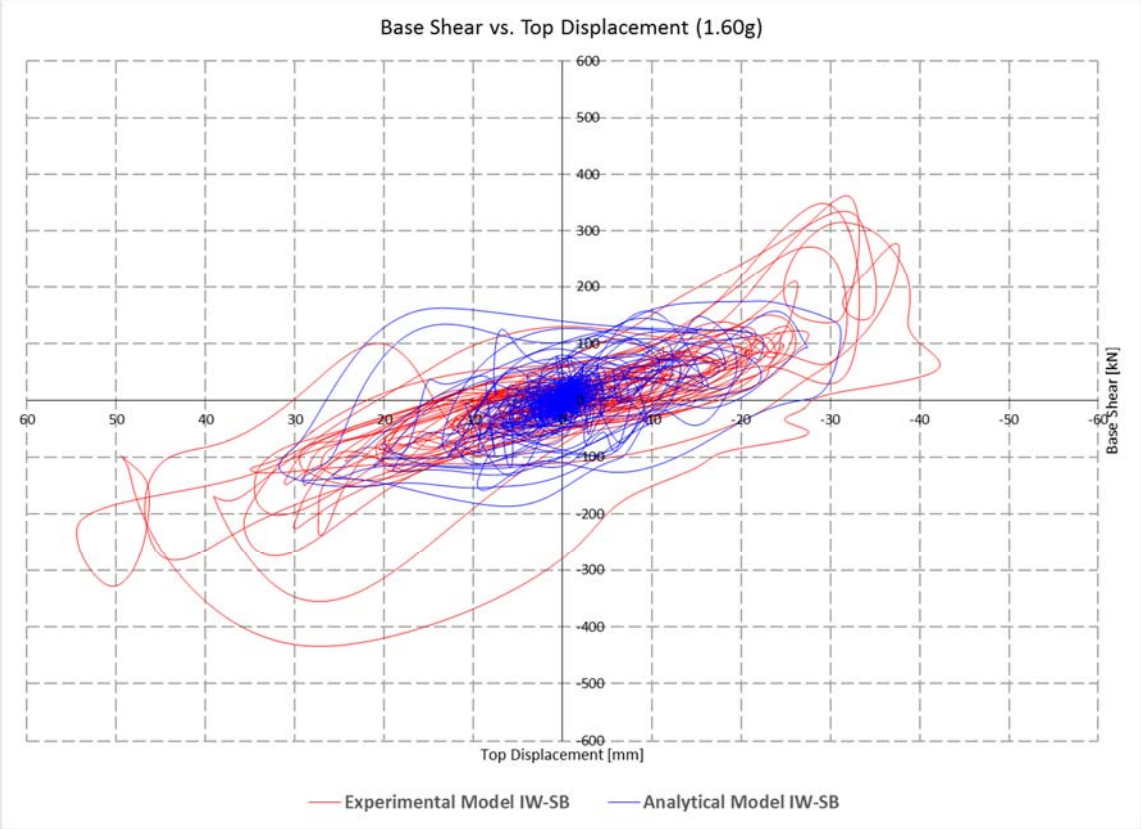

Figure 5.62 Experimental vs. Analytical [Base shear vs. top displacement for 1.60g]

From the Figures presented above, it can be concluded that the modeling approach with tuning of the infill wall material modulus of elasticity gives respectable matches of the time-histories for displacements and Force – Deformation (Base Shear vs. top displacement) results.

It is important to note that the pattern of the time-histories for the top displacements is matching foremost 0.10g and 0.60g all along the earthquake simulation.

For earthquake levels 1.00 – 1.60, it is noted that the pattern of the displacement time histories and most of the values have good match from time interval of 0.00 – 12.00 seconds, while afterwards it can be seen that the analytical results are showing bigger damping in the interval of 12 – 30.00 seconds, having in mind that the experimental displacements time history in this interval is showing bigger displacements.

The Force – Displacements relationships (Base Shear vs Top Displacement hysteresis loop) also shows quite good match for the earthquake level of 0.10g and 0.60g. There are several leaps of the loop in the diagram for 0.60g which are beyond the analytical results, but these values are expected due to the imperfections of the experimental process and they can be filtrated. Furthermore, for intensities of 1.00g, 1.20g and 1.60g there is also respectable match of the diagrams, although it should be clear that the earthquake intensities are with significant magnitude and exact match is impossible. The most important is that the analytically obtained hysteresis inclination (given the stiffness of the structure) is almost the same with the experimental results.

5.4.2. Analytical vs. Experimental results comparison and verification for Model 1

A comparison of selected analytical and experimental results for Model 1 is also done for calibrating the selected modeling approach. Comparison of the top displacements, along with a Base Shear – Top displacement time-histories for selected earthquake intensities of 0.10g, 0.60g, 1.00g and 1.60g, obtained from the nonlinear direct integration time-history analysis for the 3D modeled structure for Model 1 and experimental shake table tests results for the considered model are presented in the Figures 5.63-5.70, accordingly.

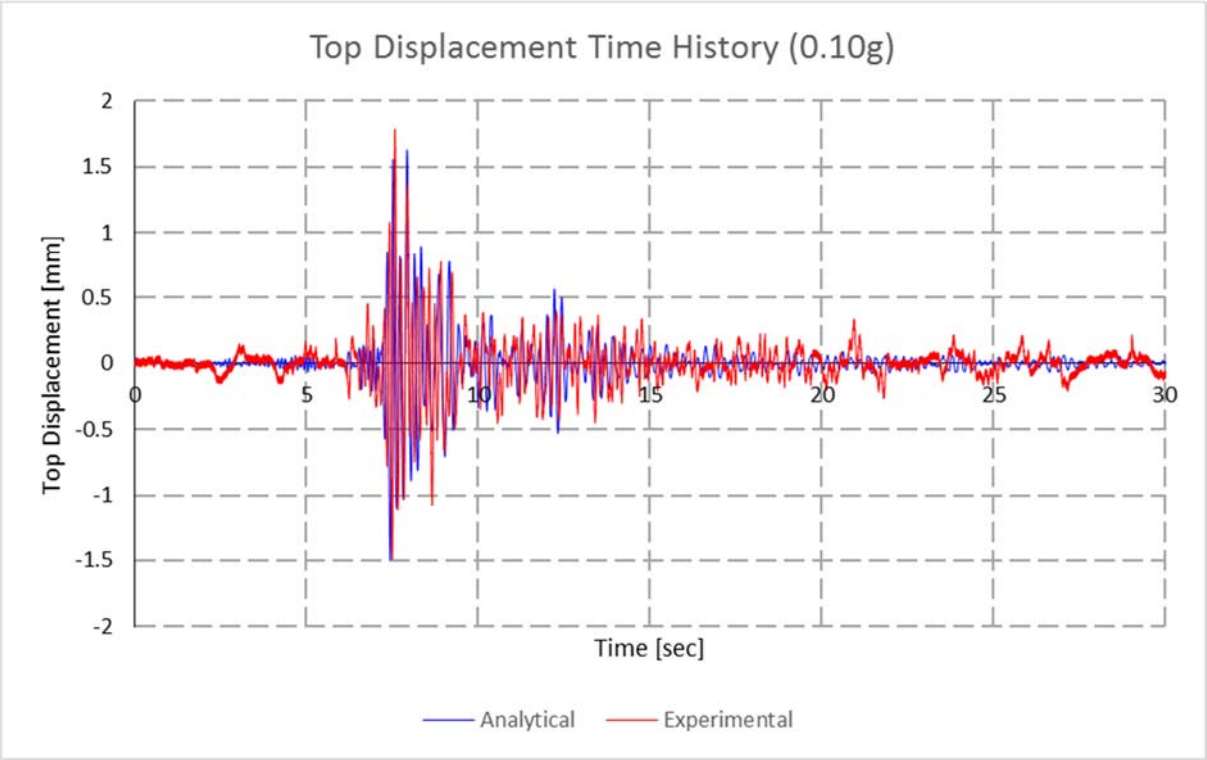

Figure 5.63 Comparison of Top Displacement Time Histories for 0.10g

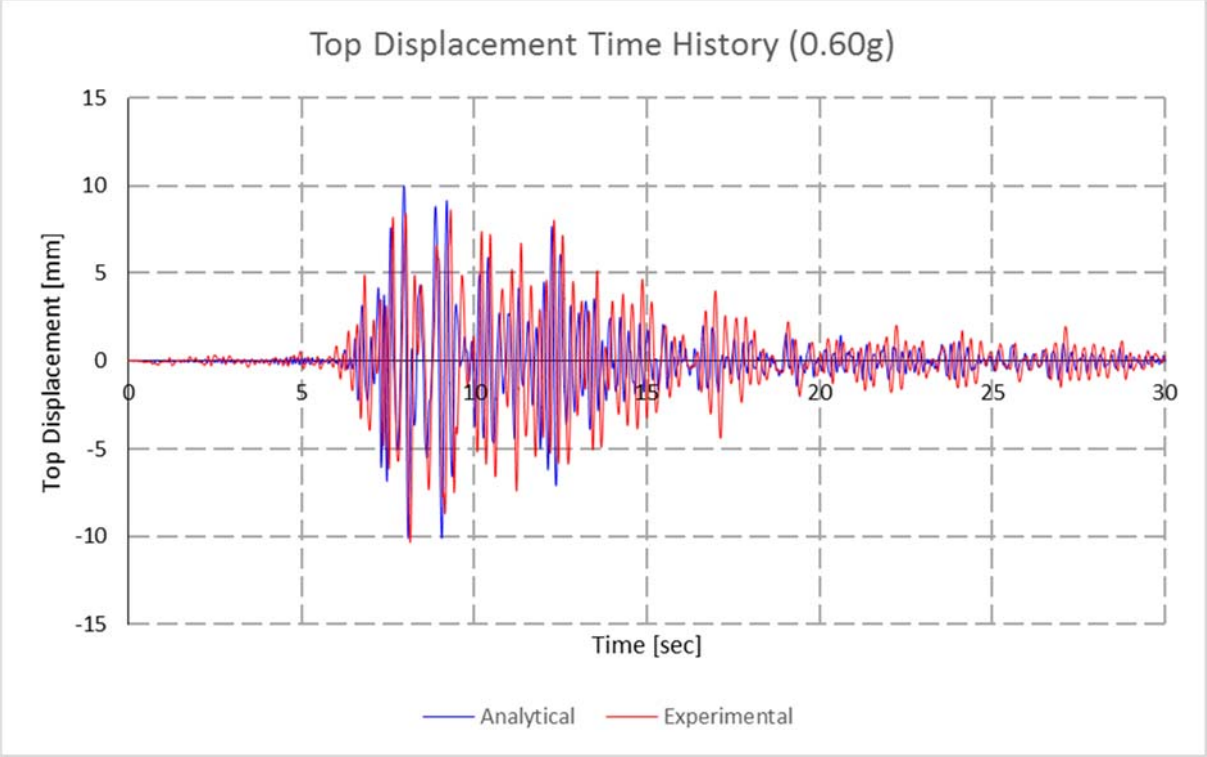

Figure 5.64 Comparison of Top Displacement Time Histories for 0.60g

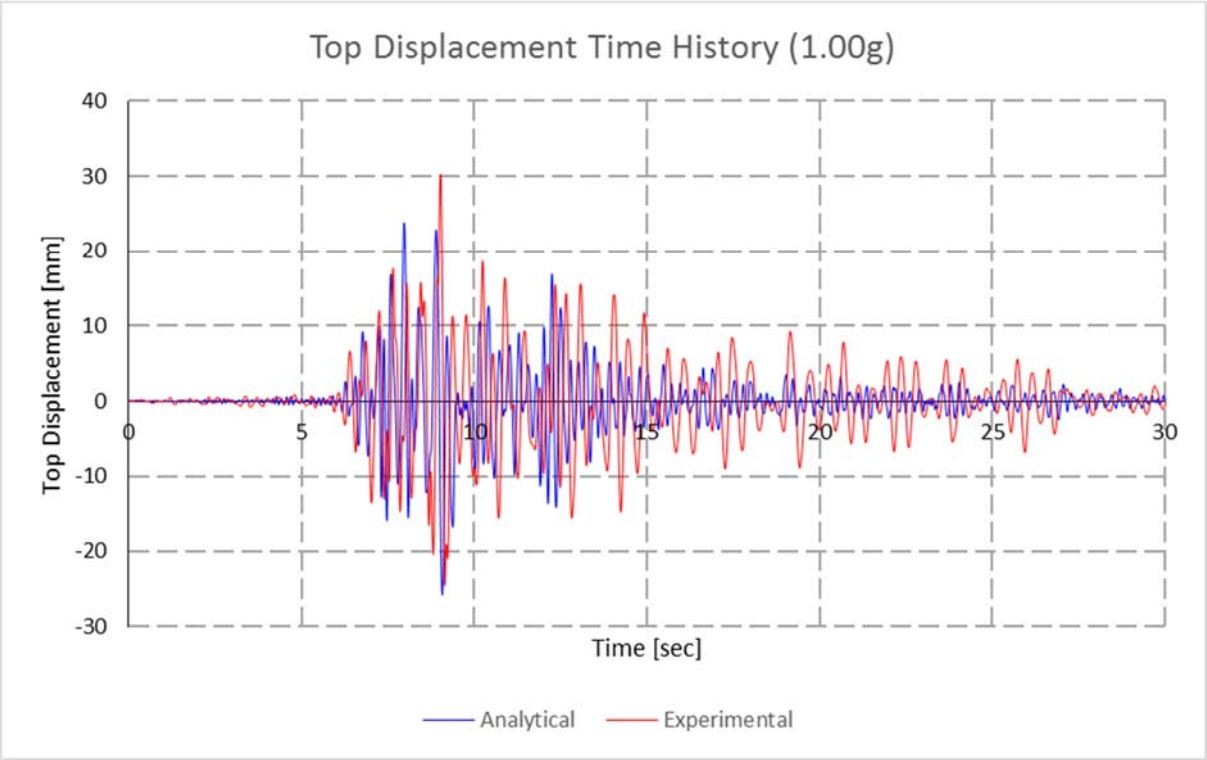

Figure 5.65 Comparison of Top Displacement Time Histories for 1.00g

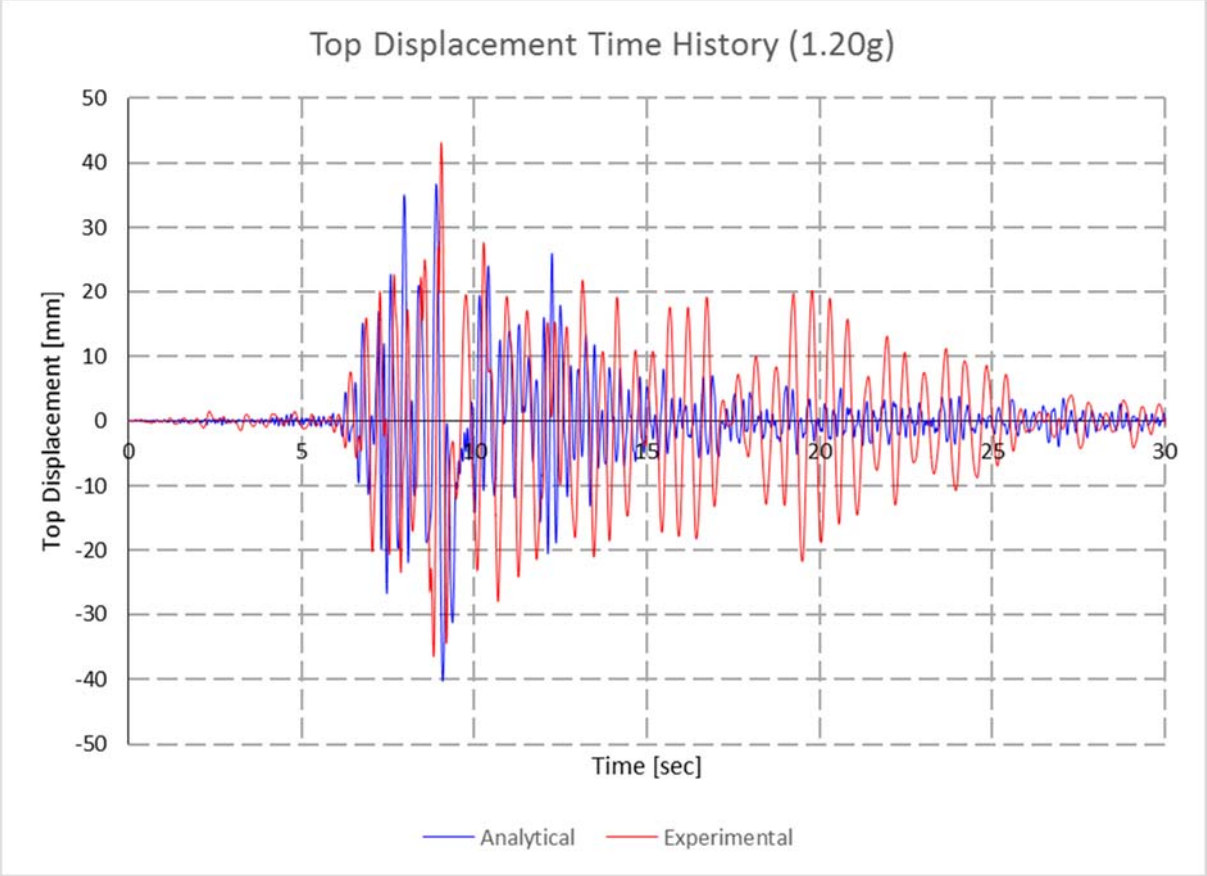

Figure 5.66 Comparison of Top Displacement Time Histories for 1.20g

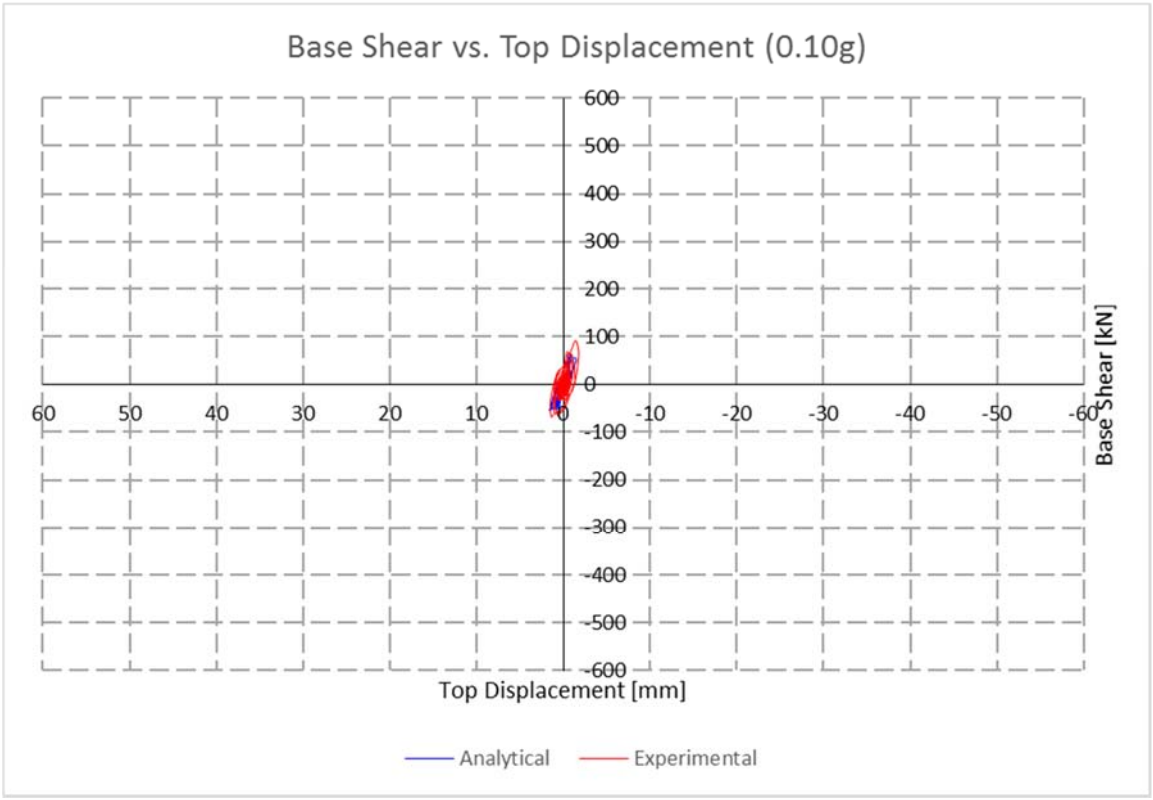

Figure 5.67 Experimental vs. Analytical [Base shear vs. top displacement for 0.10g]

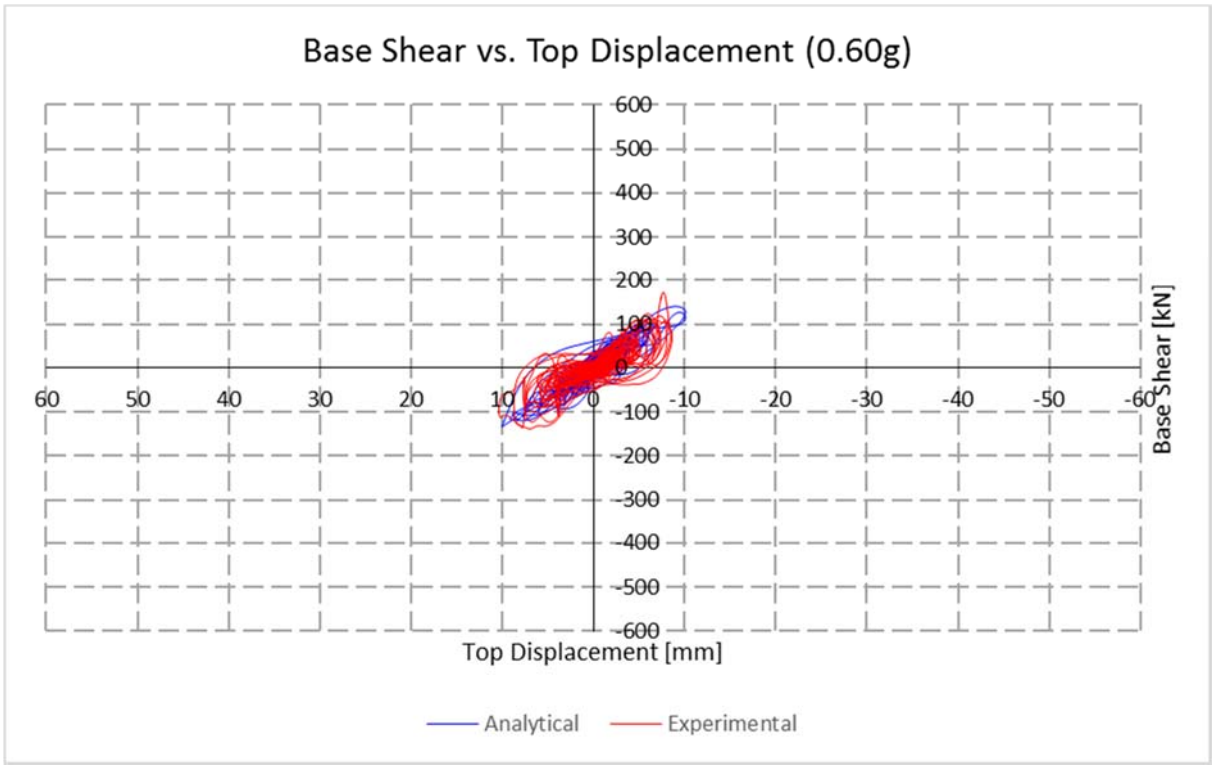

Figure 5.68 Experimental vs. Analytical [Base shear vs. top displacement for 0.60g]

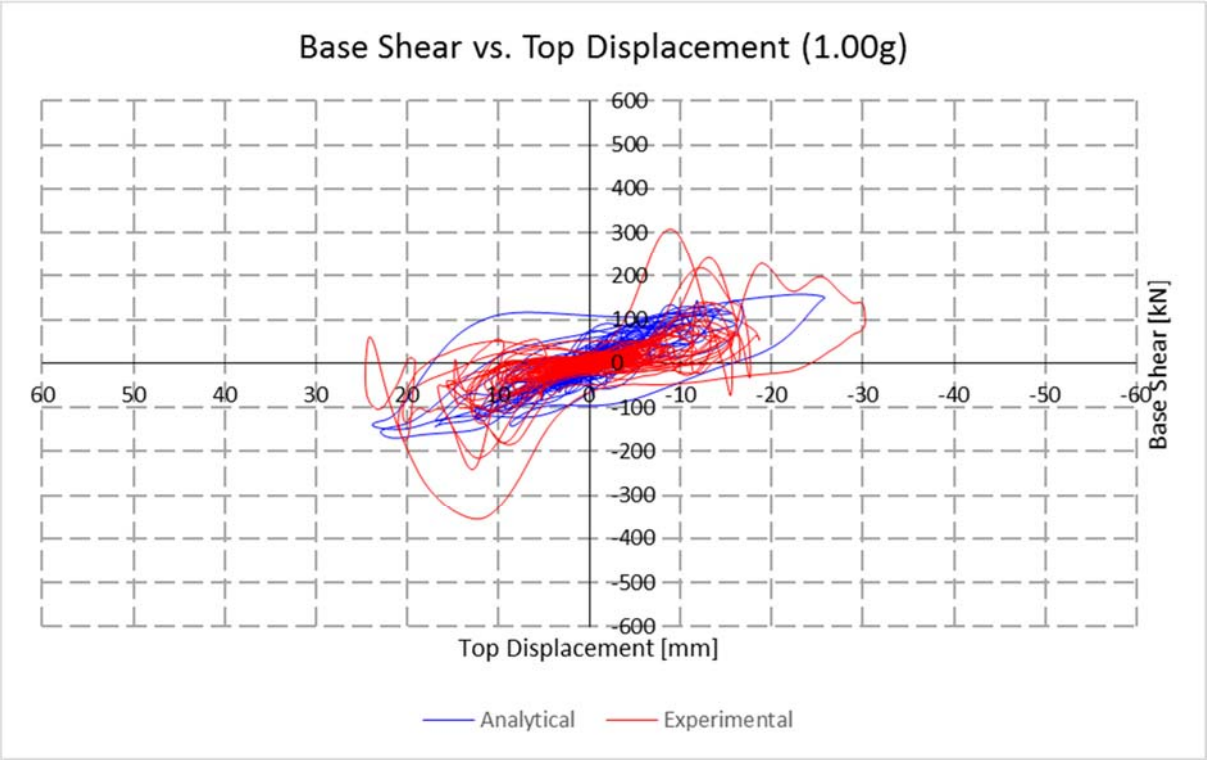

Figure 5.69 Experimental vs. Analytical [Base shear vs. top displacement for 1.00g]

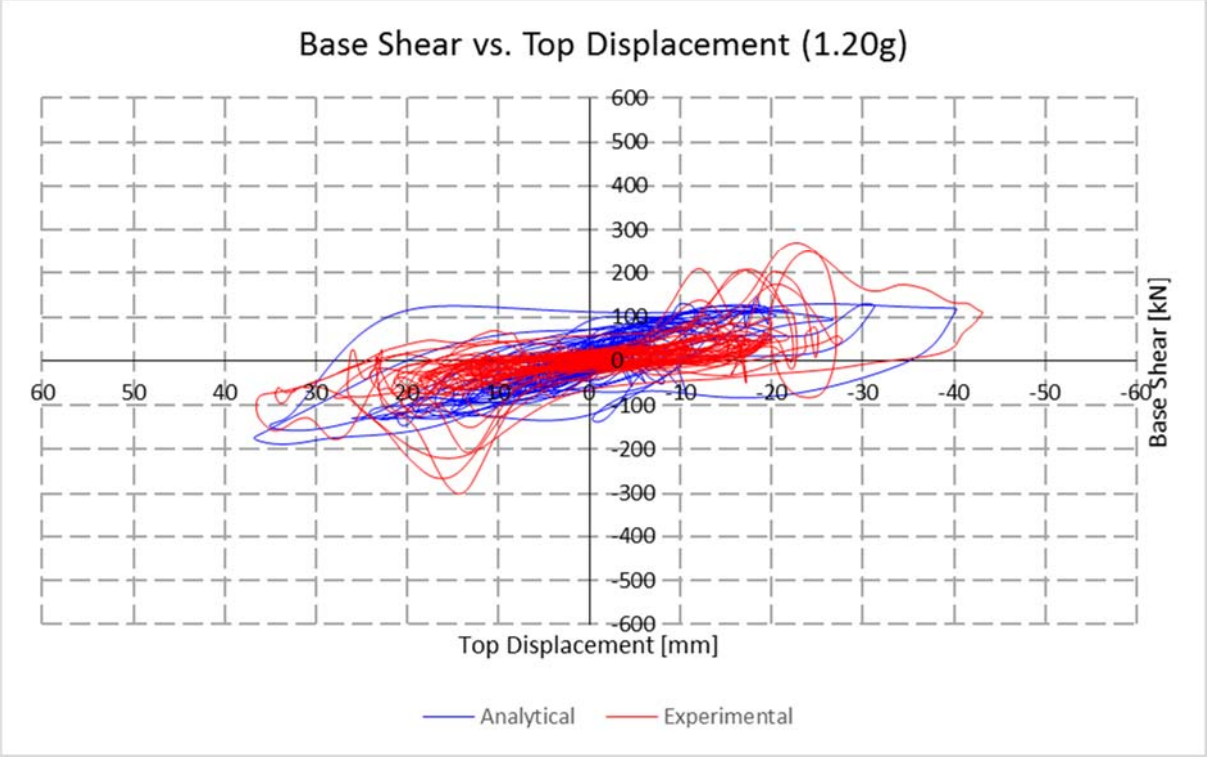

Figure 5.70 Experimental vs. Analytical [Base shear vs. top displacement for 1.20g]

Similar comments can be pointed for verification of Model 1 analytical and experimental results as for Model IW-SB (Section 5.4.1).

As in the previous case the pattern of the time-histories for the top displacements is matching foremost 0.10g and 0.60g all along the earthquake simulation.

The same disorder of the displacement values is noted here as well for earthquake levels 1.00 – 1.20. The pattern of the displacement time histories and most of the values have respectable match from time interval of 0.00 – 12.00 seconds, while afterwards it can be seen that the analytical results are showing bigger damping in the interval of 12 – 30.00 seconds, having in mind that the experimental displacements time history in this interval is showing bigger displacements.

The Force – Displacements relationships (Base Shear vs Top Displacement hysteresis loop) also shows quite good match for the earthquake level of 0.10g and 0.60g as in the case of Model IW-SB. For intensities of 1.00g, 1.20g and 1.60g there is also good match of the diagrams, although the same principle stands here that at these magnitudes an exact match is impossible.

The most important is that the analytically obtained hysteresis inclination (given the stiffness of the structure) is almost the same with the experimental results.

5.4.3. Comparison of capacity of Model IW-SB, Model 1 and Bare Frame Model according to nonlinear static (pushover) analysis results

While the results from the nonlinear time-history analysis gave quite good matching with the experimental results, the aim here is to show a comparison of the capacity of the three different models (Model IW-SB, Model 1 and the Bare Frame system) in the aim of the nonlinear static (pushover) analysis results. The three capacity curves (Base-Shear vs. Top Displacement) curves are shown on Figure 5.70. It can be noted that the infill modeling have significant influence of the seismic response of the structure in the terms of both strength and corresponding deformation capacities of the structure. The proposed infill connection of the Model IW-SB gives best results in comparison with Bare Frame Model and the referent Model 1.

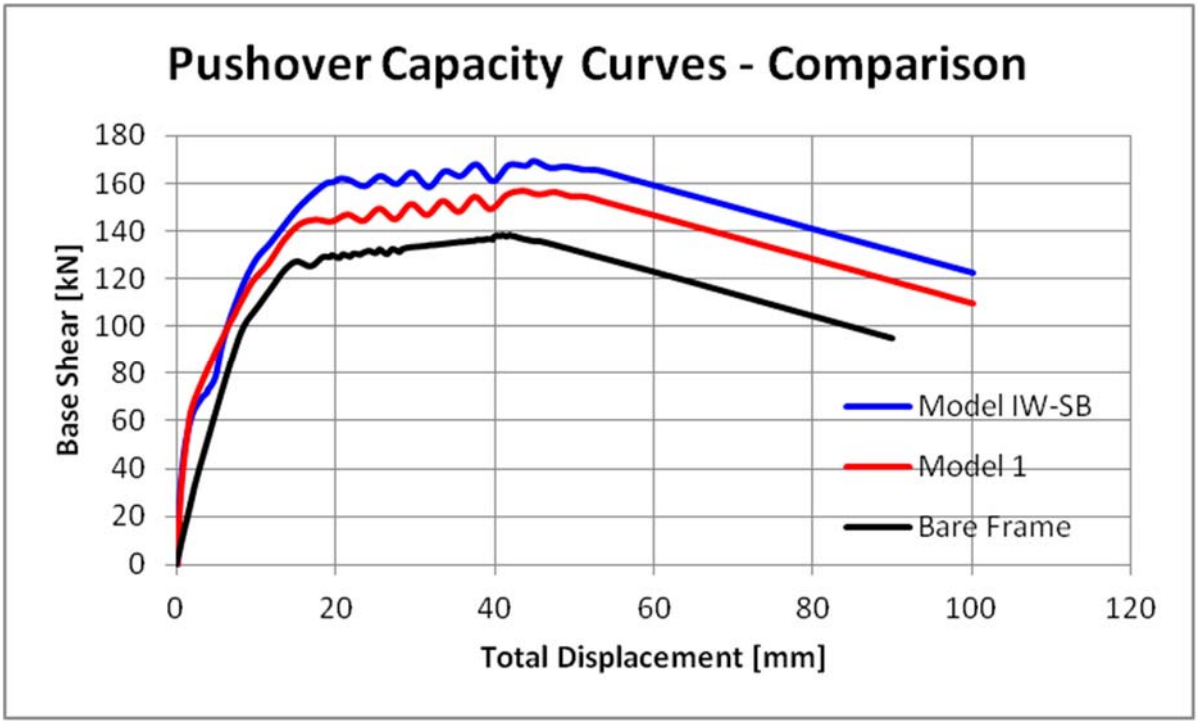

Figure 5.71 Pushover Capacity curves comparison (Model IW-SB, Model 1 & Bare Frame Model)

5.5. General guidelines for the possible application of the IW-SB method in infill walls

As a result of the extensive analytical and experimental research carried out, some general guidelines can be given on the possible application of the innovative method for infill walls in standard reinforced concrete buildings.

The analysis of one single span / single level model with appropriate dimensions (Figure 5.72) has been selected. Two types of models have been analyzed: a model with standard infill wall connection (as referred of Model 1) with no use of the proposed method and the model with placing the IW-SB at certain distances. For these models, diagrams of stresses derived from equivalent seismic force analysis are displayed, as well as appropriate horizontal displacements. Finally, general guidelines for applying this method are given.

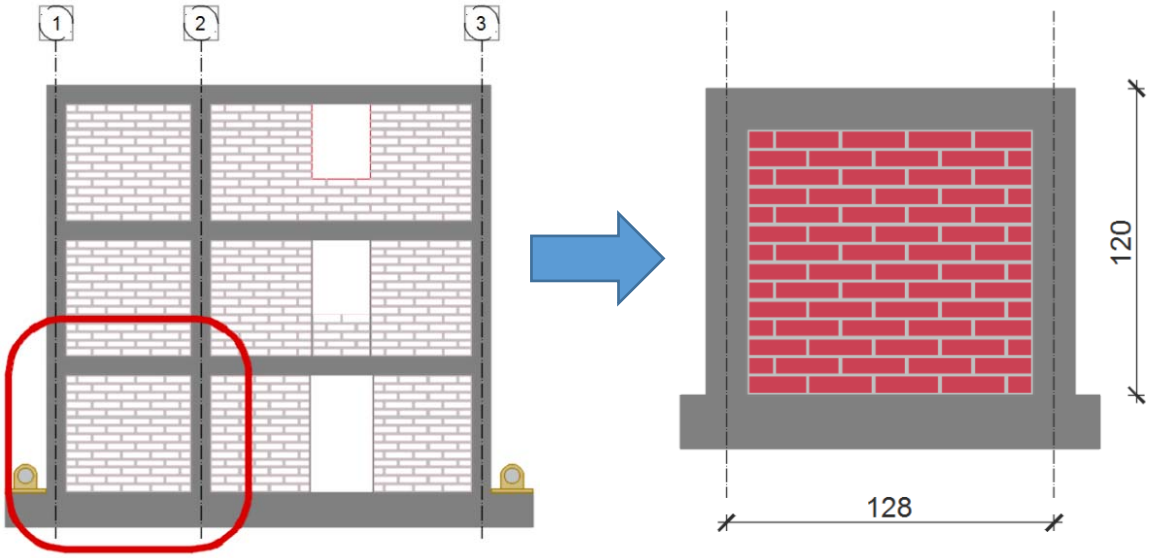

Figure 5.72 Single span / single level frame model selected for analysis

5.5.1. Analysis of selected single span / single level model

A various combinations of models with implementation of the proposed IW-SB method has been selected for analysis in order to get appropriate results for the general guidelines for the application in infill walls (Figure 5.73). A simple linear analysis for all of the selected models has been done using the SAP 2000 computer software. The reinforced concrete frame elements (columns and beam) is modeled using the line elements option and the infill wall bricks are modeled as shell elements with appropriate geometric and material properties. The IW-SB elements are modeled as frame elements with unconfined concrete and two bars of Ø6 mm added in the cross section properties (Figure 5.74). Constant force at the top left corner is applied and the stress intensities and distribution along with the axial force values in the IW-SB elements and total displacements of the integral frame has been analyzed for all models. The results are presented for the S-INF (as referent model) and IW-SB_2td_1m (as selected most adequate model) in the following Figures 5.75 and 5.76 and Table 5.3.

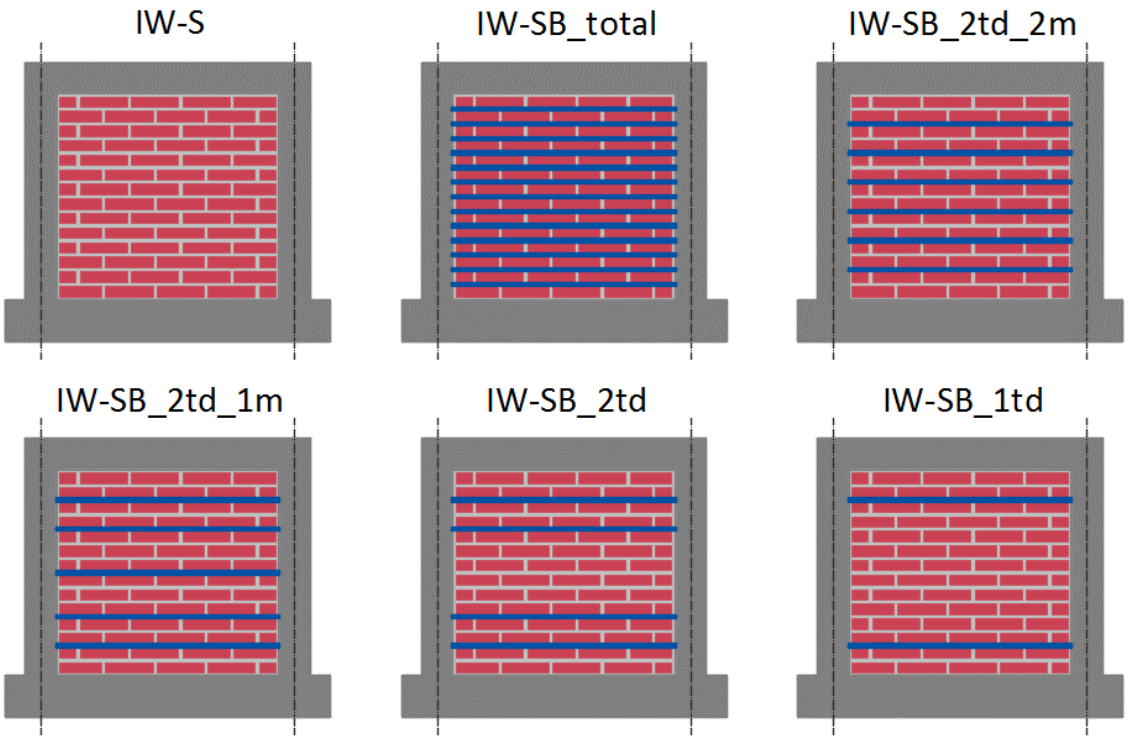

Figure 5.73 Selected different models with implemented IW-SB method for analysis

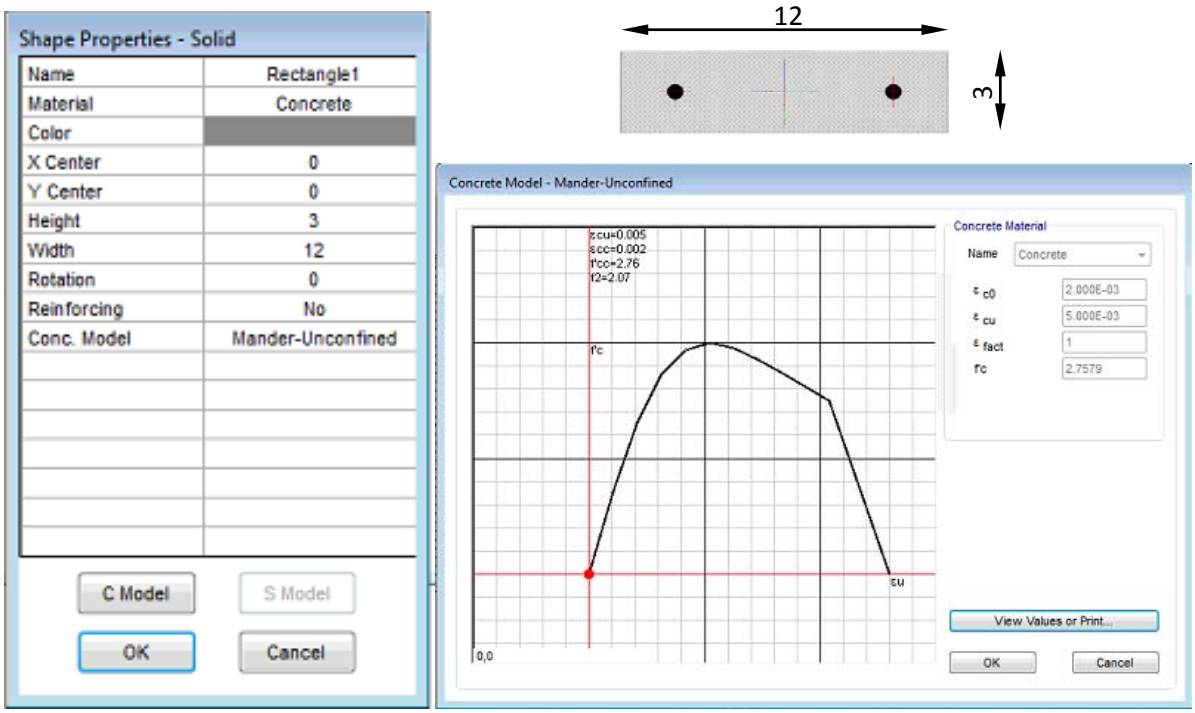

Figure 5.74 Defined Section Properties for IW-SB elements

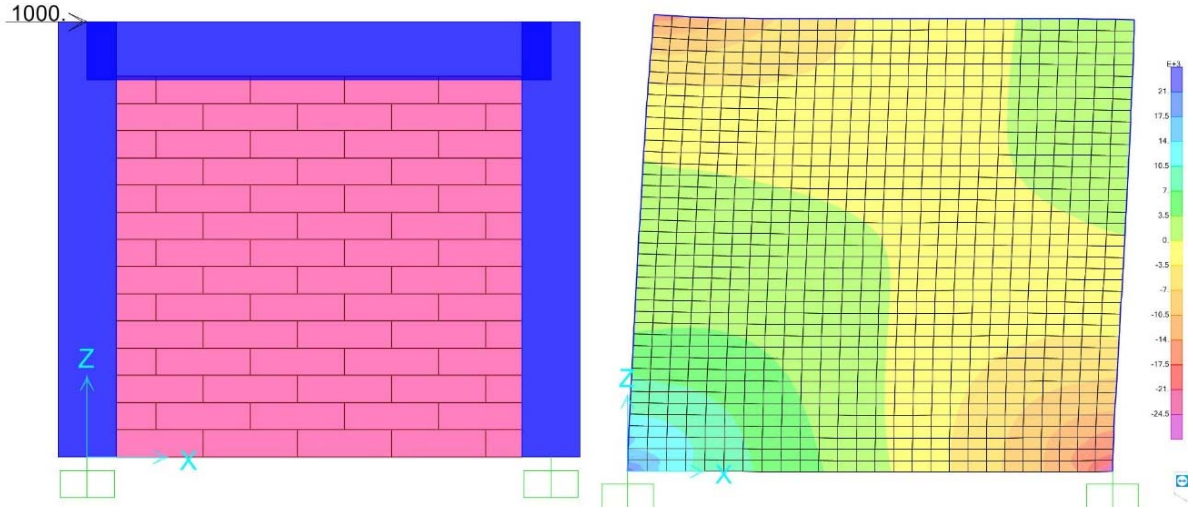

Figure 5.75 Stress distribution for Model IW-S

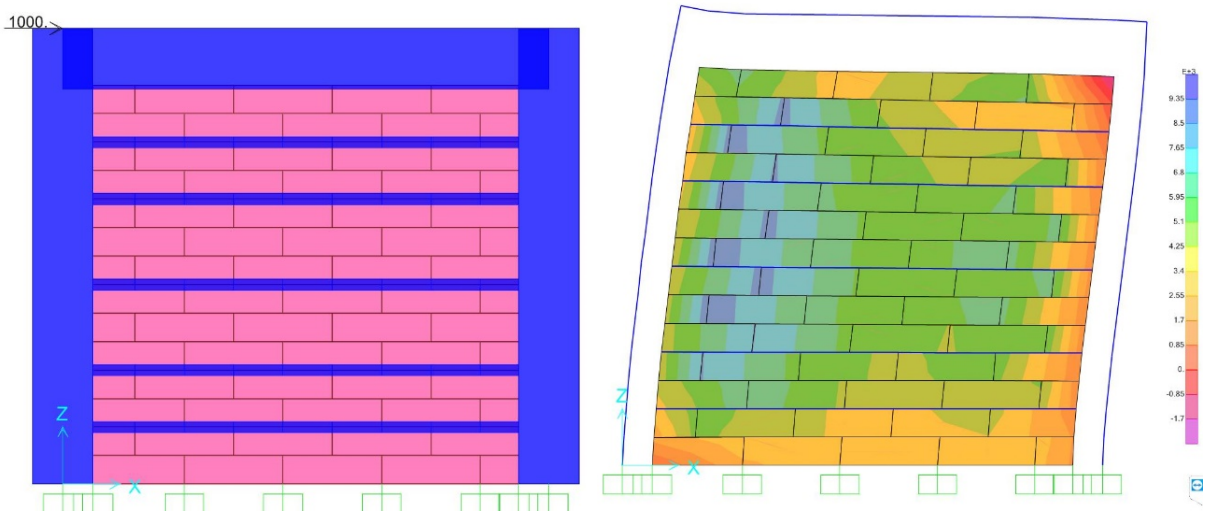

Figure 5.76 Stress distribution for Model IW-SB_2tb_1m

Table 5.13 Difference from analysis results from Model IW-S and IW-SB_2tb_1m

Type of Model	displacement [cm]	Stiffness - K [kN/cm]	Stress Range [kN/m^2]
IW-S	0.7057	1417	16.000 – 21.000
IW-SB_2tb_1m	0.5206	1921	7.000 – 9.000

It is important to note that the stress distribution diagram for the infill wall for Model IW-S (referent model) and Model IW-SB_2tb_1m was corresponding to the damage pattern that was observed during the experimental tests of the models (Figure 5.77 and 5.78) which confirms the right modeling approach.

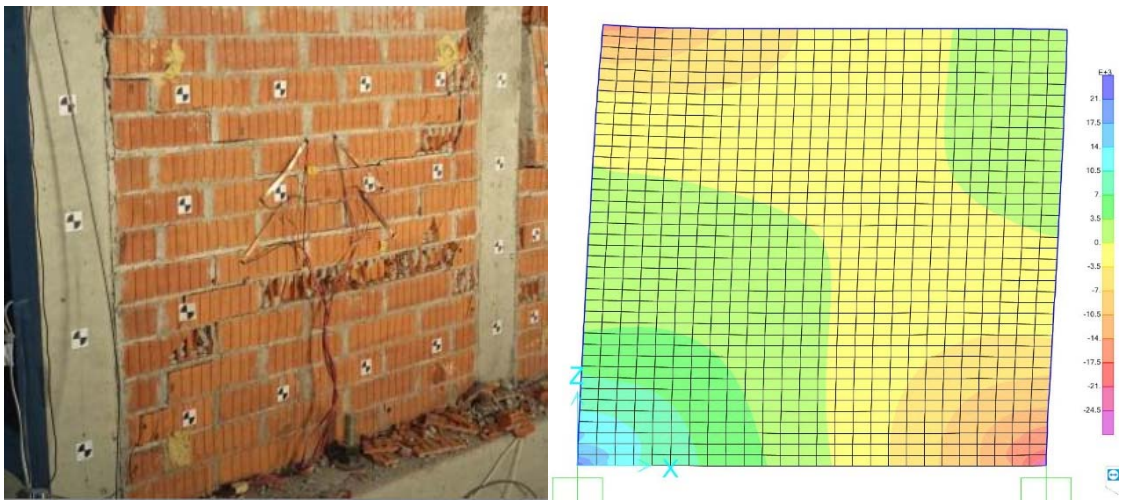

Figure 5.77 Infill wall damage from experiments and Stress distribution for Model IW-S (FRAMA Model 1)

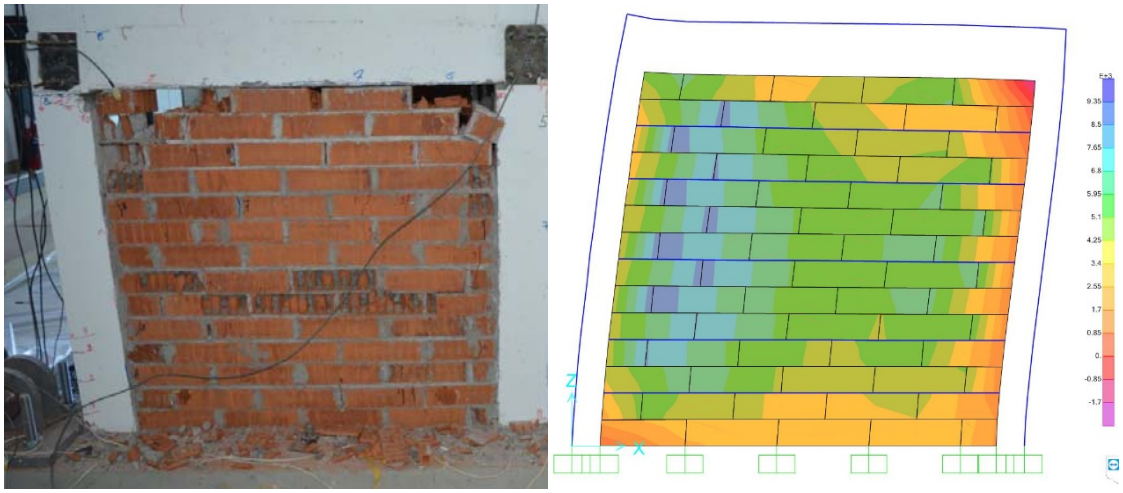

Figure 5.78 Infill wall damage from experiments and Stress distribution for Model IW-SB_2tb_1m

5.5.2. General guidelines

The general guidelines for applying the innovative method IW-SB can be classified into several points:

- According to the shown distribution of stresses, which largely coincides with damage pattern of the infill walls of Model IW-SB from the experimental investigations, it is obvious that the best results for the positive impact of this method in standard reinforced concrete buildings can be obtained if the same method is applied in two rows in the first and last third of the corresponding height of the infill wall and one

row between the second third. In terms of larger, non-standard heights, two lines from the IW-SB method can be predicted in the second and third quarters of the height of the filler respectively (Model IW-SB_2tb_2m).

- It is recommended to install vertical ties around all openings (doors and windows).
- The diameter of the reinforcing bars can be determined depending on the level of the defined seismic force, i.e. the corresponding axial tensile strength obtained in the IW-SB replacement element.
- By applying the IW-SB method, greater reliability and out-plane behavior on the infill walls is achieved. For more detailed guidelines in this direction, it is recommended to carry out additional experimental and analytical research.
- The incorporation and application of the IW-SB method is very simple without the use of additional performance technology. The cost of both the materials and the corresponding required technology for application of the method is minor and insignificant compared to the safety that can be achieved by applying this method.

6. CONCLUSIONS AND RECOMMENDATIONS

Catastrophic failure of masonry infilled reinforced concrete frame structures, with tremendous risk to human life and property, have been extensively reported in almost every disastrous earthquake during the past few decades. These facts reveal that inherent problems relating to design and analysis methods of tight-fit masonry infilled frames remain unsolved. Improperly designating tight-fit infill panels as non-structural elements in design could cause an unexpected structural performance during severe earthquake excitations.

This dissertation aims to develop an optimal solution, which can considerably mitigate the undesirable interaction between infill panels and bounding frames, protect the frames and infills from premature shear failure, and provide structural redundancy during high levels of lateral displacement. With the simple proposed connection detailing method, the structural system can exhibit minimal damage, while both in-plane and out of-plane infill stability are still achieved. Generally, the designer can have control over the seismic performance and failure mode of infilled frame structures by adopting the connection method.

To achieve the stated goals of this dissertation and to propose certain design guidelines, a comprehensive research programme has been carried out. The entire study involved three main phases as summarized below.

The first phase, as presented in Chapter 1, Chapter 2 and Chapter 3, gave an inclusive review of the seismic performance and current design methods and considerations relating to masonry infilled reinforced concrete frames. Vulnerabilities are summarized at global and local levels based on lessons learnt from past earthquakes. Simplified macro models such as single and multiple diagonal strut models were reviewed by comparing their merits and shortcomings. Localized micro-models for numerically simulating the infill and mortar were introduced, followed by a review of some informative shake-table experiment results. Generally, the structural reliability and adequacy of masonry infilled frame buildings cannot be guaranteed by current design and analysis methods. The proposed concept of connections is essential for further realization with detailed experimental investigations and numerical simulation.

In the second phase of the study (Chapter 4), the whole test programme including introduction of the available shake-table system, derivation of the similitude law, design and construction of models, and their instrumentation are specifically introduced. All the material properties used in this study were given. Also, real earthquake record for use as input was selected and scaled based on the models' properties and the boundary conditions. A test protocol was programmed with the purpose of gradually inducing damage to the structure by subjecting it to ground motions of increasing intensity. The second phase of the study besides the testing procedures presents also the results from the shake-table tests.

The new proposed connection involves spaced steel bars, and two variant solutions were analyzed: a) where the connection between masonry infill and frame is only done by the steel reinforcement and b) the infill panel is separated from columns with two finite width vertical gaps filled with polystyrene foam. Comprehensive experimental program is performed to investigate whether proposed column-infill connection details can effectively improve the seismic performance of masonry-infilled RC frame structures. The test results indicate that the proposed column-infill connection details can effectively improve the seismic performance of masonry-infilled RC frame structures. In addition, the displacement ductility and energy dispassion capacity of the frame system can be considerably improved. Considerable in-plane and out-of-plane stability together with a notable energy dissipation capacity were achieved.

In the third phase of the study, in order to represent and validate the experimental results, 3D series of analyses including dynamic excitation and monotonic loading were performed in SAP2000, using shell one-strut diagonal model for the masonry infill. The simulation results were compared with experimental observations and further validated the advantages of the proposed columns-infill connection.

The primary objective of the research, which proposes an innovative technical solution for infilled frame structures and looks to thoroughly validating its applicability and effectiveness through experimental investigation and numerical simulations, have been attained. Based on the results generated, the following conclusions are drawn, and corresponding general guidelines for the possible application of the IW-SB method in infill walls are given.

- The innovative connection detailing method proposed in this research has been proved to be an effective and favorable solution in high seismicity areas. For low seismic excitation, minor cracks could be observed on the infill panels, and the frame members tended to behave as the expected mode according to the structural analysis. For medium and high seismic excitation, the infill walls interact with the bounding frame and provide structural redundancy to resist the horizontal actions, and because of steel wire connections deployed in the mortar layers, the satisfying in-plane and out-of-plane stability and integrity of the infill panels can be achieved until an ultimate level of excitation.

- According the design of the innovative connection in this research, at each second layer of bricks starting from up and down two steel reinforcement bars with ϕ6 mm were installed, while in the middle part the distance between the bars was three layers of bricks. The procedure of the construction was the following: First two layers of bricks were set, on which above the mortar was installed. After that in both frames, at the columns anchors with length of one third of the span were connected. In the middle, reinforcement bar was put with length of the clear span which was connected with small wires to the reinforcement anchored in the columns from left and right in order to have continuous length of the reinforcement installed in the infill. Above the reinforcement another layer of mortar with same depth is installed. The procedure is repeated with all other layers above in the infill panel. At the bays where there were no columns, the anchorage was performed in the vertical tie. At frame B, the second variant of the proposed solution for connection was installed, where vertical gaps were put with length of 2.5 cm filled with polystyrene foam (Figure 4.3).

- Extensive experimental and numerical global analysis of the tested structure was performed and compared to a referent model with tight-fit hollow brick infill – Model 1 from FRAMA project (Necevska-Cvetanovska et al. 2015, Guljas et al. 2018, Anic et al. 2018).

Experimental results comparison - Model IW-SB vs. Model 1

- *Visual observations of damage after the final tests.* Before the test at 0.4 g, in both test series the structure experienced negligible-to-slight damage in the first story

walls. At 0.4 g in both test series, cracks began to form around the perimeter of the infill walls with some crushing at the corners. At 0.8 g in Model 1, the first and second story infill walls began to develop inclined cracks at isolated locations. These cracks formed in both directions. At the end of test sequences of Model 1 (PGA = 1.2g), the infill wall adjacent to the door opening had collapsed, and significant diagonal cracks occurred in the infill panels. In contrast, infill damage at the end of test sequences of Model IW-SB (PGA=1.6g) was only concentrated on the connections of the panel to the RC frame (Figure 4.51). The infill panels in Model IW-SB were being engaged more effectively in resisting the lateral demands, and kept their integrity until the last level of excitation of 1.6g. This observation contributed to the statement that with reinforcement bars the seismic capacity and in-plane and out-of plane stability of the infill is significantly improved.

- *Acceleration and displacement time histories.* The peak values of the accelerations and displacements of Model IW-SB comparing to Model 1 has lower values almost for all excitation level which also points to better seismic performance of Model IW-SB.

- *Strain in the reinforcement of the column of RC frame.* Results from comparison of the strain measurements show that maximum values measured for strain for Model 1 are higher that the values measured for Model IW-SB (Figure 4.58). This fact indicate also better seismic performance of Model IW-SB.

- *Interstory drifts.* Interstory drift ratios were calculated for each level of seismic excitation, (Figures 4.52-4.57), spanning from are 0.02% for 0.1g, 0.37% for 0.6g, 1.86% for 1.2g and 2.89% for 1.6g. These obtained drifts were compared with results obtained for Model 1 presented in Guljas et al. (2018). Results pointed out that Model IW-SB is having lower values than Model 1 which indicates to the conclusion that the proposed method for connection between the infill and the RC frame improves the seismic performance of the overall structure in general.

Analytical vs. Experimental results comparison and verification for Model IW-SB

Results from shake table tests of the referent Model 1 (Guljas et al., 2018) and Model IW-SB investigated in this study are compared with results obtained from numerical analysis. Within the doctoral dissertation two types of analysis are carried out: nonlinear static (pushover analysis) and time history nonlinear analysis. For both models, base shear vs. top displacements and top displacements time history obtained from numerical analysis are compared with experimental results (Figures 5.53-5.70).

General conclusion can be drawn that the results from the experiments fit well with the results from numerical analysis. This contributes to the fact that the simplified one diagonal strut model used in the numerical analysis for modelling of the infill gives satisfying results. This model can be used in design and analysis in everyday engineering practice for modelling of masonry infill in RC structures. For seismic excitation of 0.1g and 0.6 g there is very low difference between the experiments and numerical results, while for 1.2g and 1.6g this difference is slightly higher. Having in mind that the value of intensities like 1.2g and 1.6g are with significant magnitude, yet it can be confirmed that the results are satisfying. Results from comparative analysis point out that Model IW-SB has better capacity for strength and deformation, especially for high seismic excitation.

- From the extensive experimental and numerical investigation performed in this study it can be concluded that the proposed innovative connection detailing method could effectively mitigate undesirable damage for masonry infilled RC frame structures. The proposed technical solution is consisted of connection of the infill panel with bounding columns with steel wire connections which are deployed in mortar layers and anchored to columns. The proposed simple connection is practical, cheap and easy to implement without any specific technology, which is very important for developing countries in seismic regions such as Macedonia. Globally, the structural stability and integrity, displacement ductility, and energy dissipation capacity of masonry infilled RC frame are substantially improved. In view of the large number of masonry-infilled frame buildings in

Macedonia, the presented research is expected to provide useful guidance for seismic assessment and the design of safer frame structures.

- Considering that the infill walls constitute a considerable part of the gravity load in the reinforced frame structures, it is recommend to use regular infill walls as partitions only in low-seismicity areas. In this way, masonry infill walls actually provide structural redundancy for vertical load transfer in the frame system, increase the in-plane stiffness of structure, and act as the first line of earthquake defense.

- In high- seismicity areas, severe damage and poor seismic performance of infilled frame structures have been extensively demonstrated. The bracing effects dramatically change the dynamic characteristics. The load transfer path of frame structures under high storey drift ratio demand can cause sudden failure especially for very stiff masonry panels, which exposes the frame members to enormous shear force demand and the subsequent strength and stiffness degradation cause failure or collapse of the whole structure. It should be noted that the cost of repairing a severely damaged infilled frame may exceed the expense of building a new one.

- The general design recommendation for moderate to high seismicity areas for infilled RC frame system are summarized as below:

    - The rationale of the proposed connection method is to effectively mitigate the undesirable effects between infill panels and bounding columns during moderate levels of excitation, and provide a certain degree of beneficial strengthening effect at high levels of storey drift. The shake-table experimental results indicated that under this drift level both the frame members and infill panels exhibited minor damage. Analyzing the selected procedure for the calculation of the strut width, it is concluded that with the increase of the modulus of elasticity of the infill panel (Eme), the width of the diagonal strut (aw) is increasing, so the strength of the wall itself will become bigger. Moreover, the increasing of the Modulus of elasticity of the masonry material will give bigger strength in the analysis of the structural system itself. Regarding the modelling, if the proposed connection method is applied, than the infill panel should be modelled in the analysis as a structural element using simplified procedures.

Recommendation for future work

Comprehensive experimental research has been performed as basis for the investigations presented in this study. Yet, the experimental results can be significant starting point for investigation of the following topics:

- In plane vs out of plane failure mechanism
- Door and window openings, which are functional and inevitable, have been reported to considerably change the failure mode and seismic performance of infilled RC frames during earthquake excitation. Most of the analytical methods, especially diagonal strut models, would be ineffective when taking openings in infill panels into consideration. Further investigations, both numerical and experimental, should be carried out for masonry infilled RC frames with openings to provide an intensive seismic performance evaluation.
- Further investigation variant solution of the connection, for ex. for larger bays / width of the infill panel
- It is recognized that the high computational effort and complicated model assembly of the discrete modelling approach can inhibit its application in designing high-rise infilled frame structures. A new simplified modelling approach needs to be developed in the future to save analysis time and model assembly efforts. The macro strut models which were applied in this study demonstrates that this simplified method could be applicable for preliminary design analyses. Strut and tie models that consider the pre-cracking and post-cracking mechanism of infill panels need to be developed in the future to accurately reveal the bracing effect induced in bounding frames.
- Different dissipative materials adopted at beam-to-column interfaces or panel-to-panel interfaces in infilled frame structures are also of research interest.
-
-

7. REFERENCES

Angel, R. E. (1994). *Behavior of reinforced concrete frames with masonry infill walls* (Doctoral dissertation, University of Illinois at Urbana-Champaign).

Angel, R. I. C. H. A. R. D., Abrams, D. P., Shapiro, D. A. N. I. E. L., Uzarski, J., & Webster, M. A. R. K. (1994). *Behavior of reinforced concrete frames with masonry infills*. University of Illinois Engineering Experiment Station. College of Engineering. University of Illinois at Urbana-Champaign.

Anić, F., Penava, D., Varevac, D., & Sarhosis, V. (2018). Influence of Clay Block Masonry Properties on the Out-of-Plane Behaviour of Infilled RC Frames. *Tehnički vjesnik: znanstveno-stručni časopis tehničkih fakulteta Sveučilišta u Osijeku*, *26*(3), 1.

Akin, L. A. (2006). Behavior of reinforced concrete frames with masonry infills in seismic regions.

Al-Chaar G. (2002). Evaluating Strength and Stiffness of Unreinforced Masonry Infill Structures. ERDC/CERL TR-02-1, US Army Corps of Engineers, Construction Engineering Research Laboratory, 2002.

Apostolska R., Necevska-Cvetanovska G., Cvetanovska J., Gjorgjievska E. (2010). Influence of masonry infill on seismic performance of RC frame buildings. Proc. of 14 European Conference on Earthquake Engineering, Ohrid, 2010.

Apostolska R., Golubka Necevska-Cvetanovska, Julijana Cvetanovska. (2010). Analytical investigations of seismic behaviour of RC frame buildings with masonry infill. Structural Engineer, Journal of MASE, ISBN 9989-9785-3-0 (No.9/2010).

Apostolska R., Necevska-Cvetanovska G., Cvetanovska J., Jankovska B. (2010). Analytical investigations of seismic behaviour of RC building structures with masonry infill, Proc.of the GNP, February, Zabljak, Montenegro, 2010.

Apostolska R., Necevska-Cvetanovska G et al. (2017). Shaking table tests of three-storey RC building with hollow and solid masonry infill. 17th Symposium of MASE Ohrid, Macedonia.

Aristizabal-Ochoa, J. D., & Sozen, M. A. (1976). *Behavior of ten-story reinforced concrete walls subjected to earthquake motions* (No. 431). Urbana: University of Illinois.

Aschheim, M., & Black, E. F. (2000). Yield point spectra for seismic design and rehabilitation. *Earthquake Spectra*, *16*(2), 317-336.

Asteris, P. G., Cotsovos, D. M., Chrysostomou, C. Z., Mohebkhah, A., & Al-Chaar, G. K. (2013). Mathematical micromodeling of infilled frames: state of the art. *Engineering Structures*, *56*, 1905-1921.

ATC, 1996, Seismic evaluation and retrofit of concrete buildings, Vol. 1, ATC 40, Applied Technology Council, Redwood City, CA.

Bertero, V., & Brokken, S. (1983). Infills in seismic resistant building. *Journal of Structural Engineering*, *109*(6), 1337-1361.

Building Code Requirements and Specification for Masonry Structures: Containing Building Code Requirements for Masonry Structures (TMS 402-08/ACI 530-08/ASCE 5-08), Specification for Masonry Structures (TMS 602-08/ACI 530.1-08/ASCE 6-08) and Companion Commentaries. Masonry Society, 2008.

Burilo, D., Penava, D., Guljaš, I., Laughery, L., & Pujol, S. (2018, January). Influence of Masonry Walls on Unintended Torsional Response of Framed-Masonry Building. In *9th International Congress of Croatian Society of Mechanics*.

Calvi, G. M., Bolognini, D., & Penna, A. (2004). Seismic performance of masonry-infilled RC frames: benefits of slight reinforcements. *Invited lecture to "Sísmica*, *6*, 14-16.

Canadian Standards Association. (2004). CSA S304. 1-04: Design of masonry structures. *Mississauga, ON, Canada*.

Cavaleri, L., Fossetti, M., & Papia, M. (2005). Infilled frames: developments in the evaluation of cyclic behaviour under lateral loads. *Structural Engineering and Mechanics*, *21*(4), 469-494.

Cavaleri, L., & Di Trapani, F. (2014). Cyclic response of masonry infilled RC frames: Experimental results and simplified modeling. *Soil Dynamics and Earthquake Engineering*, *65*, 224-242.

China Ministry of Construction (CMC). (2010). Code for Seismic Design of Buildings (GB50011-2010).

Crisafulli, F. J. (1997). Seismic behaviour of reinforced concrete structures with masonry infills.

Crisafulli, F. J., & Carr, A. J. (2007). Proposed macro-model for the analysis of infilled frame structures. *Bulletin of the New Zealand Society for Earthquake Engineering*, *40*(2), 69-77.

Chrysostomou, C. Z. (1991). *Effects of degrading infill walls on the nonlinear seismic response of two-dimensional steel frames* (Doctoral dissertation, Cornell University).

Chrysostomou, C. Z., Gergely, P., & Abel, J. F. (2002). A six-strut model for nonlinear dynamic analysis of steel infilled frames. *International Journal of Structural Stability and Dynamics*, *2*(03), 335-353.

Council, B. S. S. (2000). Prestandard and commentary for the seismic rehabilitation of buildings. *Report FEMA-356, Washington, DC*.

Dolšek, M., & Fajfar, P. (2008). The effect of masonry infills on the seismic response of a four-storey reinforced concrete frame—a deterministic assessment. *Engineering Structures*, *30*(7), 1991-2001.

Doudoumis, I. N., & Mitsopoulou, E. N. (1986). Non-linear analysis of multi-storey infilled frames for unilateral contact condition. In *Proc., 8th European Conf. on Earthquake Engineering* (Vol. 3, pp. 63-70). Istanbul, Turkey: European Association for Earthquake Engineering (EAEE).

El-Dakhakhni, W. W., Elgaaly, M., & Hamid, A. A. (2003). Three-strut model for concrete masonry-infilled steel frames. *Journal of Structural Engineering*, *129*(2), 177-185.

EuroCode, P. (2005). Eurocode 8: Design of structures for earthquake resistance-part 1: general rules, seismic actions and rules for buildings. *Brussels: European Committee for Standardization*.

Fardis, M. N. (2006, September). Seismic design issues for masonry-infilled RC frames. In *Proceedings of the first European conference on earthquake engineering and seismology. Paper* (Vol. 313).

Fardis, M. N., Bousias, S. N., Franchioni, G., & Panagiotakos, T. B. (1999). Seismic response and design of RC structures with plan-eccentric masonry infills. *Earthquake engineering & structural dynamics*, *28*(2), 173-191.

Fardis, M. N., & Panagiotakos, T. B. (1997). Seismic design and response of bare and masonry-infilled reinforced concrete buildings part II: infilled structures. *Journal of Earthquake Engineering*, *1*(03), 475-503.

FEMA, F. (1997). NEHRP guidelines for the seismic rehabilitation of buildings. *FEMA 273*.

FEMA 306. (1998). Evaluation of earthquake damaged concrete and masonry wall buildings: Basic procedures manual. *ATC, Redwood City, CA, USA*.

Fiore, A., Netti, A., & Monaco, P. (2012). The influence of masonry infill on the seismic behaviour of RC frame buildings. *Engineering structures*, *44*, 133-145.

Flanagan, R. D., & Bennett, R. M. (1999). Arching of masonry infilled frames: Comparison of analytical methods. *Practice Periodical on Structural Design and Construction*, *4*(3), 105-110.

Flanagan, R. D., & Bennett, R. M. (2001). In-plane analysis of masonry infill materials. *Practice Periodical on Structural Design and Construction*, *6*(4), 176-182.

Furtado, A., Rodrigues, H., & Arêde, A. (2015). Modelling of masonry infill walls participation in the seismic behaviour of RC buildings using OpenSees. *International Journal of Advanced Structural Engineering (IJASE)*, *7*(2), 117-127.

Gavrilovic et al. (1992). Behaviour of infill in reinforced concrete frame systems under seismic effect. IZIIS report

Griffith, M. (2008). Seismic retrofit of RC frame buildings with masonry infill walls: literature review and preliminary case study. *JRC Scientific and Technical Reports*.

Grünthal, G. (1998). *European macroseismic scale 1998*. European Seismological Commission (ESC).

Guljaš, I., Penava, D., Laughery, L., & Pujol, S. (2018). Dynamic Tests of a Large-Scale Three-Story RC Structure with Masonry Infill Walls. *Journal of Earthquake Engineering*, 1-29.

Gulkan, P., & Sozen, M. A. (1974, December). Inelastic responses of reinforced concrete structure to earthquake motions. In *Journal Proceedings* (Vol. 71, No. 12, pp. 604-610).

Hashemi, A., & Mosalam, K. M. (2006). Shake-table experiment on reinforced concrete structure containing masonry infill wall. *Earthquake engineering & structural dynamics*, *35*(14), 1827-1852.

Henderson, R. C., Fricke, K. E., Jones, W. D., Beavers, J. E., & Bennett, R. M. (2002). SUMMARY OF LARGE-AND SMALL-SCALE UNREINFORCED MASONRY TEST PROGRAM by.

Hermanns, L., Fraile, A., Alarcón, E., & Álvarez, R. (2014). Performance of buildings with masonry infill walls during the 2011 Lorca earthquake. *Bulletin of Earthquake Engineering*, *12*(5), 1977-1997.

Hidalgo, P., & Clough, R. W. (1974). Earthquake Simulator Study of a Reinforced Concrete Frame, Report No. EERC 74–13. *Earthquake Engineering Research Center, University of California, Berkeley, CA*, *14*.

Holmes, M. (1961). Steel frames with brickwork and concrete infilling. *proceedings of the Institution of civil Engineers*, *19*(4), 473-478.

Huang, Y., Zhang, Y., Zhang, M., & Zhou, G. (2014). Method for predicting the failure load of masonry wall panels based on generalized strain-energy density. *Journal of Engineering Mechanics*, *140*(8), 04014061.

Idrizi I. (2013). Innovative HD systems with infill as a way of reduction of seismic risk for reinforced concrete buildings. Doctoral dissertation IZIIS.

Jankovska, B. (2009). Seismic performance of RC frame buildings with masonry infill. Master thesis, IZIIS.

Kakaletsis, D. J., & Karayannis, C. G. (2009). Experimental Investigation of Infilled Reinforced Concrete Frames with Openings. *ACI Structural Journal*, *106*(2).

Kappos, A. J., Stylianidis, K. C., & Michailidis, C. N. (1998). Analytical models for brick masonry infilled R/C frames under lateral loading. *Journal of Earthquake Engineering*, *2*(01), 59-87.

Kaushik, H. B., Rai, D. C., & Jain, S. K. (2006). Code Approaches to Seismic Design of Masonry-Infilled Reinforced ConcreteFrames: A State-of-the-Art Review. *Earthquake Spectra*, *22*(4), 961-983.

Klingner, R. E., & Bertero, V. V. (1978). Earthquake resistance of infilled frames. *Journal of the structural division*, *104*(6), 973-989.

Koutromanos, I., Stavridis, A., Shing, P. B., & Willam, K. (2011). Numerical modeling of masonry-infilled RC frames subjected to seismic loads. *Computers & Structures*, *89*(11-12), 1026-1037.

Krstevska L. (2002). Development and application of nonlinear micromodels for evaluation of seismic behavior of reinforced concrete frame structures with infill of unreinforced and reinforced masonry. Doctoral dissertation IZIIS.

Kuang, J. S., & Yuen, Y. P. (2013). Simulations of masonry-infilled reinforced concrete frame failure. *Proceedings of the Institution of Civil Engineers-Engineering and Computational Mechanics*, *166*(4), 179-193.

Kyriakides, M. A., & Billington, S. L. (2008). Seismic retrofit of masonry-infilled non-ductile reinforced concrete frames using sprayable ductile fiber-reinforced cementitious composites. In *14th World Conf. on Earthquake Engineering* (pp. 1-7).

Lee, H. S., & Woo, S. W. (2002). Effect of masonry infills on seismic performance of a 3-storey R/C frame with non-seismic detailing. *Earthquake engineering & structural dynamics*, *31*(2), 353-378.

Liauw, T. C., & Kwan, K. H. (1983). Plastic theory of non-integral infilled frames. *Proceedings of the Institution of Civil Engineers (London)*.

Liauw, T. C., & Kwan, K. H. (1983). Plastic theory of infilled frames with finite interface shear strength. *Proceedings of the Institution of Civil Engineers (London)*.

Liauw, T. C., & Kwan, K. H. (1985). Static and cyclic behaviours of multistorey infilled frames with different interface conditions. *Journal of Sound and Vibration*, *99*(2), 275-283.

Lotfi, H. R., & Shing, P. B. (1994). Interface model applied to fracture of masonry structures. *Journal of structural engineering*, *120*(1), 63-80.

Lourenço, P. B. (1996). A user/programmer guide for the micro-modeling of masonry structures. *Report*, *3*(1.31), 35.

Lourenço, P. B., & Rots, J. G. (1997). Multisurface interface model for analysis of masonry structures. *Journal of engineering mechanics*, *123*(7), 660-668.

Madan, A., Reinhorn, A. M., Mander, J. B., & Valles, R. E. (1997). Modeling of masonry infill panels for structural analysis. *Journal of structural engineering*, *123*(10), 1295-1302.

Mander, J. B., Nair, B., Wojtkowski, K., & Ma, J. (1993). An experimental study on the seismic performance of brick-infilled steel frames with and without retrofit.

McDowell, E. L., McKee, K., & Sevin, E. (1956). Arching action theory of masonry walls. *Journal of the Structural Division*, *82*(2), 1-8.

Mehrabi, A. B., & Shing, P. B. (1997). Finite element modeling of masonry-infilled RC frames. *Journal of structural engineering*, *123*(5), 604-613.

Moretti, M. L. (2015). Seismic design of masonry and reinforced concrete infilled frames: a comprehensive overview. *American Journal of Engineering and Applied Sciences*, *8*(4), 748.

Mosalam, K. M. A. (1996). *Experimental and computational strategies for the seismic behavior evaluation of frames with infill walls*. Cornell University, August.

Mosalam, K. M., White, R. N., & Gergely, P. (1997). Static response of infilled frames using quasi-static experimentation. *Journal of Structural Engineering*, *123*(11), 1462-4169.

Mosalam, K. M., Ayala, G., White, R. N., & Roth, C. (1997). Seismic fragility of LRC frames with and without masonry infill walls. *Journal of Earthquake Engineering*, *1*(04), 693-720.

Murty, C. V. R., Brzev, S., Faison, H., Comartin, C. D., & Irfanoglu, A. (2006). At risk: the seismic performance of reinforced concrete frame buildings with masonry infill walls. *Earthquake Engineering Research Institute, Publication No. WHE-2006-03,*, *70*.

Necevska-Cvetanovska G., Apostolska R., Shendova V., Stojanoski B., Zurovski A. (2015). “Frame-Masonry Composites for Modelling and Standardizations (FRAmed-MAsonry)”. *Report IZIIS* 2015-31.

Necevska-Cvetanovska et al. (2015). Nonlinear analysis of RC frames with types of infill characteristics for Macedonia and Croatia, Joint Macedonian-Croatian project.

Necevska-Cvetanovska G. (2015). 50 years of seismic design and assessment of RC building structures in IZIIS, Skopje, Macedonia. Proc. of the international conference to mark 50 years of IZIIS.

Necevska-Cvetanovska, G, Apostolska R, Sendova V, Vitanova M, Cvetanovska J (2014) Geo-referenced Inventory toward Seismic Safety of Existing Building – Case Strudy Karposh Municipality Skopje, Proceeding on the Second European Conference on Earthquake Engineering and Seismology, Istanbul, August 25-29, 2014.

Necevska-Cvetanovska, R. Apostolska. (2012). Methodology for seismic assessment and retrofitting of RC building structures. Proc. of 15 World Conference on Earthquake Engineering, Lisboa, September 24-28, 2012, (Paper ID 2149).

Necevska-Cvetanovska, G, Apostolska R. (2010). Methodology for Seismic Design of R/C Building Structures, Proceedings of the 12th World Conference on Earthquake Engineering/ New Zealand, 2010.

Necevska-Cvetanovska, G, Apostolska et al. (2018) METHOD FOR SEISMIC UPGRADING OF MASONRY INFILLS IN RC BUILDINGS. 16th European Conference on Earthquake Engineering, Thessaloniki, Greece.

Nocevski N. (1993). Definition of empirical and theoretical models for definition of vulnerability level of high-rises. Doctoral Dissertation IZIIS.

Otani, S., & Sozen, M. A. (1972). *Behavior of multistory reinforced concrete frames during earthquakes*. University of Illinois Engineering Experiment Station. College of Engineering. University of Illinois at Urbana-Champaign..

Polyakov, S. V. (1960). On the interaction between masonry filler walls and enclosing frame when loaded in the plane of the wall. *Translations in Earthquake Engineering, Earthquake engineering Research Institute, Oakland, California*, 36-42.

Preti, M., Migliorati, L., & Giuriani, E. (2015). Experimental testing of engineered masonry infill walls for post-earthquake structural damage control. *Bulletin of Earthquake Engineering*, *13*(7), 2029-2049.

Saneinejad, A., & Hobbs, B. (1995). Inelastic design of infilled frames. *Journal of Structural Engineering*, *121*(4), 634-650.

Sendova et al. (2013). Experimenatl verification of inovative technique for seismic retrofitting of traditional masonry buildings, Report IZIIS 2013-44.

Sezen, H., Whittaker, A. S., Elwood, K. J., & Mosalam, K. M. (2003). Performance of reinforced concrete buildings during the August 17, 1999 Kocaeli, Turkey earthquake, and seismic design and construction practise in Turkey. *Engineering Structures*, *25*(1), 103-114.

Shing, P. B., & Mehrabi, A. B. (2002). Behaviour and analysis of masonry-infilled frames. *Progress in Structural Engineering and Materials*, *4*(3), 320-331.

Smith, B. S. (1966). Behavior of square infilled frames. *Journal of the Structural Division*, *92*(1), 381-404.

Somers, P., Campi, D., Holmes, W., Kehoe, B. E., Klingner, R. E., Lizundia, B., & Schmid, B. (1996). Unreinforced masonry buildings. *Earthquake Spectra*, *12*(S1), 195-217.

Stafford Smith, B., & Carter, C. (1969). A method of analysis for infilled frames. *Proceedings of the institution of civil engineers*, *44*(1), 31-48.

Stavridis, A., Koutromanos, I., & Shing, P. B. (2012). Shake-table tests of a three-story reinforced concrete frame with masonry infill walls. *Earthquake Engineering & Structural Dynamics*, *41*(6), 1089-1108.

Syrmakezis, C. A., & Vratsanou, V. Y. (1986). Influence of infill walls to RC frames response. In *Proceedings of the eighth European conference on earthquake engineering* (Vol. 3, pp. 6-5).

Taghavi, S., & Miranda, E. (2003). *Response assessment of nonstructural building elements*. Pacific Earthquake Engineering Research Center.

Thiruvengadam, V. (1985). On the natural frequencies of infilled frames. *Earthquake engineering & structural dynamics*, *13*(3), 401-419.

Tu, Y. H., Chuang, T. H., Liu, P. M., & Yang, Y. S. (2010). Out-of-plane shaking table tests on unreinforced masonry panels in RC frames. *Engineering Structures*, *32*(12), 3925-3935.

Uva, G., Raffaele, D., Porco, F., & Fiore, A. (2012). On the role of equivalent strut models in the seismic assessment of infilled RC buildings. *Engineering Structures*, *42*, 83-94.

Varum, H., Furtado, A., Rodrigues, H., Dias-Oliveira, J., Vila-Pouca, N., & Arêde, A. (2017). Seismic performance of the infill masonry walls and ambient vibration tests after the Ghorka 2015, Nepal earthquake. *Bulletin of Earthquake Engineering*, *15*(3), 1185-1212.

Žarnić, R., Gostič, S., Crewe, A. J., & Taylor, C. A. (2001). Shaking table tests of 1: 4 reduced-scale models of masonry infilled reinforced concrete frame buildings. *Earthquake engineering & structural dynamics*, *30*(6), 819-834.

Yuen, Y. P., & Kuang, J. S. (2011, December). Seismic failure of infilled RC frames: discrete modelling approach with damage-based cohesive crack representation. In *The third international symposium on computational mechanics*.

Yuen, T. Y., Kuang, J. S., & Ali, B. S. M. (2016). Assessing the effect of bi-directional loading on nonlinear static and dynamic behaviour of masonry-infilled frames with openings. *Bulletin of Earthquake Engineering*, *14*(6), 1721-1755.

Yuen, Y. P., & Kuang, J. S. (2013). Fourier-based incremental homogenisation of coupled unilateral damage–plasticity model for masonry structures. *International Journal of Solids and Structures*, *50*(20-21), 3361-3374.

Zhang, H. (2015). *Strategies of Seismic Damage Mitigation for Infilled RC Frames: Shake-table Tests* (Doctoral dissertation, Hong Kong University of Science and Technology).